THE FORMATION AND REDUCTION PROCESSES OF RIVER DELTAS AND THEIR CONTROL(Dissertation_全文)

AUTHOR(S):

REFAAT, Hossam El-din A.A.

THE FORMATION AND REDUCTION PROCESSES OF RIVER DELTAS AND THEIR CONTROL

by

Hossam El-din A. A. Refaat

April 1990

THE FORMATION AND REDUCTION PROCESSES OF RIVER DELTAS AND THEIR CONTROL

by

Hossam El-din A.A. Refaat

April 1990

ACKNOWLEDGEMENTS

First of all I would like to express my deep gratitude and appreciation to Professor Y. Tsuchiya, Disaster Prevention Research Institute, Kyoto University, who introduced me to this topic, for his support, continuous guidance, invaluable discussions and advise, encouragement, and for critical reading of the manuscript. Without his support this thesis would never been written.

I also wish to direct my thanks to Associate Professor Y. Kawata for his guidance, and support throughout my staying in Japan. Sincere thanks are also to every member of Prof. Tsuchiya's Laboratory in which I stayed during the course of this work, for the congenial and stimulating atmosphere which all the laboratory members have created. I am particularly grateful for Dr. H. Yoshioka, Dr. T. Yamashita, Dr. A.S. Dadang (from Indonesia), Dr. J.R. Tallent (from U.S.A.) and Mr. Mishima. Numerous discussions with them in the field of Coastal Engineering have been helpful.

I would like also to acknowledge my gratitude to Cairo University, Egyptian Ministry of Higher Education, Kyoto University and the Japanese Ministry of Education for providing me the opportunity to pursue my studies in Japan and for granting me the financial support.

To my wife and daughter : Thank you for being understanding and patient during the last months of constant work. Believe it or not, "Al-hamedollah" the thesis is finished !, and finally I want to express my greatest appreciations and present this work to my parents and to all members of my family.

ABSTRACT

This study describes the formation and reduction processes of river deltas and their control. Based on the similarity process between the flow motion within the boundary layer and the nearshore currents within the surf zone, the concept of the boundary layer theory is introduced. The theory is authorized by two essential assumptions; they are the velocity profiles of longshore currents are similar and wave set-up is independent of longshore direction. Employing these assumptions, the nearshore current equations can be simplified to arrive a single equation for non-uniform longshore currents. This equation is similar to the boundary layer equation and contains integration coefficients which depend only on the velocity profiles of longshore currents. Therefore, an experimental study on the similarity of velocity profiles in non-uniform longshore currents was carried out. The experimental results reveal that the coefficients which appeared in the equation of non-uniform longshore currents are not functions of longshore direction nor time.

An extension is made to Tsuchiya and Yasuda's formulation of longshore sediment transport rate to include the non-uniform terms. The new formulation of non-uniform longshore sediment transport includes the effects of sediment size, beach slope and bed roughness, and has been verified with the field and laboratory data plotted in the well known Komar's figure.

The physical description of river delta formation is investigated through studying two field cases: the Nile Delta coast, Egypt and the major river deltas in Lake Biwa, Japan. The formation process of river deltas is investigated analytically and experimentally. The effect of longshore variation of beach slope on the configuration of river delta is studied. The theoretical and experimental results reveal that; for river-dominated delta type, beach slope is remarkably varied along the river delta with steeper beach slope at the river mouth and milder one at the end sides of the river delta. Thus, the configuration of river delta is sharply formed. In the contrary, for wave-dominated delta type, the longshore variation of beach

slope is very small resulting in gently curved shape of river delta. With normal wave incident, symmetrical configuration of river delta is arrived. When waves approach the beach obliquely asymmetrical configuration of river delta is observed.

The reduction process of river delta due to decrease or lack of sediment input form the river is experimentally investigated. The experimental results reveal that the reduction process is significantly different from the formation process. For the reduction process, the shoreline of the river delta is rapidly eroded, while the front line of the river delta retreats shoreward at a very slow rate. For the formation process, both the shoreline and the front line of the river delta propagate at the same rate, they are almost parallel.

A theory of formation of stable beaches is derived based on the new formulation of non-uniform longshore sediment transport and the aid of one-line theory. The applicability of the theory of formation of stable beaches is examined using data of stable beaches at Amanohashidate beach.

The final goal of this study is to control beach erosion of river delta, which occurs due to decrease or lack of sediment input from the river. The methodology of beach erosion control is investigated by introducing the previous and new methods for beach erosion control. A new proposal is made for beach erosion control of river delta based on Tsuchiya's ideal methodology for beach erosion control and the concept of formation of stable beaches. Two ideal examples are presented for controlling beach erosion of symmetrical and asymmetrical river delta configurations.

CONTENTS

LIST OF FIGURES

LIST OF TABLES

LIST OF TABLES

Chapter 1 INTRODUCTION

1.1 Objectives of The Study

The River delta areas have been recognized as a natural resource for the activities of human beings, particularly in those countries, especially in Egypt, which greatly depends on the Nile River for cultural as well as economic activities. The coasts of river delta have been developed to support agriculture, industry, residential areas, and recreational usage. In recent years utilization of coastal areas have steadily increased. Development of the coastal areas and river basins has frequently resulted in severe beach erosion, for example the construction of river dams which intercept the flow of sediment from the river to the coast resulting in serious beach erosion.

The history of man's intervention in the flow of the Nile River is very long, it dates back to Pharaonic times when Senusret built a canal from the ancient Pelusiac branch of the Nile to the Red Sea (circa 1900 B.C.). Since the completion of the High Aswan Dam in 1964, which has trapped all of the sediment load, a severe beach erosion takes place especially at the river mouths. For example at Rosetta promontory the erosion rates for the periods proceeding the surveys in 1926, 1965, 1973 and 1982 were 18, 20, 125 and 211 m/yr, respectively. The "new" Rosetta Lighthouse which was 1 km inland in 1970, became an offshore island in 1976. Therefore, the study of the formation and reduction processes of river deltas is one of the important aspects not only for Egypt but also for all countries of the world. The methods of preventing beach erosion and reclaiming land from the sea around river delta areas and adjacent coasts are the principal goals of this study.

In Japan, coastal projects have developed all over the country in order to protect human life from disasters caused by storm surge and tsunami (tidal waves). These projects also aim to stabilize the shoreline and preserve coastal environment. In addition to these purposes, it has recently become important to reclaim the land for increasing recreational areas.

The interactions between waves, currents, and bottom sediments are extremely complex. The incoming waves are transformed as they propagate into shallow water where they, at some critical depth, place the sediment in motion. This sediment is transported by coastal currents which are generated by the waves or other meteorological phenomena resulting in significant bathymetric changes. The objectives of the present study can be summarized as:

(1) A new formulation of total rate of non-uniform longshore sediment transport is made theoretically based on the applying of the concept of the boundary layer theory to the nearshore current equations in order to derive a single equation for non-uniform longshore currents as a function of time and space.

(2) A geographical and topographical investigation of the coastal areas around the river mouths and adjacent coasts is made for two field cases: the Nile Delta coast, Egypt, and the major river deltas in Lake Biwa, Japan.

(3) The total sediment discharge from the river is estimated using data records from sediment input analysis or by estimating from the shape of the river delta.

(4) The formation process of river deltas is investigated analytically and experimentally by applying the one-line theory and the formulation of non-uniform longshore sediment transport rate. The effect of beach slope change along the delta on the formation process of river delta is also presented. An experimental study is carried out to specify the main parameters in the formation process. The reduction process of river deltas due to decrease or lack of sediment input from the river is also experimentally investigated.

(5) An analytical solution for predicting the shoreline configuration of stable beaches is derived by the formulation of non-uniform longshore sediment transport associated with the

aid of one-line theory. Applicability of this theoretical formation is examined by use of field data of stable beaches.

(6) And the methods of controlling or preventing the coastal areas from beach erosion are investigated by introducing the previous and new methods for beach erosion control. A new proposal is made for beach erosion control of river delta based on Tsuchiya's ideal methodology for beach erosion control and the concept of formation of stable beaches. Two ideal examples are presented for controlling beach erosion of symmetrical and asymmetrical river delta configurations.

1.2 River Deltas in the World

Delta result from the relative importance of deposition of river sediments which build the delta seaward, versus the action of waves and currents which transport the sediments and erode the delta. Historically, the term *delta* was first applied by the Greek historian Herodotus, circa 450 B.C., to the triangular alluvial deposit at mouth of the Nile River. Deltas may occur wherever a stream debauches into an ocean, gulf, inland sea, bay, or lake. Consequently, deltas of various sizes can be found throughout the world. Table 1.1 gives the locations of some of the world's largest modern deltas (Wright, 1985). In addition to these major deltas, literally thousands of minor deltas are distributed over all the world's coasts.

For existence of a delta there are certain requirements, the first prerequisite for a significant deltaic accumulation is the existence of large drainage basin in which sediments are supplied by failure and erosion of the basin due to a heavy rainfall. The sediment-water discharge from the drainage basin is then transported to the coast by way of the alluvial valley that confines the stream. The general configuration of delta is then dependent of the relative importance of the deposited river sediment and the transported one by the action of waves and currents.

Previous researches have shown that configuration of delta is a function of numerous

Table 1.1 Some major deltas and their locations.

River	Land mass	Receiving body of water	Coordinates	
			Lat.	Long.
Amazon	South America	Atlantic Ocean	0	52°W
Burdekin	Australia	Coral Sea	19°S	147°E
Chao Phraya	Asia	Gulf of Siam	13°N	101°E
Colville	North America	Beaufort Sea	71°N	151°W
Danube	Europe	Black Sea	43°N	28°E
Dneiper	Asia	Black Sea	47°N	32°E
Ebro	Europe	Mediterranean Sea	41°N	02°E
Ganges–Brahmaputra	Asia	Bay of Bengal	32°N	90°E
Grijalva	North America	Gulf of Mexico	18°N	93°W
Huang Ho	Asia	Yellow Sea	37°N	118°E
Indus	Asia	Arabian Sea	24°N	67°E
Irrawaddy	Asia	Bay of Bengal	16°N	94°E
Klang	Asia	Straits of Malacca	3°N	101°E
Lena	Asia	Laptev Sea	73°N	125°E
Mackenzie	North America	Beaufort Sea	68°N	139°W
Magdalena	South America	Caribbean Sea	12°N	69°W
Mahakam	Borneo	Makassar Strait	1°S	117°E
Mekong	Asia	South China Sea	10°N	107°E
Mississippi	North America	Gulf of Mexico	30°N	90°W
Niger	Africa	Gulf of Guinea	4°N	7°E
Nile	Africa	Mediterranean Sea	32°N	31°E
Ord	Australia	Timor Sea	16°S	120°E
Orinoco	South America	Atlantic Ocean	8°N	62°W
Paraná	South America	Atlantic Ocean	33°S	58°W
Pearl	Asia	South China Sea	22°N	113°E
Pechora	Europe	Barents Sea	68°N	54°E
Po	Europe	Adriatic Sea	44°N	12°E
Purari	Papua New Guinea	Gulf of Papua	8°S	144°E
Red	Asia	Gulf of Tonkin	21°N	107°E
Sagavanirktok	North America	Beaufort Sea	70°N	148°W
São Francisco	South America	Atlantic Ocean	11°S	37°W
Senegal	Africa	Atlantic Ocean	17°N	16°W
Shatt-al-Arab	Asia	Persian Gulf	30°N	49°E
Shoalhaven	Australia	Pacific Ocean	35°S	151°E
Tana	Africa	Indian Ocean	2°S	42°E
Volga	Europe	Caspian Sea	47°N	48°E
Yangtze	Asia	East China Sea	32°N	122°E

process variables. Attempts to incorporate some or all of the process of variables into models for discriminating delta types have resulted in at least three classification themes. Fisher, Brown, Scott and McGowen (1969) proposed high constructive and high destructive delta types based on relative intensity of river discharge and waves action. Colemen and Wright (1971) and Wright, Coleman and Ericson (1974), using a board range of parameters, quantified the process variable, then used statistical techniques to array deltas into discrete grouping. More recently, Wright (1985) proposed a classification scheme based on the earlier work of Galloway (1975), wherein deltas were plotted on a ternary diagram to define general field of river, wave, and tide dominance. The most significant aspect of these studies is the addressing of the role of physical processes in producing specific and predictable answer.

Examination of a few major modern world river deltas indicates that although a large number of variations exists, there are generalized trends and most exceptions can be logically explained. Coleman and Roberts (1987) illustrated in Figure 1.1 the river discharge (m^3/sec) for several modern world deltas. In this figure the Amazon river has a largest river discharge with about $16x10^5$ m^3/sec, while the Sao Francisco river has a smallest river discharge of about 130 m^3/sec. This large variation does not indicate whether the Amazon delta is belong to a river-dominated type or not. For example, although the magnitude of Mississippi river discharge is relatively smaller than the magnitude of Amazon river discharge, the Mississippi delta will be the most river-dominated type while the Amazon delta will be classified as a tidal-dominated type .

A quantitative evaluation of wave power ($x10^7$ ergs/sec/m of coast) of seventeen river deltas is shown in Figure 1.2. The wave power parameter shown extremely wide variation, the Senegal delta experiences nearly 1,000 times more wave energy than the Mississippi delta. In other words, the Senegal delta receives more wave power along its coast in a little over two hours than the Mississippi delta dose all year. Such wave energy tends to smooth out the configuration of delta coastal line.

Tidal processor control the spatial relationships and geometries of configuration of

delta. There are three important characteristics of tidally dominated rivers can be identified as: 1) water-mass mixing by tidal activity destroys vertical density distribution, 2) for part of year tides account for the highest percentage of the sediment-transport energy and flow both in shoreward and seaward of the river mouth, and 3) the zone of wave-river interactions is greatly extended both vertically and horizontally (Wright, 1985). These characteristic effects result in widely different geometries for the delta development at the river mouth. Tidal processes are difficult to quantify, but Coleman and Roberts (1987) show in Figure 1.3 the average tidal range (in m) for 27 river deltas. The configuration of a low tide river delta such as the Nile or the Mississippi would be severely altered in a short period of time if it was subjected to tidal of nearly 6 m as in the case of the Ord river delta of Western Australia.

The relationship between river discharge and delta area of major world rivers is illustrated in Figure 1.4, which shows that as river discharge increases delta area increases. However, there is a very wide variation in delta area for any given river discharge, this is because of numerous interacting parameters. For example, the Sao Francisco river delta of Brazil is relatively small for the magnitude of its river discharge but this delta is characterized by extremely high wave action. In contrast, the Mekong delta of Vietnam is relatively large for the magnitude of its river discharge, the delta is rather stable and is significantly influenced by tidal processes, (Coleman and Roberts 1987). Later in Chapter 3, the data shown in Figures 1.1, 1.2 and 1.3 are used to adapt a modified version of a ternary diagram proposed by Galloway (1975).

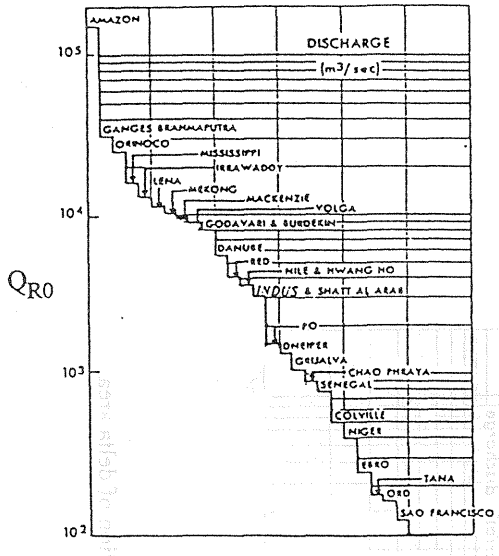

Figure 1.1 River discharge of selected river deltas.

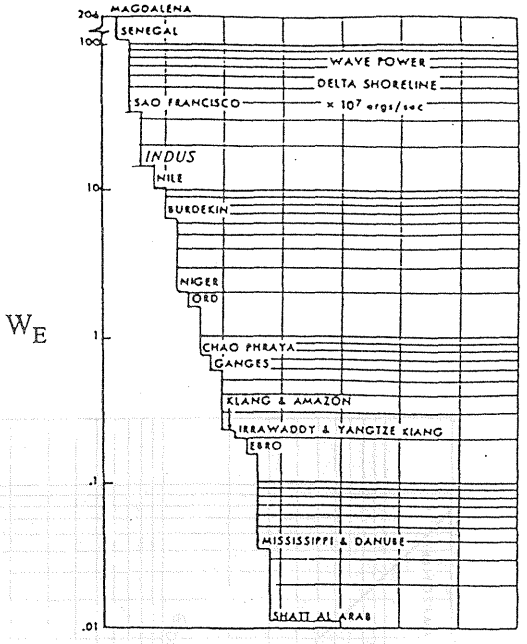

Figure 1.2 Wave power of selected river deltas.

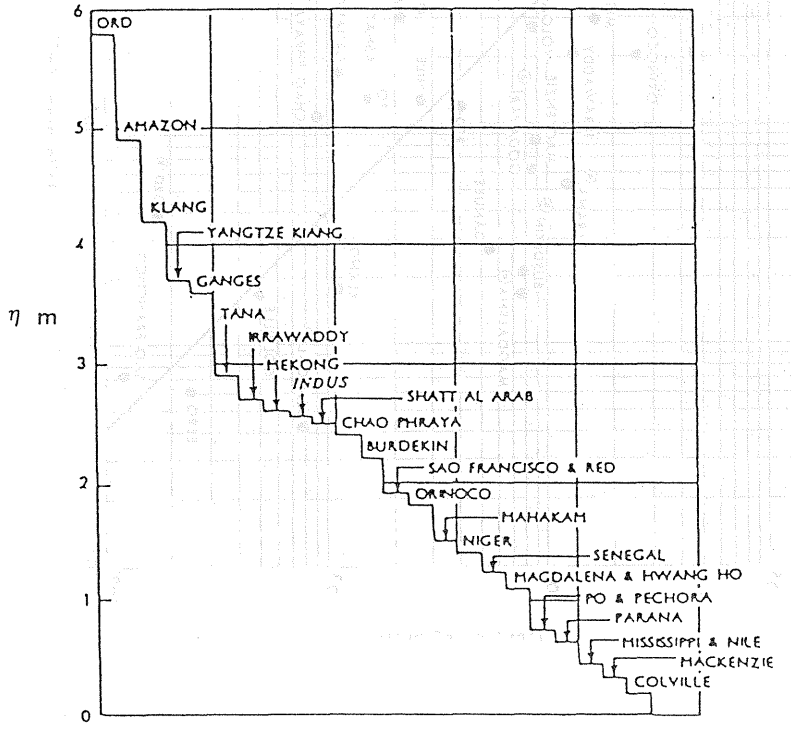

Figure 1.3 Average tidal range of selected river deltas.

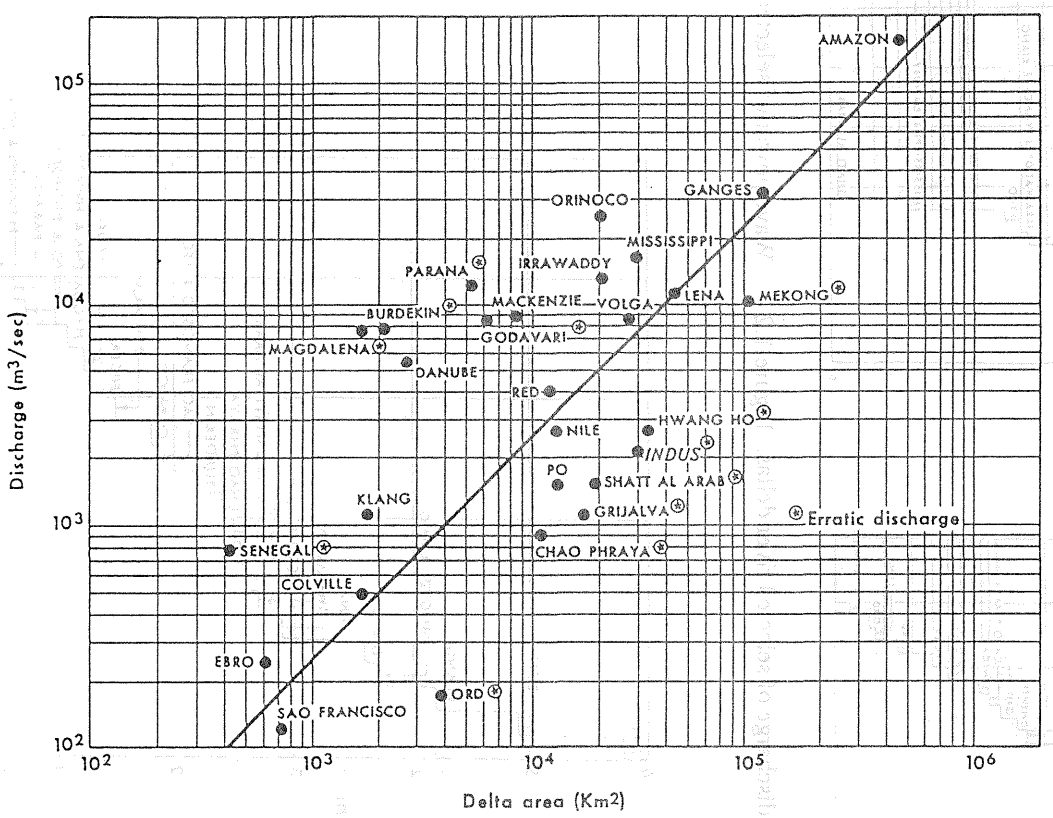

Figure 1.4 River discharge of major modern world deltas as a function of delta area.

1.3 Outline of Thesis

This thesis presents an investigation of the formation and reduction processes of river deltas, and methodology of beach erosion control of river deltas. Chapter 2 presents a new equation of non-uniform longshore currents based on the concept of boundary layer theory. An experimental study on the similarity of velocity profiles in non-uniform longshore currents was carried out. The experimental results reveal that the coefficients appeared in the new equation of non-uniform longshore currents are not functions of longshore direction nor time. Tsuchiya and Yasuda's (1979) formula for estimating of the total rate of longshore sediment transport is extended to include the non-uniform terms. This new formulation of non-uniform longshore sediment transport rate includes the effects of sediment size, beach slope and bed roughness, and has been verified with the field and laboratory data plotted in the well known Komar's figure.

In Chapter 3, firstly, the physical description of river deltas is presented through studying two field cases: the Nile Delta coast, Egypt, and the major river deltas in Lake Biwa, Japan. A brief description of the fundamental of the one-line theory will be discussed following by an overview of the previous analytical work related to the theory. Several analytical solutions for shoreline evolution of river deltas will be derived based on the aid of the one-line theory and the new formulation of non-uniform longshore sediment transport. In addition, an experimental study on the formation process of river deltas was carried out to specify the main parameters in the formation process. Finally, the analytical solutions of shoreline evolution of river deltas are applied to the experimental data and to the river deltas in Lake Biwa.

In Chapter 4 the reduction process of river deltas due to decrease or lack of sediment input from the river is experimentally investigated. An analytical solution for predicting the shoreline configuration of stable beaches will be derived based on the formulation of non-uniform sediment transport associated with the one-line theory. A theory of shoreline

configuration of stable sandy beaches is derived and its applicability is examined by using data of stable beaches at Amanohashidate beach, Japan. The last portion of the chapter presents the methodology of beach erosion control. A new proposal is made for beach erosion control of river delta based on Tsuchiya's ideal methodology for beach erosion control and the concept of formation of stable beaches. Two ideal examples are presented for controlling beach erosion of symmetrical and asymmetrical river delta configurations.

REFERENCES

Coleman J. M. and Roberts H. H. , 1987 " Deltaic Coastal Wetlands " Proc. of the symp. on Coastal Lowlands Organized by the Royal Geological and Mining Society of the Netherlands (KNGMG).

Coleman, J. M. and Wright L. D. 1971, " Analysis of Major River System and their Deltas: Procedures and Rationale, with two Examples ", coastal studies Institute, Louisiana State University, Techn. Rept. 95 : 125 pp.

Fisher, W. L. , Brown L. F. ,Scott A. T. and McGowen J. H. 1969, " Delta Systems in the Exploration for Oil and Gas " Bur. Econ. Geol., Univ. of Texas Austen: 78 pp.

Galloway, W. E. 1975 " Process Framework for Describing the Morphologic and Stratigraphic Evaluation of Deltaic Depositional Systems ", in M. L. Broussared (ed.): Deltas, models for exploration, Houston Geol. Soc. , Houston, Texas, pp. 87-98.

Tsuchiya, Y. and Yasuda, T., 1979," A Mathematical Model for Beach Change," Proc. 25th Japanese Conf. on Coastal Eng., JSCE, pp. 36-40 (in Japanese).

Wright, L. D. 1985 " River Deltas " In: R. A. Davis (ed.) : " Coastal Sedimentary Environments", second edition, Springer-Verlag pub. New York : pp. 76.

Wright, L. D , Coleman J. M. and Ericson M. W. , 1974 " Analysis of Major River Systems and their Deltas ", coastal studies Institute, Louisiana State University, Techn. Rept. 156, 114 pp.

Chapter 2 NON-UNIFORM LONGSHORE SEDIMENT TRANSPORT

2.1 Introduction

In recent years, the coastal region has become an area of intense human activity for industry, transportation, recreation, as well as for coastal protection works. The longshore sediment transport has a significant influence on changes in the shoreline positions as well as beach profiles. The prediction the longshore sediment transport rate is of great importance for the coastal engineers.

In the deep water, the propagation of waves is generally not associated with wave mass transport. However, as the waves travel closer to the shore, outside the surf zone, the wave mass transport gradually increases. Inside the surf zone, wave mass slowly moves shoreward, this is in addition to the to-and-fro motions produced by the waves. Closer to the shore, due to the presence of the beach, the water is redirected into a longshore current. The return flow of water offshore takes place in strong, narrow currents known as rip currents which flow seaward from the surf zone. This phenomenon is typically observed in nature.

Waves, currents and the properties of the bottom material determine the occurrence and magnitude of sediment transport in the coastal zones. The shoreline is simply defined as the boundary between sea and land. The geometry of the beaches is determined from the pattern and rate of sediment transport as well as the influence of man-made structures and other human activities in the nearshore zones.

The process of longshore sediment transport in coastal zones is extremely complex. Breaking and reforming waves, changing in space and time, generate a three-dimensional turbulence field acting over an irregular and constantly changing bottom topography. In

addition to the complexity just described other parameters of major importance for the longshore sediment transport such as grain size, beach slope and bed roughness must be considered. A complete theoretical description of all these parameters is for beyond the scope of presently available literature. Instead, simplified models must be used.

The aim of this chapter is to gain more insight into the dynamics of longshore sediment transport generated by waves and currents. In the following subsections, the overview of the previous works on longshore currents and associated longshore sediment is shown. Based on the concept of boundary layer theory, a new equation of non-uniform longshore currents is derived. This equation is similar to the boundary layer integral equation. An experimental study on the similarity of velocity profiles in non-uniform longshore currents was carried out to examine the applicability of the assumptions of the boundary layer concept in nearshore region. A new formula for total rate of non-uniform longshore sediment transport is derived based on the formula of Tsuchiya and Yasuda (1979). This formula includes the effect of sediment size, beach slope, bed roughness, and has been verified using the field and laboratory data plotted in the well known Komar's figure. With this formula, the empirical CERC formula could be modified.

2.2 Overview of Previous Work

2.2.1 Longshore sediment transport

Numerous investigations have been attempted to formulate the total rate of longshore sediment transport. Inman and Bagnold (1963) empirically correlated the longshore sediment transport rate to the longshore component of the incoming wave energy flux. They presented the first dimensionally correct expression for this correlation. This expression is now commonly known as the CERC (Coastal Engineering Research Center) formula. Bagnold (1963) extended his concept of work performed by water in moving sediment particles to include wave effects. He assumed that the longshore sediment transport depends on the

combined effect of waves and currents. Once the sediment is in motion due to waves, it becomes available to transport by longshore currents. His approach is known as the energetic model approach. In the literature there have been, and still are, many discussions about the value of the CERC formula coefficient.

Gourlay (1982) extended Bagnold's model to include an expression for the longshore current velocity resulting from the effects of both breaking angle and a longshore gradient of breaking wave height. Similar relations to the longshore current velocity proposed by Gourlay (1982) have been proposed by several authors (e.g. Motyka and Willis, 1975; Ozasa and Brampton, 1980). This type of expression has recently been recognized as useful for application of the one-line theory of beach evolution, especially for beaches with coastal structures (Hanson and Kraus, 1986).

In other approach known as bottom shear stress approach (or mass flux approach), the physical process of the mechanism of sediment transport is studied in more detail than the previous energetic approach. Consequently, this approach requires detailed knowledge of the important physical parameters such as bottom shear stress under combined waves and current, bottom slope, grain size distribution, the reduction of wave height due to breaking, and estimation of the diffusion coefficients both in non-breaking and breaking fields. Bijker (1971) assumed that mechanism of sediment movement is governed by the bottom shear stress alone. He combined the Kalinske-Frijlink bed load equation with the suspended load relation proposed by Einstein (1950) to get the total transport rate. Recently Tsuchiya and Yasuda (1979) proposed a new formulation of the total rate of longshore sediment transport based on the mass flux model, in which the longshore sediment transport is proportional to the averaged concentration of sediment and the longshore current velocity. This formula will be discussed in detail later in this chapter with extended it to include the non-uniformity of longshore sediment transport. Also, the formula will be verified using field and laboratory data plotted in the well known Komar's figure.

2.2.2 Longshore currents

Since Longuet-Higgins and Stewart (1964) laid down the principles and gave the physical meaning behind the concepts of radiation stress for water waves, the theory of longshore currents induced by wave breaking obliquely on beaches has progressed considerably. Eagleson (1965) measured the characteristics of breaking waves and the resulting longshore currents for 34 combinations of wave height (up to 0.22 ft), period (0.40 to 1.50 sec), and breaker angle (up to 32°) along a 20 ft test section of a 30 ft plane. The beach used in his experiment was smooth concrete with slope of 0.104. Observations and measurements show that most of the fluid in the surf zone remains there, and that longshore current velocity initially increases downstream from an obstacle. He explained the increasing of velocity along the beach due to the fluid forming the breaking wave has been withdrawn from the surf zone and thus already has a longshore component of motion of the breaking wave. A differential equation for this non-uniform flow agrees qualitatively with the measured variation of velocity with breaker angle and with distance from an obstacle.

Horikawa and Sasaki (1968) reviewed and summarized literature though 1967 including Japanese and Russian efforts. They conducted laboratory model tests with movable-bed and irregular topography using submerged float to measure the longshore current. Some fixed-bed model tests also conducted using Iwabana Harbor topography. Their results were well predicted values using the Eagleson (1965) formula. No quantitative comparison of model and theory was given in order to draw conclusions. The influence of the Reynolds number on bottom friction coefficients was also discussed.

Bowen (1969) investigated theoretically the generation of longshore currents on a beach, using the concept of radiation stress to describe the flux of momentum associated with the incoming waves. With reasonable assumptions, the theory leads to a complete description of the velocity field as a function of the distance from the shoreline. The model provides a mathematical framework for testing the various possible assumption by comparing them with reliable experimental data.

James (1974) proposed a theory of non-linear longshore currents. The present theory uses a combination of third-order hyperbolic waves (an approximation to cnoidal waves) near the shore and Stokes waves farther out. This is shown to be suitable assumption for the case of spilling breakers on gentle slopes. The momentum and energy fluxes given by this model are calculated and the consequences for wave shoaling and set-up are discussed.

Gourlay (1976) conducted hydraulic experiments for non-uniform longshore currents. Experimental data show that the form of the non-uniform wave-generated current system resulting from diffraction behind an offshore breakwater is essentially determined by the beach breakwater geometry while its magnitude depends upon the wave height. Furthermore, the current may produce significant increases in the magnitude of the wave set-up within three-dimensional system.

Liu and Dalrymple (1978) developed the analytical forms of the time-averaged bottom shear stress, including the effects of the angle between the direction of wave propagation and the mean current, and a large angle of wave incidence is also included in the study. Two different friction models are obtained based on the relative magnitudes of wave orbital velocity and that of mean currents. These two friction models are applied to longshore currents generated by obliquely incident waves. The lateral mixing is ignored and the beach contours are assumed to be straight and parallel. The strong current model, used when the mean currents are greater than the waves orbital velocity, is compared with laboratory data. A good agreement is found. The regions of validity of these two theories are discussed in terms of the angle of incident waves, the slope of the beach, and the bottom friction coefficient.

Kraus and Sasaki (1979) obtained an analytical solution of the steady longshore current on a plane beach. The simple form of the solution, which is essentially an extension of the Longuet-Higgins (1970), isolates the effects due to a moderately large incident wave angle and the lateral mixing parameter. Predictions of the model are verified with new detailed laboratory and field measurements. From comparison with observation it appears that mixing parameters less than about 0.1 describe most steady longshore currents. Values of both the

bottom friction and lateral mixing coefficients are determined by fitting the theory with the data.

Visser (1984) performed of laboratory experiments on uniform longshore currents and computed of the data with longshore current profiles predicted by a mathematical model. For the mathematical model it is assumed that longshore current generation occurs between the plunge line and the shoreline. Good agreement between theory and laboratory data is achieved with realistic values of the bottom roughness.

Recently, Thornton and Guza (1986) compared their analytical and numerical models for longshore currents generated by obliquely incident random waves with field observations. The longshore current models are based on balancing the gradient of the radiation stress with the longshore bed shear and Reynolds stresses, assuming stationary wave conditions and straight and parallel bottom contours. Optimal agreement between observed and predicted longshore currents was satisfied with a bed shear stress coefficient C_f = 0.006. They found that the eddy viscosity is not important, at least for the nearly planar topography present during the observations.

The previous theories have used some assumptions that are rather crude or even invalid. But, as Longuet-Higgins (1972) remarked :" it need do little harm to adopt special, but inapplicable, theories as a first step towards understanding a phenomenon, provided that we realize what we are doing and are prepared to make improvement later on". Good and reliable data are very important in the process of improving theory: both to guide this process and to evaluate the results.

2.3 Formulation of Non-uniform Longshore Currents

Many investigators have studied uniform longshore currents, but only a few such as Eagleson (1965), Horikawa and Sasaki (1968), James (1974) and Gourlay (1976) have concentrated on the phenomenon of non-uniform longshore currents. More recently,

Tsuchiya, Kawata and Refaat (1989) studied experimentally the velocity profiles of non-uniform longshore currents. They verified the existence of the similarity of velocity profiles of non-uniform longshore currents in the longshore direction. The phenomenon of non-uniform longshore currents can be seen clearly in the vicinity of reefs and headlands, as well as coastal structures. The velocity profile starts to grow near the initial current movement and increases rapidly, downcoast the structure, to reach a constant shape, which represents the velocity profile of uniform longshore current. Therefore, we may say that the non-uniform longshore currents are responsible for occurring a rapid erosion or accretion around these structures.

The shoreline is a boundary between sea and land. Immediately seaward of the shoreline there exist a narrow band of fluid known as the surf zone. The surf zone is characteristic of complex fluid motion induced by the rapid dissipation of the incoming wave energy. Moreover, in the field of hydraulics, particularly in the open channel flow, there exist a thin layer near the bed, within this layer the influence of viscosity is confined. Consequently, it may be possible to describe the longshore current motion in the surf zone using the boundary layer concept. Based on this analogy, the concept of boundary layer theory is introduced to the nearshore region.

The concept of boundary layer theory is well known in the fluid motion. The theory is authorized by two essential assumptions; they are the similarity in velocity profiles is existed and the pressure in a boundary layer is practically constant. Using these assumptions, Navier-Stokes equations can be simplified (Schlichting, 1960).

Similarly, in the nearshore region the assumptions of the boundary layer theory are introduced as: the velocity profiles of longshore currents are similar and wave set-up is independent of longshore position, see Figure 2.1. By employing these assumptions the nearshore currents equations can be simplified to arrive a single equation for non-uniform longshore currents, which is similar to the boundary layer integral equation.

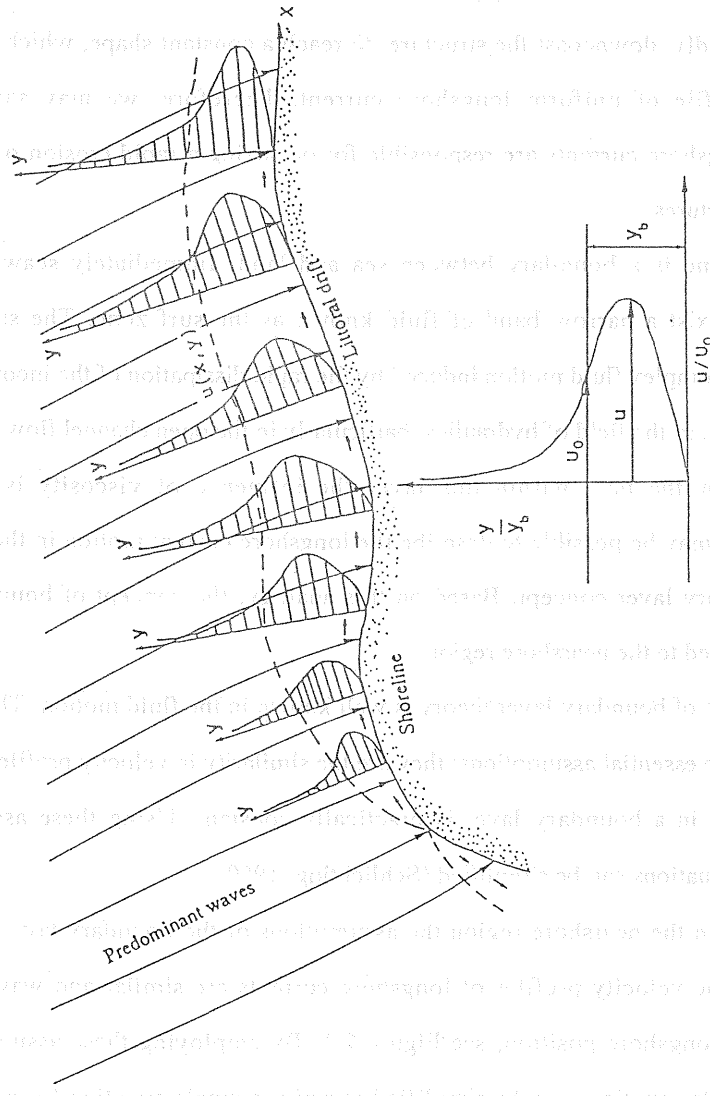

Figure 2.1 Schematic of similarity of velocity profiles of longshore currents.

The processes of simplification of the basic equations of nearshore current dynamics are straightforward as follows; 1) transformation of basic equations into a dimensionless form, 2) determination of order of magnitude of terms of basic equations by using stretching scale method, 3) separation of the basic equations into uniform and non-uniform, and 4) substitution of the equations of mass conservation and momentum conservation in cross-shore direction into the equation of momentum conservation in longshore direction to drive a single equation, and finally integration of that equation over the cross-shore direction. The resulted partial differential equation will be function of x (in longshore direction) and t (time) and contains integration coefficients which depend only on the velocity profiles of longshore currents. Since the velocity profiles are similar, the integration coefficients will not be functions of x nor t.

2.3.1 Basic equations of nearshore currents

In order to investigate the generation of nearshore currents, it is normally assumed that the fluid is homogeneous and the velocity field is independent of the water depth, so that only two-dimensional (horizontal) motion is allowed. The conservation of mass and momentum equations for waves superimposed on currents are derived by integrating the continuity and Navier-Stokes equations over the total water depth and then by taking a time average over the wave period. The detailed derivation of the equations is given by Phillips (1977) and by Mei (1983). The time- and depth-averaged mass and momentum conservation equation for unsteady flow in a homogeneous fluid are formed, respectively, as:

$$\frac{\partial h}{\partial t} + \frac{\partial (hu)}{\partial x} + \frac{\partial (hv)}{\partial y} = 0 \tag{2.1}$$

$$\frac{\partial u}{\partial t} + u\frac{\partial u}{\partial x} + v\frac{\partial u}{\partial y} = -\frac{1}{\rho h}\left(\frac{\partial S_{xx}}{\partial x} - \frac{\partial S_{xy}}{\partial y}\right) - g\frac{\partial \bar{\eta}}{\partial x}$$

$$+ \frac{1}{\rho h}\left(\frac{\partial T_{xx}}{\partial x} + \frac{\partial T_{xy}}{\partial y}\right) - \frac{1}{\rho h}\tau_x \tag{2.2}$$

$$\frac{\partial v}{\partial t} + u\frac{\partial v}{\partial x} + v\frac{\partial v}{\partial y} = -\frac{1}{\rho h}\left(\frac{\partial S_{yy}}{\partial y} - \frac{\partial S_{yx}}{\partial x}\right) - g\frac{\partial \bar{\eta}}{\partial y}$$

$$+\frac{1}{\rho h}\left(\frac{\partial T_{yy}}{\partial y} + \frac{\partial T_{yx}}{\partial x}\right) - \frac{1}{\rho h}\tau_y \qquad (2.3)$$

where u , v are the depth-averaged and time-averaged velocity components; S_{xx} , S_{xy} , etc. are the radiation stress components; T_{xx} , T_{xy}, etc. are the components of the Reynolds stress tensor expressed in lateral stresses; τ_x , τ_y are the time-averaged bottom shear stress components; and $\partial \bar{\eta} / \partial x$, $\partial \bar{\eta} / \partial y$ are the gradients of water surface in the x- and y-directions.

The momentum conservation equations, Eqs. (2.2) and (2.3), are equivalent to those for nearly horizontal free-surface flows if the radiation stress gradients are neglected. The radiation stress is defined as the excess momentum flux induced by wave motion. Longuet-Higgins and Stewart (1964) laid down the principles and gave the physical meaning behind the concepts of radiation stress for water waves. The lateral stress components shown in the momentum conservation equations, Eqs. (2.2) and (2.3) are described as the combined momentum fluxes due to both horizontal mixing length of turbulent eddies and deviations of local velocity from its depth-averaged value. Due to the weak understanding of the surf zone dynamics, the lateral stresses are usually described in terms of an eddy viscosity coefficient associated with velocity gradients (Vreugdenhil, 1980).

2.3.2 Processes of simplification of basic equations

To simplify the basic equations, first we transform these equations into a dimensionless form, then determine the order of magnitude of the basic equations terms by using stretching scale method. Finally, the separation of the basic equations into uniform and non-uniform can be done. The detail of the simplification processes is straightforward.

(1) Dimensionalization of basic equations

Before drawing the processes of simplification, the dimensionless of the basic

equations is first be required. Physically, surf zone is very narrow comparing with global view of the ocean, therefore, a certain distance, l, in longshore direction is introducing as the representative length to facilitate the dimensionless process, in which the uniformity of longshore current velocity is satisfied. The velocity of uniform longshore current is given by a modified Longuet-Higgins formula as:

$$U_b = \frac{5\pi}{16}\frac{\gamma}{C_f} g h_b \left(\frac{b}{c_b}\right) m \cos\alpha_b, \tag{2.4}$$

where $$m = \partial h / \partial y = \tan\beta / \left(1 + \frac{3}{8}\gamma^2\right) = (1 - k)\tan\beta \tag{2.5}$$

$$k = \left(1 + 8/3\,\gamma^2\right)^{-1}$$

in which, $\gamma = H_b/h_b$ is the breaker index, $\tan\beta$ is beach slope, C_f is the bottom frictional coefficient due waves and currents, $c_b = \sqrt{g h_b}$ the breaking wave celerity, g is the acceleration of gravity, with the definition, $b = \sin\alpha_b$, to simplify the notation and the subscript b denotes the values at the breaker line. U_b is selected as the representative velocity to facilitate the dimensionless process. The dimensionless quantities are introduced as:

$$x^* = \frac{x}{l}\ ,\quad y^* = \frac{y}{l}\ ,\quad h^* = \frac{h}{l}\ ,\quad t^* = \frac{t U_b}{l}\ ,$$
$$\bar{\eta}^* = \frac{U_b^2 \bar{\eta}}{g l^2}\ ,\quad u^* = \frac{u}{U_b}\ ,\ \text{and}\quad v^* = \frac{v}{U_b}\ , \tag{2.6}$$

Substitution of Eq. (2.6) into the basic equations, Eqs. (2.1), (2.2) and (2.3) , yields the dimensionless form of the mass and momentum conservation equations, respectively, as:

$$\frac{\partial h^*}{\partial t^*} + \frac{\partial (h^* u^*)}{\partial x^*} + \frac{\partial (h^* v^*)}{\partial y^*} = 0 \tag{2.7}$$

$$\frac{\partial u^*}{\partial t^*} + u^*\frac{\partial u^*}{\partial x^*} + v^*\frac{\partial u^*}{\partial y^*} = -\left(\frac{\partial S_{xx}^*}{\partial x^*} - \frac{\partial S_{xy}^*}{\partial y^*}\right) - \frac{\partial \bar{\eta}^*}{\partial x^*} + \left(\frac{\partial T_{xx}^*}{\partial x^*} + \frac{\partial T_{xy}^*}{\partial y^*}\right) - \tau_x^* \tag{2.8}$$

$$\frac{\partial v^*}{\partial t^*} + u^*\frac{\partial v^*}{\partial x^*} + v^*\frac{\partial v^*}{\partial y^*} = -\left(\frac{\partial S_{yy}^*}{\partial y^*} - \frac{\partial S_{yx}^*}{\partial x^*}\right) - \frac{\partial \bar{\eta}^*}{\partial y^*} + \left(\frac{\partial T_{yy}^*}{\partial y^*} + \frac{\partial T_{yx}^*}{\partial x^*}\right) - \tau_y^* \tag{2.9}$$

where the asterisk represents the dimensionless terms.

(2) Ordering of magnitude of terms of basic equations

The phenomenon of longshore currents deals with a narrow zone in cross-shore direction and a wide length in longshore direction. Hypothesis used are: 1) u is large in comparison with v; and 2) the derivatives with respect to y are large compared to the derivatives with respect to x. In order to clearly see the phenomenon of longshore currents, the longshore direction must be stretched, while the cross-shore direction remains constant. For this purpose, we introduce the stretching scale method. Application of the stretching scale method requires the specification of a small parameter $\varepsilon = h_b / l$, thus

$$h_b << l \quad , \quad u >> v \quad \text{and} \quad \partial / \partial y >> \partial / \partial x \tag{2.10}$$

where h_b is the water depth at the breaker line. Although, the longshore direction will be stretched by ε^m , where m is a positive number, the other dimensionless quantities in Eq. (2.5) will be stretched by another small parameters ε_1, ε_2, ...etc., because they are functions of x^*, y^* and t^*. The stretching quantities are then set as:

$$x_0 = \varepsilon^m x^* \quad , \quad y_0 = y^* \quad , \quad h_0 = \varepsilon_1 h^* \quad , \quad \bar{\eta}_0 = \varepsilon_1 \bar{\eta}^* \quad ,$$

$$u_0 = \varepsilon_2 u^* \quad , \quad v_0 = \varepsilon_3 v^* \quad , \text{and} \quad t_0 = \varepsilon_4 t^* \quad , \tag{2.11}$$

where the subscript 0 and the superscript * represent, respectively, the stretching and dimensionless quantities. The stretching parameters ε_i, i=1,4, will be determined as follows: From Eq. (2.10), the local acceleration term, the convective acceleration term, and the pressure gradient term , in longshore direction , are in the same order , thus

$$0\left(\frac{\partial u^*}{\partial t^*}\right) = 0\left(u^* \frac{\partial u^*}{\partial x^*}\right) = 0\left(v^* \frac{\partial u^*}{\partial y^*}\right) = 0\left(\frac{\partial \bar{\eta}^*}{\partial x^*}\right)$$

$$\text{or} \quad \frac{\varepsilon_4}{\varepsilon_2} = \frac{\varepsilon^m}{\varepsilon_2^2} = \frac{1}{\varepsilon_2 \varepsilon_3} = \frac{\varepsilon^m}{\varepsilon_1} \tag{2.12}$$

Longuet-Higgins has mentioned that the radiation stress gradient $\partial S_{xy} / \partial y$ and the bottom shear stress τ_x are of order one , then

$$0\left(\frac{\partial S^{*}_{xy}}{\partial y^{*}}\right) = 0\left(\tau^{*}_{x}\right) = 0(1) \quad \text{or} \quad \frac{1}{\varepsilon_1} = \frac{\varepsilon_1^{1/2}}{\varepsilon_2} = 1 \tag{2.13}$$

From Eqs. (2.12) and (2.13) we get:

$$\varepsilon_1 = \varepsilon_2 = 1 \;,\; \varepsilon_3 = \varepsilon^{-m} \quad \text{and} \quad \varepsilon_4 = \varepsilon^{m} \tag{2.14}$$

Substitution of Eqs. (2.11) and (2.14) into Eqs. (2.6), (2.7) and (2.8) , yields the mass and momentum conservation equations, respectively, in the form:

$$\varepsilon^m\left(\frac{\partial h_0}{\partial t_0} + \frac{\partial (h_0 u_0)}{\partial x_0} + \frac{\partial (h_0 v_0)}{\partial y_0}\right) = 0 \tag{2.15}$$

$$\varepsilon^m\left(\frac{\partial u_0}{\partial t_0} + u_0\frac{\partial u_0}{\partial x_0} + v_0\frac{\partial u_0}{\partial y_0} + \frac{\partial S_{xx0}}{\partial x_0} + \frac{\partial \bar{\eta}_0}{\partial x_0}\right) - \varepsilon^{2m}\frac{\partial T_{xx0}}{\partial x_0}$$

$$-\varepsilon^{2m}\frac{1}{h_0}\frac{\partial}{\partial y_0}\left(\upsilon_0 h_0 \frac{\partial v_0}{\partial x_0}\right) = \frac{\partial S_{xy0}}{\partial y_0} + \frac{1}{h_0}\frac{\partial}{\partial y_0}\left(\upsilon_0 h_0 \frac{\partial u_0}{\partial y_0}\right) - \tau_{x0} \tag{2.16}$$

$$\varepsilon^m\left(\frac{\partial S_{yx0}}{\partial x_0} + \frac{\partial T_{yy0}}{\partial y_0} + \frac{1}{h_0}\frac{\partial}{\partial x_0}\left(\upsilon_0 h_0 \frac{\partial u_0}{\partial y_0}\right) - \tau_{y0}\right) - \varepsilon^{2m}\left(\frac{\partial v_0}{\partial t_0}\right.$$

$$\left. + u_0\frac{\partial v_0}{\partial x_0} + v_0\frac{\partial v_0}{\partial y_0}\right) + \varepsilon^{3m}\frac{1}{h_0}\frac{\partial}{\partial x_0}\left(\upsilon_0 h_0 \frac{\partial v_0}{\partial x_0}\right) = \frac{\partial S_{yy0}}{\partial y_0} + \frac{\partial \bar{\eta}_0}{\partial y_0} \tag{2.17}$$

where υ is the kinematic turbulent viscosity. It is noted from Eq. (2.15) that the mass conservation equation is of order ε^m, this is because for the uniform condition, the gradient of the longshore currents with respect to the longshore direction is nil, i.e. $\partial u/\partial x = 0$ and therefore, no effect of cross-shore velocity component v on longshore velocity component u. In Eqs. (2.16) and (2.17), the model of Vreugdenhil (1980) was used to express the lateral stress components in terms of eddy viscosity coefficient associated with velocity gradients.

(3) Separation of basic equations into uniform and non-uniform

It is now convenient to separate the possible equations into two classes, uniform and non-uniform equations, depending on the stretching parameter ε^m. The uniform basic equations consist of terms of order one, while the non-uniform basic equations consist of the

uniform terms plus the terms of order ε^m. The higher order terms ε^{2m} and ε^{3m} will be neglected. In the following subsections the solution for uniform and non-uniform nearshore current equations is discussed.

2.3.3 Uniform nearshore current equations

Referring to Eqs. (2.16) and (2.17), terms of order one show, respectively, the equation of uniform longshore current and the equation of wave set-up as:

$$\frac{\partial S_{xy0}}{\partial y_0} + \frac{1}{h_0}\frac{\partial}{\partial y_0}\left(\upsilon_0 h_0 \frac{\partial u_0}{\partial y_0}\right) - \tau_{x0} = 0 \qquad (2.18)$$

$$\frac{\partial S_{yy0}}{\partial y_0} + \frac{\partial \bar{\eta}_0}{\partial y_0} = 0 \qquad (2.19)$$

The analytical solutions of Eqs. (2.18) and (2.19) have been given, respectively, by Longuet-Higgins (1972) to derive a model for longshore current profiles, and by Bowen, Inman and Simmons (1968) to derive wave set-up and set-down. The solutions are straightforward.

(1) Uniform longshore velocity profiles

Longuet-Higgins (1972) solved Eq. (2.18) showing that the velocity profile of the longshore current is dependent only of the nondimensional parameter P. He assumed that turbulent energy dissipation in breaking wave takes place shoreward of the breaker line. The ratio between the breaker height H_b and the breaker depth h_b is assumed constant, and is defined as, a breaker index $\gamma = H_b / h_b = H / h$. The parameter P is formed as:

$$P = \frac{N \pi m}{\gamma C_f} \qquad (2.20)$$

where N is a dimensionless constant being greater or equal to 0.016, C_f the bottom frictional resistance coefficient due to both waves and currents, and m the gradient of the water surface. The parameter P now represents the relative importance of lateral turbulent mixing of

the wave orbital motion to the bottom frictional resistance. Longuet-Higgins obtained the following results, for $P \neq 0.4$

$$U = A\,Y + B_1\,Y^{P1} \qquad 0 \le Y \le 1 \qquad (2.21a)$$

$$U = B_2\,Y^{P2} \qquad Y \ge 1 \qquad (2.21b)$$

where $U = u / U_b$, $Y = y / y_b$,

$$A = \frac{1}{(1 - \frac{5}{2}P)} \quad , \quad P1 = -\frac{3}{4} + \sqrt{\frac{9}{16} + \frac{1}{P}} \quad , \quad P2 = -\frac{3}{4} - \sqrt{\frac{9}{16} + \frac{1}{P}}$$

$$B_1 = \frac{P2 - 1}{P1 - P2}\ A \ , \quad B_2 = \frac{P1 - 1}{P1 - P2}\ A \qquad (2.21c)$$

so that all the constants (A, P1, P2, B_1, and B_2) in Eq. (2.21) depend upon the parameter P. The effect of parameter P on the velocity profiles is shown, for some representative P values, in Figure 2.2. These velocity profiles demonstrate that the magnitude of the longshore current velocity decreases with increasing magnitude of the parameter P. This is because taking larger P values gives more lateral stresses to smooth and spread the theoretical longshore current profile across the surf zone and beyond the breaker line. And using the lower P values shifts the maximum longshore current toward the breaker line. Taking P=0 for no lateral stress gives U=1 at Y=1 and a triangular solution is formed inside the surf zone with U=0 outside the breaker line.

(2) Wave set-down & set-up

Bowen, Inman and Simmons(1968) solved Eq. (2.19) and showed that for a plane beach of slope $\tan\beta$, the wave set-down is expressed as:

$$\frac{d\,\bar{\eta}}{d\,y} = -(1 + 8/3\,\gamma^2)^{-1} \tan\beta = -k \tan\beta \qquad (2.22)$$

This means that the mean water surface slope, wave set-down, is proportional to the beach slope. Integration of Eq. (2.19) to find $\bar{\eta}$, wave set-up, on a plane beach reduces to a simple trigonometric analysis. Thus $\bar{\eta}$ can be specified by the magnitude of the breaker index γ, the location of the break point, and the magnitude of wave set-down at the break point, $\bar{\eta}_b$.

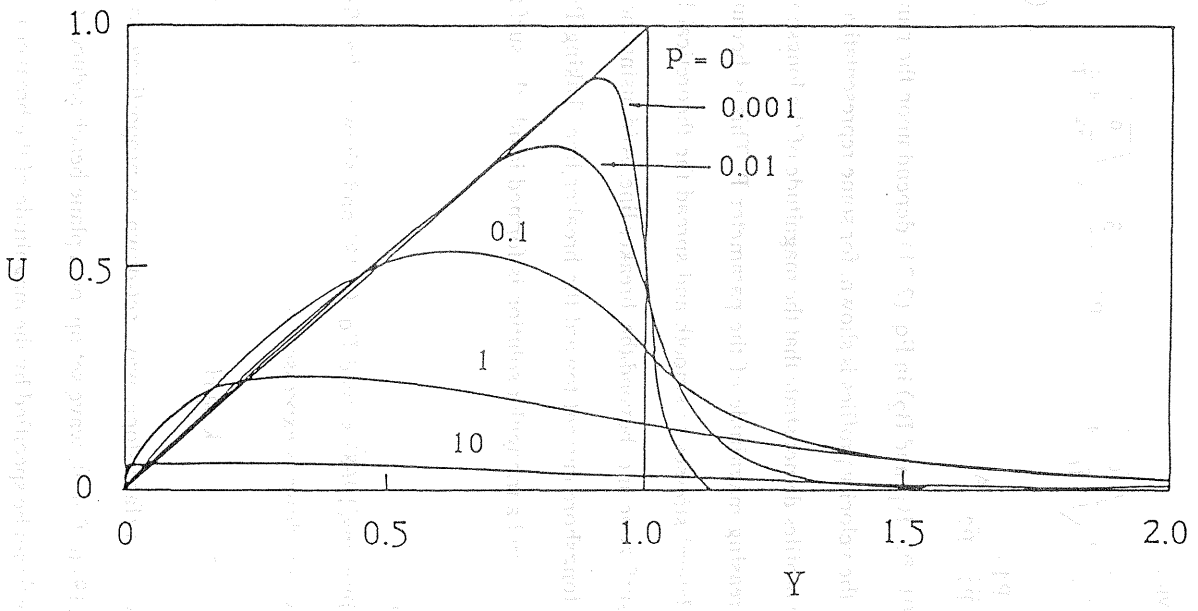

Figure 2.2 Dimensionless longshore velocity profiles as function of P - parameter (after Longuet-Higgins, 1972).

2.3.4 Non-uniform nearshore current equations

Returning to Eqs. (2.15), (2.16) and (2.17), the non-uniform basic equations can be extracted by neglecting terms of order higher than ε^m as:

$$\frac{\partial h}{\partial t} + \frac{\partial (hu)}{\partial x} + \frac{\partial (hv)}{\partial y} = 0 \tag{2.23}$$

$$\frac{\partial u}{\partial t} + u\frac{\partial u}{\partial x} + v\frac{\partial u}{\partial y} = -\frac{\partial S_{xx}}{\partial x} + \frac{\partial S_{xy}}{\partial y} - \frac{\partial \bar{\eta}}{\partial x} + \frac{1}{h}\frac{\partial}{\partial y}\left(\upsilon h \frac{\partial u}{\partial y}\right) - \tau_x \tag{2.24}$$

$$\frac{\partial \bar{\eta}}{\partial y} = -\frac{\partial S_{yy}}{\partial y} + \frac{\partial S_{yx}}{\partial x} + \frac{1}{h}\frac{\partial}{\partial x}\left(\upsilon h \frac{\partial u}{\partial y}\right) + \frac{\partial T_{yy}}{\partial y} - \tau_y \tag{2.25}$$

The subscript 0 has been dropped for convenience. Equations (2.23) and (2.24) are two simultaneous equations for the two velocity components u and v. While, Eq. (2.25) shows the non-linearity of wave set-up in a cross-shore direction. In the next section we will show how can these two simultaneous equations be transform into a single equation for non-uniform longshore currents.

2.3.5 Non-uniform longshore current velocity

In previous section a set of two simultaneous equations for the two velocity components u and v was derived. The substitution of the mass conservation equation, Eq. (2.23), into the momentum conservation equation, Eq. (2.24), results a single equation for a non-uniform longshore velocity. The velocity of non-uniform longshore current in this equation will be a function of the radiation stress gradients, mean water surface slope, lateral stress and bottom shear stress. This equation will be integrated over the cross-shore direction to eliminate the derivative with respect to y and to remain only the derivative with respect to x and t. Therefore, this integration requires us to specify the velocity profile of the longshore current in y-direction. For this purpose, a model proposed by Longuet-Higgins will be used in order to simplify the integration process. Also, to estimate the wave set-up, the model proposed by Bowen, Inman, and Simmons (1968) will be used. We should mention that any model for estimation of longshore velocity profiles can be used to evaluate the integration

quantities. Now the substitution of Eq. (2.23) into Eq. (2.24) and integrating over cross-shore direction, yields:

$$\rho \int_0^\infty h \frac{\partial u}{\partial t} dy - \rho \int_0^\infty \frac{\partial u}{\partial y} \left(\int_0^y \frac{\partial h}{\partial t} dy \right) dy + \rho \int_0^\infty h u \frac{\partial u}{\partial x} dy - \rho \int_0^\infty \frac{\partial u}{\partial y} \left(\int_0^y \frac{\partial (hu)}{\partial x} dy \right) dy$$

$$= - \int_0^\infty \frac{\partial S_{xx}}{\partial x} dy + \int_0^\infty \frac{\partial S_{xy}}{\partial y} dy - \rho g \int_0^\infty h \frac{\partial \bar{\eta}}{\partial x} dy + \int_0^\infty \frac{\partial}{\partial y} \left(\mu h \frac{\partial u}{\partial y} \right) dy - \int_0^\infty \tau_x \, dy \qquad (2.26)$$

Equation (2.26) is rewritten in a simple form as:

$$(I_1 - I_2) + (I_3 - I_4) = - I_5 + I_6 - I_7 + I_8 - I_9 \qquad (2.27)$$

The evaluation of the integration quantities requires knowing the velocity profiles of the longshore currents. Tsuchiya, Kawata and Refaat (1989) verified experimentally that the velocity profiles of non-uniform longshore currents are similar. Therefore, a suitable expression for the velocity profile is formed, taking into consideration that expression should satisfy the similarity of velocity profiles, hence

$$\frac{u}{U_0} = f\left(\frac{y}{y_b}\right) \qquad (2.28)$$

where U_0 is the non-uniform longshore current velocity at the breaker line. Now, the evaluation of the above integration quantities given by Eq.(2. 27) is drawn as follows;

$(I_1 - I_2)$: Local inertia term

From the longshore current profile shown in Figure 2.2 , it is noted that

$$I_2 = \rho \int_0^\infty \frac{\partial u}{\partial y} \left(\int_0^y \frac{\partial h}{\partial t} dy \right) dy = - \rho \int_0^\infty u \frac{\partial h}{\partial t} dy \qquad (2.29)$$

Then

$$I_1 - I_2 = \rho \int_0^\infty \left(h \frac{\partial u}{\partial t} + u \frac{\partial h}{\partial t} \right) dy = \rho \int_0^\infty \frac{\partial (hu)}{\partial t} dy \qquad (2.30)$$

Normalizing Eq. (2.30) with U_0 and h_b, yields

$$I_1 - I_2 = \frac{\rho}{m}\frac{\partial}{\partial t}\{ U_0 h_b^2 \int_0^\infty (\frac{h}{h_b})(\frac{u}{U_0})\, d(\frac{y}{y_b}) \} = \rho \frac{\partial}{\partial t}(\alpha_1 U_0 h_b^2) \qquad (2.31)$$

in which $$\alpha_1 = \frac{1}{m}\int_0^\infty (\frac{h}{h_b})(\frac{u}{U_0})\, d(\frac{y}{y_b}) \qquad (2.32)$$

Since u / U_0 is a function of y / y_b and h/h_b can be expressed by y / y_b, the coefficient α_1 will not be a function of x nor t.

$(I_3 - I_4)$: Convective inertia term

Similar to the above, it is found that

$$I_4 = \rho \int_0^\infty \frac{\partial u}{\partial y}\left(\int_0^y \frac{\partial (hu)}{\partial x}\, dy\right) dy = -\rho \int_0^\infty u \frac{\partial (hu)}{\partial x}\, dy \qquad (2.33)$$

Then

$$I_3 - I_4 = \rho \int_0^\infty \left(hu\frac{\partial u}{\partial x} + u\frac{\partial (hu)}{\partial x}\right) dy = \rho \int_0^\infty \frac{\partial (hu^2)}{\partial x}\, dy \qquad (2.34)$$

Normalized Eq. (2.34) with U_0 and h_b , yields

$$I_3 - I_4 = \frac{\rho}{m}\frac{\partial}{\partial x}\{ U_0^2 h_b^2 \int_0^\infty (\frac{h}{h_b})(\frac{u}{U_0})^2\, d(\frac{y}{y_b}) \} = \rho \frac{\partial}{\partial x}(\alpha_2 U_0^2 h_b^2) \qquad (2.35)$$

in which $$\alpha_2 = \frac{1}{m}\int_0^\infty (\frac{h}{h_b})(\frac{u}{U_0})^2\, d(\frac{y}{y_b}) \qquad (2.36)$$

Also, α_2 is not a function of x nor t.

I_5 : Radiation stress gradient ($\partial S_{xx} / \partial x$)

In a series of papers beginning in 1960, Longuet-Higgins and Stewart laid down the principles and gave the physical meaning behind the concepts of radiation stress for water waves. They assumed that the dissipation of wave energy flux takes place shoreward of the breaker line, therefore, I_5 is reduced to

$$I_5 = \int_0^{y_b} \frac{\partial S_{xx}}{\partial x}\, dy = \frac{\partial}{\partial x}\int_0^{y_b} S_{xx}\, dy - \frac{\partial y_b}{\partial x}[S_{xx}]_{y_b} \qquad (2.37)$$

Applying the definition of the radiation stress given by Longuet-Higgins (1972) into Eq. (2.37), shows

$$I_5 = \frac{1}{16}\rho g \gamma^2 \frac{\partial}{\partial x}\{\beta_2 h_b^3 + 2\beta_3 b^2 h_b^3\} - \frac{1}{8}\rho g \gamma^2 h_b^2 (\frac{1}{2} + b^2)\frac{\partial y_b}{\partial x} \qquad (2.38)$$

in which $\beta_2 = \frac{1}{m}\int_0^1 (\frac{h}{h_b})^2\, d(\frac{y}{y_b})$ and $\beta_3 = \frac{1}{m}\int_0^1 (\frac{h}{h_b})^3\, d(\frac{y}{y_b})$ (2.39)

in which the definition, $b = \sin\alpha_b$, to simplify the notation and the subscript b notices the values at the breaker line. The coefficients β_2 and β_3 depend on the ratio of y/y_b, therefore they are geometrical constants.

I_6 : Radiation stress gradient ($\partial S_{xy}/\partial y$)

Since the dissipation of wave energy flux takes place shoreward of the breaker line the integration I_6 reduces to:

$$I_6 = \int_0^{y_b} \frac{\partial S_{xy}}{\partial y}\, dy = [S_{xy}]_{y_b} = \frac{1}{16}\rho g \gamma^2 h_b^2 \sin 2\alpha_b \qquad (2.40)$$

I_7 : Wave set-up

Bowen, Inman, and Simmons (1968) showed that the wave set-up for a planar beach of slope tanβ with normal wave incidence is expressed as:

$$\frac{d\bar{\eta}}{dy} = -k\tan\beta = -k\frac{\partial d}{\partial y}, \quad \text{where} \quad k = (1 + 8/3\gamma^2)^{-1} \qquad (2.41)$$

This meant that the mean water surface slope, wave set-up, is proportional to the beach slope. Integration of Eq. (2.41) to find $\bar{\eta}$ on a plane beach reduces to a simple trigonometric analysis. Therefore, the wave set-up relation can be written as:

$$\bar{\eta} = \frac{k}{(1-k)}(\frac{5}{6}h_b - h) = \frac{3\gamma^2}{8}(\frac{5}{6}h_b - h) \qquad (2.42)$$

Substitution of Eq. (2.42) into the integration I_7 shows:

$$I_7 = \frac{5\gamma^2}{16}\rho g \beta_1 h_b^2 \frac{\partial h_b}{\partial x} - \frac{3\gamma^2}{16}\rho g \frac{\partial}{\partial x}(\beta_2 h_b^3) + \frac{3\gamma^2}{16}\rho g h_b^2 \frac{\partial y_b}{\partial x} \qquad (2.43)$$

in which $\beta_1 = \frac{1}{m}\int_0^1 (\frac{h}{h_b})\, d(\frac{y}{y_b})$ and $\beta_2 = \frac{1}{m}\int_0^1 (\frac{h}{h_b})^2\, d(\frac{y}{y_b})$ (2.44)

Similarly, the coefficient β_1 depends on the ratio y/y_b, thus it will be a geometrical constant.

I_8 : Lateral stress term

The lateral stress combines the momentum fluxes due to both the horizontal mixing length of turbulent eddies and the deviations of local velocity from its depth-averaged value. Due to weak understanding of the dynamics of surf zone, the lateral stress is usually described in term of an eddy viscosity coefficient associated with a velocity gradient. Longuet-Higgins (1972) distinguished the effect of lateral stress on the shape of velocity profiles, addressing by a dimensionless parameter P. However, the integration I_8 shows that

$$I_8 = \int_0^\infty \frac{\partial}{\partial y}(\mu h \frac{\partial u}{\partial y})\, dy = \left[\mu h \frac{\partial u}{\partial y}\right]_{y=\infty} - \left[\mu h \frac{\partial u}{\partial y}\right]_{y=0} \qquad (2.45)$$

When the Longuet-Higgins's model for the longshore velocity profiles is applied, Eq. (2.21). The integration I_8 will be mathematically equal to zero. Physically, in the deep water area, when y goes to infinity, the wave energy is assumed conserved, therefore no lateral stress exist. Also, no lateral stress exist at the shoreline where the water depth goes to zero. This means that the lateral stress has no effect on the velocity in the longshore direction. In fact, we can explain this phenomenon from a point of view of similarity of velocity profiles as; since the lateral stress has been addressed by the parameter P which plays an essential part for changing the shape of the velocity profile in the cross-shore direction and since the similarity of the velocity profiles in the longshore direction has been verified experimentally, therefore, the parameter P will be independent of the longshore direction and consequently, the lateral stress will have no effect on the non-uniformity of the current velocity in longshore

direction.

I_9 : Bottom shear stress

For the time average bottom shear stress τ_x Longuet-Higgins derived

$$\tau_x = \frac{2}{\pi} C_f \rho \left| u_m \right| u \qquad (2.46)$$

where; C_f is the bottom frictional resistance coefficient due to both waves and longshore currents, and $|u_m|$ is the absolute value, maximum wave orbital velocity near the bottom for sinusoidal motion, thus I_9 can be written as:

$$I_9 = \frac{\gamma}{\pi} C_f \rho \alpha_3 c_b U_0 h_b, \quad \text{in which } \alpha_3 = \frac{1}{m} \int_0^{\infty} \left(\frac{h}{h_b}\right)^{1/2} \left(\frac{u}{U_0}\right) d\left(\frac{y}{y_b}\right) \qquad (2.47)$$

The evaluation of the above integration quantities creates coefficients α_i and β_i, i = 1, 2, 3. The estimation of these coefficients requires knowing the longshore velocity profiles and the local depth ratio (h/h_b). Employing the similarity of velocity profiles in non-uniform longshore currents shows that the coefficients α_i and β_i are not functions of x nor t. They are functions of the shape of the longshore current velocity, which can be represented by Longuet-Higgins parameter P. The detail of evaluation of these coefficients using the model of Longuet-Higgins is summarized in next subsection. Therefore, Eq. (2.27) is rewritten finally as:

$$\alpha_1 \frac{\partial}{\partial t}(U_0 h_b^2) + \alpha_2 \frac{\partial}{\partial x}(U_0^2 h_b^2) + \alpha_3 \frac{\gamma C_f c_b}{\pi} U_0 h_b = f(x) \qquad (2.48)$$

and

$$f(x) = \frac{\gamma^2}{16} g h_b^2 \{ \sin 2\alpha_b - 2 \cos^2 \alpha_b \frac{\partial y_b}{\partial x} (5\beta_1 - 6\beta_2 + 6\beta_3 \sin^2 \alpha_b) \frac{\partial h_b}{\partial x} - 2\beta_3 h_b \sin 2\alpha_b \frac{\partial \alpha_b}{\partial x} \} \qquad (2.49)$$

where U_0 is the non-uniform longshore current velocity at the breaker line, $\gamma = H_b/h_b$ is the breaker index, $c_b = \sqrt{g h_b}$ is the breaking wave celerity, g is the acceleration of gravity, and

α_i and β_i , i = 1, 2, 3, are the integration coefficients. Regarding to the similarity of the velocity profiles, these coefficients will be dependent of the predicted shape of the velocity profiles. Any model for predicting the velocity profiles of the longshore currents can be used with Eq. (2.48), however, for simplifying the mathematical process, the model of Longuet-Higgins will be used here.

Equation (2.48) is a nonlinear partial differential equation with only one unknown, the longshore current velocity U_0. The analytical solution of this equation gives a complete description for the phenomenon of longshore currents, which is the final goal. However, the equation is excessively complicated to permit analytical treatment since too many variables are described in one formulation. Therefore, to obtain a closed form solution to the non-uniform longshore currents, a simple mathematical formulation has to be used, but one which still preserves the important mechanism concerned. Since the concept of the boundary layer is introduced here, it is expected that the derived equation for describing the non-uniformity of longshore currents is similar to the boundary layer integral equation. An interesting theoretical analogy can be made between these two equations, such that, the integration coefficients appeared in both equations are dependent of the velocity distribution in a direction perpendicular to the direction of the main flow. For example, in the boundary layer integral equation two coefficients appeared, they are called the displacement thickness δ^* and the momentum thickness θ, and defined by

$$\delta^* U = \int_{y=0}^{\infty} (U - u) \, dy \tag{2.50}$$

and

$$\theta U^2 = \int_{y=0}^{\infty} u (U - u) \, dy \tag{2.51}$$

Similarly, the coefficients appeared in the non-uniform longshore current equation, Eq. (2.48), can be distinguished as the coefficients α_i, i = 1, 2, 3, which represent the longshore

velocity profiles, and the coefficients β_i, i = 1, 2, 3, which represent the gradient of the radiation stress and wave set-up. A comparison between the coefficients of the boundary layer equation and the coefficients of the non-uniform longshore currents equation leads to some interesting points, that; (1) The coefficient α_1 is similar to the displacement thickness δ^*, and α_2 is similar to the momentum thickness θ, while α_3 represents the effect of the bottom shear stress due to wave actions, (2) the coefficient β_i, i = 1, 2, 3, represent the pressure gradient, which is assumed constant in the boundary layer equation and assumed here independent of the longshore direction.

2.3.6 Closed form solution for non-uniform longshore current

The closed form solution of Eq. (2.48) depends upon the estimation of the coefficients α_i and β_i, as will as the given boundary conditions. An analytical solution of Eq. (2.48) for steady and constant waves conditions, and with the boundary condition at x = 0 , $U_0 = \bar{U}_0$ is derived as:

$$\frac{(1-\bar{U}_0/U_b)\exp(1-U_0/U_b)}{(1-U_0/U_b)\exp(1-\bar{U}_0/U_b)} = \exp(B\,x) \qquad (2.52)$$

where

$$U_b = \frac{5\pi\gamma m}{16\,C_f} g\,h_b \left(\frac{\sin\alpha_b}{c_b}\right)\cos\alpha_b , \quad \text{and}$$

$$B = \left(\frac{8\,C_f}{5\pi m}\right)^2 \frac{2}{\alpha_2 h_b \sin 2\alpha_b} \qquad (2.53)$$

Equation (2.52) demonstrates the development of non-uniform longshore current velocity at the breaker line. Figure 2.3 shows a family of solutions of Eq. (2.52) for some representative $\bar{U}_0/U_b$ values . The longshore current velocity increases rapidly to reach a constant value which corresponds to the uniform longshore current velocity U_b .

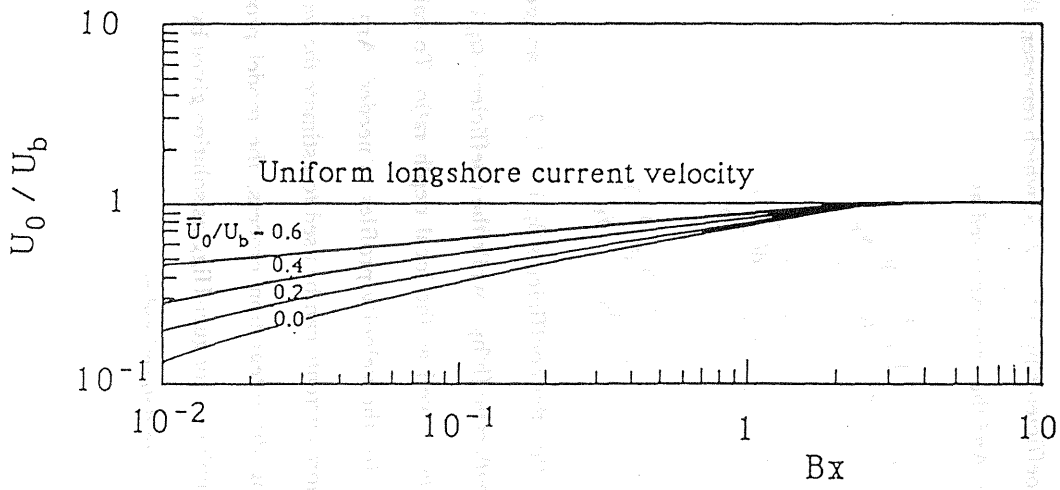

Figure 2.3 Distribution of non-uniform longshore current velocity for some representative $\bar{U}_0 / U_b$ values.

2.3.7 Coefficients of non-uniform longshore current equation

In section 2.3.5 an equation for non-uniform longshore currents was derived, Eq. (2.48). This equation has coefficients which appeared due to the integration over the cross-shore direction, and they are dependent of the velocity profiles of longshore current, which are similar, as well as the uniformity of wave set-up in longshore direction. These coefficients can be distinguished as the coefficients α_i, i = 1, 2, 3, which represent the longshore velocity profiles, and the coefficients β_i, i = 1, 2, 3, which represent the gradient of the radiation stress and wave set-up. And they are expressed as:

$$\alpha_1 = \frac{1}{m}\int_0^{\infty} \left(\frac{h}{h_b}\right)\left(\frac{u}{U_0}\right) d\left(\frac{y}{y_b}\right), \quad \beta_1 = \frac{1}{m}\int_0^{1} \left(\frac{h}{h_b}\right) d\left(\frac{y}{y_b}\right)$$

$$\alpha_2 = \frac{1}{m}\int_0^{\infty} \left(\frac{h}{h_b}\right)\left(\frac{u}{U_0}\right)^2 d\left(\frac{y}{y_b}\right), \quad \beta_2 = \frac{1}{m}\int_0^{1} \left(\frac{h}{h_b}\right)^2 d\left(\frac{y}{y_b}\right) \qquad (2.54)$$

$$\alpha_3 = \frac{1}{m}\int_0^{\infty} \left(\frac{h}{h_b}\right)^{1/2}\left(\frac{u}{U_0}\right) d\left(\frac{y}{y_b}\right), \quad \beta_3 = \frac{1}{m}\int_0^{1} \left(\frac{h}{h_b}\right)^3 d\left(\frac{y}{y_b}\right)$$

It is clearly seen in Eq. (2.54), that the coefficients β_i, i = 1, 2, 3, are geometrical constants, depend only on the local depth ratio (h/h_b), while the coefficients α_i, i = 1, 2, 3, are dependent of the velocity profiles as well as the local depth ratio. To calculate the coefficients α_i a suitable expression for the velocity profiles is needed. Any model for predicting velocity profiles of longshore currents can be used to estimate the values of the coefficients, however, for simplifying the integration process, the model proposed by Longuet-Higgins will be used here. Applying Longuet-Higgins solution given by Eq. (2.21), the coefficients α_i and β_i, i = 1, 2, 3, are determined as:

$$\alpha_1 = \frac{1}{3m}(1-P)^{-1}, \quad \beta_1 = \frac{1}{2m}$$

$$\alpha_2 = \frac{A}{4m} + \frac{2AB_1}{m(P1+3)} + \frac{B_1^2}{2m(P1+1)} - \frac{B_2^2}{2m(P2+1)}, \quad \beta_2 = \frac{1}{3m} \qquad (2.55)$$

$$\alpha_3 = \frac{2}{5m}, \quad \beta_3 = \frac{1}{4m}$$

where the constants A, P1, P2, B_1, and B_2 are dependent upon the Longuet-Higgins parameter P. Figure 2.4 illustrates the influence of the parameter P on the coefficients α_i and β_i. The coefficients β_i do not affect by the parameter P, because they are geometrical constants as indicated in Eq. (2.54). The coefficients α_1 and α_2 are affected by the parameter P, while the coefficient α_3 has been held constant. The reason for this is explained as follows; in Eq. (2.48) the coefficients α_1 and α_2 present , respectively, the influence of unsteady and non-linear terms of longshore currents which are affected by the changes of velocity in the longshore direction, while the coefficient α_3 presents the influence of uniform longshore current term.

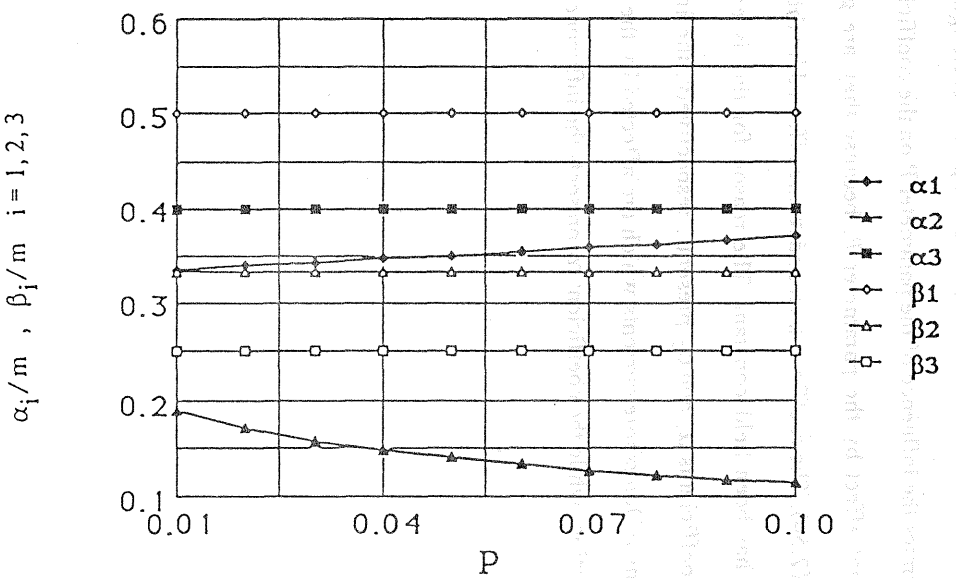

Figure 2.4 Integral coefficients for non-uniform longshore currents as function of Longuet-Higgins parameter P.

2.4 Experimental Study on Similarity of Velocity Profiles

Based on the similarity between the flow motion within the boundary layer and the longshore current within the surf zone, the concept of boundary layer theory is introduced to the nearshore region. The theory is authorized by two assumptions, they are: the velocity profiles of longshore currents are similar, and wave set-up is independent of longshore position. As discussed in the previous section, these assumptions were employed to simplify the nearshore current equations. Therefore, a series of experiments on longshore currents was performed. The purposes of these experiments were to examine the applicability of the assumption that the velocity profiles in non-uniform longshore currents are similar and to examine the uniformity of wave set-up in the longshore direction. The experiments were performed using regular waves.

2.4.1 Experimental set up

The experiments were performed in the fan-shaped wave basin (semicircular part: r=17.5 m; rectangular part: 35 x 10 m) of Ujigawa Hydraulics Laboratory, Disaster Prevention Research Institute, Kyoto University. A smooth concrete beach was constructed with slope 1:10. Two smooth wave guide walls were installed in the normal direction to the wave board, The upstream guide wall was closed to the beach and downstream one was ended near the toe of the fixed bed, see Figure 2.5. The purpose for having a guide wall closed to the beach in upstream is to keep the wave height uniform along the beach. While, the opening at downstream guide wall helps to minimize the water circulation between the guide walls and to carry it away behind at the still water area.

In Figure 2.5, the sloping part of the wave basin was marked by a 20 square cm grid. Measurements of current velocity were made at every grid line perpendicular to the shoreline. Two different types of colored tracers were used; 3 cm square shaped paper tracers and 2.5 cm ball tracers. The tracer trajectories within each grid was recorded by using a video camera

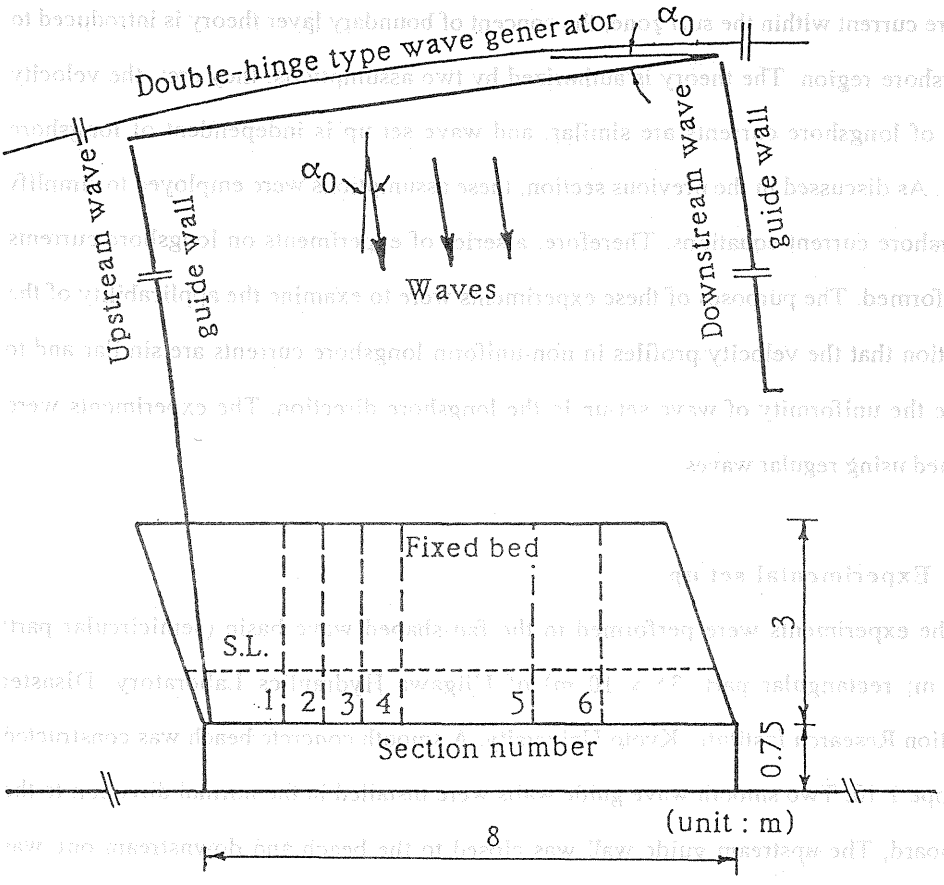

Figure 2.5 Schematic diagram of experimental arrangement of similarity of velocity profiles in non-uniform longshore currents.

system. Measurements of wave heights in the constant depth of the basin were made with capacitance type wave gauges. While on the sloping part, measurements of wave heights and mean water level were made over the entire grid area using capacitance type wave gauge and low frequency filter, respectively. The wave gauge and low frequency filter were installed on a vehicle mounted on rails controlled by personal computer. The angles of incoming wave incidence were measured at the constant depth part by measuring the angles of inclination of the wave generator to the beach. Snell's law and linear wave theory were used to estimate the angles of wave incidence at the breaker line.

2.4.2 Experimental results

In order to develop a more realistic model for non-uniform longshore currents, it is necessary to employ regular waves under various conditions. To carry out this investigation, eight experiments were performed under the conditions that the still water depth at the constant depth part is 30.6 cm, the wave period is 1.13 sec, the range of angle of incidence is 15° to 55°, and the wave height is varied from 3.8 cm to 8.5 cm, (see Table 2.1). The experimental results are classified mainly into two categories which are given as:

(1) Similarity of velocity profiles

Figures 2.6 and 2.7 show an example of the measured longshore velocity, for two incident wave angles 17° and 45°, compared with the theoretical curve of Longuet-Higgins (1972). The rate of agreement between measured and computed longshore current profiles is influenced by the choice of Longuet-Higgins parameter P. The curves were fitted to the data by using the method of least square. It is noted that for all experiments Longuet-Higgins parameter P is less than 0.2. From these figures it is obvious that:

(1) The similarity of velocity profiles is very satisfactory. The shape of the velocity distribution starts to grow from the initial boundary until to reach constant shape, which represents uniform velocity profile.

Table 2.1 Experimental conditions of non-uniform longshore currents.

Ex. No.	H'_0 (cm)	α_0 deg.	H_b (cm)	h_b (cm)	γ (H_b/h_b)	α_b deg.	W_b (cm)	P
R1	3.80	17.0	5.68	6.05	0.94	7.32	80	0.20
R2	5.10	17.0	6.73	7.87	0.86	8.36	100	0.09
R3	8.50	17.0	11.61	11.72	0.99	10.22	150	0.10
R4	4.50	35.0	7.98	8.80	0.91	17.56	90	0.05
R5	5.20	45.0	7.21	8.03	0.90	20.81	100	0.10
R6	7.75	45.0	9.63	11.80	0.82	25.51	130	0.10
R7	5.50	55.0	7.74	9.48	0.82	26.56	100	0.10
R8	6.65	55.0	8.60	10.03	0.86	27.38	120	0.08

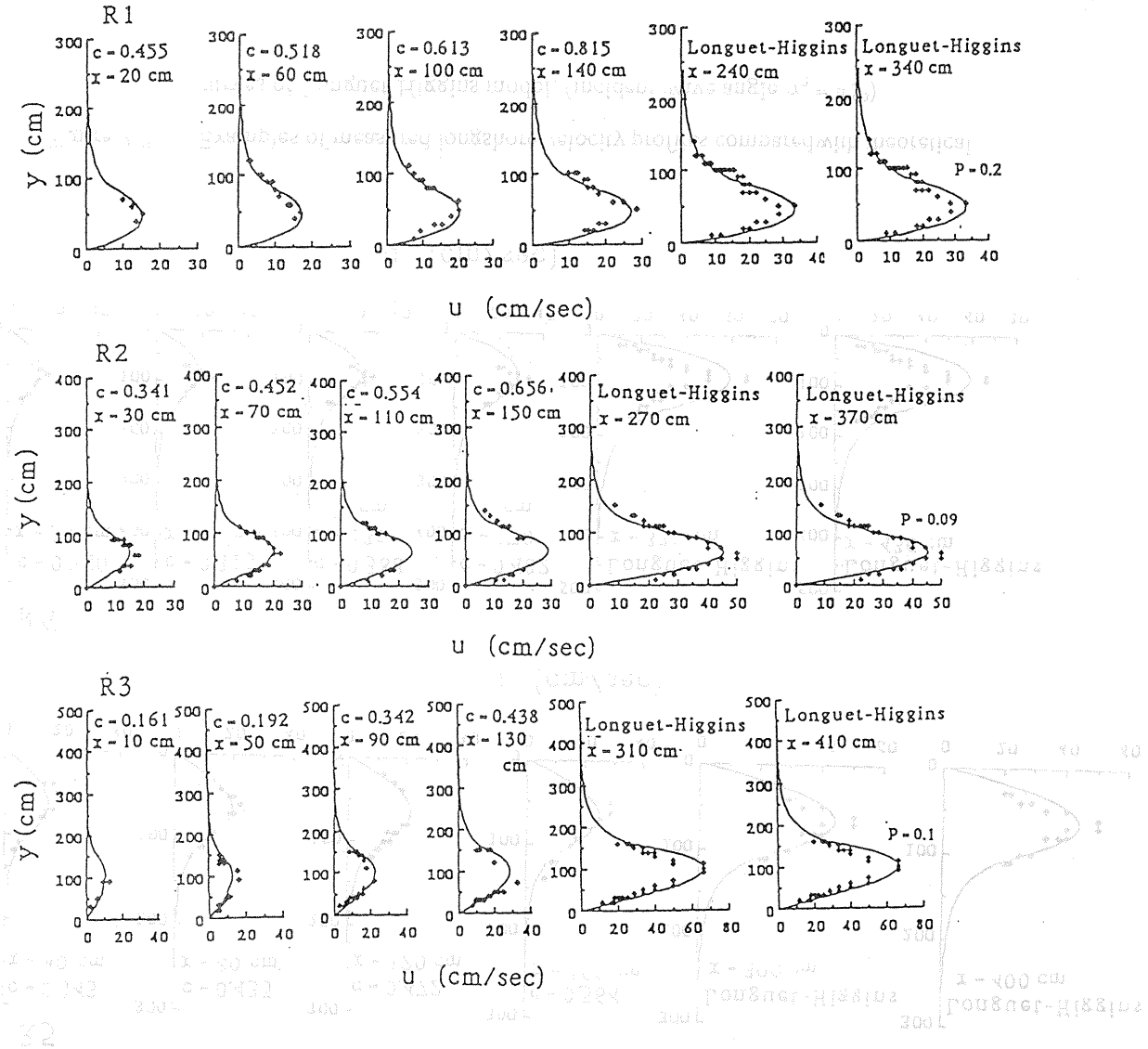

Figure 2.6 Examples of measured longshore velocity profiles comparedwith theoretical curves of Longuet-Higgins model, (incident wave angle α_0 =17°).

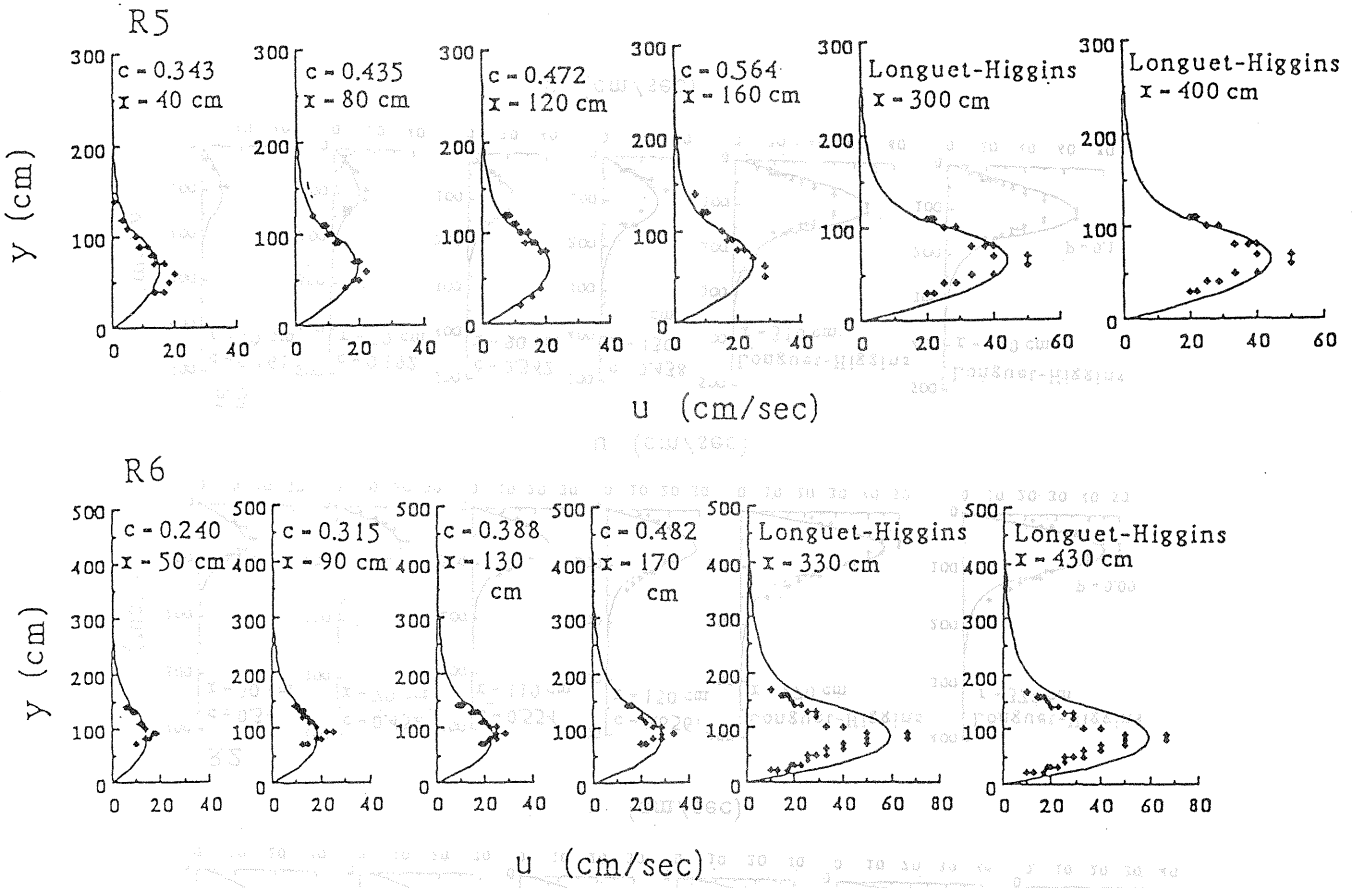

Figure 2.7 Examples of measured longshore velocity profiles comparedwith theoretical curves of Longuet-Higgins model, (incident wave angle $\alpha_0 = 45^o$).

(2) For a small angle of incident, the agreement between the measured velocities and Longuet-Higgins curve is good. While in the case of large angle of incident, the agreement is less.

The development of non-uniform longshore current velocity at the breaker line is shown in Figure 2.8, where the longshore distance is normalized by Eagleson's factor B expressed as:

$$B = \frac{2}{5}\left[\frac{C_f'}{h_b \cos\beta \sin\alpha_b}\right] \tag{2.56}$$

where, h_b is the breaker depth, α_b the breaking wave angle, β the beach slope, and C_f' is the Darcy–Weisbach friction coefficients. The longshore current velocity increases rapidly from zero to a constant value which corresponds to the uniform longshore current velocity. The measured longshore current velocities clearly show the tendency of non-uniform longshore currents.

(2) Uniformity of wave set-up

Figures 2.9(a) and 2.9(b) illustrate the distribution of measured wave height for Run 2 and the mean water level for Run 3 over the entire fixed bed area. In these figures the horizontal axis represents the cross-shore direction, while the longshore direction represented by the third axis. The uniformity of wave height and wave set-up alongshore are clearly seen in these figures. Figure 2.10 shows the cross-shore measurements of wave field for Run 2. The lower part of the figure shows the measured wave height computed with the calculated one by linear wave theory. In the experiments, the breaking wave is plunging type, this means that the wave height continues increases up to the breaker point. The effect of nonlinearity is so small, so that the measured values fit the calculated one well. The upper part of the figure shows the changes in the mean water level presented by waves. Bowen's formula (1968) for wave set-down was used to fit the measured data. It's clear from this figure that the wave set-up increases linearly toward the shoreline. Therefore we can conclude from Figures 2.9 and 2.10, that the wave set-up is uniform alongshore and

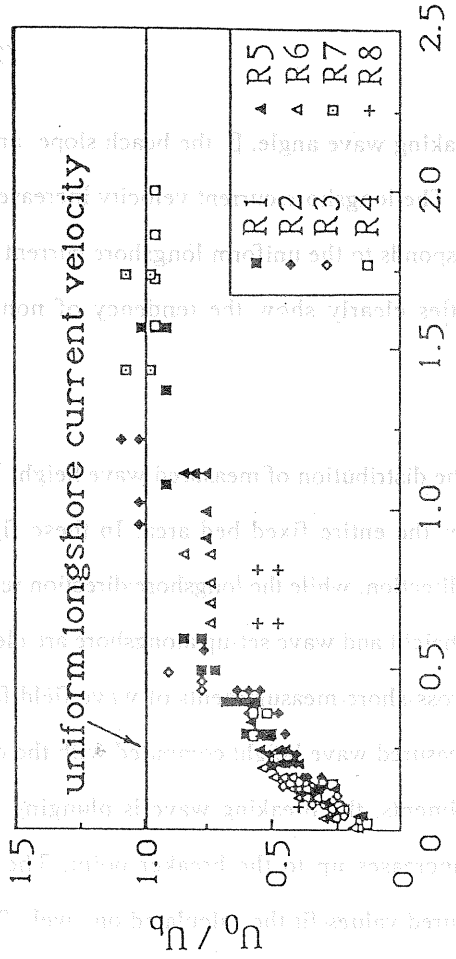

Figure 2.8 Development of non-uniform longshore current velocity.

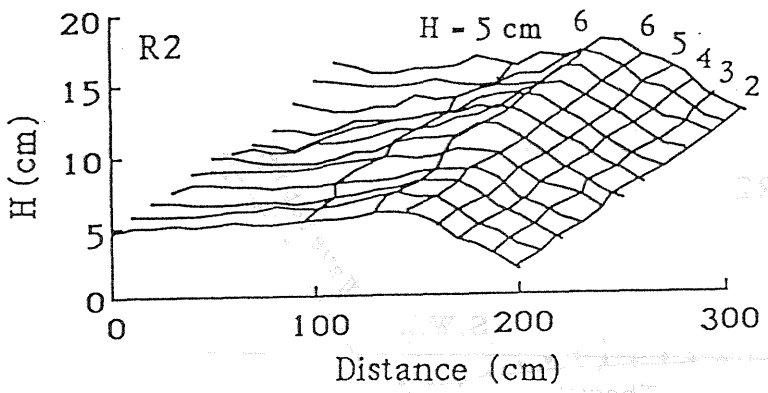

(a) Distribution of measured wave height (Run2).

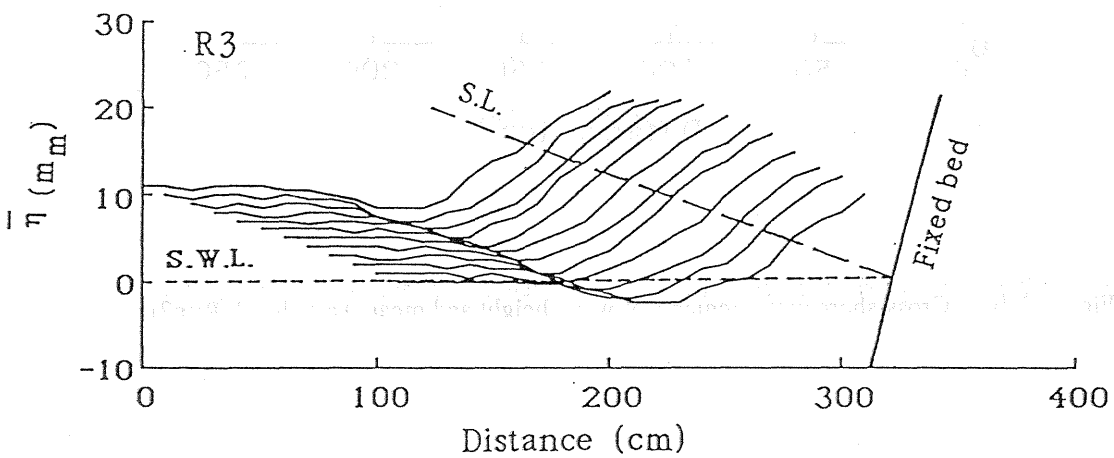

(b) Distribution of measured mean water level (Run3).

Figure 2.9 Distribution of measured wave height and mean water level over the entire fixed bed area.

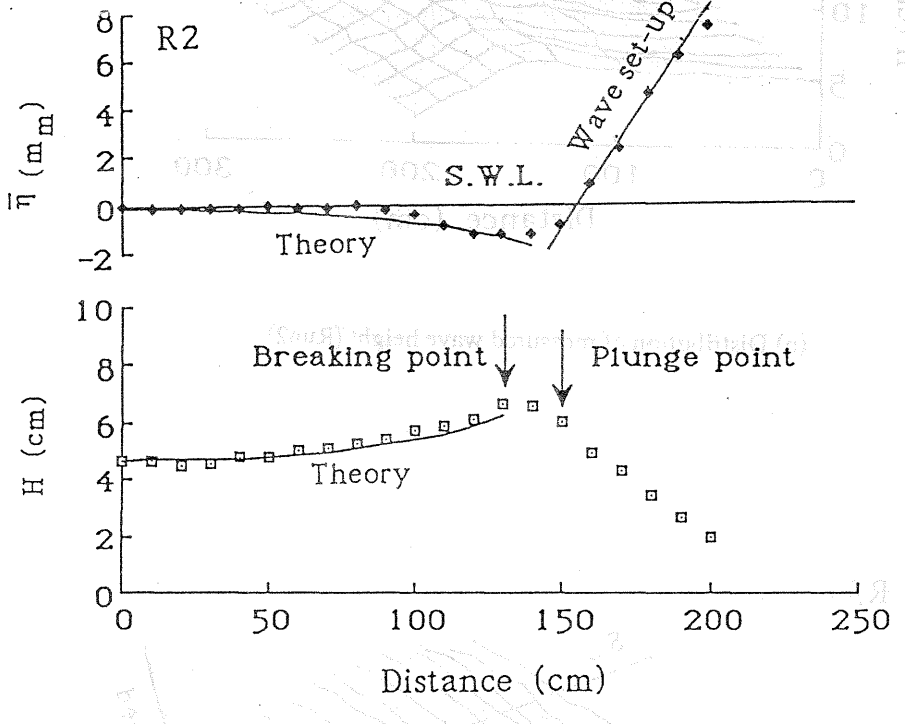

Figure 2.10 Cross-shore measurements of wave height and mean water level (Run2).

increases linearly toward the shoreline.

Figure 2.11 illustrates the variation of the measured wave set-up along the shoreline. The measured values used in this figure are 20 cm from the initial shoreline because the limitation of measurements at this region. But, fortunately, the wave set-up increases linearly, thus we can use this value instead of the maximum wave set-up value. In this figure Run 2 shows the maximum variation of wave set-up which is less than 7%, other cases are much smaller. Therefore, we may conclude that the wave set-up is uniform alongshore. Furthermore, it's well known that wave set-up is a function of breaker index, H_b/h_b. Figure 2.12 demonstrates the uniformity of breaker index, H_b/h_b, along the shoreline, therefore Bakker's formula can be used to estimate wave set-up along the shoreline. In this figure, the value of the breaker index, H_b/h_b, is laid between 0.8 and 1.0.

2.5 Comparison with Experimental Data

In the previous section, series of experiments on longshore currents were carried out. The main purpose of these experiments was to examine the applicability of the boundary layer assumptions, by studying the phenomenon of non-uniform longshore currents generated by regular waves. An example of the measured longshore velocity compared with the theoretical curve of Longuet-Higgins (1972) is shown in Figure 2.6. The degree of agreement between measured and computed longshore current profiles is influenced by the choice of Longuet-Higgins parameter P. The curves were fitted to the data by using the method of least square. It is noted that for all experiments Longuet-Higgins parameter P is less than 0.2. The similarity of velocity profiles is very satisfactory. Therefore, the coefficients of integration in Eq. (2.48) are dependent of the predicted shape of the velocity profiles and the local depth ratio, h/h_b. The comparison between the experimental measurements of non-uniform longshore currents and the theoretical curve given by Eq. (2.52) for boundary condition at x=0, $\bar{U}_0=0$, is shown in Figure 2.13. Each plot in the figure

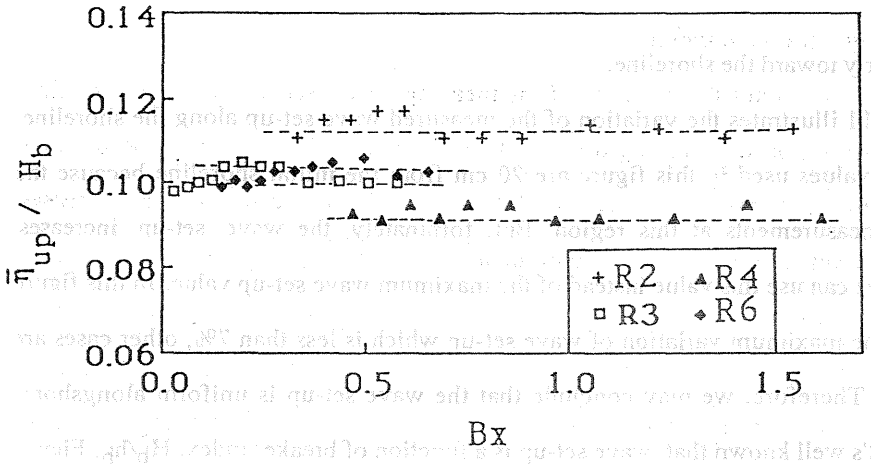

Figure 2.11 Longshore variation of measured wave set-up, normalized by breaking wave height, H_b.

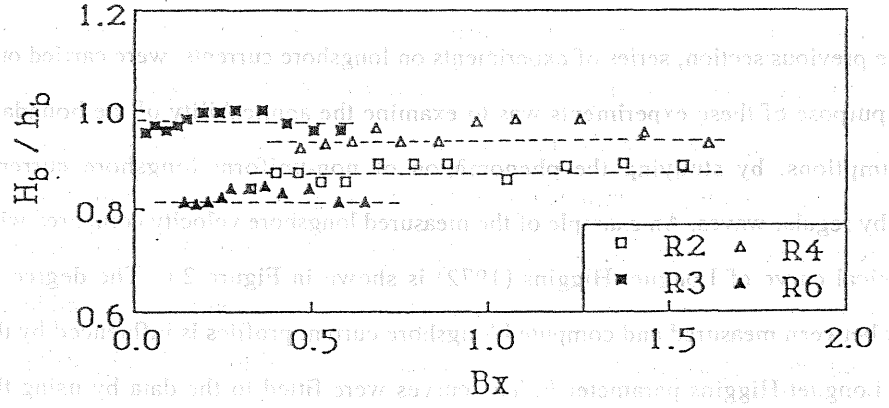

Figure 2.12 Longshore variation of measured breaker index, H_b / h_b.

is identified by the plotting symbol corresponding to each run in the experimental measurements. It is seen that most of the points lie around the theoretical curve derived by Eq. (2.52). The theoretical curve given by Eagleson (1965) is also shown in Figure 2.13 for a comparison. The longshore current velocity increases rapidly from zero, at the initial condition, to a constant value which corresponds to the uniform longshore current.

From Figures 2.6 and 2.13, It can be pointed out that the shape of the velocity profile starts to grow near the initial condition and increases rapidly, upcoast of the structure reaching a constant shape which represents the velocity profile of the uniform longshore currents. Therefore, the theoretical curve given by Eq. (2.52) describes not only the non-uniform longshore velocity at the breaker line but also at any given relative local depth ratio, h / h_b. Consequently, the phenomenon of non-uniform longshore currents can be described analytically by solving Eq. (2.48) with the given boundary conditions and with the estimation of the integration coefficients by the aid of similarity of velocity profiles.

2.6 Rate of Longshore Sediment Transport

The process of longshore sediment transport in coastal area is extremely complex. Breaking and reforming waves, changes in space and time, the generate of a three-dimensional turbulence field, all these acting over an irregular and constantly changing bottom topography.In addition to the complexity of this picture there are also other parameters of major importance for the longshore sediment transport such as grain size, beach slope, or bed roughness. A complete theoretical description of all these parameters is for beyond the present literature. Instead, simplified models have to be used. Among the several formulas for the longshore sediment transport rate there are three basic approaches which are distinguished; the wave power approach, the energetic model approach, and the bottom shear stress (or mass flux) approach. A brief discussion on these three approaches is given below, in which it is restricted to the general relationships describing each approach.

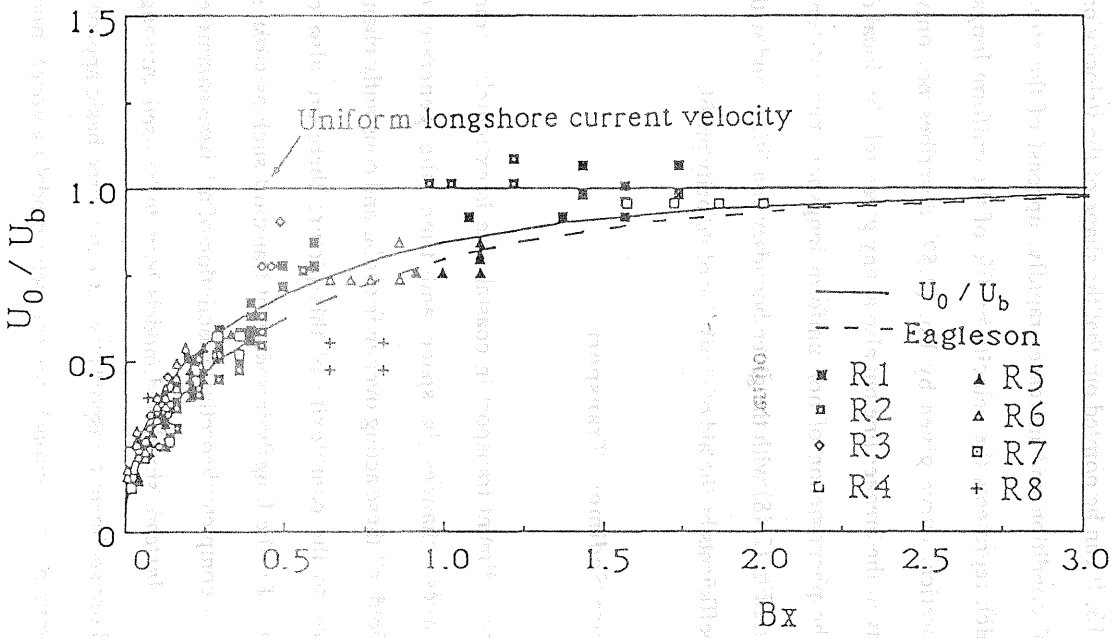

Figure 2.13 Comparison of measured and computed non-uniform longshore current velocity.

2.6.1 Wave power approach

Numerous investigations have been attempted to correlate the longshore sediment transport rate Q_x to the longshore component of the incoming wave energy flux P_l (e.g.Caldwell, 1965; Manohar, 1962). The first dimensionally correct expression was presented by Inman and Bagnold (1963):

$$Q_x = \frac{k' P_l}{(\sigma - \rho) g (1 - \lambda)} \tag{2.57}$$

where k' is a non-dimensional proportionality constant, σ and ρ the densities of the sediment and water, g is the acceleration of gravity, and λ is the sediment porosity. The longshore component of wave energy flux (wave power) P_l is written as:

$$P_l = (E c_g)_b \sin\alpha_b \cos\alpha_b \tag{2.58}$$

where E is the wave energy, c_g the group velocity, α the angle of wave crests to the shoreline, and the subscript b denotes the breaking condition. Longuet-Higgins (1971) has objected to the terminology for P_l. He showed that P_l is incorrect and has no physical meaning since scaler quantities, such as power or energy, cannot have components. Bearing this in mind, but still finding the terminology illustrative and consistent with many other studies. Equations (2.57) and (2.58) form together what is commonly known as the CERC formula (Shore Protection Manual, 1984) for which k' is set to 0.77. In the literature there have been, and still are, many discussions about the true of the CERC formula coefficient. Over the years, the recommended value of k' has been varied. More recently, Bailard (1985) and Kamphuis, Davies, Nairn and Sayao (1986) suggested that instead of being constant, k' is a function of parameters such as breaker angle, grain size, breaker index, H_b / h_b, and bottom slope. The CERC formula has several limitations. It does not explicitly take into account the effect of grain size, beach slope or bed roughness. In spite of this and although it is basically empirically derived, without any considerations of the mechanism of sediment transport, the CERC formula has been successfully applied in immeasurable engineering projects. In next section a trial is made to adapt the well known Komar's figure, in which the

relationship between the immersed-weight sediment transport rate and longshore component of wave power is computed with both field and laboratory data, by using a new formulation for the rate of longshore sediment transport.

2.6.2 Energetic model approach

Bagnold (1963) extended his concept of work performed by water in moving sediment particles to include wave effects. Here, the longshore sediment transport rate is assumed to depend on the combined effect of waves and currents. Once the sediment is in motion due to the waves, it becomes available for transport by longshore current velocity U. Then, the total immersed-weight transport rate can be expressed as:

$$I_l = k'' \, (E c_g \cos\alpha)_b \, \frac{U}{u_m} \qquad (2.59)$$

where k" is non-dimensional proportionally constant, and u_m is the maximum near-bottom orbital velocity at wave breaking. Komar and Inman (1970) found for several sets of data that K" is equal to 0.28. As opposed to CERC formula, Eq. (2.59) can be used when the longshore current velocity, U, is uniform or non-uniform. As shown by Gourlay (1982), it is possible to derive an expression for the longshore current velocity resulting from the effects of both breaking angle and a longshore gradient of breaking wave height. Equation (2.59) becomes identical to the CERC formula when the breaking wave angle is small and the longshore gradient of the breaking wave height is set to zero. This type of expression has recently been recognized as useful for application of the one-line theory of beach evolution, especially for beaches with coastal structures (Hanson and Kraus, 1986).

2.6.3 Bottom shear stress (mass flux) approach

In the bottom shear stress approach, the physical process of the mechanism of sediment transport is considered in more detail than the previous two approaches. Consequently, this

approach requires detailed knowledge about important physical parameters such as bottom shear stress under combined waves and current, bottom slope, grain size distribution, the reduction of wave height due to breaking, and estimation of the diffusion coefficients both in non-breaking and breaking fields. Bijker (1971) assumed that the mechanism of sediment movement is governed by the bottom shear stress alone. He combined the Kalinske-Frijlink bed load equation with the suspended load relation proposed by Einstein (1950) to get the total transport rate. Recently Tsuchiya and Yasuda (1979) proposed a new formulation of the total rate of longshore sediment transport based on the mass flux model, in which the longshore sediment transport is proportional to the averaged concentration of sediment and the longshore current velocity. This formula will be discussed in detail in next section where it is extended it to include the non-uniformity of longshore sediment transport. Also, the formula will be verified using field and laboratory data plotted in well known Komar's figure.

2.7 Non-uniform Longshore Sediment Transport

In the previous section three types of approaches to determine the longshore sediment transport rate were discussed. The first type, leading to the CERC formula, is purely empirical and has proved to give reasonable results in many coastal applications. Its major limitation is the inability to account for non-uniform longshore currents generated. The third type models the physical process of sediment transport in more detail that the other two. Unfortunately, the use of this technique in engineering applications is still beyond the state of considerable. However, as progress is being made, as in this section, this type of approach is believed to become more available for engineering use.

In general, sediment are transported downcoast by longshore currents through a to-and-fro motion even as they are undergoing sliding or saltation due to wave action. Einstein (1972) indicated that the motion of sediment transported by fluid can be expressed

universally by a formula for sediment load. Tsuchiya and Yasuda (1979) expressed the mechanism of longshore sediment transport as:

$$q_x = \bar{c}_0 \cdot h \cdot u \tag{2.60}$$

in which q_x is the rate of longshore sediment transport per unit width, u the longshore current velocity, and $\bar{c}_0$ the averaged concentration of sediment. The averaged concentration of sediment can be expressed (according to Tsuchiya and Kawata, 1971) as:

$$\bar{c}_0 = c_0 \left(\frac{\rho}{\sigma}\right)\left(1 - \frac{\tau^*_c}{\tau^*}\right) \tag{2.61}$$

in which c_0 is approximately equal to 0.2, although it varies slightly with the shields parameter τ^*, ρ/σ the specific gravity of sediment, and τ^*_c the critical value of shields parameter at the threshold of sediment movement. The shields parameter τ^* is defined as:

$$\tau^* = \frac{\tau/\rho}{(\sigma/\rho - 1)\, g\, D} \tag{2.62}$$

where

$$\tau/\rho = \frac{1}{2} f u_m^2 \tag{2.63}$$

in which f is the bottom friction coefficient, D is the sediment size, g is the acceleration of gravity, and u_m is the maximum near-bottom orbital velocity. The value for u_m can be expressed approximately by:

$$u_m = \begin{cases} \frac{1}{2}\gamma\sqrt{g\,h}\,; & 0 \le Y \le 1 \\ \frac{1}{2}\left(\frac{H}{H_0}\right)\left(\frac{L}{L_0}\right)\left(\frac{H_0 L_0}{T h}\right); & 1 \le Y < \infty \end{cases} \tag{2.64}$$

in which L is the wave length, H the wave height, T the wave period, h the water depth, $Y=y/y_b$, and the subscripts 0 and b refer to wave properties at the deep water limit and at the breaking, respectively. The substitution of Eqs. (2.61) to (2.64) into Eq. (2.60) leads to:

$$q_x = \begin{cases} c_0 \left(\frac{\rho}{\sigma}\right)\left(1 - F_r^2 \frac{h_b}{h}\right) h\, u & 0 \le Y \le 1 \\ c_0 \left(\frac{\rho}{\sigma}\right)\left(1 - R^2 F_r^2 \frac{h^2}{h_b^2}\right) h\, u & 1 \le Y < \infty \end{cases} \qquad (2.65)$$

where

$$R^2 = \frac{\gamma^2 \pi}{2} \left(\frac{H_0}{H}\right)^2 \left(\frac{L_0}{L}\right)^2 \left(\frac{h_b}{H_0}\right)^2 \left(\frac{h_b}{L_0}\right) \qquad (2.66)$$

and

$$F_r^2 = \frac{8}{\gamma^2} \frac{u_c^{*2}}{f\, g\, h_b} \qquad (2.67)$$

in which R^2 represents a function of wave characteristics and F_r^2 represents a square of Froude number of threshold of sediment movement. In order to integrate q_x over the domain of sediment drift in the cross-shore direction it is necessary to specify the cross-shore distribution of longshore current velocity. For this purpose, the Longuet-Higgins (1972) equation for longshore current is used. Now, the total rate of non-uniform longshore sediment transport is derived by integrating Eq. (2.65) over the domain of sediment drift while applying the non-uniform longshore current velocity U_0 given in section 2.3, as:

$$Q_x = \frac{c_0}{m} \left(\frac{\rho}{\sigma}\right) I(R, F_r)\, h_b^2\, U_0 \qquad (2.68)$$

where

$$I(R, F_r) = a_0 - b_0 F_r^2 - d_0 (RF_r)^{e_0} + d_0 (RF_r)^2 \qquad (2.69)$$

in which $a_0 = 0.298$, $b_0 = 0.124$, $d_0 = 0.373$, and $e_0 = 1.11$ when $P = 0.2$.

Figure 2.14 illustrates the change in $I(R, F_r)$ versus F_r^2 and R^2 when Longuet-Higgins parameter P is set to 0.2. It is obvious form this figure that; 1) For a small value of F_r^2 the function $I(R, F_r)$ becomes nearly constant say 0.3, and 2) The function $I(R, F_r)$ decreases with increasing F_r^2, it becomes very small when F_r^2 reaches 1.0. Consequently, in

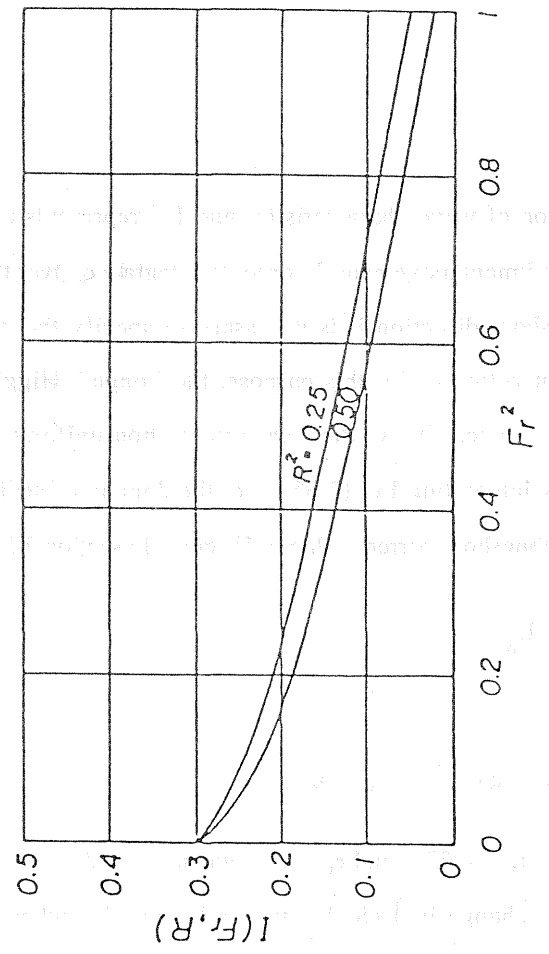

Figure 2.14 Change in $I(R,F_r)$ with the parameter R and F_r (after Tsuchiya, 1982).

the field coast the function $I(R, F_r)$ is nearly constant because of the parameter F_r^2 includes the ratio of sediment size to break water depth, which is very small. On the other hand, in laboratory experiment, the ratio of sediment size to break water depth becomes much larger than the one in field coast, and therefore the function $I(R,F_r)$ becomes much affectable by the ratio of sediment size to break water depth as well as the characteristics of waves and sediment.

Now we consider the empirical relationship for the total rate of longshore sediment transport derived by wave power approach, which known as the CERC formula and the well known figure prepared by Komar and Inman (1970), which shows the verification of CERC formula with both of field data and laboratory data. In their figure, the laboratory data are plotted considerably below the CERC formula which fits the field data well.

Tsuchiya and Yasuda (1979) followed the same derivation steps, but they used Longuet-Higgins expression for uniform longshore currents. Their formula can be derived from Eq. (2.48) by neglecting the non-uniform terms. Their formula for total rates of uniform longshore sediment transport, Q_m, is expressed by:

$$Q_m = C\left(\frac{\rho}{\sigma}\right) I(R, F_r)\, h_b^2 \sqrt{g h_b}\, \sin 2\alpha_b \qquad (2.70)$$

in which $$C = \frac{5\pi}{32} \frac{c_0 \gamma}{f} \qquad (2.71)$$

Equation (2.70) shows that the total rate of longshore sediment transport is proportional to the longshore component of wave energy flux (wave power) and the function $I(R,F_r)$. In field, the function $I(R,Fr)$ is nearly constant, therefore the total rate of longshore sediment transport will be directly proportional to the longshore component of wave power, and the formula given by Eq. (2.70) will be equivalent to the empirical CERC formula derived by wave power approach. Equation (2.70) can be expressed as an immersed-weight rate, I_m, as:

$$I_m = (\sigma - \rho) g (1 - \lambda) Q_m = k''' I(R,F_r) (E\ c_g \sin\alpha \cos\alpha)_b \qquad (2.72)$$

where k''' is a non-dimensional proportionality constant. In the field, this constant multiplied

by the value of the function $I(R,F_r)$ will be equivalent to the CERC proportionality constant, which is set to 0.77, the situation mathematically expressed as:

$$k'' I(R,F_r)_f = k' = 0.77 \qquad (2.73)$$

in which $I(R,F_r)_f$ represents the value of the function at the field coasts. Substitution of Eq. (2.73) into Eq. (2.72), gives:

$$I_m = (\sigma-\rho) g (1-\lambda) Q_m = k' \frac{I(R,F_r)}{I(R,F_r)_f} (E c_g \sin\alpha \cos\alpha)_b \qquad (2.74)$$

The new expression proposed by Eq. (2.74) takes into account the effects of grain size, beach slope, and bed roughness. Equation (2.74) implies that in the field, the expression will be similar to the CERC formula. This formula will be verified with field and laboratory data presented in the well known Komar's figure in next section. Equation (2.70) can be rewritten using uniform longshore current velocity U_b and breaker water depth h_b as:

$$Q_m = \frac{c_0}{m} \left(\frac{\rho}{\sigma}\right) I(R,F_r) h_b^2 U_b \qquad (2.75)$$

The comparison between Eq. (2.68) for non-uniform longshore sediment transport and Eq. (2.75) for uniform longshore sediment transport shows that both the equations are similar in every term except for the longshore current velocity. For example, the function $I(R, F_r)$ will have the same values in uniform and non-uniform longshore sediment transport, this can be explained by the function $I(R, F_r)$ which is proportional to velocity profiles, or the Longuet-Higgins parameter P. Moreover, the similarity of velocity profiles has been previously verified. Thus, the function $I(R, F_r)$ will not be affected whether the longshore current velocity is uniform or non-uniform. Therefore, the total rate of longshore sediment transport will be directly proportional to the longshore current velocity, mathematically expressed as:

$$\frac{Q_x}{Q_m} = \frac{U_0}{U_b} \qquad (2.76)$$

2.8 Verification of Longshore Sediment Transport Formula

The judgment of validity of any formula is its ability to be applied to laboratory and field studies. For that purpose, the laboratory and field data used in Komar's figure have been recalculated with using the new formulation for the immersed-weight transport rate given by Eq. (2.74), in which the function $\mathrm{I}(R, F_r)$ plays an essential part in the verification. A complete description with a more comprehensive presentation of field and laboratory data used in this verification is found in Das (1971). From Das's report, both the immersed-weight transport rate and the longshore component of wave power for the field and laboratory data are recalculated using the new formula expressed by Eq. (2.74). The results are plotted in Figure 2.15. In comparing of Figure 2.15(b) with Komar's figure (Figure 2.15(a)) it can observe that the laboratory data are sifted and the agreement between the new formula and the data is much better. The results imply that by using the new formula, Eq. (2.74), the empirical CERC formula could be modified to include the function $\mathrm{I}(R,F_r)$ which takes into account the effect of sediment size, beach slope and bed roughness.

2.9 Conclusions

The process of longshore sediment transport in coastal zone was investigated. A new equation of non-uniform longshore currents was derived based on the the applying the concept of the boundary layer theory to the nearshore current equations. The applicability of the assumptions of the boundary layer which are the velocity profiles in non-uniform longshore currents are similar and the wave set-up is uniform in the longshore direction, was examined by performing an experimental study. The experimental results reveal that the similarity of the velocity profiles is very satisfactory. Therefore the integration coefficients appeared in the new equation of non-uniform longshore currents are not functions of longshore direction nor time. Moreover, the maximum longshore variation of wave set-up

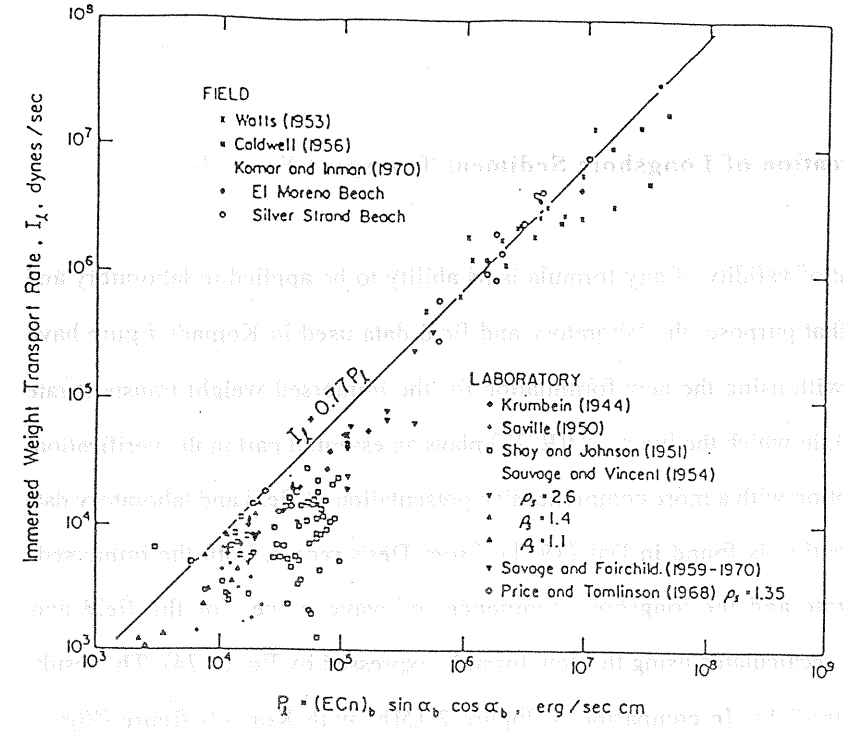

(a) Before introducing the function $I(R,F_r)$, (after Komar, 1977).

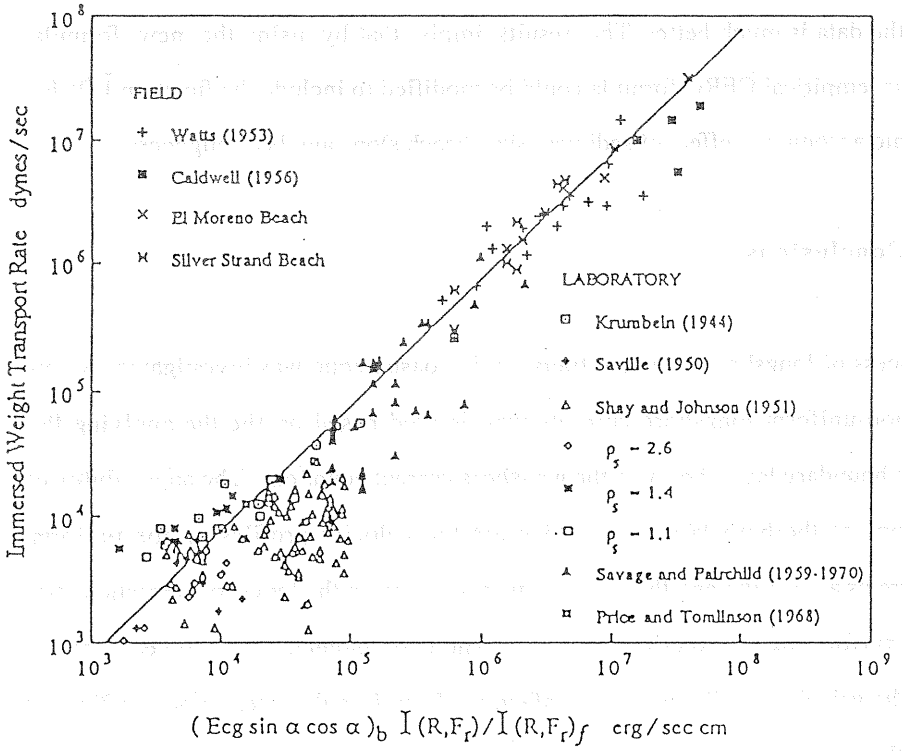

(b) After introducing the function $I(R,F_r)$.

Figure 2.15 Total immersed weight rate of longshore sediment transport as function of wave energy flux and $I(R,F_r)$.

was (more or less) small and wave set-up increases linearly shoreward.

From the comparison of the new equation of non-uniform longshore currents with the experimental data, it is observed that the degree of agreement between measured and computed longshore current profiles is influenced by the choice of Longuet-Higgins parameter P. The shape of the velocity distribution starts to grow from the initial boundary until reaching a constant shape which represents uniform velocity profile. Therefore the theoretical curve given by the new equation of non-uniform longshore currents describes not only the non-uniform longshore velocity at the breaker line but also at any given relative local depth ratio, h/h_b. Consequently, the phenomenon of non-uniform longshore currents can be described analytically by solving the new equation with the initial and boundary conditions and with estimation of the integration coefficients by the aid of similarity of velocity profiles.

A new formula for estimating of the total rate of longshore sediment transport was derived based on the formula of Tsuchiya and Yasuda (1979). This formula includes the effect of sediment size, beach slope and bed roughness. The verification of the new formulation of non-uniform longshore sediment transport rate was made using the field and laboratory data plotted in the well known Komar's figure. The result of the verification reveals that the function $I\,(R, F_r)$ plays an essential role in the verification. The laboratory data have been rearranged using the new formula, as a result the agreement between the new formula and the data is much better. Furthermore, the empirical CERC formula can be modified to include the function $I\,(R, F_r)$ which takes into account the effect of sediment size, beach slope and bed roughness.

REFERENCES

Bagnold, R.A., 1963," Mechanics of Marine Sedimentation," The Sea, edited by M.N. Hill, Vol. 3, Interscience, New York, pp. 507-528.

Bailard, J.A., 1985," A Simplified Model for Longshore Sediment Transport," Proc. 19th

Coast. Eng. Conf., ASCE, pp. 1454-1470.

Bijker, E.W., 1971," Longshore Transport Computation," Jour. of the Waterways, Harbors and Coastal Engineering Division, Vol. 97, No. ww4, pp. 687-701.

Bowen, A.J., Inman, D.L. and Simmons, V.P., 1968," Wave Set-down and Set-up," Journal of Geophysical Research, Vol. 73, No. 8, pp. 2569-2577.

Caldwell, J.W., 1965," Wave Action and Sand Movement near Anaheim Bay, California," Technical Memorandum, US Army Corps of Engineers, Beach Erosion Board, 21 pp.

Das, M.M., 1971," Longshore Sediment Transport Rate: A Compilation of Data," Miscellaneous paper No. 1-17, US Army Corps of Engineers, Coastal Engineering Research Center, 75 pp.

Eagleson, P.S., 1965," Theoretical Study of Longshore Currents on a Plane Beach," Report R65-28, Massachusetts Institute of Technology, Department of Civil Engineering, Cambridge, Mass.

Einstein, H.A., 1950," The Bed-load Function for Sediment Transportation in Open Channel Flow," Technical Bulletin No. 1026, US Department of Agriculture, Soil Conservation Service.

Einstein, H.A., 1972," Sediment Transport by Wave Action," Proc. 13th Coast. Eng. Conf., ASCE, pp. 933-952.

Gourlay, M.R., 1976," Non-uniform Alongshore Currents," Proc. 15th Conf.on Coastal Eng., ASCE, Vol. 1, pp. 701-720.

Gourlay, M.R., 1982," Nonuniform Alongshore Currents and Sediment Transport - a One Dimensional Approach," Research Report No. CE31, Department of Civil Eng., Univ. of Queensland, Australia, 67 pp.

Hanson, H. and Kraus, N.C., 1986," Seawalls Boundary Condition in Numerical Models of Shoreline Change," Technical Report CERC-86-3, US Army Engineer Waterways Experiment Station, Coastal Engineering Research Center, 59 pp.

Horikawa, S. and Sasaki, T., 1968," Some Studies on Longshore Currents Velocity," Proc. 18th Japanese Conf. on Coastal Eng., JSCE, pp. 126-135 (in Japanese).

Inman, D.L. and Bagnold, R.A., 1963," Littoral Processes," The Sea, edited by M.N. Hill, Vol. 3, Interscience, New York, pp. 529-553.

James, I.D., 1974," A Non-linear Theory of Longshore Currents," Estuarine and Coastal Marine Science, Vol. 2, pp. 235-249.

Kamphuis, J.W., Davies, M.H., Nairn, R.B. and Sayao, O.J., 1986," Calculation of Littoral Sand Transport Rate," Jour. of Coastal Eng., ASCE, Vol. 10, pp. 1-21.

Komar, P.D. and Inman, D.L., 1970," Longshore Sand Transport on Beaches," Jour. of Geophysical Research, Vol. 73, No. 30, pp. 5914-5927.

Kraus, N.C. and Sasaki, T.O., 1979," Effect of Wave angle and Lateral Mixing on the Longshore Current," Coastal Engineering in Japan, Vol. 22, pp. 61-74.

Liu, P.L.-F and Dalrymple, R., 1978," Bottom Frictional Stresses and Longshore Currents due to Waves with large angles of incidence," Sears Foundation: Jour. of Marine Research, Vol. 36, No. 2, pp. 357-375.

Longuet-Higgins, M.S., 1972," Recent Progress in the Study of Longshore Currents," Waves on Beaches and Resulting Sediment Transport, R.E. Meyer, ed., 1st ed., Academic Press, Inc., New York, pp. 203-248.

Longuet-Higgins, M.S., and Stewart, R.W., 1964," Radiation Stress in Water Waves; a Physical Discussion with Applications," Deep-Sea Research, Oxford, England, Vol. 11, No. 4, pp. 529-562.

Manohar, M., 1962," Laboratory Determination of Littoral Transport Rate," Jour. of the Waterways, Harbors, and Coastal Eng. Division, Vol. 88, No. ww4, pp. 144-147.

Mei, C.C., 1983," The Applied Dynamics of Ocean Surface Waves," John Wiley & Sons, Inc.

Motyka, J.M. and Willis, D.H., 1975," Alongshore Sediment Transport due to Variation in Wave Height," UK Department of Environment, Hydraulics Research Station, HRS

Notes 17, pp. 6-7.

Ozasa, H. and Brampton, A.H., 1980," Mathematical Modeling of Beaches Backed by Seawalls," Jour. of Coastal Engineering, Vol. 4, No. 1, pp. 47-64.

Phillips, O.M., 1977," The Dynamics of the Upper Ocean," Cambridge University press, Cambridge, Mass., 2nd ed.

Schlichting, H., 1960," Boundary Layer Theory," Translated by J. Kestin, 4st ed., McGrow-Hill, Inc., New York.

Shore Protection Manual, 1984, 4th ed., 2 Vols., US Army Engineer Waterways Experiment Station, Coastal Engineering Research Center, US Government Printing Office, Washington, DC.

Tsuchiya, Y. and Kawata, Y., 1971," The Rate of Sediment Transport by Mechanics of Saltation," Proc. 15th Japanese Conf. on Hydraulics, JSCE, pp. 7-12 (in Japanese).

Tsuchiya, Y., Kawata, Y. and Refaat, H., 1989," Similarity of Velocity Profiles in Non-uniform Longshore Currents," Proc. 35th Japanese Conf. on Coastal Eng., pp. 234-238 (in Japanese).

Tsuchiya, Y. and Yasuda, T., 1979," A Mathematical Model for Beach Change," Proc. 25th Japanese Conf. on Coastal Eng., JSCE, pp. 36-40 (in Japanese).

Thornton, E.B. and Guza, R.T., 1986," Surf Zone Longshore Currents and Random Waves: Field data and Models," Jour. of Physical Oceanography, American Meteorological Society, Vol. 16, pp. 1165-1178.

Visser, P.J., 1984," Uniform Longshore Current Measurements and Calculations," Proc. 19th Coastal Eng. Conf., ASCE, pp. 2192-2207.

Vreugdenhil, C.B., 1980," A Method of Computation for Unsteady Wave-Driven Coastal Currents," Report No. 1174, Pt. 1, Delft Hydraulic Laboratory, Delft, The Netherlands.

Chapter 3 FORMATION PROCESS OF RIVER DELTAS

3.1 Introduction

In view of the variability of modern deltas, a single delta model is no longer adequate. Instead a series of models is required and several schemes have been proposed, based primarily on the physical processes operative within the delta (Galloway, 1975). Based on Galloway's classification , the river deltas are categorized as:

(1) River-dominated type; in which the river discharge is predominant and wave energy is minimal. The characteristics of delta of this type are mainly governed by the river region, the wave action is nearly negligible, as such as prevails along the coast of the Mississippi delta.

(2) Wave-dominated type; which represents higher wave energy situations, where powerful waves have slowed down the advance of the delta and redistributed the river sediments such that the delta plane takes on a smooth and gentle shape. This type of delta can be observed along the coast of the Senegal delta.

(3) Tidal-dominated type; where the oceanic tidal currents are impinging on coastal waters near river deltas cause river discharged sediments to be transported and dispersed along the coast at considerable distances from the river mouth. In a few instances, unidirectional tidal currents may be as swift as the river outflow itself. Probably the most prominent example of a delta influenced by strong tidal currents is the Ord river of Western Australia, in which the spring tide rang of about 5.9 m sweeps the delta and reveals flood and ebbs currents in excess of 3 m/s (Wright, Coleman and Ericson, 1974).

Based on the data collected by Coleman and Roberts (1987) presented in Chapter 1, Figures 1.1, 1.2, and 1.3, and a ternary diagram proposed by Wright (1985) and by Galloway (1975), a modified version of a scheme proposed by Galloway (1975) is adapted. This scheme is shown in Figure 3.1, in which a ternary diagram is used to define general regions of river-, wave- and tidal-dominated deltas. Applying the scheme the positions of individual deltas are plotted qualitatively, in which it can be seen that the Mississippi delta is the most river-dominated type, whereas the Ord delta is the most tidal-dominated type and the Senegal delta is the most wave-dominated type. Although the definition of these parameters are not restrictive, they are helpful in qualitatively understanding the delta classification.

In this chapter, firstly, the physical description of the river delta formation is presented by investigating two field cases; the Nile Delta coast in Egypt and the major river deltas in Lake Biwa, Japan. The fundamental of the physical description will include the study of the history of the set and shoreline changes, the sediment characteristics, and wave climate conditions.

Secondly, a brief description of the fundamental of the one-line theory will be discussed following by an overview of the previous analytical work related to the theory. Thirdly, by employing the one-line theory associated with the formula of non-uniform longshore sediment transport rate, presented in Chapter 2, several analytical solutions for evolution of shoreline of river deltas will be derived under various boundary conditions.

Fourthly, an experimental study was carried out. The main objectives of this work are, to demonstrate the process of formation of river deltas, to declare the change of the beach profiles along the shoreline of the delta, to verify the relationship between shoreline change and cross- sectional area of beach profiles, and finally to study the effect of oblique wave incident on the symmetry of river delta configuration and on the process of formation of river deltas. Finally, the application of the analytical solutions to experimental study and to river deltas in Lake Biwa will be discussed.

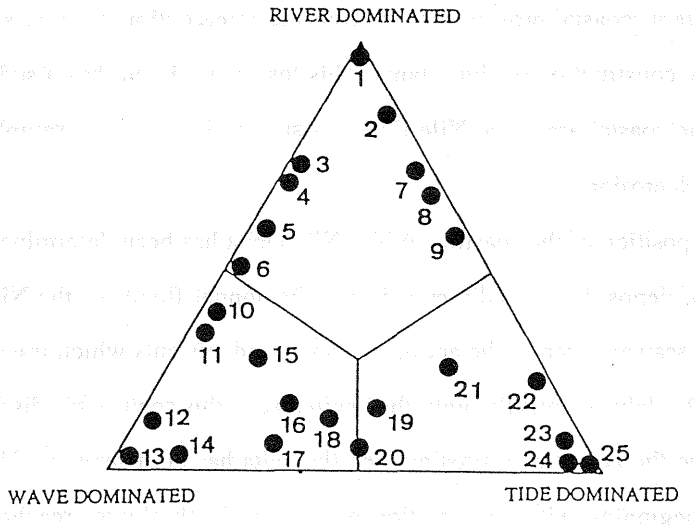

1. Mississippi ; 2. Shatt Al Arab ; 3. Po ; 4. Danube;
5. Jaba ; 6. Ebro ; 7. Irrawaddy ; 8. Huang ; 9. Mahakam ;
10. Nile ; 11. Rhone ; 12. Sao Francisco ; 13. Senegal ;
14. Shoal Haven ; 15. Orinoco ; 16. Indus ; 17. Burdekin ;
18. Niger ; 19. Mekong ; 20. Copper ; 21. Purari ; 22. Amazon ;
23. Ganges-Brahmaputra ; 24. Gulf of Papua ; 25. Ord.

Figure 3.1 Ternary diagram of delta types, based on the relative importance of river, wave, and tide processes and delta shape, (modified after Galloway, 1975; Wright, 1985).

3.2 Nile Delta Coast

Man's intervention in coastal processes takes many form, however, the most serious large scale and long term coastal erosion results from the interception of river sediment supply to the coast by construction of river dams. This loss of sediment has a sudden and disasters effects on the coastal area. The Nile Delta coast is an impressive example of the effect of dams on beach erosion.

Historically the position of the coastline of the Nile Delta has been determined by the relative importance of deposition of sediments during the annual floods of the Nile River which build the delta seaward, versus the action of waves and currents which transport the sediments and erode the delta. Generally, until the beginning of this century the discharge of sediment has exceeded the potential of erosion, and the delta has built seaward. However, man's intervention, beginning with construction of barriers in the lower reaches of the Rosetta and Damietta branches and with the construction of the Low Aswan Dam in 1902, changed the pattern to one of erosion, construction of the High Aswan Dam, which began filling in 1964, has resulted in a total absence of Nile river discharge as active sediment source for the delta. As a consequence, the action of waves and currents, which have remained undiminished, are in the process of eroding and changing the configuration of the coastline of the Nile Delta.

The present Nile Delta covers an onshore area of about 25,000 km^2 and an about equal offshore, down to the 200 m water depth. The coastline of the Nile Delta from Alexandria to Port Said is about 300 km long. The southern apex of the Delta is at 30° N, some 30 km north of Cairo, where the Nile River splits into the Rosette branch in western and Damietta branch in eastern (Figure 3.2).

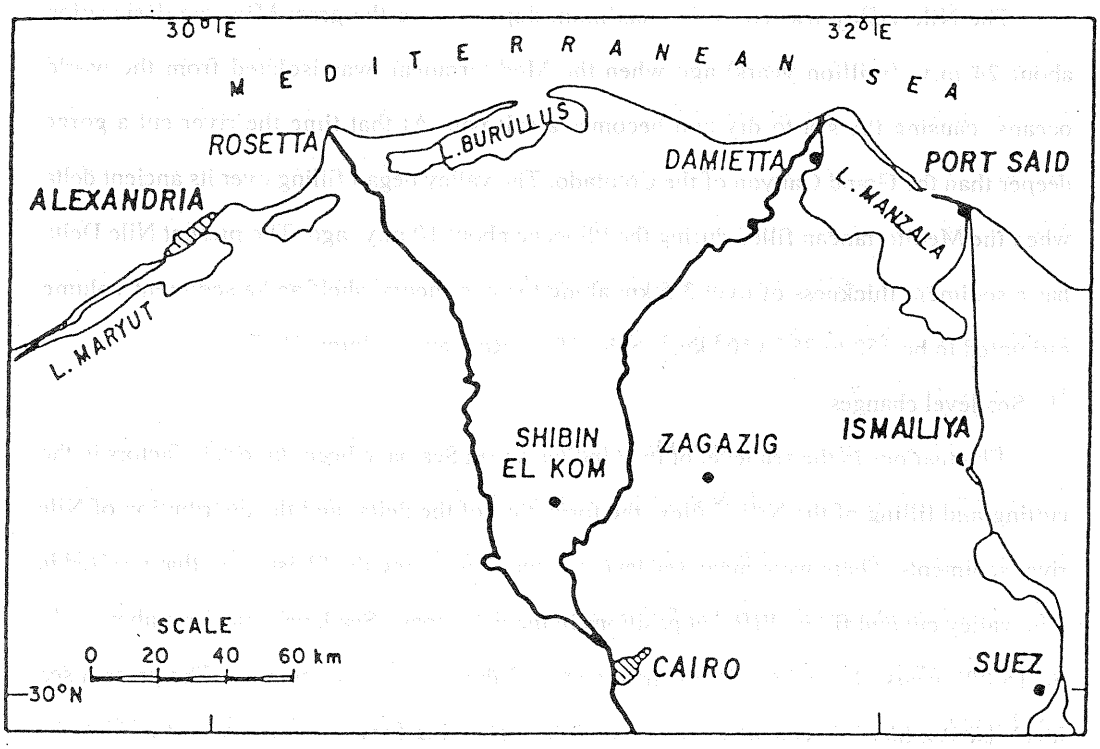

Figure 3.2 General plan of the Nile Delta.

3.2.1 History of Nile valley

The Nile valley was cut to its maximum depth during the great Miocene desiccation about 24 m.y. (million years) ago when the Mediterranean was isolated from the world oceans, causing the sea to dry and becomes a salt pan. At that time the river cut a gorge deeper than the Grand Ganyon of the Colorado. The valley began filling over its ancient delta when the Mediterranean filled during the Pliocene about 10 m.y. ago. The present Nile Delta has a sediment thickness of over 3.5 km along the continental shelf and a sediment volume estimated to be 350 to 387 $x10^3$ km^3 (Said, 1981; Ross and Uchupi, 1977).

(1) Sea level changes

Fluctuations in the sea level of the Mediterranean Sea have been important factors in the cutting and filling of the Nile Valley, the formation of the delta, and the distribution of Nile river sediments. There were many sea level fluctuations during the Pleistocene that resulted in Nile valley cut and fill in different positions in the delta coast. Sea level rose form about -140 m, 15,000 years ago and is still rising at a rate of about 15 cm per century. The present sea level rise is a factor in coastal erosion, possible accounting for a shoreline retreat of 10 to 15 m per century (Inman and Jenkins, 1984).

(2) Nile river discharges

The Nile river derives its water from the Lake Plateau of Tanzania and Kenya (White Nile) and from the Ethiopian highlands (Blue Nile). It has a drainage of about 3 x 10^6 km^2 and a length of 6,800 km. The Nile traverses 35 degrees of latitude in its long northerly flow from its source in Tanzania to the Mediterranean Sea. Before the construction of the High Aswan Dam, the river discharged annually 86 x 10^9 m^3 of water (Hurst, 1952; Said, 1981). The sediment supplied by the Nile River has been estimated to be about 88 to 120 x 10^6 ton/ yr, (Holeman, 1968). Some of this sediment have been transported to the coast by the prevailing waves and currents, while the remainder has been deposited as part of the delta formation.

Man's intervention in the flow of the Nile dates back at least to Pharaonic times when

Senusret had a canal built from the ancient Pelusiac branch of the Nile to the Red Sea (circa 1900 B.C.). Modern intervention began with construction of the Delta Barrage below Cairo in 1861. The barrage sluices opened to pass flood waters, of which about 70 percent flowed out the Rosetta mouth, and 30 percent through the Damietta. The barrage was the beginning of perennial intervention versus basin irrigation and the extensive use of Nile silts and clays as nutrients in agriculture. This intervention continued with the construction of Low Aswan Dam in 1902, up until the High Aswan Dam was completed in 1964, which trapped all of the sediment load.

Before 1861, probably most of the sediment was carried during the flood months, July through November, and deposited off the Mediterranean to form the delta of the Nile. The erosion of Rosette promontory which began about the turn of this century was probably in part due to a decreased of sediment supply caused by the present of Low Aswan Dam.

The flood months of the Nile River are usually taken as July, through November, with the maximum monthly discharge of about 17 and 21 x 10^9 m^3 during August and September respectively. However, measurements show that the rising phase of the flood in August carries the highest percentage of suspended load. A minimum water discharge of 1.5 x 10^9 m^3 occurs in May. The sediment transported by the Nile are made up of bed load and suspended load. The investigations carried out in the pre-High Dam period have shown that the bed load transport was only 1 to 2% of the total sediment transport. It accordingly became customary to consider the total sediment load equal to the suspended load, (Shahin, 1985).

Shahin (1985) investigated the suspended load measured during the flood season from 1928 to 1963. The main conclusions drawn from his investigation are as follows:

(1) 98% of the annual sediments are brought by the Nile during the flood season. The annual volume of sediments reaching Aswan to be about 125 x 10^6 tons.

(2) The percentages of clay, silt and sand fractions in the suspended load changes with time during the flood season. The monthly average percentage are shown in Table 3.1.

Table 3.1 Monthly average percentage of clay, silt and sand fractions in suspended load.

Month	Clay < 0.002 mm	Silt 0.002 - 0.02 mm	Sand 0.02 - 0.2 mm
August	35	45	20
September	30	45	25
October	30	45	25
November	35	35	30

3.2.2 Longshore sediment characteristics

The grain size of littoral sediments typically varies in the longshore direction. This variability is caused in part, by the influence of sediment source and by selective transport and selective deposition of specific fraction of the available sediment. The local sediment size, frequently characterized by the median diameter, d_{50}, is well correlated with the beach slope of the equilibrium beach profile of the Nile Delta as shown in Figure 3.3, which is an significant parameter in the classification of beach profiles. The fact that the coarser material is correlated with a steeper slope is clearly verified in this figure.

Mineralogical studies of coastal sediments from Alexandria eastward to Sinai show that the Nile River has been the source of sediment for beaches and coastal dunes. Fishawi, Fahmy, Sestinine and Shawki (1976) show in Figure 3.4 the average longshore grain size of the Nile Delta Coastline for the period 1973 to 1975. Also in this figure shown are the data from United Nations Development Program, UNDP, (1973), and the data from the 1980 sediment survey performed by Coastal Research Institute, CRI, Water Research Center, Ministry of Irrigation, Egypt (1980). Two distinct areas are apparent. The first is the area from Abou Quir Bay to the Gamasa-Ras El Bar, characterized by coarser sediments of 0.25 to 0.3 mm, and the second is the area east of the Damietta mouth where grain size is relatively constant at about 0.15 to 0.2 mm. From Figure 3.4 it is noted that the Fishawi, Fahmy, Sestinine and Shawki (1976) data show a minimum grain size in the vicinity of the distributary

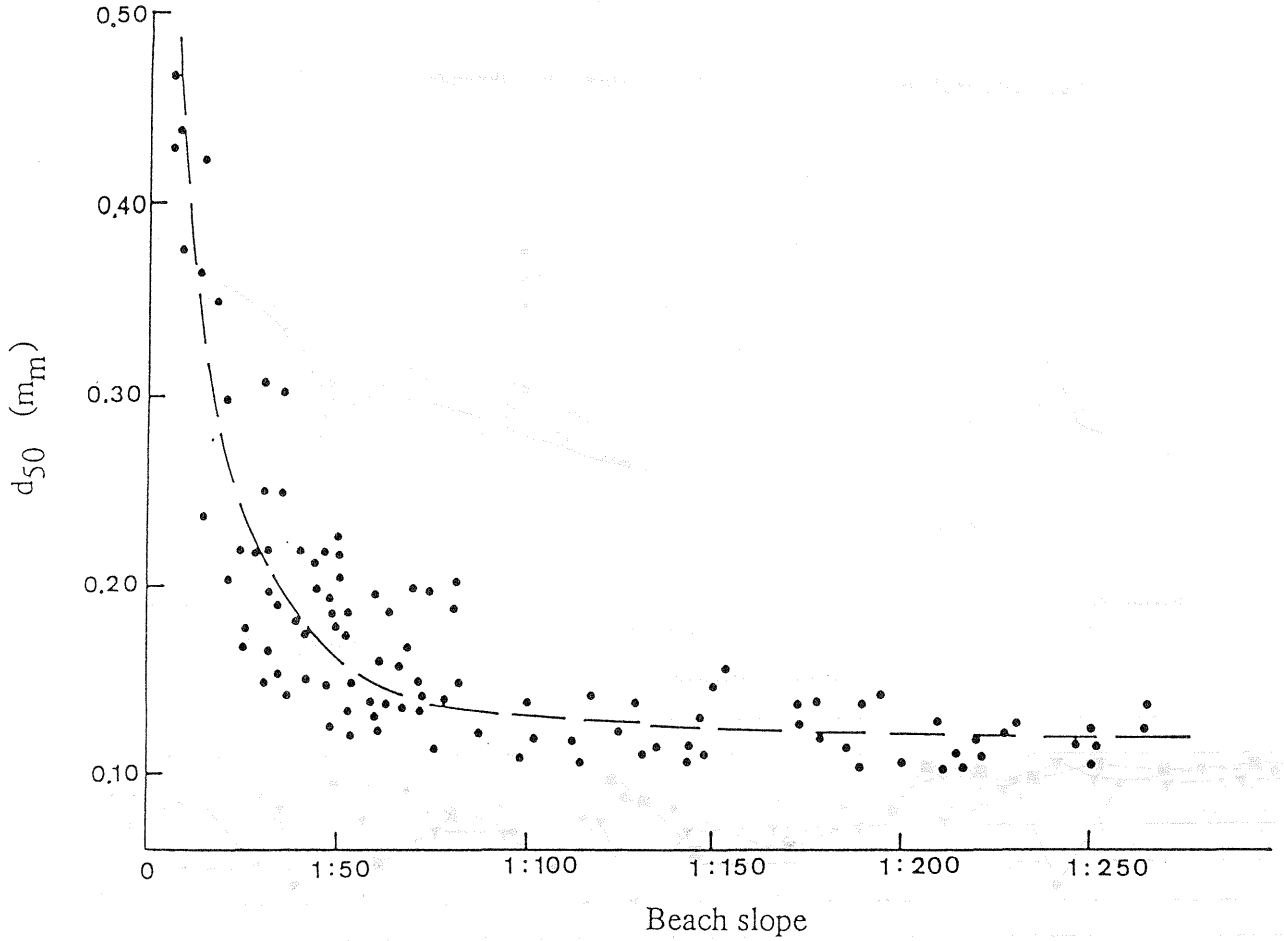

Figure 3.3 Relation between beach slope and sediment size of Nile Delta coast, (after Manohar, 1975).

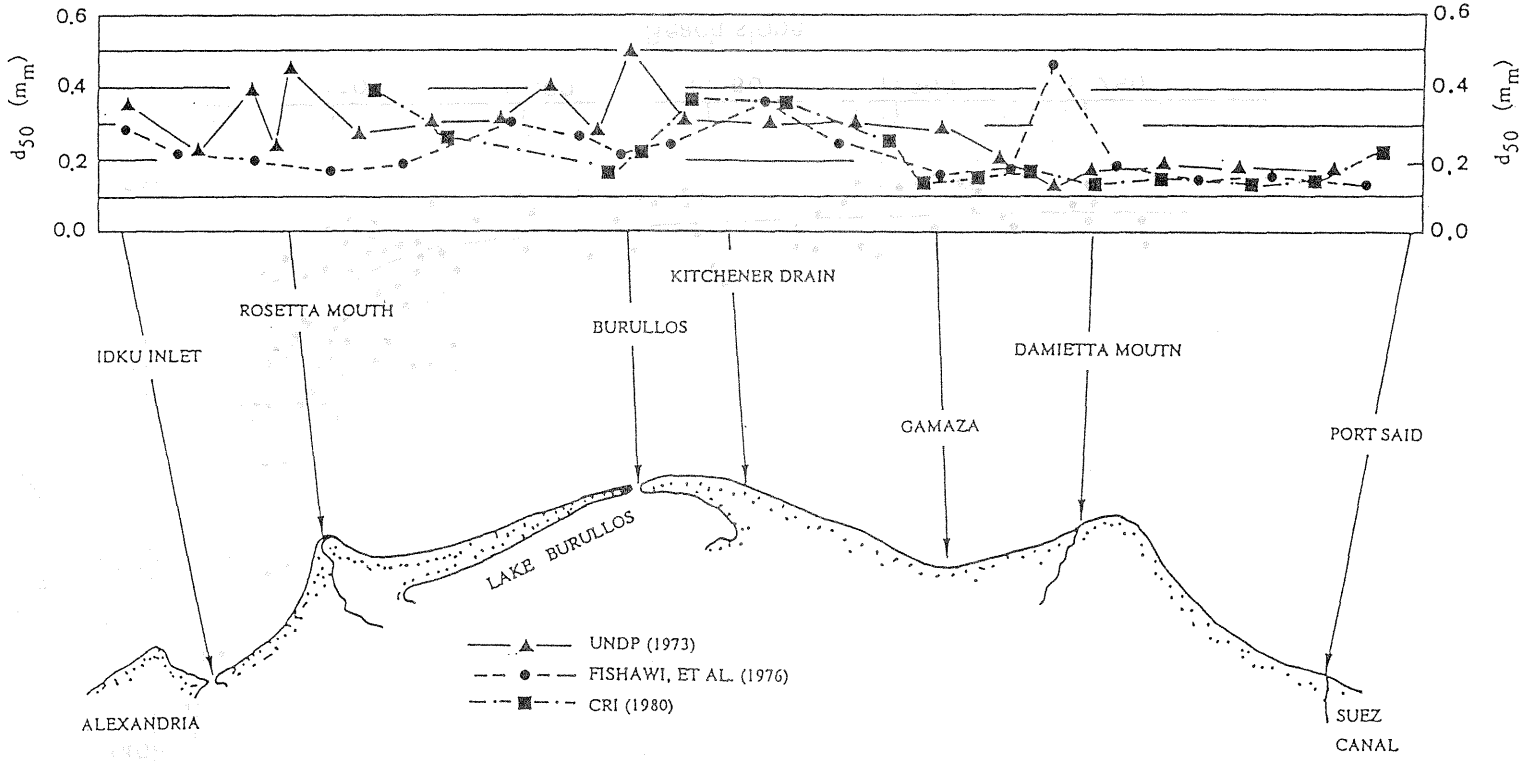

Figure 3.4 Sediment characteristics along the Nile Delta coast (after CRI, 1980).

mouths. While, UNDP (1973) data show a maximum at the Rosetta mouth, and the CRI (1980) data show a local maximum at Ras El Bar, near the Damietta mouth. This natural temporal variability makes it difficult to describe a specific grain size at any position along the coast. From a practical point of view, however, the range of variability is less than 0.4 mm for d_{50}, which is still characterized as fine to medium sand. Thus, characterization of the shoreline sediment as 0.25 mm west of Ras El Bar and 0.15 mm east of Damietta mouth is a reasonable approximation for engineering purposes.

3.2.3 History of shoreline change

Accretion and erosion are common to sandy coasts exposed to waves and currents. The stability of any particular section of shoreline depends upon the balance between the quantity of sediment supplied to that section and that carried away. If the sediment supplied is equal to that transported away, then the coastal section is said to be in dynamic equilibrium and the beaches are not subject to net erosion or accretion.

Historical shoreline changes are usually analyzed using available maps, charts, aerial photography and profile information. Comparison of surveys shows that the shoreline of the Nile river has retreated off the delta promontories following the construction of the Low Aswan Dam at an annual rate of about 18 m / yr at the Rosetta branch. In contrast there has been a modest shoreline advance (accretion) of about 8 m / yr at the Gamasa outlet during the period 1947 to 1965, (Kadib, 1969; Mobarek, 1972). The historical maps for Rosetta promontory allow for an analysis of shoreline changes back to 1800. During the period 1600 to 1898 Rosetta promontory probably extended seaward about 8 or 9 km (Sestini, 1975). Figure 3.5 demonstrates the historical shoreline changes of Rosetta promontory. The promontory extended 3.6 km (37 m / yr) between the surveys of 1806 and 1898, then remained nearly stationary from 1898 to 1909, or in other word the shoreline of Nile Delta was in a case of dynamic equilibrium stage. From the turn of this century to the present the seaward portion of the promontory has eroded at a progressively more rapid rate. The erosion rates for the periods

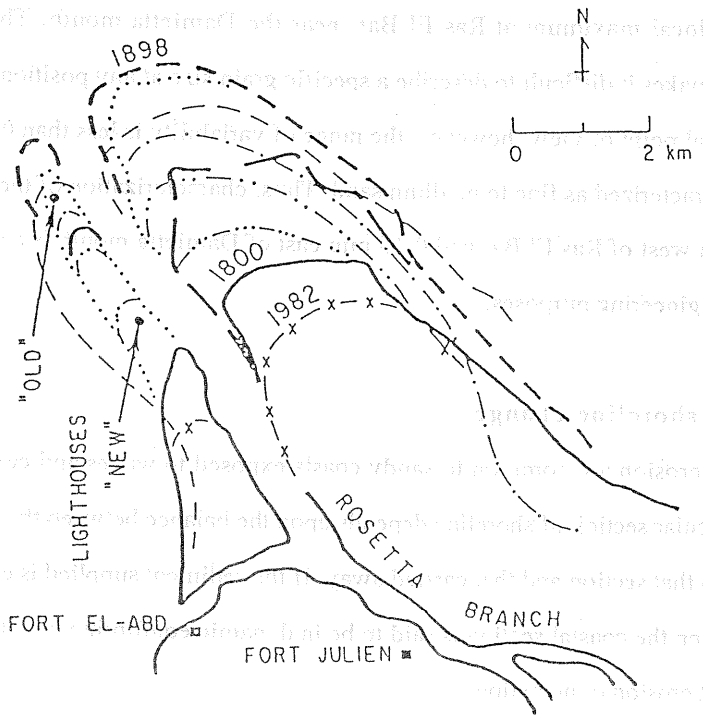

Figure 3.5 Historical shorelines of Rosetta Promontory, (after Inman and Jenkins, 1984).

proceeding the surveys in 1926, 1965, 1973 and 1982 are 18, 20, 125 and 211 m / yr, respectively (Figure 3.5). The "new" Rosetta Lighthouse which was 1 km inland in 1970, became an offshore island in 1976 (Nielsen, 1977; Khafagy et al., 1981).

The establishment in 1971 a series of beach profiles extending from Abu Quir Bay to east of Ras El Bar was an essential part of the erosion study. Repeated surveys along these profiles have proved to be the most effective means of monitoring the erosion. Comparison of beach profiles shows that the coastline has retreated of the delta promontories averaging 160 m/yr between 1971-1972 and 211 m/yr between 1973-1982 on the Rosetta branch, and 143 m/yr between 1943-1973 on the Damietta promontory (UNDP, 1973).

3.2.4 Wave climate

The large scale meteorological systems that give rise to the occurrence of waves along the Nile Delta coastline have been roughly studied . The cool season in the region of the Nile Delta extends from November to April; the warm season occurs between June and September; and May and October are transitional months with October generally accompanied by a very calm sea states. Storms, associated with moving depressions mainly following a W to NW path, occur regularly during the cool season. During the warm season a stable, wide Arabo-Bersion depression extends towards the eastern coasts of the Mediterranean Sea. The corresponding surface winds over the eastern Mediterranean blow mainly from the N to NW path during the period from mid of June to mid of September producing swell waves which reach the Nile Delta coast. The storms may occur every 6 to 7 days and their centers are often fast moving, with migration velocities of 900 to 1000 km/day. This migration rate is comparable with the speed of the waves, causing the wave height to be enhanced. The waves typically have deep water height of 3 to 6 m and periods of 8 to 10 sec and sometimes up to 15 sec, (Inman and Jenkins, 1984).

The nearshore wave data along the Nile Delta coast have been observed. From technical report presented by UNDP (1978) the available measured nearshore wave data around the Nile

Delta are summarized as (measurement depth ranged from 4m to 11m):

(1) The frequency of occurrence of maximum, significant wave heights and wave periods measured at Abou Quir, Burullus, and Ras El Bar wave observed stations is shown in Table 3.2.

(2) Table 3.3 lists the maximum record significant wave heights at Abou Quir during the period 1970 through 1974, and its associated wave period and wind direction

3) The maximum significant wave heights and periods during the storms of 1972/1973 are presented in Table 3.4.

3.2.5 Longshore sediment transport

Theoretical analysis and field measurements of waves and longshore sediment transport show that the total rate of longshore sediment is proportional to the longshore component of wave energy flux. Elwany, et al. (1984) estimated the average annual deep water wave energy flux to be about 2.5 kw/m. But along the Nile Delta coast the rate of longshore sediment transport is markedly varied. A refraction diagram for 8 sec waves from N 60° W, the predominant wave direction, is shown in Figure 3.6(a). In this figure the pronounced zones of wave convergence and divergence are shown, which resulting in strong gradients of wave height and breaker angle along the coast. This means that the longshore sediment transport rate, Q_x is not constant but varies with distance along the coast as shown in Figure 3.6(b). This variation in Q_x results in areas of erosion and accretion along the Nile Delta coast. The rate of erosion and accretion are given by the gradient of the littoral drift $\partial Q_x / \partial x$ as shown in Figure 3.6(c). It is noted that positive values of $\partial Q_x / \partial x$ indicate erosion while negative values indicate accretion. Inman, Aubray and Pawka (1975) estimated the rates of longshore sediment transport to be about 86 $x10^4$ m^3/yr move to the east near Rosetta and Damietta promontories, about 62 x 10^4 m^3/yr at Burullus inlet, about 38 x 10^4 m^3/yr on the westward facing beach between Rosetta and Burullus, and about 20 x 10^4 m^3/yr on the eastward facing beach between Burullus and Damietta.

Table 3.2 Frequency of occurrence of wave height and period.

% equal to exceeding	Abou Quir			Burullos			Ras El Bar		
	$H_{1/3}$ (cm)	H_{max} (cm)	T (sec)	$H_{1/3}$ (cm)	H_{max} (cm)	T (sec)	$H_{1/3}$ (cm)	H_{max} (cm)	T (sec)
80	85	120	8.5	75	115	7.3	75	115	8.4
50	95	135	8.7	105	148	8.2	105	135	9.0
20	110	155	9.2	140	175	9.2	112	158	9.4

Table 3.3 Maximum significant wave height, wave period and wind direction.

Month / year	$H_{1/3}$ max (m)	T (sec)	Wind Direction
Sept 1971	1.47	10.2	NE
Dec 1971	1.90	9.4	NE
April 1972	2.04	8.0	NNW
May 1972	0.82	7.7	NE
June 1972	1.18	8.0	NNE
Aug 1972	0.79	7.4	N
Nov 1973	1.89	9.8	NNW
Dec 1973	1.87	10.8	NW
Feb 1974	1.57	7.2	NE
Mar 1974	1.41	7.1	NE
April 1974	1.80	6.4	NE
May 1974	0.68	6.5	NE

Table 3.4 Maximum significant wave height and period during the storms.

Name of storm	$H_{1/3}$ max (m)	T_{max} (sec)
Waknassa	2.23	7.26
Kasem	2.15	7.23
El-Pida El-Saghira	1.39	6.83
Ras El Sanaa	1.58	6.52
El Keram	1.847	8.78
El Shames El Akhira	1.50	7.78
El Shames El Kebera	2.13	6.79

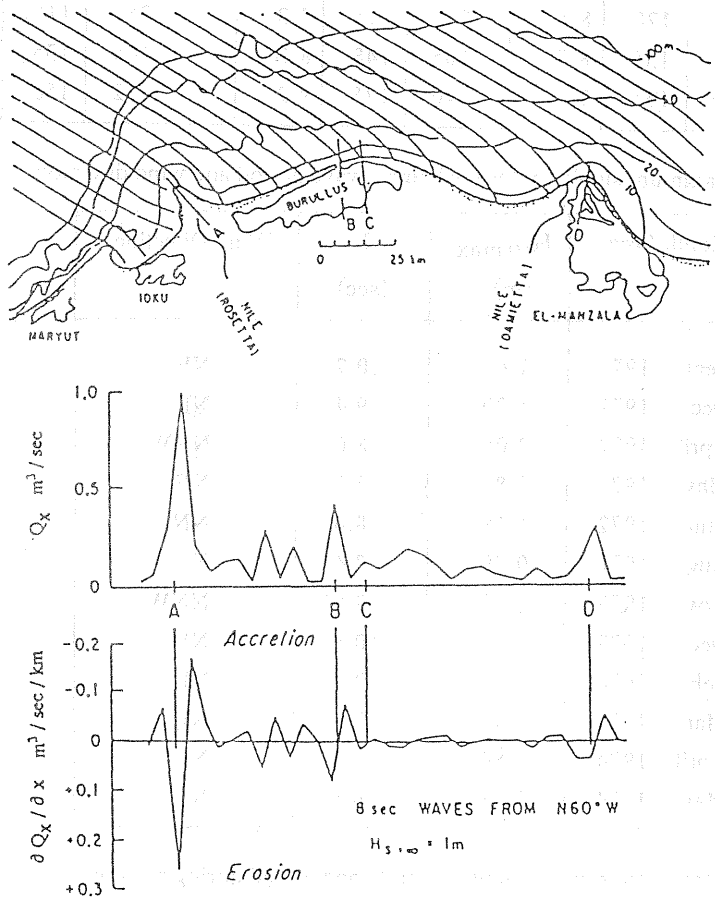

Figure 3.6 Wave refraction and variation of longshore sediment transport along the Nile Delta coast for a 1 m wave height, 8 sec wave period, coming from N 60° W, (after Inman and Jenkins, 1984).

3.3 River Deltas in Lake Biwa

Lake Biwa, the largest lake in Japan, is located in the central of Honshu Island, in Shiga Prefecture at 34° 58' - 35° 31' N and 135° 52' - 136° 17' E. The total surface area and total length of shoreline are 674 km^2 and 235 km, respectively. The maximum water depth of the lake is 104 m. The total volume of the storage water is 27.5 x 10^9 m^3, with an area of drainage basin of 3,174 km^2.

Lake Biwa was born some five million years ago and is therefore one of the oldest lakes in the world, geologically. In ancient days the lake was called Ohmi Basin. The word "Ohmi" means a big, fresh body of water in old Japanese now Ohmi means the sea. While, the meaning of the word "Biwa" is an old musical instrument of Japan, similar to the mandolin. Lake Biwa, together with Mt. Fuji, has been a symbol of natural beauty for the Japanese, and still attracts many sightseers every year. The lake has been used largely as a water resource and for recreation and tourism.

Some 460 streams of various sizes flow into the lake, but the Seta River is the only natural outlet flowing from the southern end of the lake. The Seta is a tributary of the Yodo River, which drains into the Seto Inland Sea of Japan at Osaka. In 1906, a dam was built at Uji, the uppermost end of Seta to control Lake Biwa water level and the river flux.

The sediment of Lake Biwa basin consists of gravel, sand and clay, and is divided by forty layers of volcanic ash, carried from volcanically active areas in western Japan. The lake drainage basin is surrounded by mountain ranges about 1,000 m above sea level, and is 4.7 times as wide as the lake itself. The asymmetrical basin occupied by the lake has steeper beach profiles on the western margin than on the eastern margin, as a result the river deltas located on the western margin are much narrower then these located on the eastern margin, (see Figure 3.7).

Among this large number of rivers flow into the lake, eight largest rivers are selected to be investigated. These rivers have big drainage areas and consequently big deltaic areas. Five

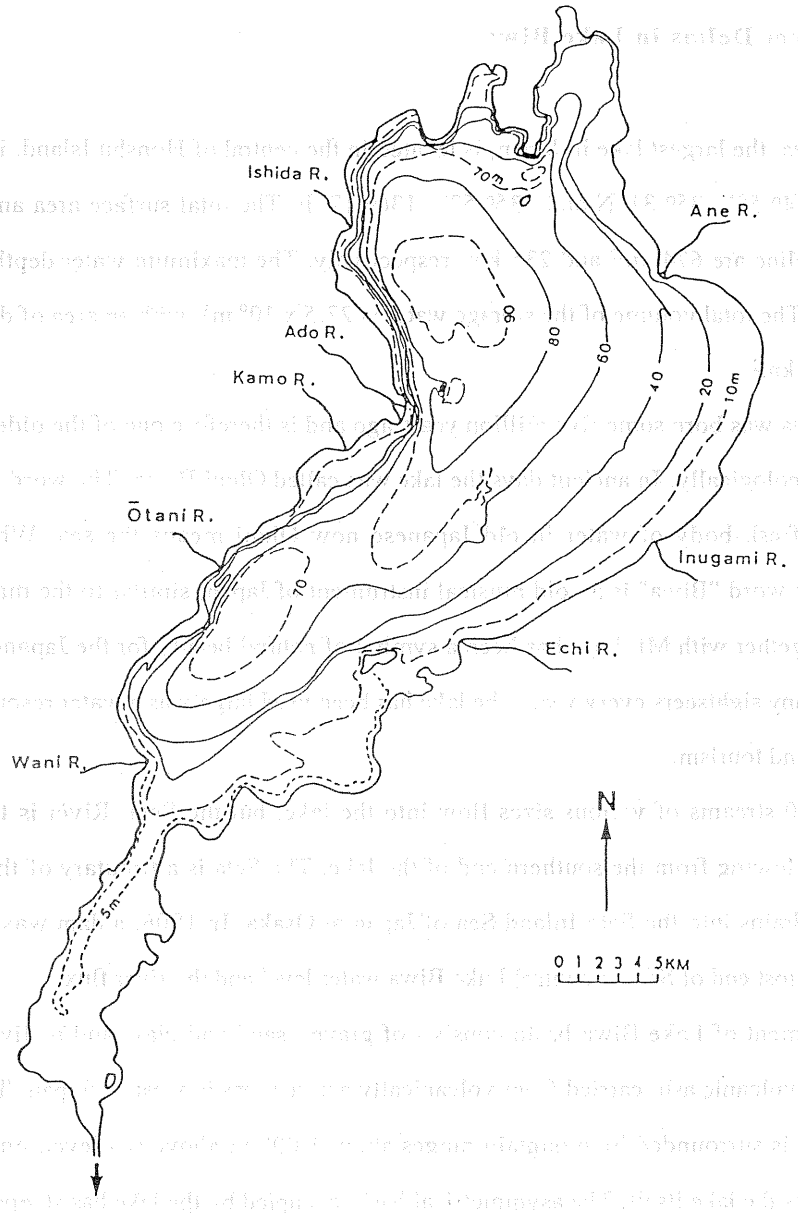

Figure 3.7 Bathymetric map of Lake Biwa and selected river deltas.

of the selected rivers located on the western margin of Lake Biwa, they are Ishida R., Ado R., Kamo R., Otani R. and Wani R., and three located on the eastern margin, they are Ane R., Inugami R, and Echi R., (see Figure 3.7).

3.3.1 Estimation of river sediment discharge

The water discharges of the selected rivers are analyzed from the twenty year recorded data from the period 1961 to 1981 presented by Local Office of the Ministry of Construction, Shiga Prefecture. From the disaster records of the Lake Biwa during the same period, the annual average number of floods has been deduced individually for each river. Using an empirical relationship between sediment discharge from river and water discharge proposed by Local Government Office of Shiga Prefecture with the associated tables, the rates of sediment input from the selected rivers have been estimated. Table 3.5 shows the estimated sediment discharge rates for the selected rivers.

3.3.2 Sediment characteristics and beach profiles

The sediment size typically varies along the coast of river delta. This variation is caused in part, by the influence of river sediment and by the littoral drift. The coarser materials are deposited in the vicinity of the river mouth area, while finer materials are transported by prevailing waves and currents, and deposited at a considerable distance from the river mouth. Shibano, Yamashita, Inoue, Tsuchiya (1985) sampled and analyzed the sediments along the western beach of Lake Biwa. These sampling data are reanalyzed for the river deltas on the western margin of Lake Biwa in term of the medium sediment diameter, d_{50}.

Since river deltas in Lake Biwa were formed some thousand years ago, their beach profiles have been reached a stable shape which is so called equilibrium beach profile. Dean (1977) proposed a relationship for equilibrium beach profile as:

$$h = A\, y^{2/3} \qquad (3.1)$$

where h is the water depth, y is offshore coordinate (positive seaward), and A is shape

Table 3.5 Estimation of rate of sediment discharge of Lake Biwa's rivers.

River Name	Drainge area(km^2)	Q_w $m^3/km^2/flood$	$Q_s x10^4$ $m^3/flood$	no. of floods per year	$Q_s x10^5$ (m^3/y)
ISHIDA	53.57	25000	66.963	1.6	10.714
ADO	306.90	30000	460.350	2.0	92.070
KAMO	43.07	25000	53.838	1.6	8.614
OTANI	6.83	20000	6.830	1.6	1.100
WANI	15.46	25000	19.325	1.6	3.100
ANE	369.03	30000	553.545	2.0	110.710
INUGAMI	104.67	30000	157.005	1.6	25.121
ECHI	202.27	25000	252.840	2.0	50.570

parameter which has a dimension of length to a power 1/3. Moore (1982) showed that the shape parameter A is correlated to the medium sediment diameter, d_{50}. He found that as the sediment diameter increases, the beach slope becomes steeper. To verify this relationship the beach profiles along the selected river deltas were measured using the available contour maps. The analysis for each river individually will be shown in next portions.

(1) Ishida river

The Ishida river discharges out to the lake at the upper northwest side of the lake. It has a drainage area of about 53.6 km^2 supplying annually 10.7 x 10^5 m^3 of sediment. The analysis of the sediment samples shows that the medium sediment diameter, d_{50}, along the delta coast is about 30 to 40 mm, which can be classified as a pebble or cobble. The beach profiles along the shoreline of the Ishida river delta were measured in the direction perpendicular to the shoreline. The longshore distance between the measuring beach profiles is about 100 m, see Figure 3.8.

The results of measured beach profiles compared with the equilibrium beach profile formula are shown in Figure 3.9. A good agreement is seen between the measured and the computed equilibrium beach profiles. The beach slope at the river mouth is steeper than the one near the end of the river delta. The average beach slope changes from 1 / 20 - 1 / 10 up to water depth of 5 m to 1 / 10 - 1 / 5 up to water depth of 20 m, deeper that 20 m the beach shop becomes very steep. The measurements of beach slope are shown in Figure 3.10, in which β_1 is the angle of beach slope up to 5 m water depth and β_2 is the angle of beach slope up to 20 m water depth. The longshore variation in the value of β_1 is small, which implies that the contour lines up to 5 m are nearly parallel to the shoreline. While the value of β_2 varies along the delta coast showing a bigger value at the river mouth and nearly constant one near the end of delta. The average beach slope at the river mouth is about 1/5 while near the river sides it is about 1/30. Figure 3.11 demonstrates the longshore variation of the medium sediment diameter, d_{50}, and the shape parameter A. The results of medium sediment diameter, d_{50}, show a scattering with a range of 30 to 40 mm which can be classified as a pebble or cobble. The disagreement between d_{50} and A is observed in this figure, this is probably because of the nature of Ishida

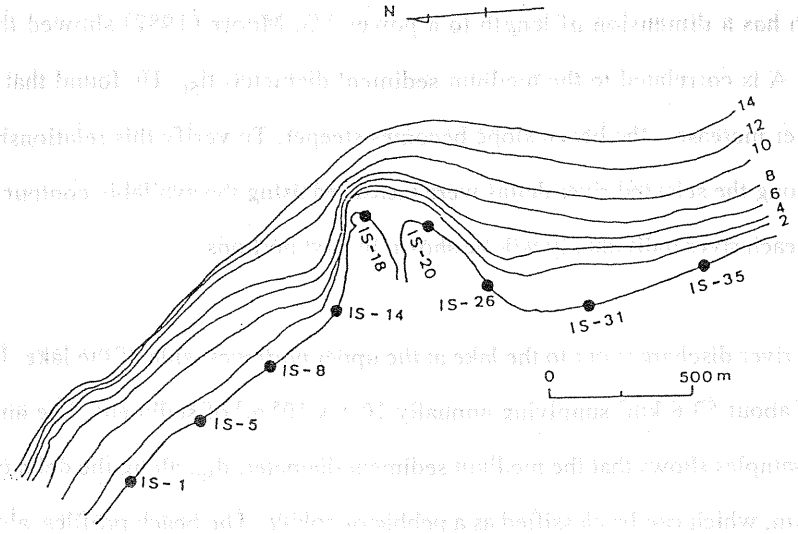

Figure 3.8 Points of measurement of beach profile along Ishida Delta coast.

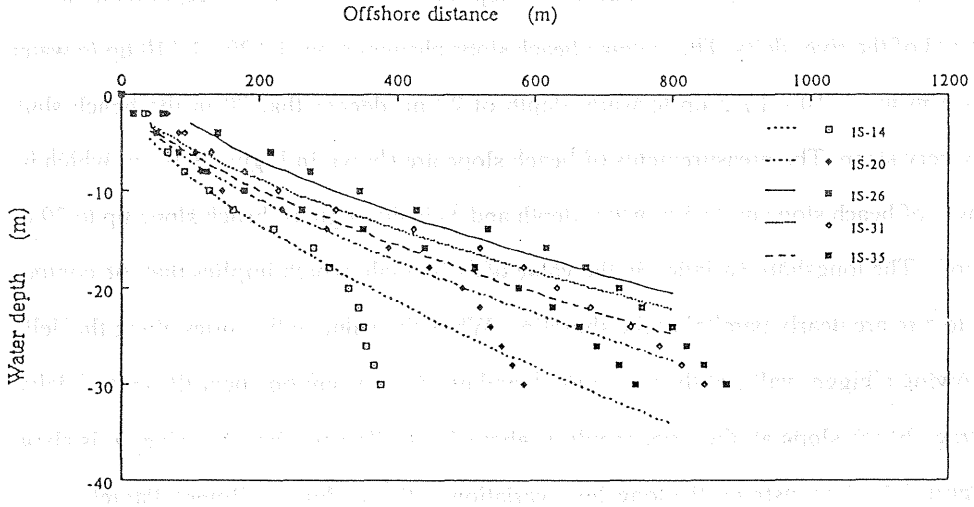

Figure 3.9 Variation of beach profiles along Ishida Delta coast compared with Dean's relationship for equilibrium beach profile.

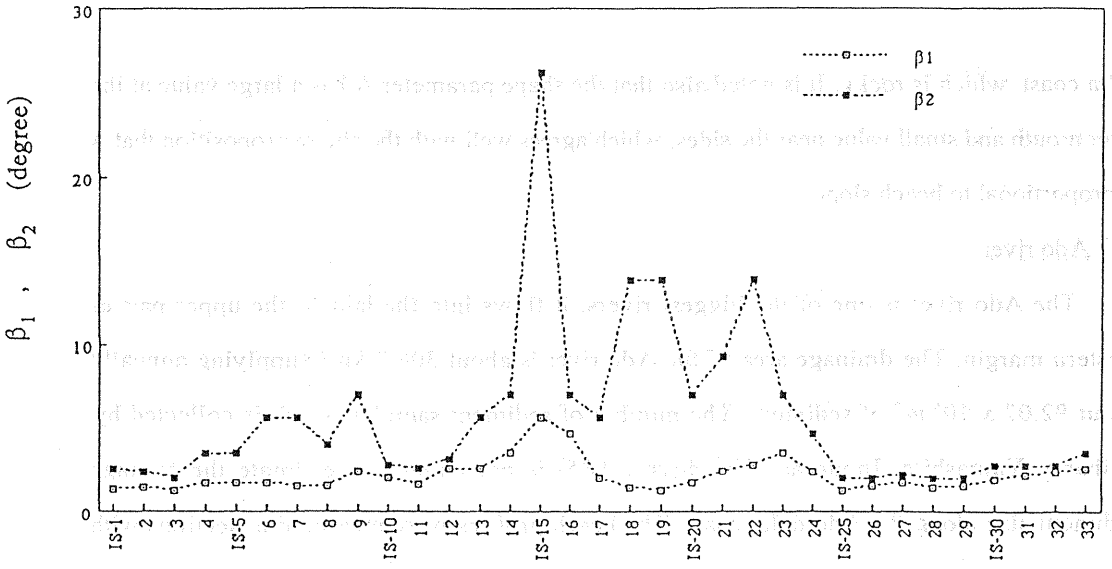

Figure 3.10 Variation of β_1 and β_2 along Ishida Delta coast.

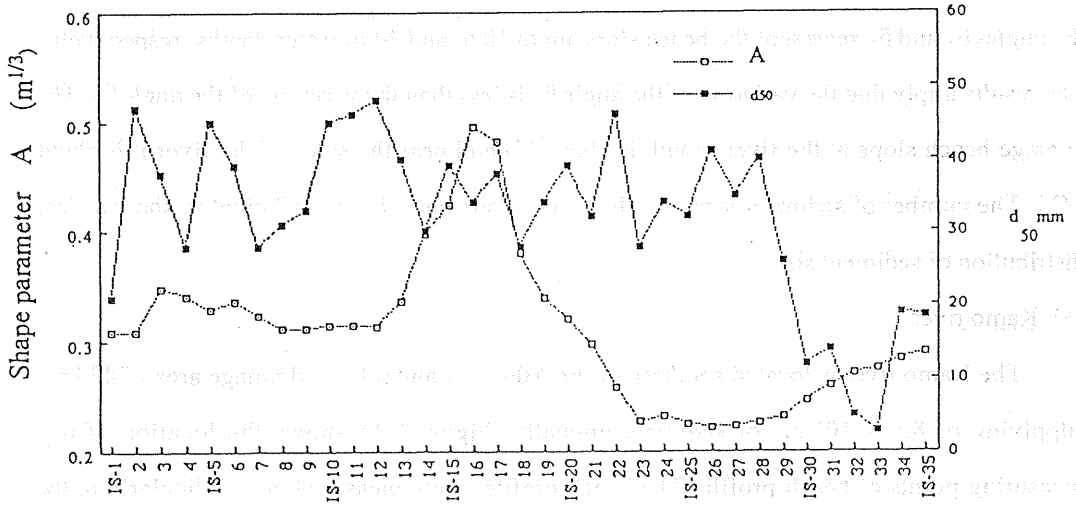

Figure 3.11 Sediment characteristics along the Ishida Delta compared with shape parameter A.

delta coast, which is rocky. It is noted also that the shape parameter A has a large value at the river mouth and small value near the sides, which agrees well with the above proposition that A is proportional to beach slope.

(2) Ado river

The Ado river is one of the biggest rivers, it flows into the lake at the upper part of western margin. The drainage area of the Ado river is about 306.9 km^2 supplying annually about 92.07 x 10^5 m^3 of sediment. The number of sediment samples which is collected by Shibano, Yamashita, Inoue and Tsuchiya (1985) is not enough to estimate the average sediment size along the Ado delta coast. The beach profiles were measured at sections with interval longshore distance of 100 m. The direction of measurements was perpendicularly to the shoreline, see Figure 3.12.

The results of measured beach profiles computed with Dean's expression for equilibrium beach profile are shown in Figure 3.13. The beach slope up to 10 m water depth is about 1 / 20 - 1 / 30 and is about 1 / 5 - 1 / 10 up to 20 m water depth. Deeper than 20 m the beach slope becomes very steep. The longshore variation of beach slope is shown in Figure 3.14, where the angles β_1 and β_2 represent the beach slope up to 10 m and 20 m water depths, respectively. The results imply that the variation of the angle β_1 is less than the variation of the angle β_2. The average beach slope at the river mouth is about 1/5 and near the sides of the river it is about 1/20. The number of sediment samples along Ado delta coast is not sufficient to show a clear distribution of sediment size.

(3) Kamo river

The Kamo river is located southern of the Ado river and it has a drainage area of 43 km^2 supplying of 8.6 x 10^5 m^3 of sediment annually. Figure 3.15 shows the location of the measuring points of beach profile. The beach profiles were measured perpendicularly to the shoreline. The results of the measurements of beach profile is shown in Figure 3.16, where the curves represent Dean's expression for equilibrium beach profile and the symbols represent the measured values. A disagreement is seen between the measured and the computed beach

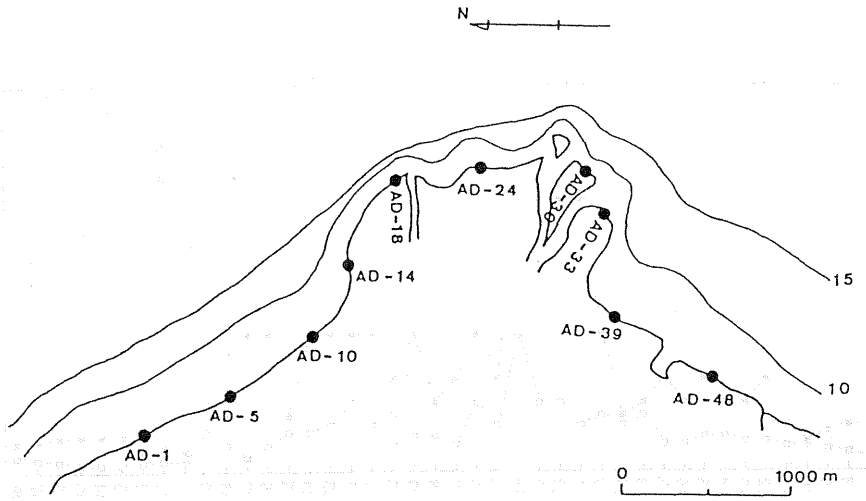

figure 3.12 Points of measurement of beach profile along Ado Delta coast.

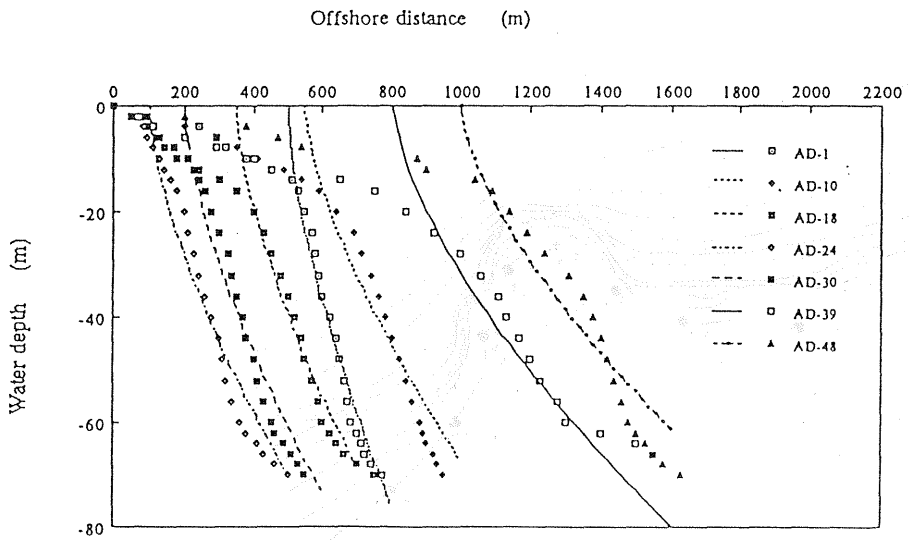

Figure 3.13 Variation of beach profiles along Ado Delta coast compared with Dean's relationship for equilibrium beach profile.

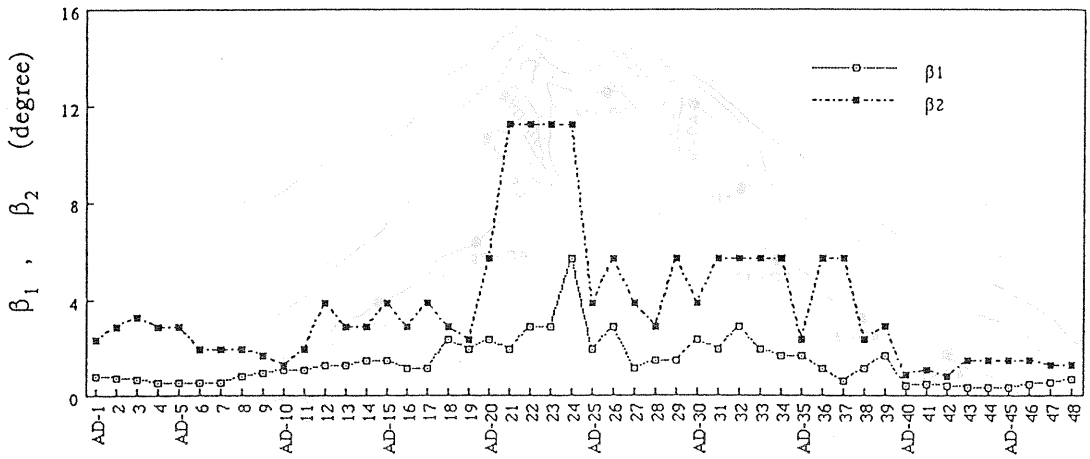

Figure 3.14 Variation of β_1 and β_2 along Ado Delta coast.

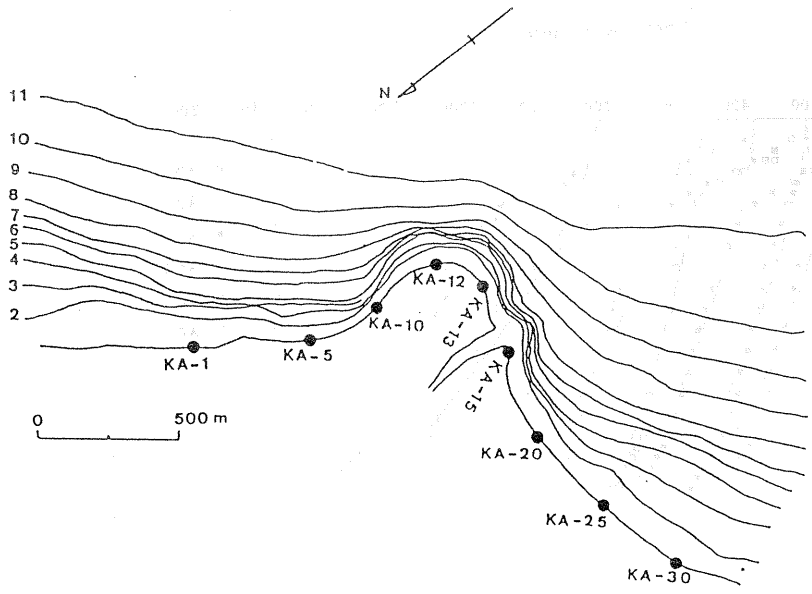

Figure 3.15 Points of measurement of beach profile along Kamo Delta coast.

profiles, which implies that the beach profile of the Kamo river has not yet reached equilibrium shape. In next subsection, it will be shown that the position of the Kamo river mouth has changed over time history.

The longshore variation of beach slope is show in Figure 3.17, where the angles β_1 and β_2 represent the beach slope up to 5 m and 10 m water depths, respectively. The general trend shows that the angles β_1 and β_2 increase at the river mouth and decrease near the sides. The average beach slope changes from about 1 / 10 at the river mouth to about 1 / 30 near the river sides. No sediment samples are available at Kamo delta coast.

(4) Otani river

The delta of the Otani river is relatively small, with the drainage area of 6.8 km^2. It is located at the middle of the western margin of Lake Biwa. The annual average sediment discharge is about 1.1 x 10^5 m^3. The beach profiles were measured at sections with interval longshore distance of 50 m, see Figure 3.18. The beach profiles were measured perpendicularly to the shoreline. Figure 3.19 illustrates the comparison between the measured beach profiles and the computed one by Dean's expression for equilibrium beach profile. A good agreement is seen between the measured and the computed beach profiles near the sides of Otani delta, while loss agreement is seen between the measured and the computed beach profiles near the river mouth.

The correlation between the sediment size represented by d_{50} and the shape parameter A is demonstrated in Figure 3.20. The sediment size on the left side of the Otani river, which is about 1.5 to 2.5 mm, is relatively coarser than the sediment size on the right side of the river which is a fine sediment of 0.5 to 1.0 mm diameter. The measurements of beach slope represented by the angles β_1 and β_2 for water depths up to 5 m and 15 m, respectively, are shown in Figure 3.21. A small variation of the angles β_1 and β_2 is observed near the sides of Otani delta, while at the river mouth the changes of β_2 are larger than the changes of β_1. The average beach slope at the river mouth is about 1/5 and near the sides of the river it is about 1/20.

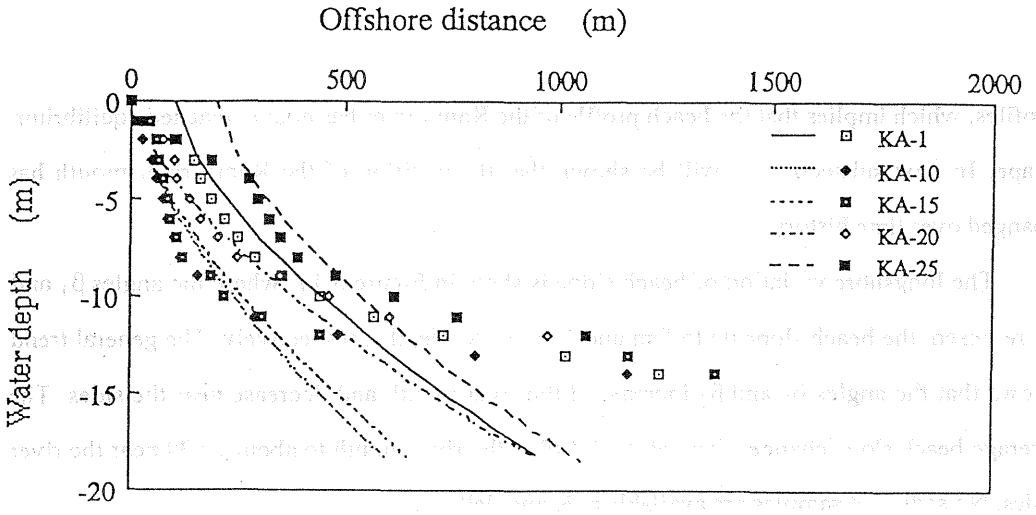

Figure 3.16 Variation of beach profiles along Kamo Delta coast compared with Dean's relationship for equilibrium beach profile.

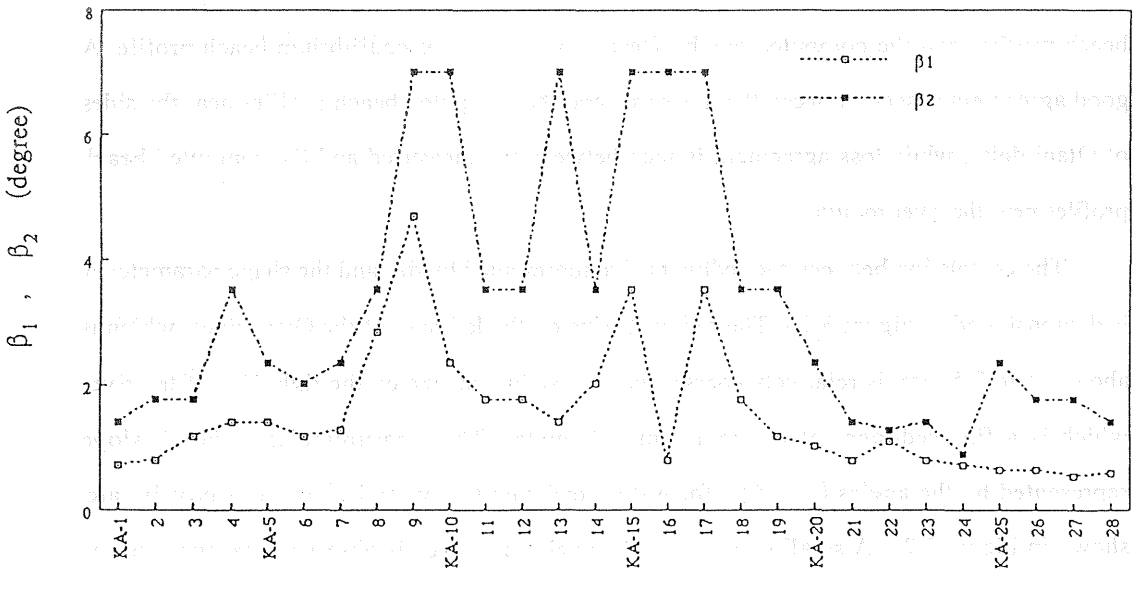

Figure 3.17 Variation of β_1 and β_2 along Kamo Delta coast.

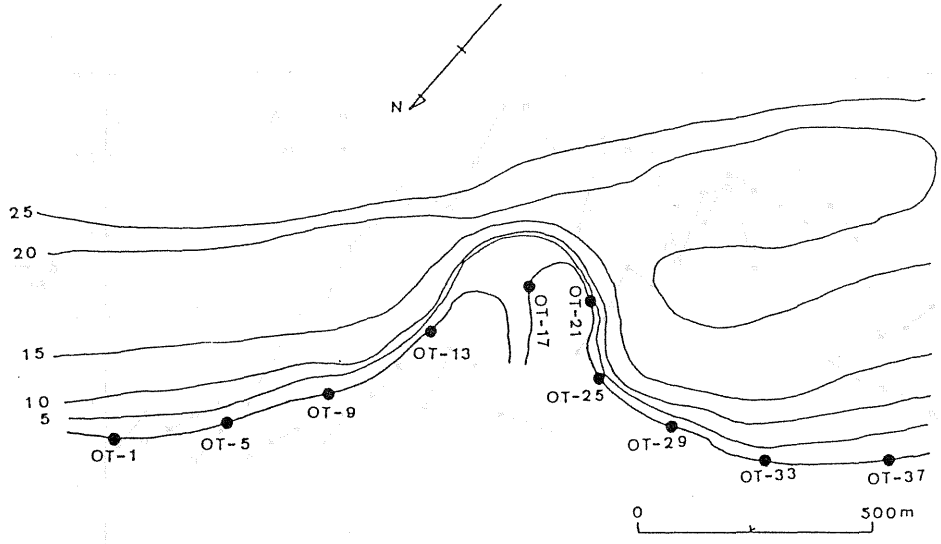

Figure 3.18 Points of measurement of beach profile along Otani Delta coast.

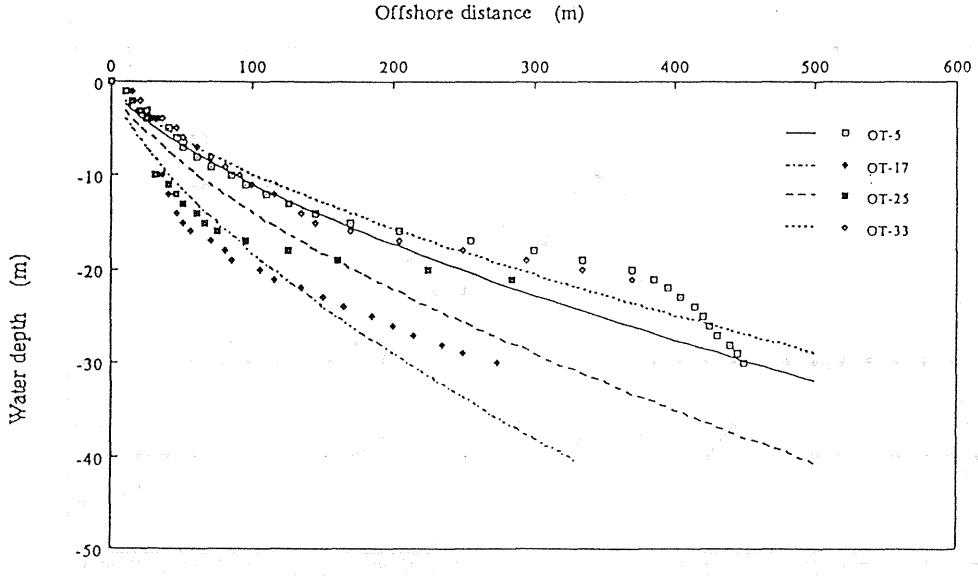

Figure 3.19 Variation of beach profiles along Otani Delta coast compared with Dean's relationship for equilibrium beach profile.

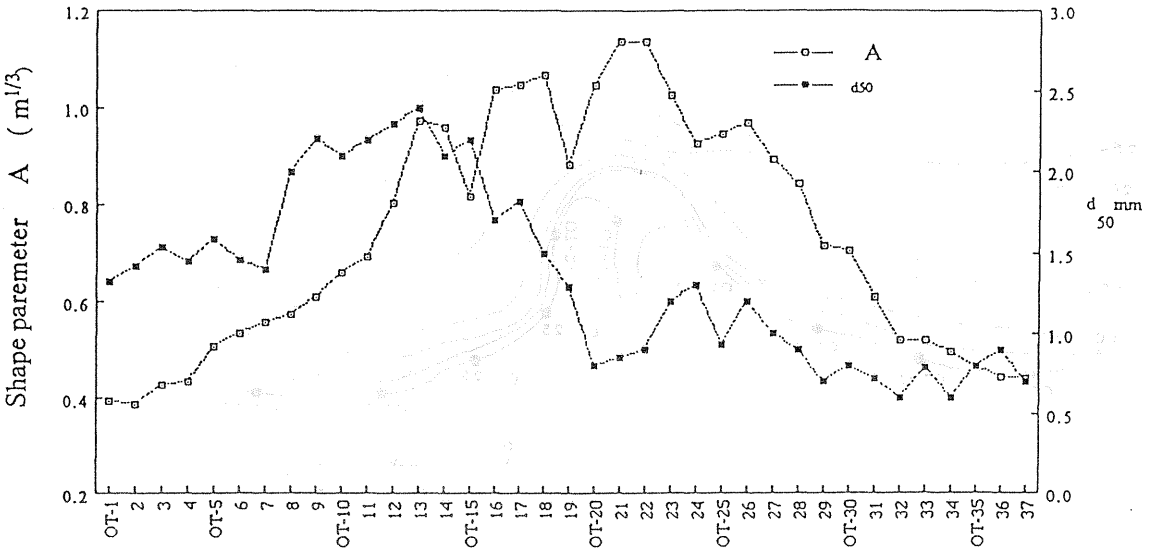

Figure 3.20 Sediment characteristics along Otani Delta coast compared with shape parameter A.

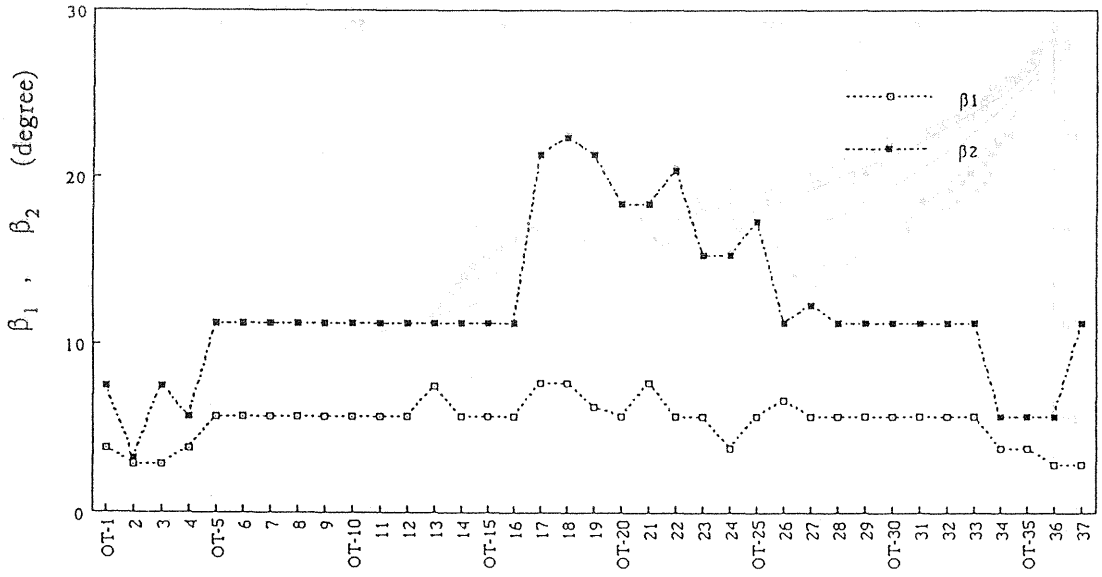

Figure 3.21 Variation of β_1 and β_2 along Otani Delta coast.

(5) Wani river

The Wani river is located at the southwest side of the lake. The drainage area is about 15.5 km^2 supplying 3.1 x 10^5 m^3 of sediment annually. The beach profiles were measured every 100 m interval distance along the Wani delta coast. The direction of measurements was perpendicularly to the shoreline, see Figure 3.22. The comparison between the measured beach profiles and the computed equilibrium profiles by Dean's expression is shown in Figure 3.23. A favorable agreement is seen between the measured profiles and the computed one. Figure 3.24 shows the longshore distribution of sediment size, represented by d_{50} and the shape parameter A. Scattering of d_{50} values indicate a disagreement with the shape parameter A. The range of sediment size is of 0.5 to 2.5 mm. The changes of beach slope alongshore of Wani delta are illustrated in Figure 3.25, where the angles β_1 and β_2 represent the beach slope up to 10 m and 20 m water depth, respectively. Although, the measured beach slopes show scattered values, the general trends of the angles increase at the river mouth and decrease near the end sides. The average beach slope at the river mouth is about 1 / 10 and near the river sides it is about 1 / 30.

(6) Ane river

The Ane river is the largest river of Lake Biwa. It flows out into the lake at the northeast side of the lake, with a drainage area of 369.0 km^2 supplying about 110.7 x 10^5 m^3 of sediment annually. Figure 3.26 shows the location of the measuring points where the beach profiles were measured perpendicularly to the shoreline. A good agreement between the measured beach profiles and the computed equilibrium profiles by Dean's expression is shown in Figure 3.27. The longshore variation of beach slope, represented by the angles β_1 and β_2 for water depths up to 10 m and 30 m, respectively, are shown in Figure 3.28. The average beach slope at the river mouth is about 1/10 and near the river end sides it is about 1/30. No sediment samples are available at Ane delta coast.

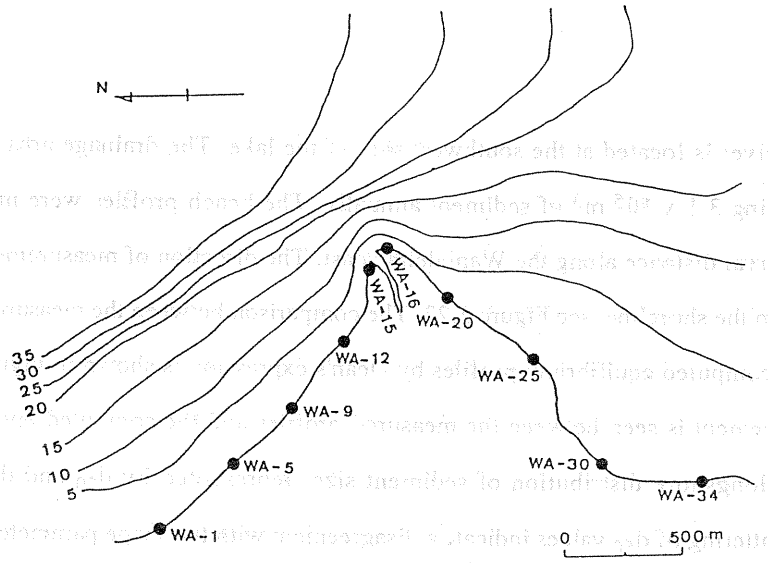

Figure 3.22 Points of measurement of beach profile along Wani Delta coast.

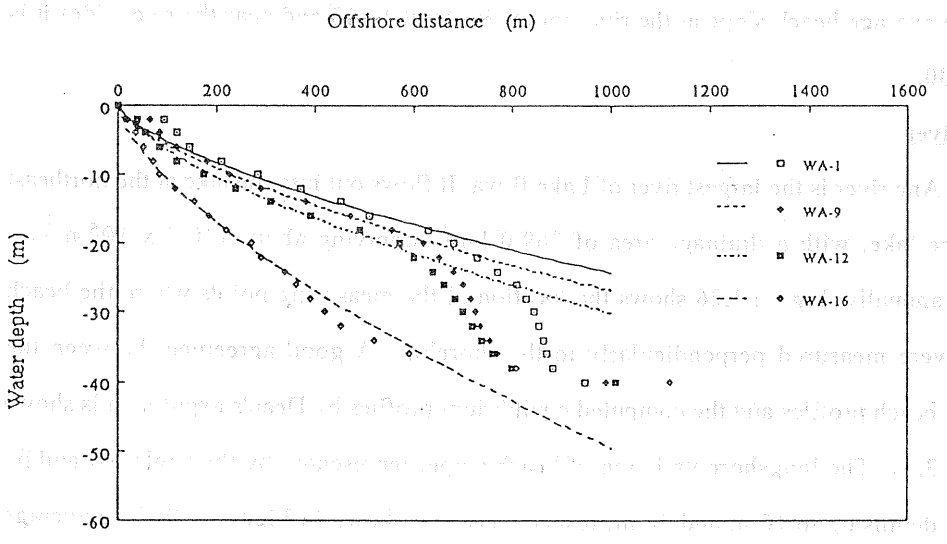

Figure 3.23 Variation of beach profiles along Wani Delta coast compared with Dean's relationship for equilibrium beach profile.

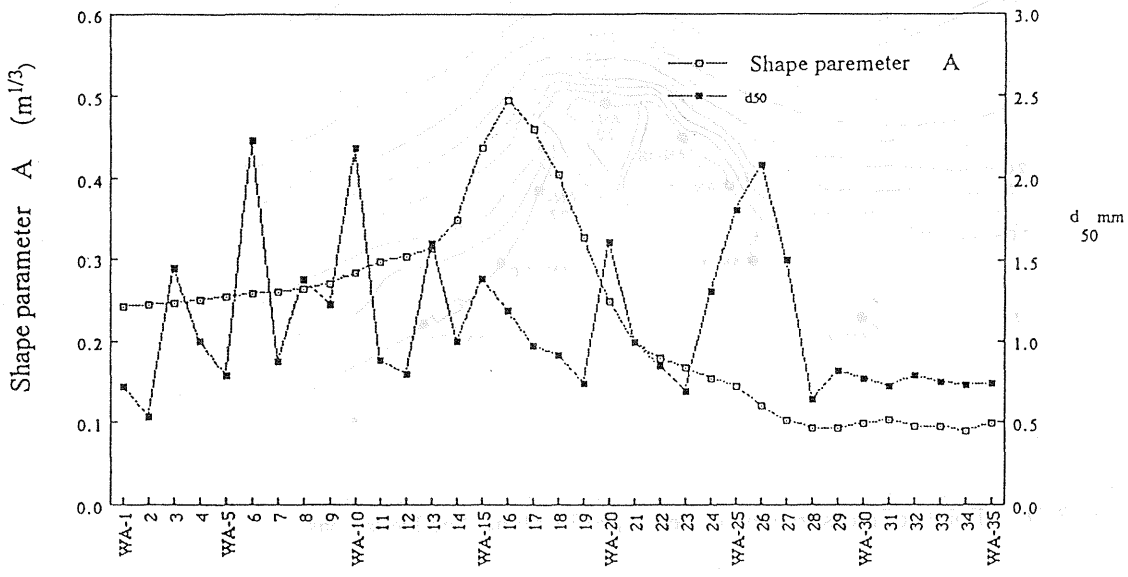

Figure 3.24 Sediment characteristics along Wani Delta coast compared with shape parameter A.

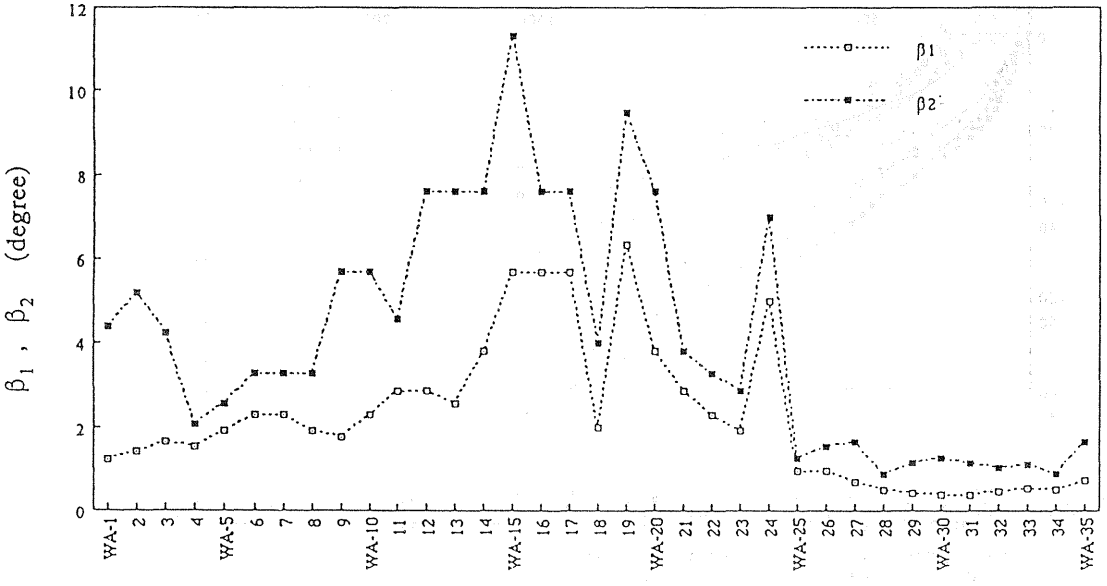

Figure 3.25 Variation of β_1 and β_2 along Wani Delta coast.

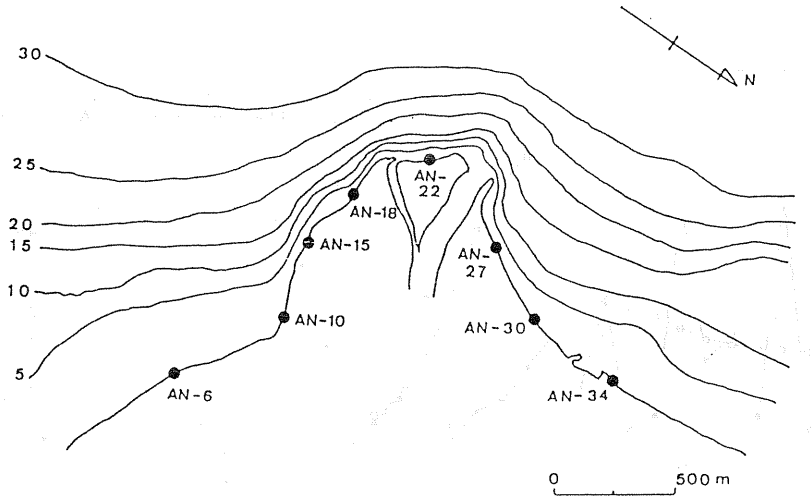

Figure 3.26 Points of measurement of beach profile along Ane Delta coast.

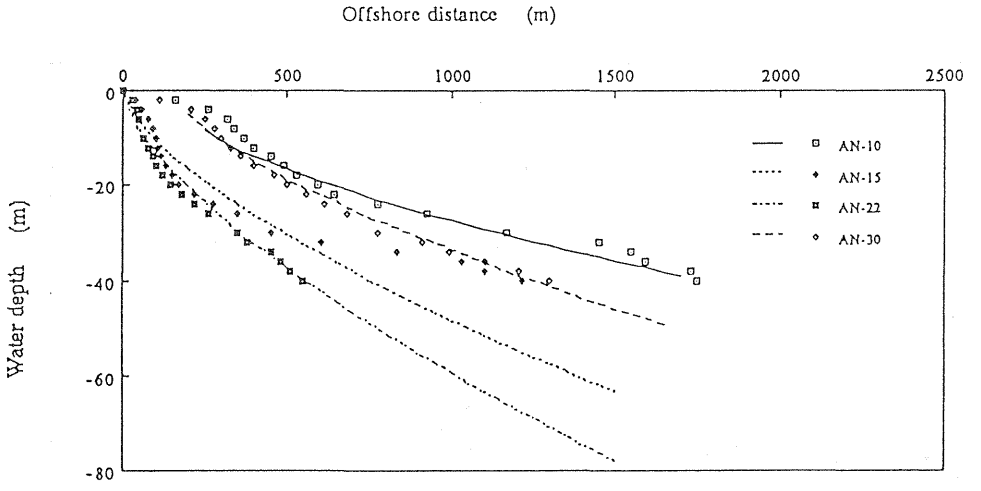

Figure 3.27 Variation of beach profile along Ane Delta coast compared with Dean's relationship for equilibrium beach profile.

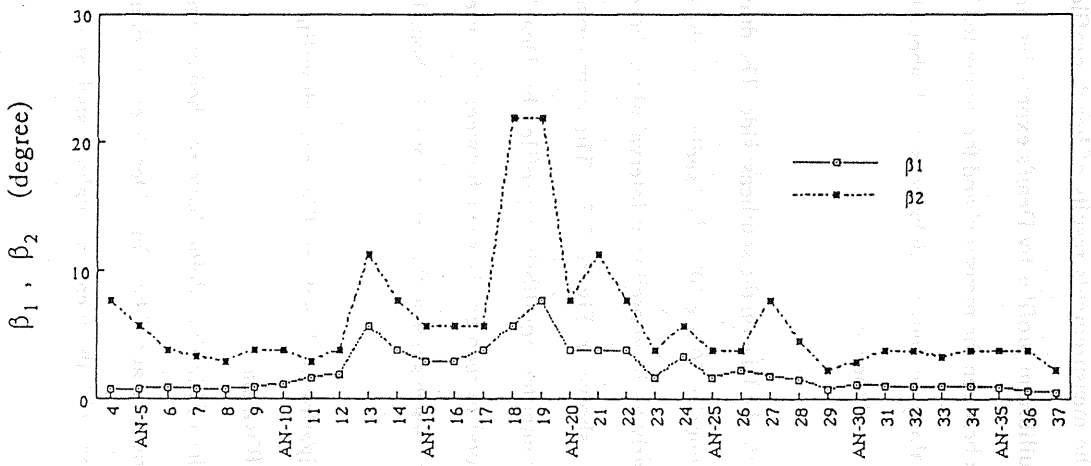

Figure 3.28 Variation of β_1 and β_2 along Ane Delta coast.

(7) Inugami river

The delta of the Inugami river is relatively small. The drainage area is about 104.7 km^2 supplying annually about 25 x 10^5 m^3 of sediment. The longshore distance interval between measured beach profiles is about 100 m, where the beach profiles were measured perpendicular to the shoreline, see Figure 3.29. The measurements results of beach profiles are shown in Figure 3.30, where the estimated equilibrium profiles by Dean's expression are also shown in the figure. The less agreement shown between the measured and the computed beach profiles is not so good. The beach slope is vary along the Inugami delta coast with about 1 / 60 at the river mouth to about 1 / 75 near the end sides of the river.

(8) Echi river

The Echi river discharges out into the lake on the southeast side. The drainage area of the river is about 202.3 km^2 supplying annually 50.6 x 10^5 m^3 of sediment to the lake. The beach profiles were measured perpendicularly to the shoreline at interval alongshore of 100 m. The location of the measuring points is shown in Figure 3.31. The comparison between the measured beach profiles and the computed equilibrium profiles by Dean's expression is demonstrated in Figure 3.32. A good agreement is seen between the measured and the computed beach profiles. The average beach slope at the river mouth is about 1/60 and near the end sides of the river is about 1/100.

It is obvious from the investigation of beach profiles and shoreline changes of the selected river deltas around the Lake Biwa that :

(1) In general, the beach profiles of big river deltas have reached an equilibrium shape, since the deltas have been formed long time ago. Therefore, Dean's expression for equilibrium beach profile shows a good agreement with the measured values, such as the Ishida R., Ado R., Wani R., Ane R. and Echi R.

(2) The beach profiles of relatively small river delta have not yet reached an equilibrium shape, and therefore Dean's expression shows a less agreement with the measured values, such as the Otani R. and Inugami R.

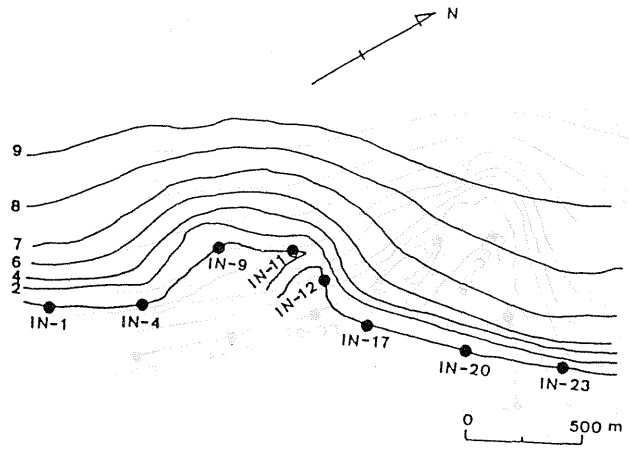

Figure 3.29 Points of measurement of beach profile along Inugami Delta coast.

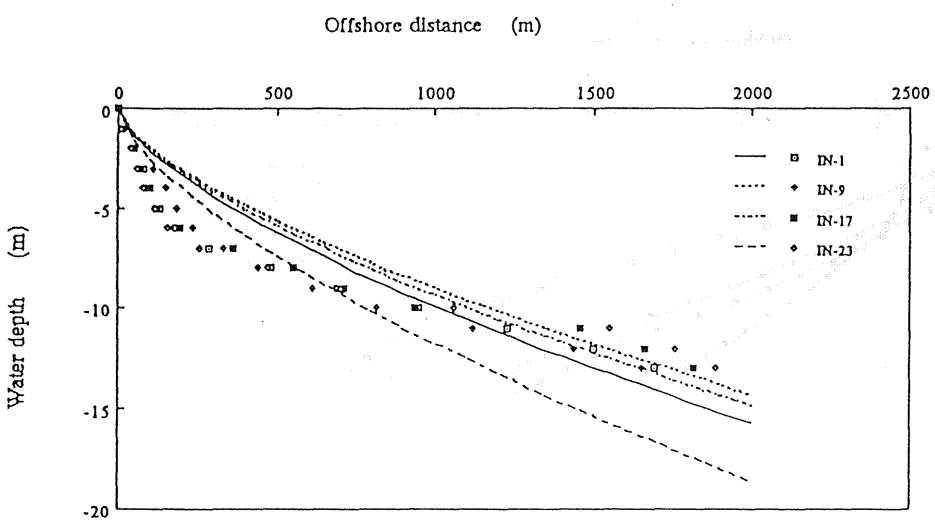

Figure 3.30 Variation of beach profile along Inugami Delta coast compared with Dean's relationship for equilibrium beach profile.

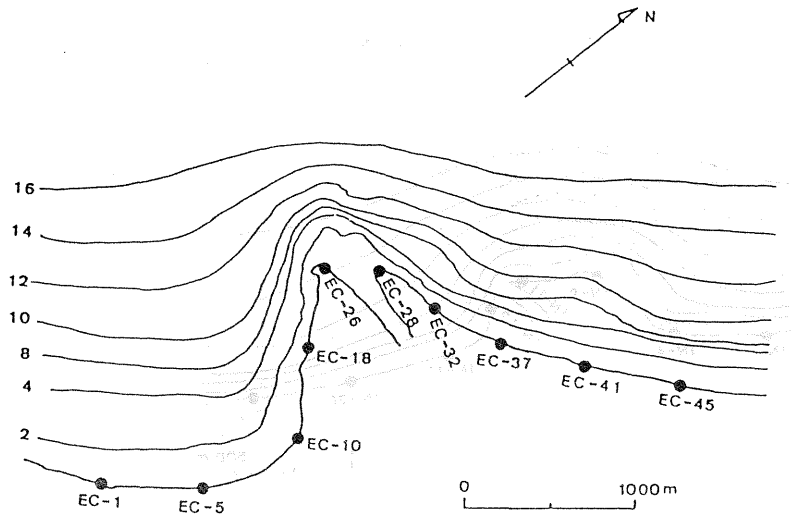

Figure 3.31 Points of measurement of beach profile along Echi Delta coast.

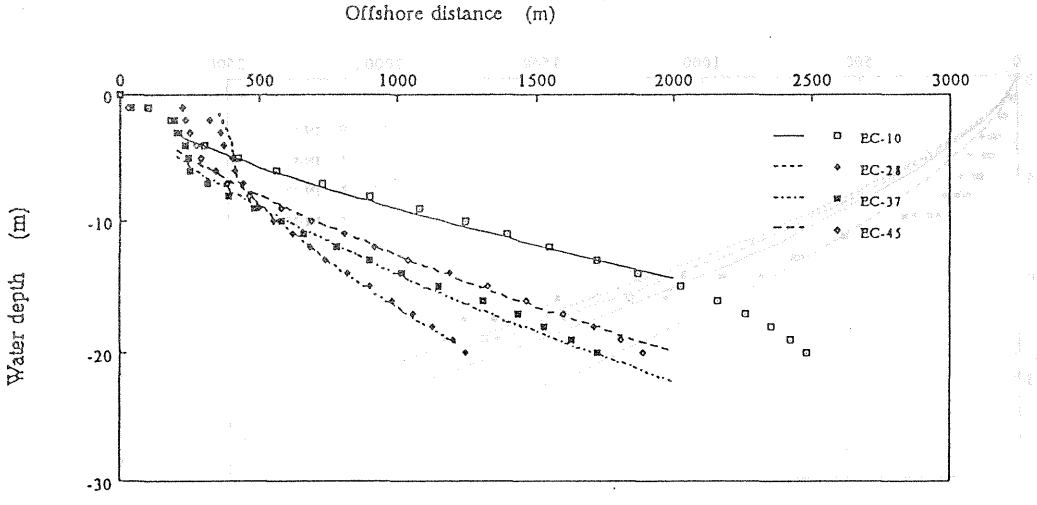

Figure 3.32 Variation of beach profile along Echi Delta coast compared with Dean's relationship for equilibrium beach profile.

(3) In general, the average beach slope varies along the river delta beach, with a steeper slope at the river mouth and milder one near the end sides of the river delta.

3.3.3 History of shoreline change

The shoreline changes are usually analyzed using the available maps, charts, aerial photography and profile information. Figure 3.33 illustrates the shoreline changes along Ishida delta, Otani delta, Wani delta, Ane delta, Inugami delta and Echi delta. From this figure it is obvious that:

(1) The comparison between two surveys performed in 1893 and 1962 for Ishida delta shows that the shoreline has slightly propagated in the north direction.

(2) The development of Otani delta during the period 1893 to 1957 indicates that the shoreline near the river mouth has propagated at a faster rate than the shoreline at the end sides of the river delta.

(3) Comparison of two surveys performed in 1893 and 1956 of Wani delta shows that the shoreline has slightly advanced in the north direction.

(4) The shoreline change of Ane delta of two surveys performed in 1893 and 1961 shows that the shoreline has been advanced at a faster rate at the river mouth than near the end sides of the river delta.

(5) The propagation of the shoreline of Inugami delta during the period 1983 to 1961 indicates that the delta has been advanced seaward with no change in river mouth position.

(6) The configuration of Echi delta was analyzed using two surveys performed in 1893 and 1959. It is observed that the shoreline on the left side has advanced at a faster rate than the right side. Asymmetric shape of delta is observed.

The historical development of Ado delta for the period 1690 to 1975 is illustrated in Figure 3.34. It is observed that during the propagation of the shoreline of the delta the river mouth position has been propagated in a constant direction. The configuration of Kamo Delta was investigated and analyzed for a period 1893 to 1982. The shoreline changes are shown in

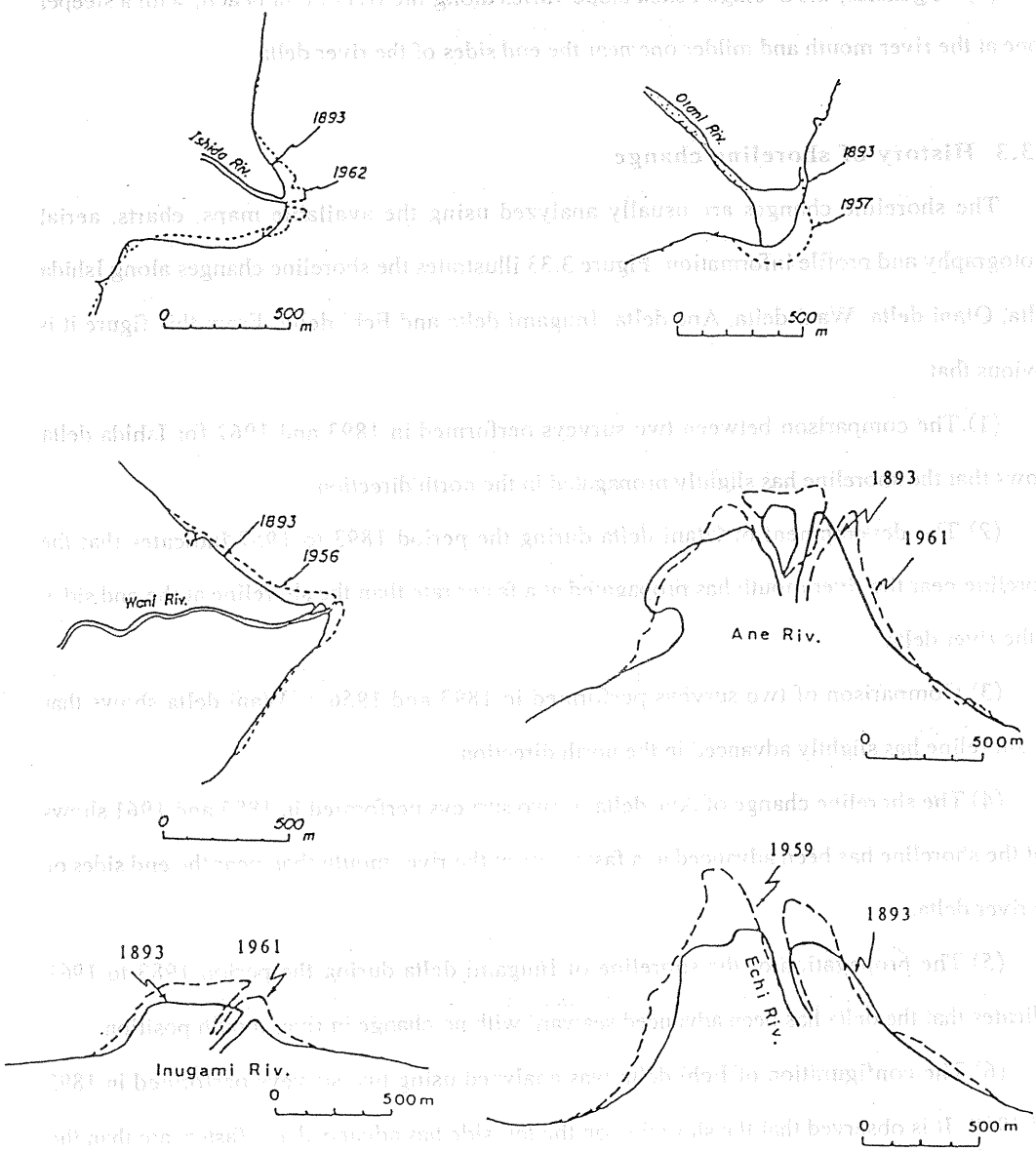

Figure 3.33 Shoreline changes along the river delta areas of Ishida River, Otani River, Wani River, Ane River, Inugami River, and Echi River.

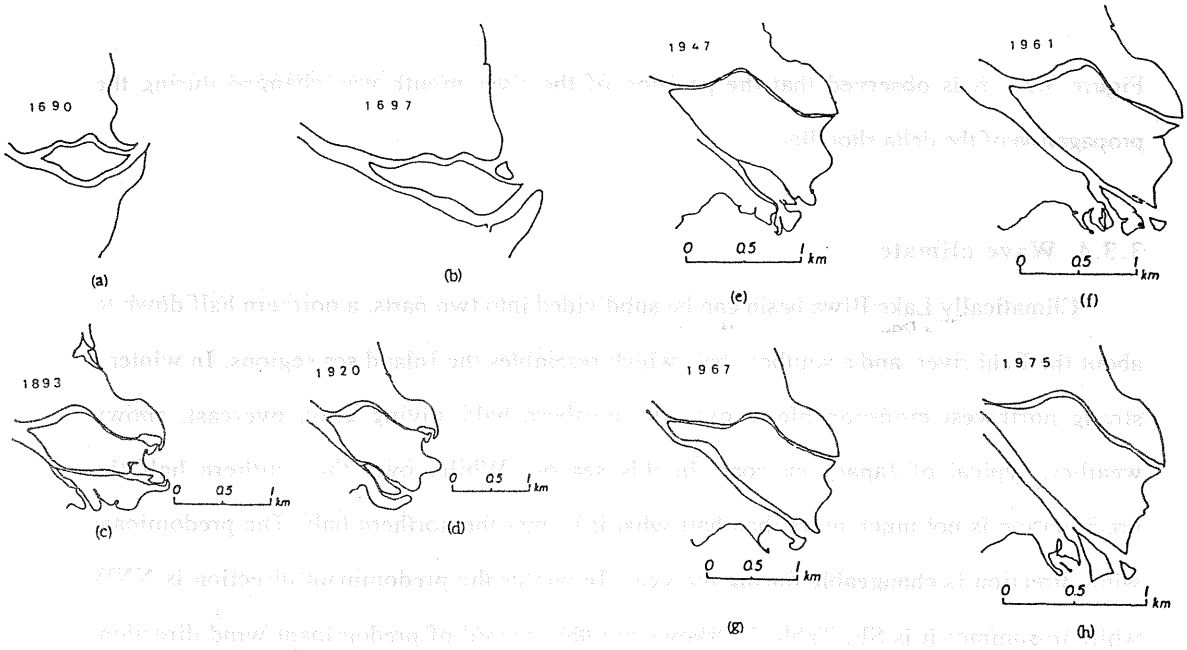

Figure 3.34 Historical changes in shoreline of Ado River Delta, (after Tsuchiya et al., 1985).

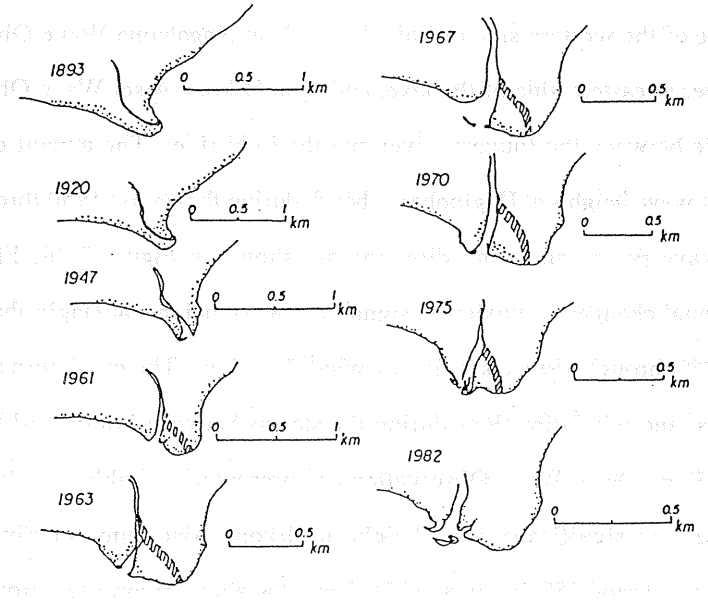

Figure 3.35 Historical changes in shoreline of Kamo River Delta, (after Tsuchiya et al., 1985).

Figure 3.35, it is observed that the position of the river mouth was changed during the propagation of the delta shoreline.

3.3.4 Wave climate

Climatically Lake Biwa basin can be subdivided into two parts, a northern half down to about the Echi river, and a southern half which resembles the Inland sea regions. In winter a strong northwest monsoon blows over the northern half, giving gray, overcast, snowy weather, typical of Japan sea coast in this season. While, over the southern half the precipitation is not much more than half what it is over the northern half. The predominant wind direction is changeable during the year. In winter the predominant direction is NNW while in summer it is SE. Table 3.6 shows monthly record of predominant wind direction, during the period of 1921-1950, observed at Ibuki mountain, located on the northeast side with 1377 m height above sea level and at Hikone, located near Inugami river on the eastern side of Lake Biwa.

Waves are observed at three locations around the Lake Biwa; 1) at Haginohama beach, located in the middle of the western side of Lake Biwa, 2) at Nagahama Wave Observation, located near Ane river at eastern side of the lake, and 3) at Hikone Aisei Wave Observation, located in the middle between the Inugami river and the Echi river. The annual changes in maximum significant wave heights at Haginohama beach during the period 1950 through 1981, and its associated wave period and wind direction are shown in Figure 3.36. Figure 3.37 demonstrates the annual changes in maximum significant wave heights at Haginohama beach during the period 1950 through 1981 classified by wind directions. The maximum significant wave height, periods, and wind directions during the storms between March and November 1975 observed at Hikone Aisei Wave Observation are presented in Table 3.7. Figure 3.38 illustrates the changes in significant wave height at Hikone Aisei and Nagahama Wave Observations during the period 1895 through 1975. From the above records it is noted that the significant wave height is about 0.5 to 1.5 m and wave period is about 4 sec.

Table 3.6 Monthly recorded of predominant wind direction in Lake Biwa.

month / location	1	2	3	4	5	6	7	8	9	10	11	12
Ibaki	NNW	NNW	NNW	NNW	NNW	SE	SE	SE	SE	NNW	NNW	NNW
Hikone	NW	NW	NW	NW	N	N	N	SE	N	NNW	NW	S

Table 3.7 Maximum significant wave height, period and wind direction during the storms.

date	time	$H_{1/3}$ (m)	$T_{1/3}$ (sec)	wind dir.
3.21	14:00	0.719	3.24	NW
3.24	1:00	1.217	3.00	NNW
3.25	13:26	0.575	2.60	NNW
4.03	3:00	0.870	2.67	NW
4.08	23:00	1.108	3.00	N
10.05	13:00	0.915	3.19	NNW
10.05	14:00	0.906	3.40	NNW
10.05	15:00	0.898	3.33	N
10.05	16:00	1.146	3.80	N
10.05	17:00	1.100	3.77	N
10.05	18:00	1.010	3.66	N
10.08	13:00	0.781	3.04	NW
10.08	20:00	0.540	2.67	NNW
10.09	16:00	0.441	2.35	N
10.10	15:00	0.512	2.67	NNW
10.13	2:00	0.497	2.58	NW
10.13	18:00	0.591	2.56	W
10.14	16:00	0.614	2.67	NW
10.15	3:00	0.874	3.30	
10.21	19:00	0.788	3.21	N
10.25	9:00	0.745	2.94	NNW
10.25	16:00	0.736	2.95	N
10.26	17:00	0.483	2.40	NW
10.30	10:00	1.122	3.65	NNW
10.30	13:00	0.996	3.45	NNW
11.02	19:00	0.607	3.18	NNW
11.03	8:00	0.650	3.09	N
11.03	17:00	0.965	3.47	NNW
11.09	13:00	1.256	3.81	NNW
11.10	0:00	0.864	3.15	N
11.11	17:00	0.483	2.40	NW
11.19	20:00	0.999	3.65	NNW
11.20	0:00	0.938	3.50	NNW
11.23	22:00	0.862	3.17	NW

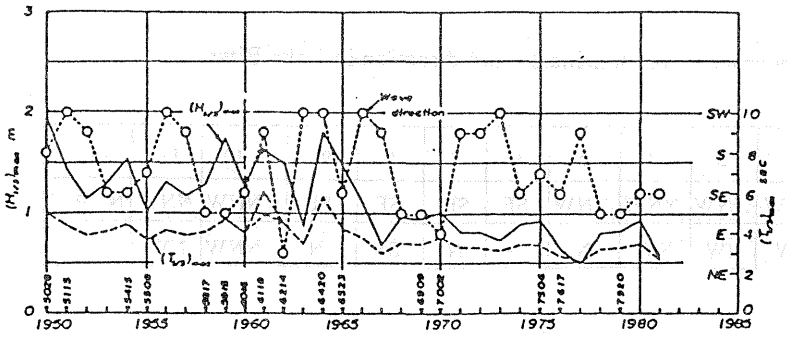

Figure 3.36 Annual changes in maximum significant wave height and period, and there direction, observed at Haginohama.

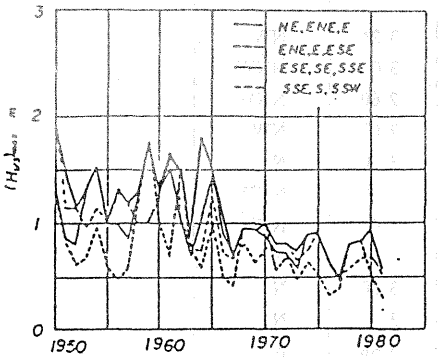

Figure 3.37 Annual changes in maximum significant wave height classified by wind direction at Haginohama.

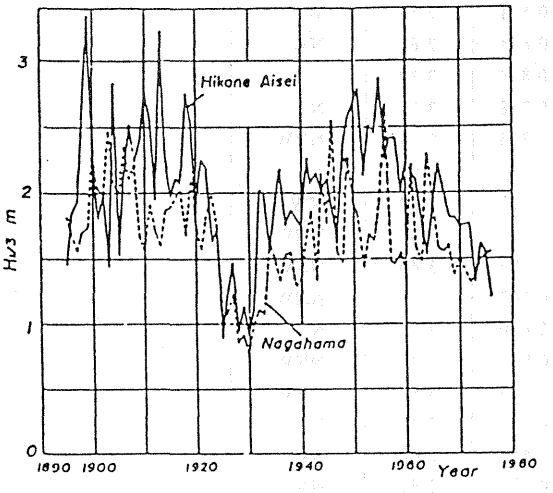

Figure 3.38 Annual changes in significant wave height observed at Hikone Aisei and Nagahama wave observation.

3.4.2 Previous analytical work of one-line theory

Pelnard-Considére (1956) was the first to employ mathematical modeling as a method of describing shoreline evolution. He introduced the so-call "One-Line" theory and verified its applicability with laboratory experiments. He then derived analytical solutions of diffusion type equation for three different boundary conditions: the shoreline evolution updrift of a groin (with and without bypassing) and the release of an instantaneous plane source of sand on the beach.

Grijm (1961) studied formation of the river delta. In the longshore sediment transport equation discussed in his article, the rate of longshore sediment transport was assumed to be proportional to twice the incident breaking wave angle to the shoreline. Only solutions which were similar in shape during the course of time are discussed. Two different analytical solutions are presented: one for which both the incident breaking wave angle and the shoreline orientation angle are small and one for which the wave angle is small in comparison with the shoreline orientation. The governing equations (longshore sediment transport and continuity of sediment transport) are expressed in polar coordinates and solved numerically. Grijm (1964) further developed this technique and presented a wide range of delta formations.

Le Méhauté and Brebner (1961) discussed solutions for shoreline change at groins, with and without bypassing of sand, and the effect of sudden dumping of material at a given point. Most of the solutions were previously derived by Pelnard-Considére (1956), but they are more precisely presented in Le Méhauté and Brebner's work, especially regarding geometric aspects of the shoreline change. The decay of an oscillating shoreline and the equilibrium shape of the shoreline between two headlands are treated.

Bakker and Edelman (1964) treated the shape of river delta by modifying the equation of longshore sediment transport rate to allow for an analytical treatment without linearization. Their solutions are more or less similar to Grijm. Komar (1973) also presented numerically

solutions of delta growth under highly simplified conditions.

Bakker (1968) extended the one-line theory to include two lines to describe beach planform change. The beach profile is divided into two parts, one relating to shoreline movement and one to movement of an offshore contour. The two lines in the model are represented by a system of two differential equations which are coupled through a term describing cross-shore transport. According to Bakker (1968), the cross-shore transport rate depends on the steepness of the beach profile; a steep profile implies offshore sand transport; and a gently sloping profile implies onshore sand transport. The analytical solutions of the two-line theory are not included in the present study.

Tsuchiya (1973) derived analytical solutions for predicting shoreline changes around river mouths. By expressing the sediment input from a river by Dirac's delta function, he could produced a modified model for the one-line theory. Tsuchiya and Yasuda (1979) further extended the analytical solutions for predicting shoreline changes around groin and river delta by introducing a new formulation for the rate of longshore sediment transport. In this study an extension of this formulation is made to include the non-uniformity of the longshore sediment transport. They also discussed analytical solutions for shoreline changes for a groin of finite length, in which a part of longshore sediment transport is entrapped, and for a river delta, of which the rate of sediment input from a river is varied.

Le Méhauté and Soldate (1979) presented a brief literature survey on the subject of mathematical modeling of shoreline evolution. Analytical solutions of the linearized equation of shoreline change are discussed along with the dispersion of sediment in a rectangular beach fill. A numerical model is derived which includes the variation in sea level, wave refraction and diffraction, rip currents, and the effects of coastal structures in connection with long-term shoreline evolution.

The most complete summary of analytical solutions to the sediment transport equation has been made by Walton and Chiu (1979). Two derivations of the continuty equation of sediment transport are presented. The differences between these two approaches, which both

arrive at the diffusion type equations, are that one approach uses the Coastal Engineering Research Center (CERC) formula for describing the longshore sediment transport rate by wave action and the other uses the formula derived by Dean (1973) based on the assumption that the majority of sediment transport occurs as suspended load. Consequently, most analytical solutions appearing in the literature were presented by Walton and Chiu (1979). Additional solutions mainly concern beach nourishment in connection with various shoreline shapes. New solutions derived by Walton and Chiu (1979) treat beach fill in a triangular shape, a rectangular gap in a beach, and a semi-infinite rectangular fill. Dean (1984) gives a brief survey of some solutions applicable to beach nourishment calculations, especially in the form of characteristic quantities describing loss percentages. One solution describes the shoreline change between two groins initially filled with sand.

Recently, Hanson and Larson (1987) proposed an analytical solution and two different numerical formulations. A comparison between these two solutions has been made based on the capabilities and limitations of each method through the study of shoreline evolution for a simple shoreline / structure configuration under idealized wave conditions.

In summary, the assumptions which comprise the one-line are given as follows; 1) The beach profile moves parallel to itself, 2) Longshore sediment transport takes place uniformly over the beach profile down to the limited depth of littoral drift, h_k, 3) Details of nearshore circulation are neglected and 4) the longshore sediment rate is proportional to the breaking wave properties.

3.5 Analytical Solutions of River Delta Formation

In the previous section the fundamentals of one-line theory were discussed. The fundamental assumption of the theory, which is that the beach profile does not change, is limited when it is applied to predicate the shoreline evolution of river deltas, especially for a river-dominated delta type. However, the shoreline evolution of the river delta can be

predicted analytically with the aid of the one-line theory, which gives a rapidly and economically estimation of shoreline evolution with a reasonable accuracy. In this section the effect of beach slope variation along the delta coast on the configuration of river deltas is considered. The analytical solutions proposed in this section are derived either from Carslaw and Jaeger (1956) solution or by the Laplace transform technique. The details of each solution is discussed in the following subsections.

3.5.1 Basic equations

The two basic equations for the prediction of shoreline changes are given as; the continuity equation of sediment transport for long time variation and an expression for the total rate of longshore sediment transport.

(1) Continuity equation of sediment transport

Iwagaki (1966) considered a control volume of sediment and formulated a mass balance during an infinitesimal interval of time to derive an equation of continuity of sediment transport. For long-time variation, Tsuchiya (1973, 1978) modified this equation by expressing the sediment input from a river by Dirac's delta function and considering the concept of one-line theory. The continuity equation of sediment transport is finally expressed as :

$$\frac{\partial y_0}{\partial t} + \frac{1}{(1-\lambda)\,h_k}\frac{\partial Q_X}{\partial x} = \frac{1}{B\,h_k} Q_R(t)\,\delta(x - x_0) \qquad (3.2)$$

in which y_0 is the shoreline position, x is the longshore direction, t is the time, λ is the correction factor for the pore space of beach sediment (approximately 0.4 for most beach deposits), h_k is the limited depth of sediment motion, Q_X is the total rate of longshore sediment transport, and $\delta(x - x_0)$ is the delta function defined by Dirac for sediment source from a river $Q_R(t)$ at $x=x_0$. In order to solve Eq. (3.2) it is necessary to specify an expression for predicting the total rate of longshore sediment transport, Q_X.

(2) Longshore sediment transport rate

In Chapter 2, a new theory for the non-uniformity of longshore currents and the non-uniformity of the total rate of longshore sediment transport is presented. The expression for the total rate of longshore sediment transport is rewritten, Eq. (2.68), as:

$$Q_x = \frac{c_0}{m} \left(\frac{\rho}{\sigma}\right) I(R, F_r)\, h_b^2\, U_0 \tag{3.3}$$

in which the function $I(R,F_r)$ includes the effect of wave properties and some effects of sediment size. The non-uniform longshore current U_0 is given by Eq. (2.48) as:

$$\alpha_1 \frac{\partial}{\partial t}(U_0 h_b^2) + \alpha_2 \frac{\partial}{\partial x}(U_0^2 h_b^2) + \alpha_3 \frac{\gamma C_f c_b}{\pi} U_0 h_b = f(x) \tag{3.4}$$

and

$$f(x) = \frac{\gamma^2}{16} g h_b^2 \{ \sin 2\alpha_b - 2\cos^2\alpha_b \frac{\partial y_b}{\partial x} - (5\beta_1 - 6\beta_2 + 6\beta_3 \sin^2\alpha_b) \frac{\partial h_b}{\partial x} - 2\beta_3 h_b \sin 2\alpha_b \frac{\partial \alpha_b}{\partial x} \} \tag{3.5}$$

in which the coefficients α_i and β_i, i= 1, 2, 3, are the integration coefficients expressed in detail in Chapter 2. Now we have a set of simultaneous equations, Eqs. (3.2), (3.3) and (3.4) which are the basic equations for the evolution of shoreline changes of a river delta. The next subsections deal with the solutions of these equations with various initial and boundary conditions.

3.5.2 Linearization of longshore sediment transport rate

The total rate of longshore sediment transport expressed by Eq. (3.3) is proportional to the breaking wave height and to the non-uniform longshore current velocity Uo. In order to obtain a closed-form solution of shoreline change a simple formulation for the total rate of longshore sediment transport must be applied. The linearization of the total rate of longshore sediment transport is made by neglecting the nonlinear terms in Eq. (3.4) to arrive at:

$$Q_x = C \left(\frac{\rho}{\sigma}\right) I(R, F_r) h_b^2 \sqrt{g h_b} \sin 2\alpha_b \qquad (3.6)$$

in which $$C = \frac{5\pi}{32} \frac{c_0 \gamma}{f} \qquad (3.7)$$

Equation (3.6) is implicitly proportional to twice the incident breaking wave angle to the shoreline and to breaking wave height. For beaches with mild slopes, it can be safely assumed that small changes in the orientation of the shoreline produce small changes in the breaking wave angles. Also, small shoreline changes produce small changes in the breaking wave height. Under these assumption the total rate of longshore sediment transport can be expressed by Taylor series and approximated to the first order as:

$$Q_x = Q_0 + \frac{\partial Q_x}{\partial \alpha_{b0}} (\alpha_b - \alpha_{b0}) + \frac{\partial Q_x}{\partial h_{b0}} (h_b - h_{b0}) + \ldots\ldots\ldots\ldots \qquad (3.8)$$

in which Q_0 denotes the total rate of longshore sediment transport at the initial wave conditions presented by the subscript 0. With reference to the above assumptions, the small changes in the breaking wave angle and height can be expressed mathematically as:

$$\Delta\alpha_b = \alpha_b - \alpha_{b0} \approx - \frac{\partial y_0}{\partial x} \qquad (3.9)$$

and

$$\Delta h_b = \Delta m \, \Delta y_0 \qquad (3.10)$$

Introducing Eqs. (3.8), (3.9) and (3.10) to Eq. (3.2), the following equation is derived as:

$$\frac{\partial y_0}{\partial t} + \varepsilon_1 \frac{\partial y_0}{\partial x} - \varepsilon_2 \frac{\partial^2 y_0}{\partial x^2} = q_R(t) \delta(x - x_0) \qquad (3.11)$$

where

$$\varepsilon_1 = \frac{\Delta m}{(1-\lambda) h_k} \left(\frac{\partial Q_x}{\partial h_b}\right)_{h_{b0}} \qquad (3.12)$$

$$\varepsilon_2 = \frac{1}{(1-\lambda)\,h_k} \left(\frac{\partial Q_x}{\partial \alpha_b}\right)_{\alpha_{b0}} \tag{3.13}$$

$$q_R(t) = \frac{1}{B\,h_k} Q_R(t) \tag{3.14}$$

Equation (3.11) is identical to the one-dimensional equation described as a linear partial differential equation. The coefficient ε_2 which has the dimensions of length squared over time, is interpreted as a diffusion coefficient. While the coefficient ε_1, having the dimension of length over time, is interpreted as the traveling speed of shoreline towards the longshore direction. In Eq. (3.12) it is clearly seen that the coefficient ε_1 is proportional to the change in beach slope, denoted by Δm. Thus, the coefficient ε_1 can not be ignored when the beach slope is changeable along the delta coast, as in the case of river-dominated delta type where the beach slope at the river mouth is steeper than the beach slope at the end sides of the river.

In fact, the one-line theory assumption of a beach profile which moves parallel to itself is limited when it is applied to the formation of a river delta of a river-dominated type, where the beach slope at the river mouth is much steeper than the beach slope at the end side of river delta. Moreover, the coefficient ε_1 causes an asymmetrical configuration of the river delta when obliquely incident waves approach the beach. The degree of the asymmetrical configuration of the river delta increases with the increasing of the incident wave angle. On the contrary, when the shoreline gently changes along the delta coast and the waves approach the beach normally, the coefficient ε_1 becomes very small and can be neglected. In other words, when a river delta is categorized as a wave-dominated type, the coefficient ε_1 is very small and Eq. (3.11) will reduce to a diffusion type equation which has a symmetrical solution for the evolution of the river delta. The linear partial differential equation presented by Eq. (3.11) can be transformed to the diffusion type equation by substitution

$$y_0 = z_0 \exp\left[\frac{\varepsilon_1}{2\varepsilon_2} x - \frac{\varepsilon_1^2}{4\varepsilon_2} t\right] \tag{3.15}$$

into Eq. (3.11), to show

$$\frac{\partial z_0}{\partial t} = \varepsilon_2 \frac{\partial^2 z_0}{\partial x^2} + q_R(t)\,\delta(x - x_0)\exp\left[-\frac{\varepsilon_1}{2\varepsilon_2}x + \frac{\varepsilon_1^2}{4\varepsilon_2}t\right] \qquad (3.16)$$

By specifying initial and boundary conditions in the areas which represent conditions prevailing in a specific shoreline evolution situation, the corresponding analytical solutions are directly applicable. Carslaw and Jaeger (1956) provided many solutions of the diffusion type equation. The analytical solutions discussed here are derived either from Carslaw and Jaeger or by direct applying the Laplace transform technique. The details of each solution is described in the following subsections.

3.5.3 General formal solution of river delta formation

The basic differential equation to solve is Eq. (3.11), together with the associated initial and boundary conditions. An infinitely long beach exposed to waves of constant properties is assumed. If the river mouth is small in comparison to the area into which it is discharging sediment, the river discharge may be approximated as a point source. Also, if the shoreline shape at time t = 0 is described by a function f(x), thus the general formal solution of river delta formation can be expressed (according to, Carslaw and Jaeger, 1959) as:

$$z_0(x,t) = \frac{1}{2\sqrt{\varepsilon_2 \pi}} \int_0^t \frac{q_R(t')\,\delta(x-x_0)}{\sqrt{(t-t')}} \exp\left[-\left[\frac{(x-x_0)^2}{4\varepsilon_2(t-t')} + \frac{\varepsilon_1}{2\varepsilon_2}x - \frac{\varepsilon_1^2}{4\varepsilon_2}(t-t')\right]\right] dt \qquad (3.17)$$

and

$$y_0(x,t) = z_0(x,t)\,\exp\left[\frac{\varepsilon_1}{2\varepsilon_2}x - \frac{\varepsilon_1^2}{4\varepsilon_2}t\right] \qquad \text{for } t > 0 \text{ and } -\infty < x < \infty \qquad (3.18)$$

where the shoreline position, denoted by y_0, is a function of x and t. The quantity t' is a dummy integration variable. Consequently, the configuration of the shoreline of river delta can be determined if Eq. (3.17) is evaluated.The simplifying analytical solutions for various river delta configurations are derive mostly from using Eq. (3.17) as well as Laplace transform technique.

3.5.4 Configuration of river delta of infinite length

Since the wave is assumed normally incident the configuration of river delta will be symmetrical with respect to the point source. If the river delta is exposed to a strong wave field, wave-dominated, the shoreline will be change gently along the delta coast. Therefore the coefficient ε_1 becomes very small and can be neglected. When the river sediment discharge is constant being q_{R0}, the solution derived from Eq. (3.17) is given as:

$$y_0(x,t) = h_k q_{R0} \sqrt{\frac{t}{\varepsilon_2}}\ \text{ierfc}\left[\frac{x - x_0}{2\sqrt{\varepsilon_2 t}}\right] \qquad \text{for } t > 0 \text{ and } -\infty < x < \infty \qquad (3.19)$$

where ierfc denotes the integral of the complementary error function erfc which is expressed as:

$$\text{ierfc}\ \omega = \int_{\omega}^{\infty} \text{erf}\ \zeta \quad d\zeta \qquad (3.20)$$

In Figure 3.39 the solution to Eq. (3.19) is illustrated. The shoreline position is normalized by the limiting depth of littoral drift, h_k, and the ratio $h_k q_{R0}/\varepsilon_2$, while the longshore distance is normalized by h_k. Since the configuration of river delta is symmetric, only half of the delta shape is presented in Figure 3.39. The quantity used to normalize the shoreline position is expressed as:

$$\frac{h_k q_{R0}}{\varepsilon_2} = \frac{Q_{R0}}{(\partial Q_x / \partial \alpha_b)_{\alpha_{b0}}} \qquad (3.21)$$

This quantity can be interpreted as a ratio between sediment discharge from the river and the derivative of longshore sediment transport rate to the breaking wave angle. The time required for the delta to reach a certain distance y_0 from the original shoreline position is calculated from the following relationship:

$$y_0(t) = h_k q_{R0} \sqrt{\frac{t}{\varepsilon_2 \pi}} \qquad \text{for } t > 0 \text{ and } (x - x_0) = 0 \qquad (3.22)$$

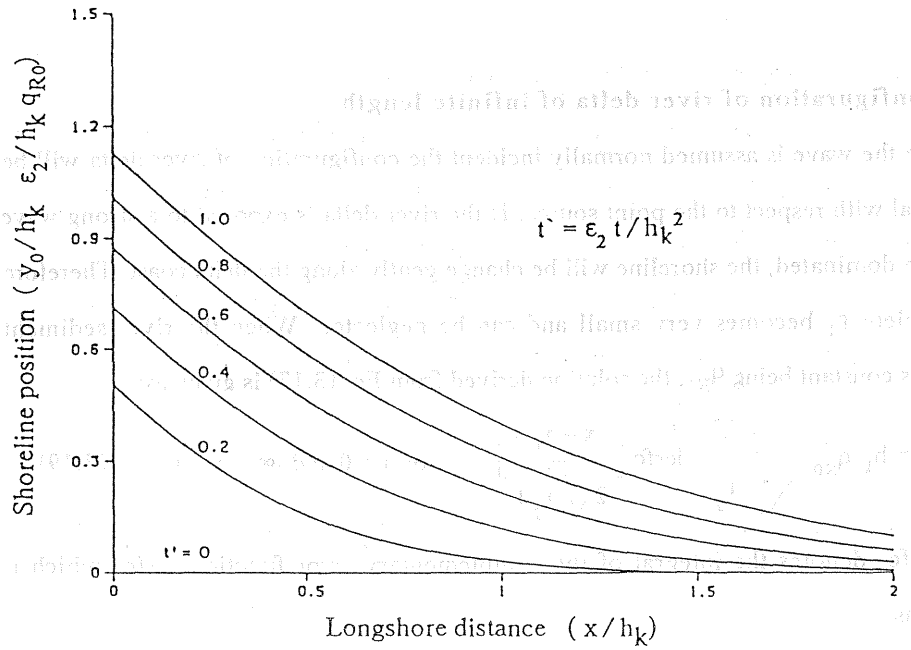

Figure 3.39 Shoreline evolution of symmetrical configuration of infinite length.

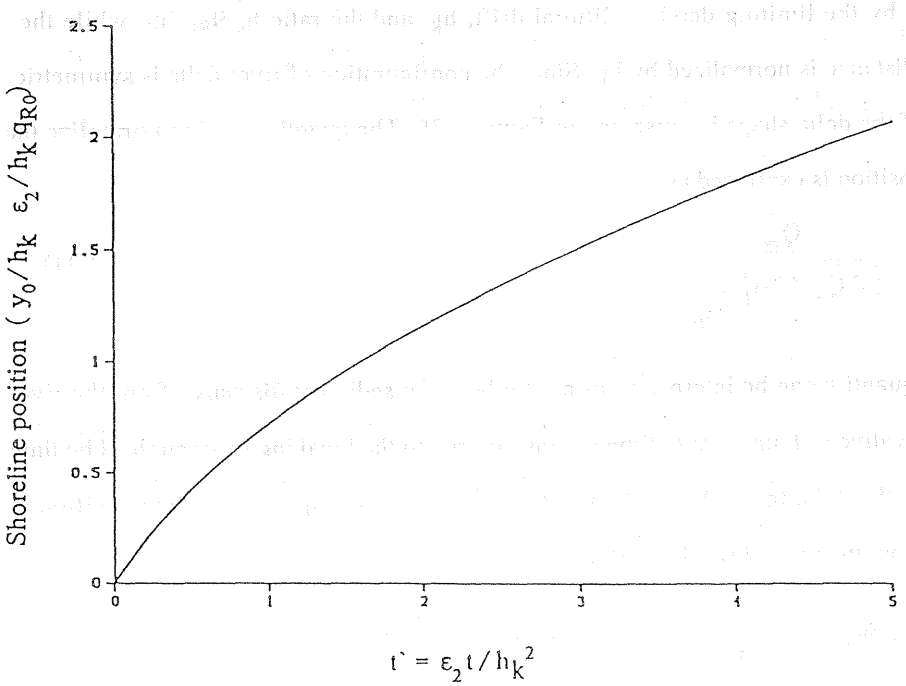

Figure 3.40 Time variation of shoreline position at the center of a river of infinite length.

Equation (3.22) is illustrated in the nondimensional diagram of Figure 3.40. For a specific wave climate, the above relation implies that an increase in the river sediment discharge has a proportional effect on the growth of the delta according to the following relation:

$$\frac{y_{01}}{y_{02}} = \frac{q_{R01}}{q_{R02}} \tag{3.23}$$

Here, the indices 1 and 2 refer to two different river sediment discharge conditions exposed to the same wave climate.

3.5.5 Configuration of river delta of finite river mouth

If the river mouth has a finite width in comparison to the area into which it is discharging sediment, an approximation by a point source is no longer accurate. Instead of supplying sediment to the beach via the delta function, the continuity equation of sediment transport will be applied twice, once over the river mouth where q_{R0} is assumed a uniformly distributed along the river mouth of a length 2a, and once outside the river mouth where q_{R0} is no longer been considered. Mathematically, the situation is expressed as:

$$\frac{\partial y_{01}}{\partial t} = \varepsilon_2 \frac{\partial^2 y_{01}}{\partial x^2} + q_{R0}; \qquad -a \le x \le a \tag{3.24}$$

and

$$\frac{\partial y_{02}}{\partial t} = \varepsilon_2 \frac{\partial^2 y_{02}}{\partial x^2}; \quad |x| > a \tag{3.25}$$

Since the configuration is symmetric with respect to the center of the river mouth, only half of the problem domain will be treated. The boundary conditions are no sediment transport through the center of the river (symmetry), and the beach must be continuous at all times between the two areas. Furthermore, the shoreline is unaffected by the river sediment discharge as x approaches infinity. According to Carslaw and Jaeger (1959), the solution is

$$y_{01}(x,t) = q_{R0}\,t\left[1 - 2\,i^2\mathrm{erfc}\left(\frac{a-x}{2\sqrt{\varepsilon_2 t}}\right) - 2\,i^2\mathrm{erfc}\left(\frac{a+x}{2\sqrt{\varepsilon_2 t}}\right)\right] \qquad (3.26)$$

for $t > 0$ and $0 \le |x| \le a$

$$y_{02}(x,t) = 2\,q_{R0}\,t\left[i^2\mathrm{erfc}\left(\frac{x-a}{2\sqrt{\varepsilon_2 t}}\right) - i^2\mathrm{erfc}\left(\frac{x+a}{2\sqrt{\varepsilon_2 t}}\right)\right] \qquad (3.27)$$

for $t > 0$ and $|x| > a$

The function ierfc, the integral of the complementary error function, is defined in Eq. (3.20) and the superscript 2 denotes a double integration. The n exponent represents n time integrations of the complementary error function. The following recurrence relation holds for $n > 1$:

$$2n\,i^n\mathrm{erfc}\,\omega = i^{n-2}\mathrm{erfc}\,\omega - 2\omega\,i^{n-1}\mathrm{erfc}\,\omega \qquad (3.28)$$

The solution to Eqs (3.26) and (3.27) is illustrated in Figure 3.41 where the shoreline position is normalized by half river width, a, and the quantity which can be interpreted as a ratio between river sediment discharge and longshore sediment transport rate. This quantity is expressed as:

$$\frac{2\,a\,q_{R0}}{\varepsilon_2} = \frac{Q_{R0}}{W_E} \qquad (3.29)$$

where Q_{R0} is the rate of sediment input from a river, and W_E denotes the effect of wave energy flux presented by the longshore sediment transport rate. In order to study the effect of the quantity given by Eq. (3.29) on the plane shape of the river delta, the longshore distance from the center of the river mouth, denoted by B, where the shoreline position is half the shoreline position at the center of the river, is plotted versus the quantity Q_{R0}/W_E. The result is shown in Figure 3.42, where B is normalized by shoreline position y_0. From this figure it is obvious that; 1) in general the distance B decreases with increasing Q_{R0}/W_E which implies that as the delta type becomes river-dominated, the delta plane shape becomes sharp with a large shoreline gradient, $|\partial y_0/\partial x|$, 2) on the contrary, as the ratio Q_{R0}/W_E becomes smaller

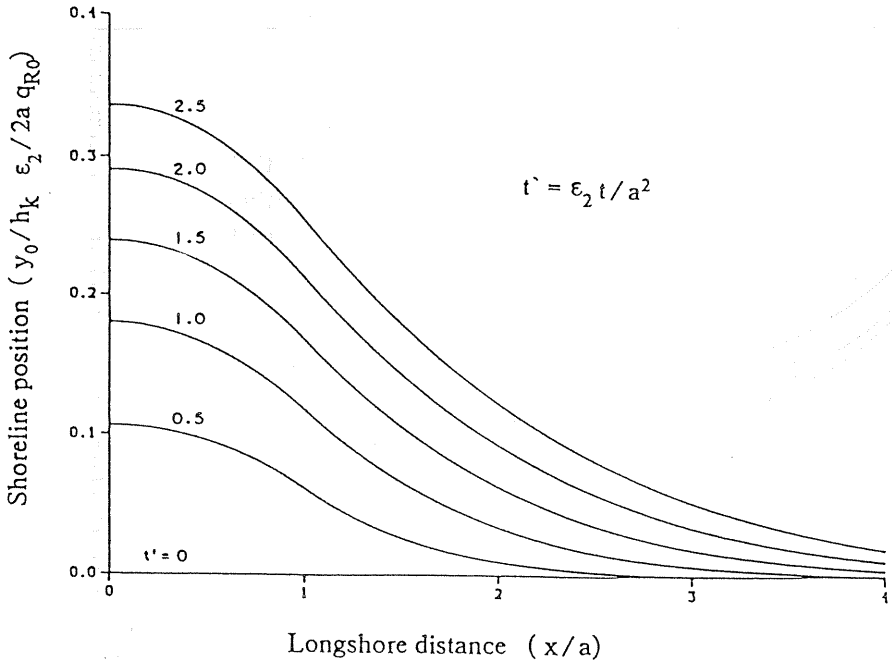

Figure 3.41 Shoreline evolution of symmetrical configuration of river delta of finite river mouth.

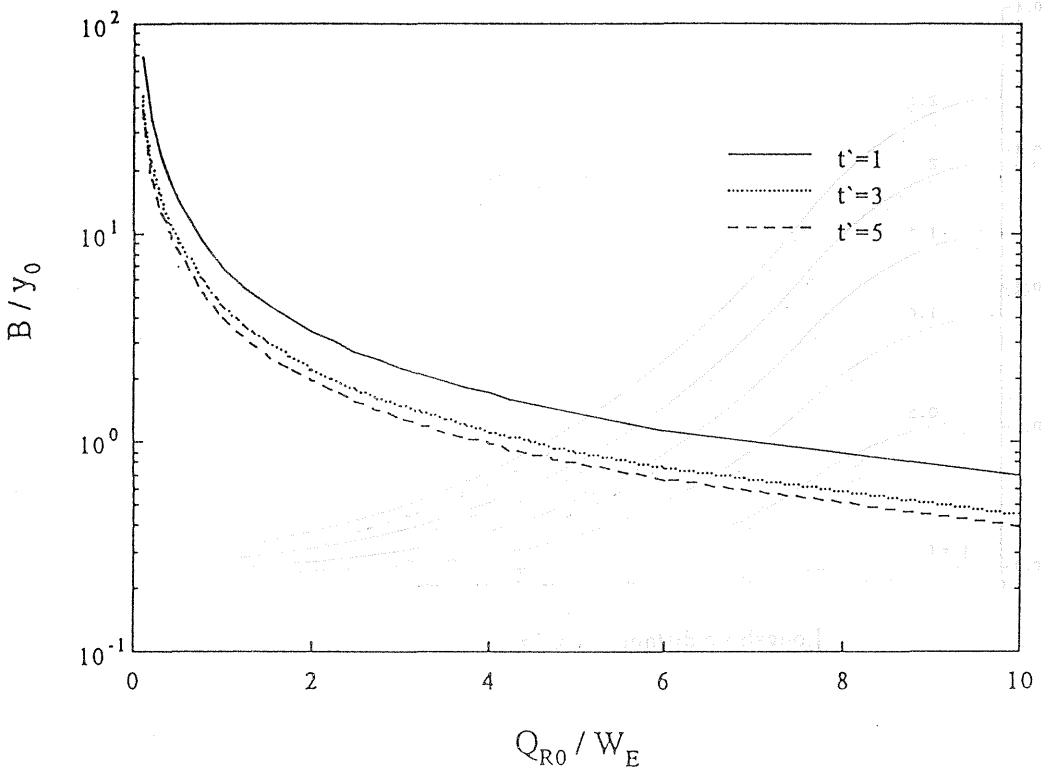

Figure 3.42 Relationship between a longshore distance B, where shoreline position is half of maximum value at the center of river mouth, and ratio between river sediment discharge and wave power.

the delta will be classified as wave-dominated type and the delta plane shape will be gently mild with a small shoreline gradient, $|\partial y_0/\partial x|$, and 3) for a specific ratio Q_{R0}/W_E, the distance B decreases with increasing the time t, which implies that the rate of deposited sediment around the river mouth increases with time.

3.5.6 Asymmetric configuration of river delta

In the previous analytical solutions the waves always approach the delta coast normally, and therefore the configurations of river delta are always symmetrical. When the waves approach the delta coast obliquely, the expected shape of the delta will be asymmetric. Consider the case where a river mouth with finite width, the continuity equation of sediment transport in the full form of Eq. (3.11) is applied as:

$$\frac{\partial y_{01}}{\partial t} = -\varepsilon_1 \frac{\partial y_{01}}{\partial x} + \varepsilon_2 \frac{\partial^2 y_{01}}{\partial x^2} + q_{R0}\,; \quad -a \le x \le a \tag{3.30}$$

and

$$\frac{\partial y_{02}}{\partial t} = -\varepsilon_1 \frac{\partial y_{02}}{\partial x} + \varepsilon_2 \frac{\partial^2 y_{02}}{\partial x^2}\,; \quad |x| > a \tag{3.31}$$

with the initial condition

$$y_{01}(x,0) = y_{02}(x,0) \tag{3.32}$$

and the boundary conditions

$$y_{02} = 0, \quad \frac{\partial y_{02}}{\partial x} = 0\,; \qquad \text{at } x \to \infty \tag{3.33}$$

$$y_{01} = y_{02}, \quad \frac{\partial y_{01}}{\partial x} = \frac{\partial y_{02}}{\partial x}\,; \quad \text{at } x = a \tag{3.34}$$

The problem consists of two coupled partial differential equations with appropriate initial and boundary conditions. By introducing the expression given by Eq. (3.15), Eqs. (3.30) and (3.31) will be transformed to the diffusion type equations and are expressed as:

$$\frac{\partial z_{01}}{\partial t} = \varepsilon_2 \frac{\partial^2 z_{01}}{\partial x^2} + q_{R0} \exp\left[-\frac{\varepsilon_1}{2\varepsilon_2} x + \frac{\varepsilon_1^2}{4\varepsilon_2} t\right]; \quad -a \le x \le a \tag{3.35}$$

and

$$\frac{\partial z_{02}}{\partial t} = \varepsilon_2 \frac{\partial^2 z_{02}}{\partial x^2}; \quad |x| > a \tag{3.36}$$

with the initial condition

$$z_{01}(x, 0) = z_{02}(x, 0) \tag{3.37}$$

and the boundary conditions

$$z_{02} = 0, \quad \frac{\partial z_{02}}{\partial x} = 0; \qquad \text{at } x \to \infty \tag{3.38}$$

$$z_{01} = z_{02}, \quad \frac{\partial z_{01}}{\partial x} = \frac{\partial z_{02}}{\partial x}; \qquad \text{at } x = a \tag{3.39}$$

In order to solve the problem with the appropriate initial and boundary conditions, the Laplace transform technique is applied. This technique is powerful for solving linear partial differential equations. It allows the target partial differential equation in the transformed plane to be used for solving one-dimensional problems in space. By using the Laplace transform technique, ordinary linear differential equations are obtained as :

$$\frac{d^2 W_1}{dx^2} - \frac{s}{\varepsilon_2} W_1 = -\frac{1}{\varepsilon_2 (s - \varepsilon_1^2/4\varepsilon_2)^2} q_{R0} \exp\left[-\frac{\varepsilon_1}{2\varepsilon_2} x\right]; \quad -a \le x \le a \tag{3.40}$$

$$\frac{d^2 W_2}{dx^2} - \frac{s}{\varepsilon_2} W_2 = 0; \qquad |x| > a \tag{3.41}$$

where the function W denotes the Laplace transformed function of z_0, and 1, 2 refer to the two applied areas. The function W is defined by the operation :

$$W = \mathcal{L}\{z_0\} = \int_0^\infty z_0(x, t)\, e^{-st}\, dt \tag{3.42}$$

The boundary conditions are transformed as;

$$W_2 = 0, \quad \frac{\partial W_2}{\partial x} = 0 ; \qquad \text{at } x \to \infty \tag{3.43}$$

$$W_1 = W_2 , \quad \frac{\partial W_1}{\partial x} = \frac{\partial W_2}{\partial x} ; \text{ at } x = a \tag{3.44}$$

The general solution for the ordinary linear differential equations is

$$W_1 = C_1 e^{xR} + C_2 e^{-xR} + \frac{q_{R0}}{(s - \varepsilon_1^2/4\varepsilon_2)} \exp\left[-\frac{\varepsilon_1}{2\varepsilon_2} x\right] ; \quad -a \le x \le a \tag{3.45}$$

$$W_2 = D_1 e^{xR} + D_2 e^{-xR} ; \quad |x| > a \tag{3.46}$$

where $$R^2 = \frac{s}{\varepsilon_2} \tag{3.47}$$

The coefficients C_1, C_2, D_1 and D_2 must be determined from the boundary conditions Eqs. (3.43) and (3.44), and they are in general, functions of the parameter s. To obtain a solution in the time domain, Eqs (3.45) and (3.46) must be inverse transforms. This can be accomplished using tables of known transforms (see, for example, Abramowitz and Stegun 1972; and Kreyszig, 1983). The solution to Eqs. (3.35) and (3.36) is then performed as:

$$z_{01}(x,t) = q_{R0}\, t \exp\left[-\frac{\varepsilon_1}{\varepsilon_2}x + \frac{\varepsilon_1^2}{4\varepsilon_2} t\right] \left[\begin{array}{l} 1 - 2\,i^2\mathrm{erfc}\left(\dfrac{a-x}{2\sqrt{\varepsilon_2 t}}\right) - 2\,i^2\mathrm{erfc}\left(\dfrac{a+x}{2\sqrt{\varepsilon_2 t}}\right) \\ + \dfrac{2\varepsilon_1}{\varepsilon_2}\, i^3\mathrm{erfc}\left(\dfrac{x-a}{2\sqrt{\varepsilon_2 t}}\right) \\ - \dfrac{2\varepsilon_1}{\varepsilon_2}\, i^3\mathrm{erfc}\left(\dfrac{x+a}{2\sqrt{\varepsilon_2 t}}\right) \exp\left(-\dfrac{\varepsilon_1}{\varepsilon_2} a\right) \end{array}\right] \tag{3.48}$$

for $t > 0$ and $0 \le |x| \le a$, and

$$z_{02}(x,t) = 2\,q_{R0}\,t\,\exp\left[-\frac{\varepsilon_1}{\varepsilon_2}x + \frac{\varepsilon_1^2}{4\varepsilon_2}t\right]\left[\begin{array}{l} i^2\mathrm{erfc}\left(\dfrac{x-a}{2\sqrt{\varepsilon_2 t}}\right) - i^2\mathrm{erfc}\left(\dfrac{x+a}{2\sqrt{\varepsilon_2 t}}\right) \\ +\dfrac{\varepsilon_1}{\varepsilon_2} i^3\mathrm{erfc}\left(\dfrac{x-a}{2\sqrt{\varepsilon_2 t}}\right) \\ -\dfrac{\varepsilon_1}{\varepsilon_2} i^3\mathrm{erfc}\left(\dfrac{x+a}{2\sqrt{\varepsilon_2 t}}\right)\exp\left(-\dfrac{\varepsilon_1}{\varepsilon_2}a\right) \end{array}\right] \tag{3.49}$$

for $t > 0$ and $|x| > a$,

in which the function ierfc represents the integral of the complementary error function and the superscript number denotes the number of integration. An expression is given by Eq. (3.29) for n time integrations of the complementary error function. Substitution of Eq. (3.16) into Eqs. (3.48) and (3.49), the solution to Eqs. (3.30) and (3.31) is obtained as:

$$y_0(x,t) = \begin{cases} \exp\left[\dfrac{3\varepsilon_1}{2\varepsilon_2}x\right] F_1(x,t); & -\infty < x \le -a \\ \exp\left[\dfrac{3\varepsilon_1}{2\varepsilon_2}x\right] F_2(x,t); & -a \le x \le 0 \\ \exp\left[-\dfrac{\varepsilon_1}{2\varepsilon_2}x\right] F_2(x,t); & 0 \le x \le a \\ \exp\left[-\dfrac{\varepsilon_1}{2\varepsilon_2}x\right] F_1(x,t); & a \le x < \infty \end{cases} \tag{3.50}$$

where

$$F_1(x,t) = 2\,q_{R0}\,t \left[\begin{array}{l} i^2\mathrm{erfc}\left(\dfrac{x-a}{2\sqrt{\varepsilon_2 t}}\right) - i^2\mathrm{erfc}\left(\dfrac{x+a}{2\sqrt{\varepsilon_2 t}}\right) \\ +\dfrac{\varepsilon_1}{\varepsilon_2}\, i^3\mathrm{erfc}\left(\dfrac{x-a}{2\sqrt{\varepsilon_2 t}}\right) \\ -\dfrac{\varepsilon_1}{\varepsilon_2}\, i^3\mathrm{erfc}\left(\dfrac{x+a}{2\sqrt{\varepsilon_2 t}}\right) \exp\left(-\dfrac{\varepsilon_1}{\varepsilon_2}a\right) \end{array} \right] \tag{3.51}$$

and

$$F_2(x,t) = q_{R0}\,t \left[\begin{array}{l} 1 - 2\,i^2\mathrm{erfc}\left(\dfrac{a-x}{2\sqrt{\varepsilon_2 t}}\right) - 2\,i^2\mathrm{erfc}\left(\dfrac{a+x}{2\sqrt{\varepsilon_2 t}}\right) \\ +\dfrac{2\,\varepsilon_1}{\varepsilon_2}\, i^3\mathrm{erfc}\left(\dfrac{x-a}{2\sqrt{\varepsilon_2 t}}\right) \\ -\dfrac{2\,\varepsilon_1}{\varepsilon_2}\, i^3\mathrm{erfc}\left(\dfrac{x+a}{2\sqrt{\varepsilon_2 t}}\right) \exp\left(-\dfrac{\varepsilon_1}{\varepsilon_2}a\right) \end{array} \right] \tag{3.52}$$

The solution to Eq. (3.50) is illustrated in Figure 3.43, in which the non-dimensional quantity describing the shoreline position is defined by:

$$y_0' = \frac{y_0}{a}\,\frac{\varepsilon_2}{2a\,q_{R0}} \tag{3.53}$$

The asymmetric shape of the delta is clearly seen in this figure. The non-dimensional quantity describing the effect of beach slope change and oblique wave incident on the configuration of river delta is defined according to $\varepsilon_1 a/\varepsilon_2$. Figure 3.44 demonstrates the effect of the quantity $\varepsilon_1 a/\varepsilon_2$ on the configuration of river delta. It is clearly seen that the configuration of river delta becomes asymmetric when $\varepsilon_1 a/\varepsilon_2$ is greater than zero. The degree of asymmetrical configuration of the river delta becomes highly significant as the quantity $\varepsilon_1 a/\varepsilon_2$ increases, which implies that as the incident wave angle increases, the asymmetrical configuration of the river delta becomes significantly remarkable. Also, it is obvious from Figure 3.44 that the shoreline gradient, $|\partial y_0/\partial x|$, becomes larger with increasing $\varepsilon_1 a/\varepsilon_2$ which means that

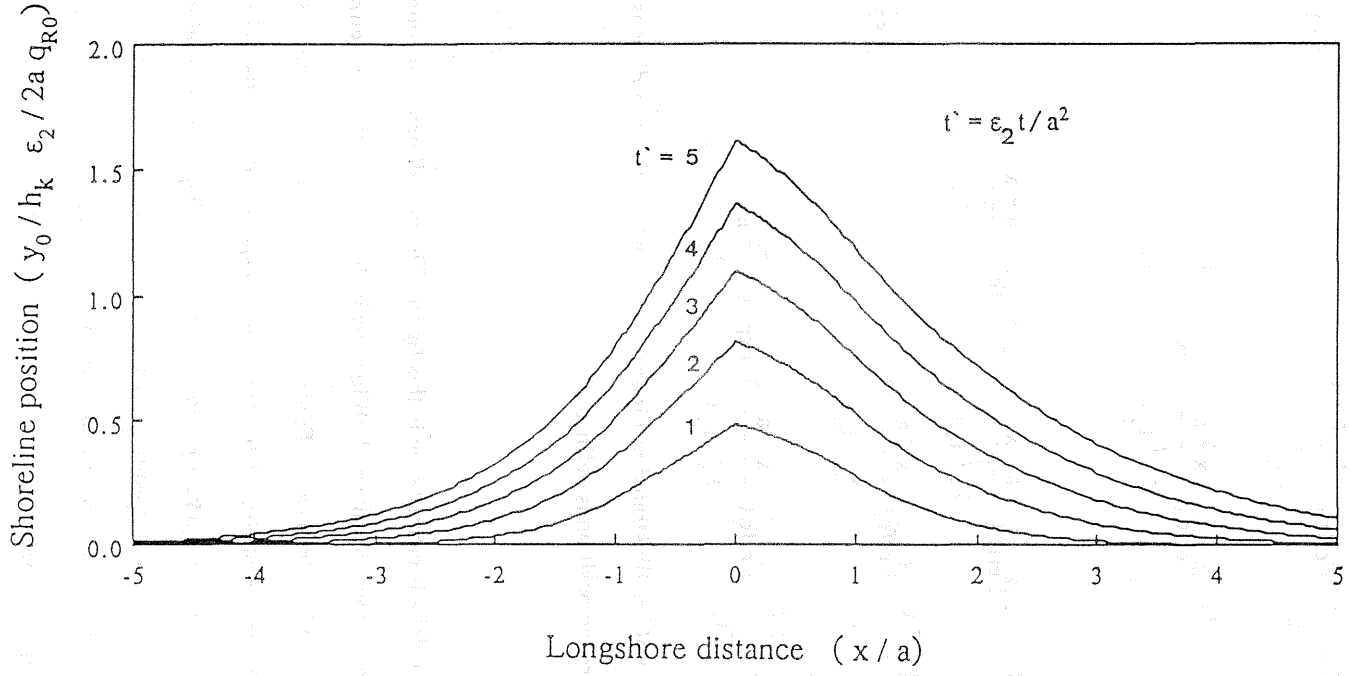

Figure 3.43 Shoreline evolution of asymmetrical configuration of river delta, ($\varepsilon_1 a / \varepsilon_2 = 0.2$).

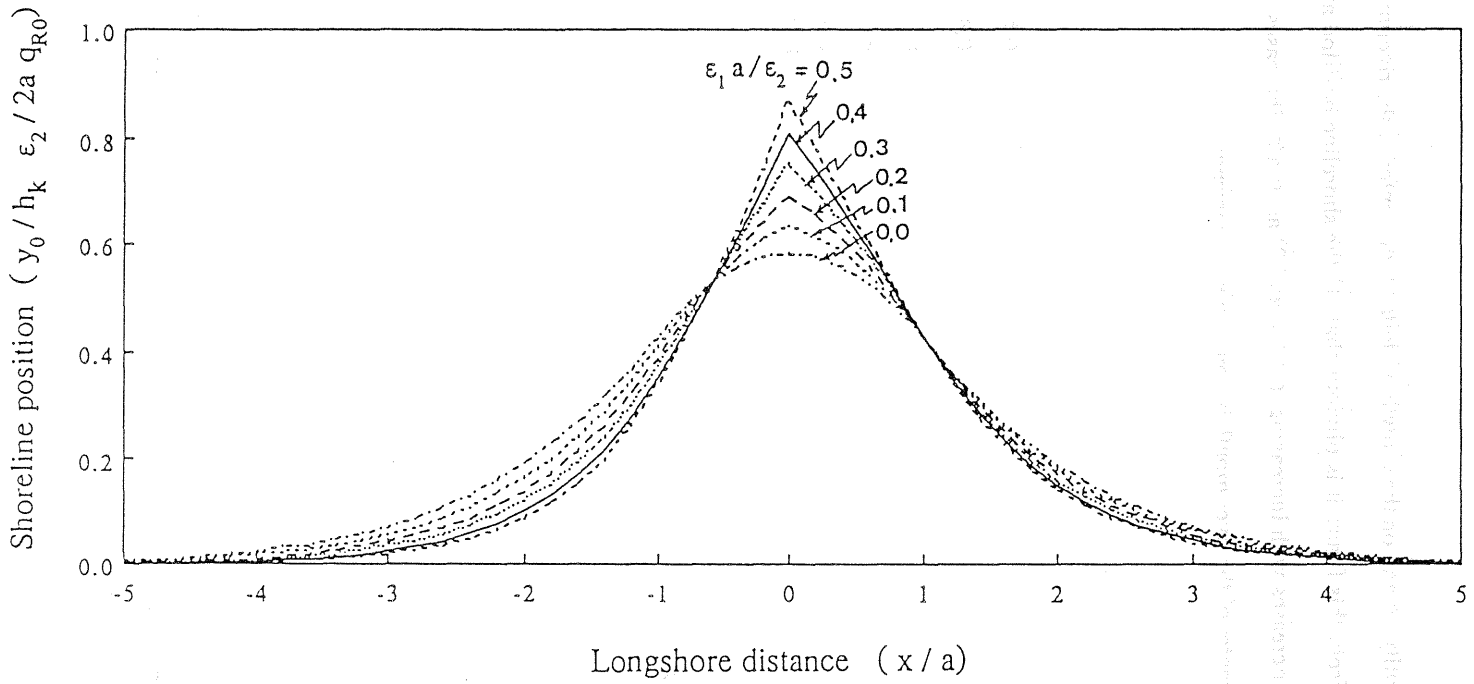

Figure 3.44 Effect of quantity $\varepsilon_1 a / \varepsilon_2$ on the configuration of river delta (t` = 2)

increasing the rate of beach slope change along the river delta causes the shape of river delta to be sharply formed.

The effect of the quantity $\varepsilon_1 a/\varepsilon_2$ on the growth of delta at the center of the river mouth is shown in Figure 3.45. From this figure it is obvious that; 1) the shoreline position at the center of the river mouth increases with increasing $\varepsilon_1 a/\varepsilon_2$, and 2) as $\varepsilon_1 a/\varepsilon_2$ increases, the rate of delta growth at the center of the river mouth becomes nearly constant.

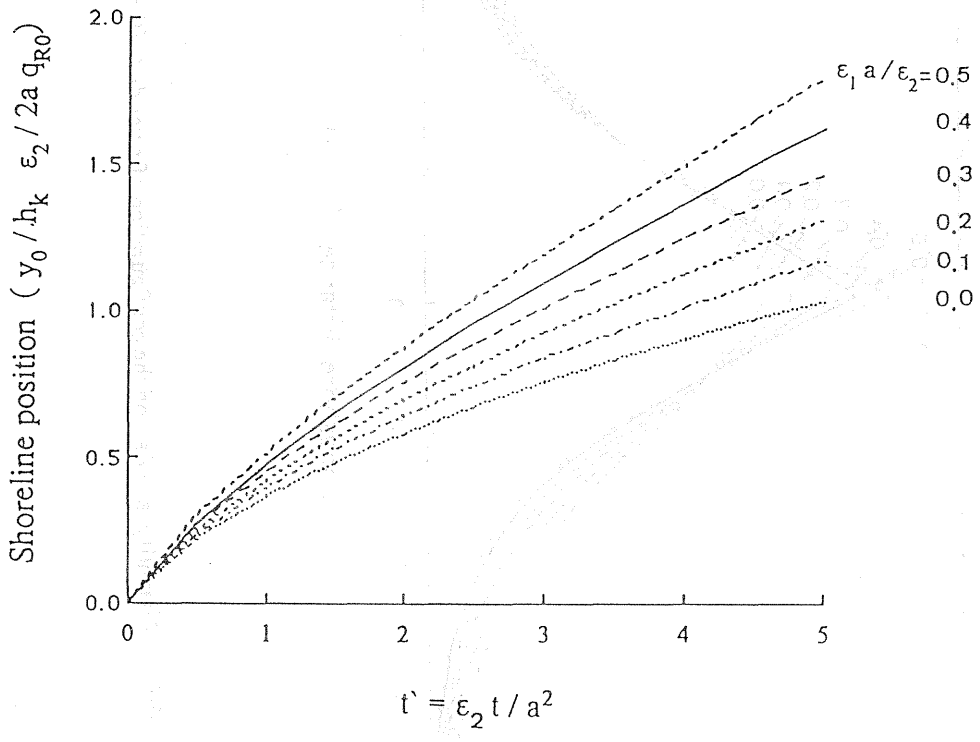

Figure 3.45 Effect of quantity $\varepsilon_1 a / \varepsilon_2$ on the time variation of shoreline position at the center of river mouth.

3.6 Experimental Study on Formation Process of River Deltas

The formation process of river deltas is controlled by the interaction between two main forces; river sediment discharge and wave power. If the rate of sediment deposition from the river is greater than the rate of sediment removal by the longshore currents, the formation process of river delta will take place. In contrast with that, if the rate of sediment deposition from the river is less than the rate of sediment removal by the longshore currents, beach erosion occurs and reduction of river delta will be remarkable.

The time scale for beach change of river deltas is on order of 100 years, therefore the seasonal changes of beach profile shape and shoreline positions during severe storms will not be considered when studying the process of formation of river deltas. In fact, the beach profile often returns to its pre-storm shape in a short time, after the storm has passed, typically on order of weeks. In contrast, imbalances in the longshore sediment transport rate cause a more gradual and permanent change in the beach plainform.

The main objectives of this experimental study are, to demonstrate the process of formation of river deltas, to determine the change of beach profiles along the shoreline of river delta, to verify the relationship between shoreline position and cross-sectional area of beach profile, and finally to study effect of oblique wave incident on the symmetrical configuration of the river delta, and on the formation process of river deltas.

3.6.1 Methods of modeling a river sediment discharge

In the hydraulic experiments modeling of river sediment discharge is not an easy task. Before the experiments on river delta formation can be carried out, the alternative methods for modeling a river sediment discharge should be examined, showing the advantage and disadvantage of every method. Finally, the most appropriate modeling method must be determined. There are three main methods to model river sediment discharge. One method deals with supplying water and sediment by using a channel, the other two methods deal with

supplying a dry sediment as a point source and as a line source. The details of each method are discussed as follows:

(1) Method of supplying water and sediment

In trying to copy nature, where the actual river flows out water carrying sediment, the most appropriate method is to construct a channel in which the water is pumped with sediment and discharged into the wave basin. To have clear understanding of this method, many factors must be considered, with discussing the effect of each factor on the formation process of river deltas and on the experimental conditions. These factors are summarized as follows:

1) Effect of stream velocity: In a case of high stream velocity the sediment is discharged and deposited out of the surf zone where the effect of longshore current is minor; resulting in formation of curved bars propagated backward by time to connect the initial shoreline. The configuration of this river delta is mainly due to river action, while the incoming waves will cause a shifting of the deformed shape to the right or to the left depending on the direction of the incident waves. Accordingly, it is implied that due to the strong water discharge, the river delta shape is so far called a fan shape river delta, and therefore, the scale and position of the alluvial fan are very unstable and severely change with time. On the contrary in a case of low velocity the sediment is deposited near the upper most end of a channel, resulting in closing a channel and no more sediment is assistance to form a river delta shape. So that, there is a critical range for the stream velocity in which, the stream velocity is able to carry sediment and deposit it within the surf zone.

2) Effect of additional water from river: It is clearly shown that the velocity of the discharged water affects the formation process of river delta, which should be taken into consideration when this method is considered. Another factor that should not be ignored the additional amount of water entering the wave basin which strongly affects the characteristics of the incoming waves via changing the water level in the wave basin. The solution to this problem is quite easy, just by discharging the same amount of water in order to keep a constant water

level in the basin.

3) Characteristics of sediment particles and rate of river sediment discharge: A sediment particle under the action of flowing water takes either a state of repose or a movement in accordance with the degree of fluid force to the resistant force of the particle. In a moving state, which is classified as either suspension or traction such as rolling, sliding and saltating, the sediment particle movement is determined by the critical shear velocity u_{*c}, which corresponds to the threshold condition of sediment movement. Generally, u_{*c} can be predicted by Shield's diagram. The sediment particle diameter is proportional to critical shear velocity and falling velocity. The particles whose falling velocities are smaller than the critical shear velocities will be kept in suspension, the other particles whose falling velocities are larger than the critical shear velocities will be deposited onto the channel bed.

The rate of sediment discharge can be controlled by using a sediment feeding system with a motor controlling device. If the rate of sediment discharge is larger than the rate of the sediment removal by wave action, the sediment will deposit at the river mouth and will accelerate the stream velocity causing a deposition of sediment on the channel bed behind the river mouth. On the contrary, if the rate of sediment discharge is smaller than the rate of sediment removal by wave action, no delta is formed and all sediment particles are carried away.

(2) Methods of supplying dry sediment

Since the sediment discharge from the river is responsible for building up a delta, and in order to avoid the effect of water discharge on the process of formation of river delta, we will consider the use of a dry sediment supplement. Although, it may be easy to model a river via dry sediment, rather than using water and sediment, some problems appear. Generally, there are two methods to model river sediment discharge using dry sediment only, they are: the point source method and the line source method. In both methods, the motor controlled sediment feeding is used to supply sediment at a constant rate. The main different between the two methods is the way of distributing the sediment over the deltaic area. The detail of

these two methods is discussed in next subsections.

1) First method (Supplying sediment as a point source): As indicated by the name of the method, the sediment is supplied at a single point, which agrees with the assumption that the river mouth width is very small compared with the finite length of the shoreline. Now, some questions arise, these questions are summarized as follows; 1) where is the best position for the point source ? and why ?, 2) which is better, to fix the position of point source or to move it, as the shoreline propagates ? and why ?, and finally 3) if it is moving, what is the rate of that movement ?.

For the first question, there are three possible positions for the point source, these positions are: 1) at the shoreline, 2) within surf zone and 3) outside surf zone. The choice of point source to be located at the shoreline makes the sediment accumulate resulting in the formation of a small hill. This is because, at the shoreline the longshore current velocity too weak to carry the sediment away. From the fact that the longshore currents are stronger inside the surf zone, the point source must be located within the surf zone. If the point source is chosen to be outside the surf zone, the longshore currents are enabled to carry the sediment particles, sufficiently. As a result, a longshore bar will form. Generally speaking, it is therefore suggested, that the position of the point source to be at the location of the maximum value of longshore sediment transport, which is just shoreward of the breaker line.

Generally, when a river delta shoreline is formed and propagates seaward, the breaker line moves seaward in a similar way. Therefore, the answer for the second and third questions is to move the position of the point source seaward at the same rate as the propagation of the shoreline of river delta. The rule of thumb is to keep the position of the point source at the location of maximum longshore sediment transport, which is just shoreward the breaker line.

(2) Second method (Supplying sediment as a line source): From the point of view of the shape of the cross-shore distribution of longshore sediment transport, which reaches a maximum value shoreward the breaker line, a line source method is proposed. The line

source consists of holes of different diameters, in which the sediment is discharged over the surf zone in distribution shape similar to distribution shape of longshore sediment transport. Although it is a good idea, the distribution shape of the longshore sediment transport must be considered, which is mainly predicted by the oblique incident waves. Additionally, around the river mouth the longshore sediment becomes non-uniform. Thus, it is believed that the point source method is easier to apply than the line source method, and it gives a reasonable accuracy for the measurements.

From the above description of the different methods of modeling river sediment discharge, the following points are drawn:

(1) The river sediment is only responsible for building up a delta, therefore the method of supplying water with sediment will be excluded, and consider only the methods of supplying dry sediment.

(2) The assumption that the river mouth is very small compared with the infinite length of the shoreline gives the point source method an advanced step over the line source method.

(3) When the line source method is used, the rate of river sediment discharge will be related to the rate of longshore sediment transport, while it should be an independent parameter. Instead the point source method gives a reasonable accuracy for the measurements.

From the above mentioned points, we decided to use the point source method for modeling the river sediment discharge. Finally, we want to mention that the experiments were carried out to verify the applicability of the point source method for modeling the river sediment discharge.

3.6.2 Experimental procedure

The experiments were performed in the fan-shaped wave basin (semicircular part : r=17.5 m ; rectangular part : 35x10 m) of Ujigawa Hydraulics Laboratory, Disaster Prevention Research Institute, Kyoto University. A smooth concrete beach was constructed

with a slope of 1:10. The beach was roughed by bonding light weight aggregate, the same material as the one whose used for modeling river sediment discharge, on to the smooth concrete. The wave guide walls, which are composed of smooth steel plates, were installed in the normal to the wave generator. The smooth steel plates were chosen such that the amplitude of refracted waves was expected to be minimal, see Figure 3.46.

On the land side, a sediment feeder machine with a controlling speed motor was set about 1.0 m from the initial shoreline, see Figure 3.46. The light weight aggregate material was chosen to model the river sediment discharge, this material is very sensitive to the wave action and has a low friction coefficient. The controlling speed motor was used to discharge sediment at a constant rate into the wave basin. Two smooth asbestos pipes of different diameters were connected to the sediment feeder machine at the output opening in order to carry the sediment to the desire position of the point source. The small diameter pipe smoothly slides inside the large diameter one allowing no sediment particles to fall between them. Thus, this system gives a free and accurate adjustment for the position of the point source. Measurements of sediment discharge rate were performed: 1) at the beginning of the experiments, and 2) at every 10 min interval time during the experiments, then the rate of sediment discharge was calculated as the average value of the measured sediment ratios.

Measurements of shoreline positions were made at 10 min intervals along the delta at 13 stations (50 cm interval distance), see Figure 3.46. At the end of each experiment, beach profiles as well as shoreline changes were measured every 10 cm interval distance along the delta. The measurements of beach profiles were made by an acoustic sensor mounted on a carriage, controlled by a personal computer. The measured profiles were transformed to digital data and recorded using a low frequency digitizer device. The formation process of river delta was observed by taking photographs every 10 minutes interval time with a 35 mm automatic camera. The camera was mounted at a height of 5 - 7 m above the water surface. The camera suspension system allows the camera to be accurately positioned and leveled.

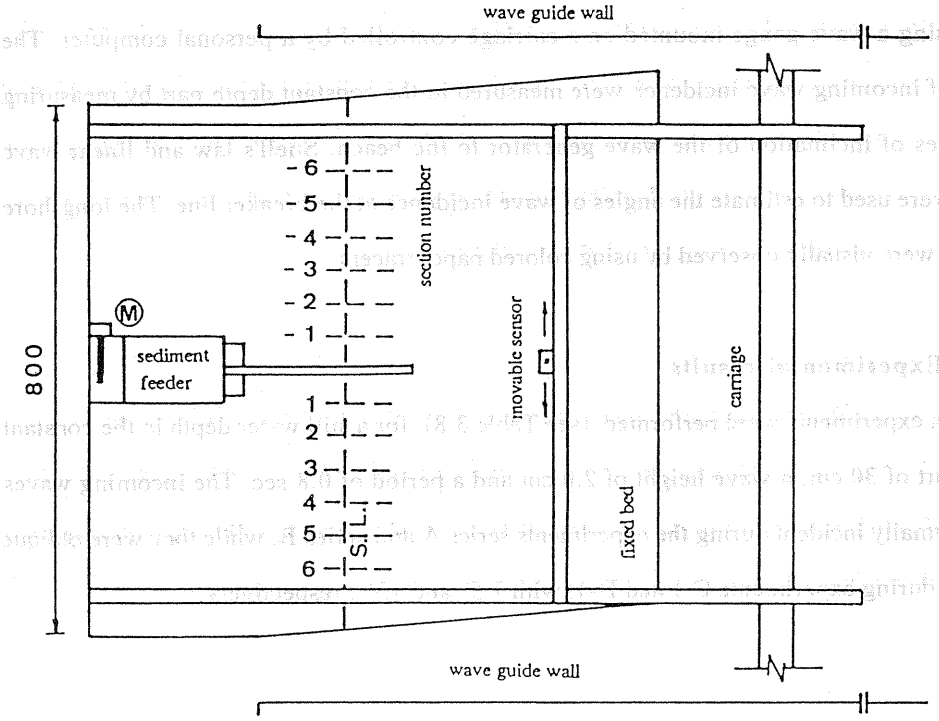

(a) Plane view.

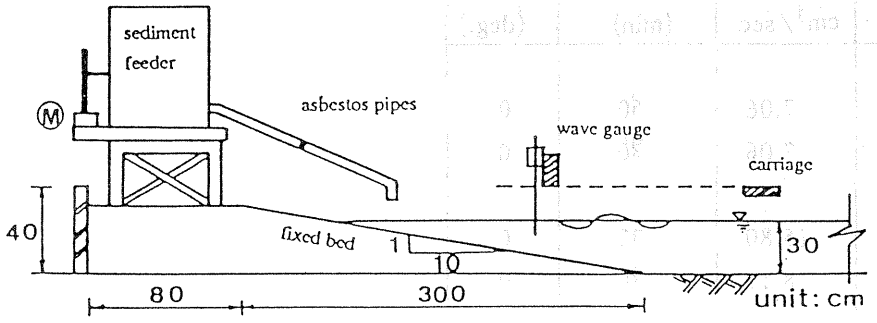

(b) Side view.

Figure 3.46 Schematic diagram of experimental arrangement of formation of river delta process.

On the wave basin side, measurements of wave heights in the constant depth part were made using capacitance type wave gauges. While on the sloping part, the measurements were made using a wave gauge mounted on a carriage controlled by a personal computer. The angles of incoming wave incidence were measured in the constant depth part by measuring the angles of inclination of the wave generator to the beach. Snell's law and linear wave theory were used to estimate the angles of wave incidence at the breaker line. The longshore currents were visually observed by using colored paper tracers.

3.6.3 Experimental results

Six experiments were performed, (see Table 3.8), for a still water depth in the constant depth part of 30 cm, a wave height of 2.0 cm and a period of 0.8 sec. The incoming waves were normally incident during the experiments series A and series B, while they were oblique incident during experiments C-1 and D-1, with 7.5° and 15° , respectively.

Table 3.8 Experimental conditions of river delta formation process.

Exp. No.	Q_R cm^3/sec	Run time (min)	α_0 (deg.)
Series A			
A-1	7.06	50	0
A-2	7.06	30	0
Series B			
B-1	15.80	30	0
B-2	8.12	30	0
Series C			
C-1	11.0	90	7.5
Series D			
D-1	11.0	180	15.0

The experimental results are as follows :

(1) General description of river delta formation process

Once the sediment feeder machine supplies sediment to the wave basin, the sediment particles spread along the coast by the effect of the longshore current. Also, a small delta is being to form on the fixed bed and propagates seaward with the nearly the same rate as the front line of delta, which means that the beach profile is moving in parallel to itself. The position of point source is moved seaward just behind the breaker point, therefore the supplying sediment particles are redistributed along the river delta by the effect of longshore currents.

It is observed that sediment particles deposit first around the river mouth then move to considerable distances from the river mouth till they deposit at the initial shoreline, forming a new shoreline. During that time other sediment particles deposit at the river mouth and once more move to considerable distances from the river mouth till they deposit at the initial shoreline and another shoreline will be formed, and so on. Finally, a series of layers appears, each layer represents a complete evolution of shoreline cycle in the formation process of river delta.

(2) Characteristics of growth of river delta

Figures 3.47 and 3.48 show the behaviors of the growth of river delta in experiments series A and B, respectively. During the experiments, the shoreline positions were measured at every 10 min and 50 cm intervals. At the end of each run, the wave generator was stopped and the shoreline positions as well as the beach profiles were measured every 10 cm interval distance in the longshore direction.

Since the rate of sediment discharge was kept constant and relatively small, Q_{R0} = 7.0 cm^3/sec, during the experiments A-1 and A-2, the measured shoreline positions shown in Figure 3.47 at t=50 min and t=80 min, respectively, are been parallel to each other. Also, the configuration of the shoreline of river delta by these experiments is gently curved. In series B, the rate of sediment discharge was relatively high, Q_{R0} = 15.0 cm^3/sec in Run B-1 and

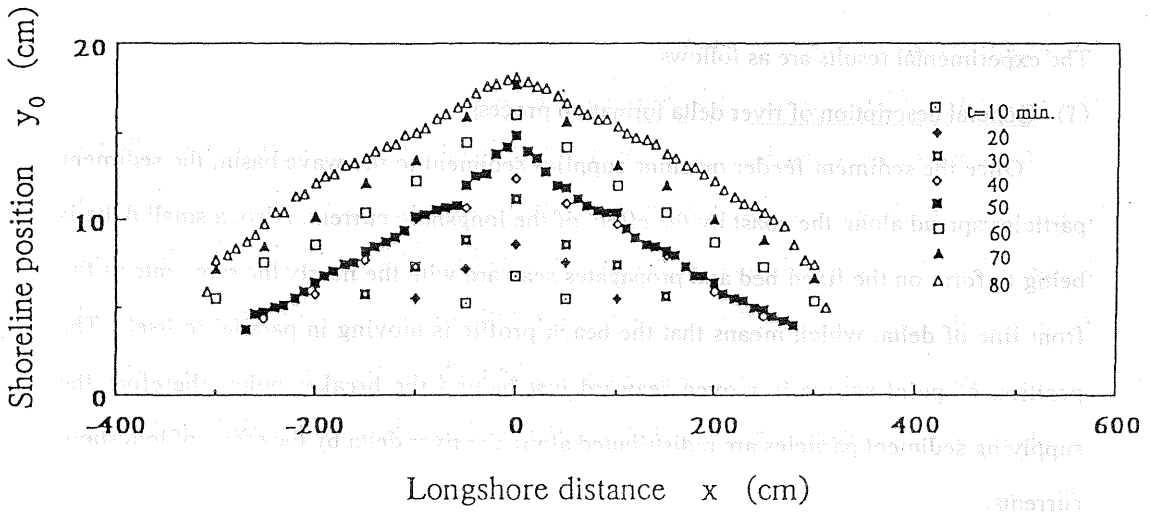

Figure 3.47 Propagation process of shoreline of river delta, (series A).

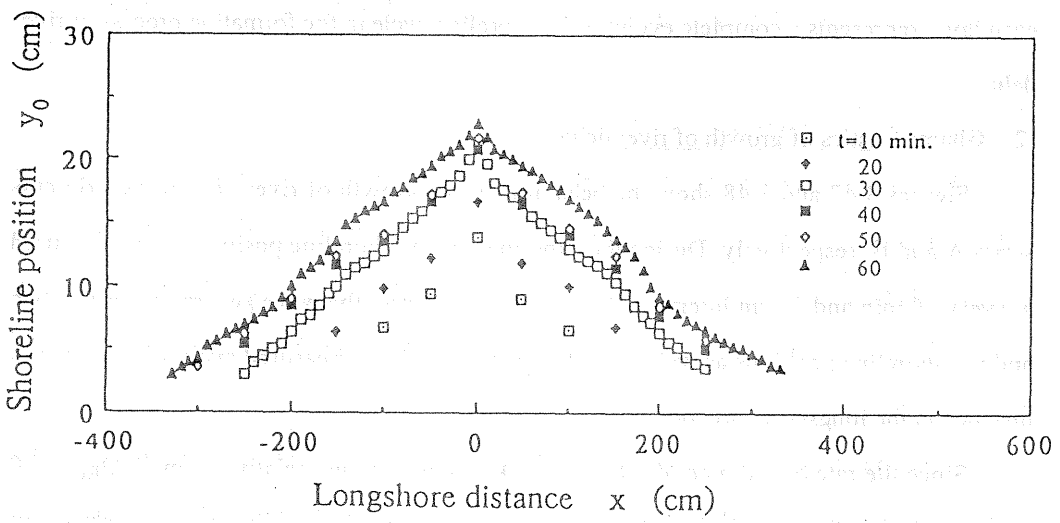

Figure 3.48 Propagation process of shoreline of river delta, (series B).

reduced by half in Run B-2. Therefore, the measured shoreline positions shown in Figure 3.48 at t=30 min and t=60 min are not perfect parallel. Moreover, much sediment particles were deposited around the point source than near the end of the delta. As a result, the configuration of the shoreline of river delta becomes sharply curved.

(3) Symmetrical shape of river delta

It is expected under a condition of normal wave incident that the configuration of river delta is symmetric. To verify this phenomenon in the laboratory, measured data of shoreline positions on the left and right sides of the delta were plotted on one side. The results are shown in Figure 3.49 for Run A-1 and Run A-2, and in Figure 3.50 for Run B-1 and Run B-2, respectively. The black symbols represent the measured data on the left side, whereas the measured data on the right side are represented by the white symbols. The symmetrical configuration of the river delta is satisfied in these figures. With oblique wave incident, an asymmetrical shape of river delta is expected. Both sides of river delta are named as a upcoast side and a downcoast side, with respect to the wave direction. The upcoast side is defined as the side of river delta which is directly affected by the wave. While, the downcoast side defined as the side of river delta where the wave effect is indirect. Figures 3.51 and 3.52 illustrate the measured data of shoreline positions in Run C-1 and Run D-1 where the angles of wave incident are 7.5° and 15.0°, respectively. The black symbols represent the measured data at the upcoast side, whereas the measured data at the downcoast side are represented by the white symbols. The asymmetrical shape of river delta is verified by these figures.

In general, oblique waves generate strong longshore currents, consequently, most of the river sediment discharge is moved in the predominant direction of littoral drift and deposited on the downcoast side. Therefore, the growth rate of the shoreline on the downcoast side is faster than the growth rate of the shoreline on the upcoast side.

(4) Effect of longshore currents on configuration of river delta

When waves approach a straight beach with an oblique angle, the component of wave power parallel to the shoreline generates the longshore currents. Therefore, in the case of

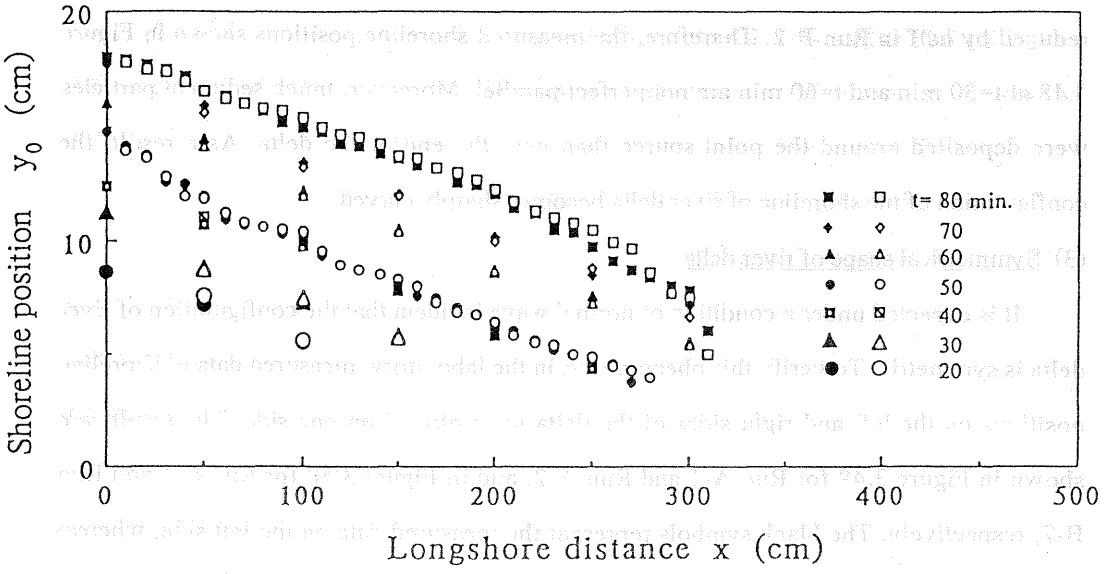

Figure 3.49 Symmetrical shape of river delta, (series A).

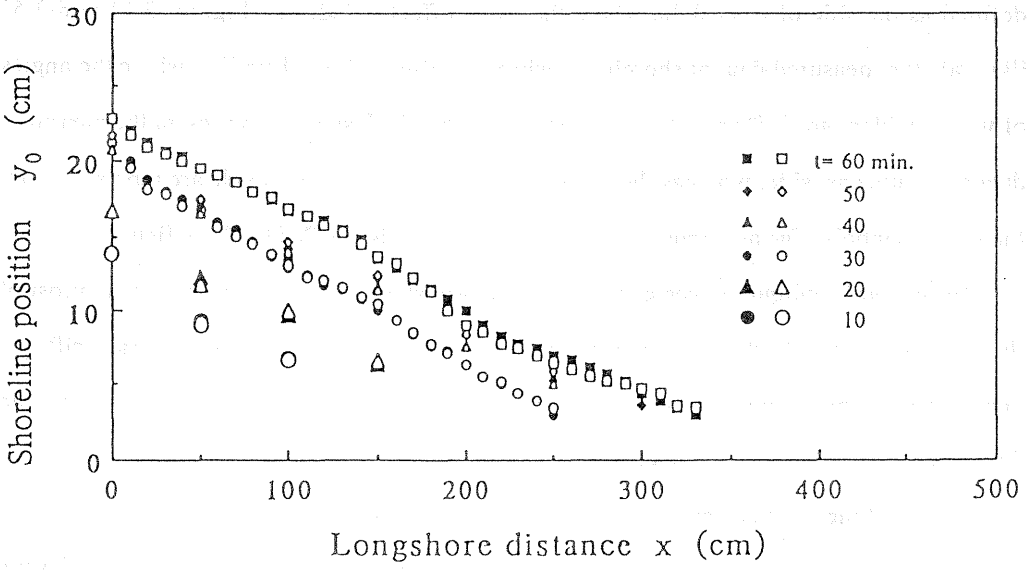

Figure 3.50 Symmetrical shape of river delta, (series B).

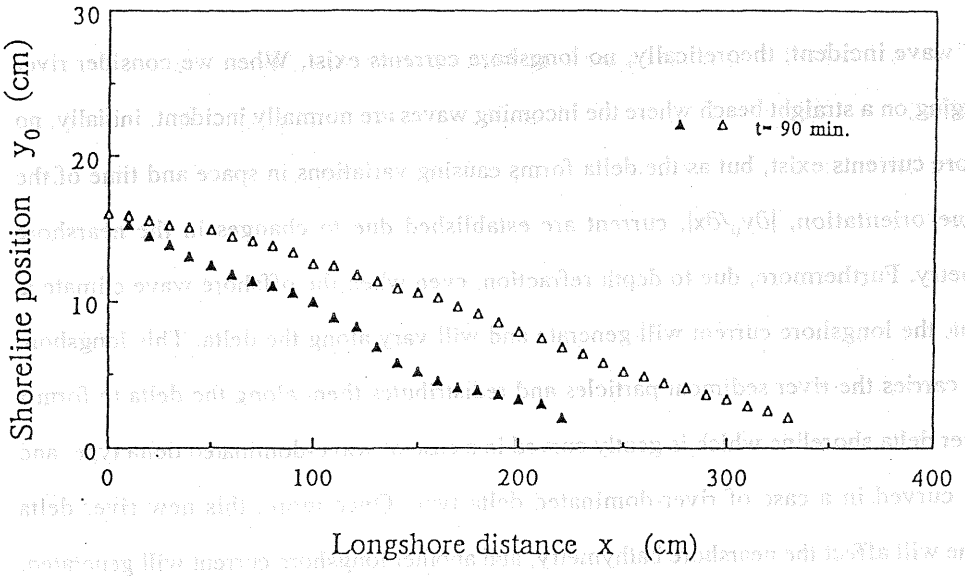

Figure 3.51 Asymmetrical shape of river delta, (run C-1).

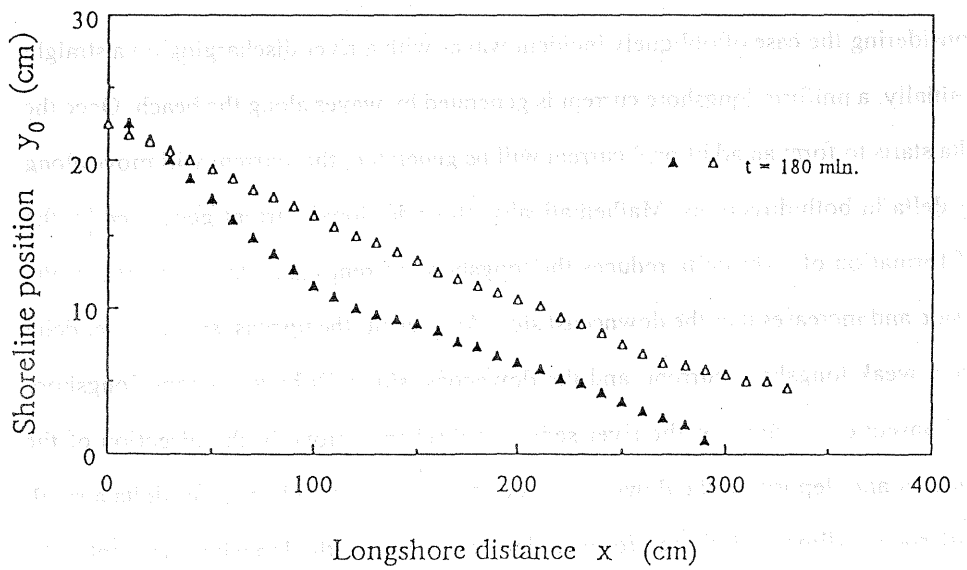

Figure 3.52 Asymmetrical shape of river delta, (run D-1).

normal wave incident, theoretically, no longshore currents exist. When we consider river discharging on a straight beach where the incoming waves are normally incident, initially, no longshore currents exist, but as the delta forms causing variations in space and time of the shoreline orientation, $|\partial y_0/\partial x|$, current are established due to changes in the nearshore bathymetry. Furthermore, due to depth refraction, even when the offshore wave climate is constant, the longshore current will generate and will vary along the delta. This longshore current carries the river sediment particles and redistributes them along the delta to form a new river delta shoreline which is gently curved in a case of wave-dominated delta type, and sharply curved in a case of river-dominated delta type. Once more, this new river delta shoreline will affect the nearshore bathymetry, and another longshore current will generated. A more realistic description of a real beach requires the incorporation of this wave-bottom interaction, which is call a feedback mechanism, that the configuration of river delta is affected by the nearshore bathymetry. Because waves are coming normal to the shoreline, the configuration of delta will be symmetric with respect to the river mouth and generated longshore currents will move along the both sides of the river delta.

Considering the case of obliquely incident waves with a river discharging on a straight beach. Initially, a uniform longshore current is generated by waves along the beach. Once the river delta starts to form an additional current will be generated, this current will move along the river delta in both directions. Mathematically, this additional current generated by the effect of formation of river delta reduces the longshore current generated by waves at the upcoast side and increases it at the downcoast side. As a result, the upcoast side of river delta will have a weak longshore current, and the downcoast side will have a strong longshore current. Consequently, most of the river sediment discharge move in the direction of the strong current and deposit on the downcoast side. At the upcoast side of river delta a small amount of river sediment discharge forms a delta and reduces the longshore current until reaching a dynamic equilibrium shape where the incoming waves approach the shoreline on that side at nearly a right angle. Thus, an asymmetrical shape of the river delta will form, (see

Figures 3.51 and 3.52).

(5) Time variation of shoreline positions

Figures 3.53 and 3.54 show the time variation of the shoreline positions for experimental series A and series B. Since the configuration of the river delta is symmetric with respect to the river mouth, half of the problem will be consider. In these figures seven idealized sections are selected, see Figure 3.46, to illustrate the time variation of shoreline positions. From these figures it is noted that:

(1) In general, the shoreline position, y_0, increases with increasing time, t. For a short time t, the shoreline position at the center of the river mouth, represented by section 0, increases rapidly, while shoreline position at the end of the delta, represented by section 6, increases in a more slowly. At the other in between sections, the shoreline positions vary between rapid and slower changes.

(2) The relation between shoreline position, y_0, and time, t, becomes linear after a long time t. In other word, the rate of propagation of the shoreline position along the river delta becomes constant.

(6) Variation of beach profile and beach slope along a delta coast

The beach profiles were measured along the river delta at every 10 cm interval distance by using acoustic sensor mounted on carriage controlled by a personal computer. Since the configuration of river delta, in experiments series A and series B, is symmetric with respect to the river mouth, only half the delta will be considered. In order to demonstrate the variation of beach profiles along the river delta, seven idealized sections are selected, (see Figure 3.46). The measured beach profiles along the river delta for experimental Run A-2, t=80 min, for the selected sections is illustrated by Figure 3.55. From this figure it is noted that the longshore variation of beach profiles are small. In fact this is, so far, true when the wave power is relatively stronger than the rate of river sediment discharge, or in other words, when the delta is categorized as a wave-dominated type, as in experimental series A, and also when the configuration of the shoreline of the river delta is gently curved. In this case the

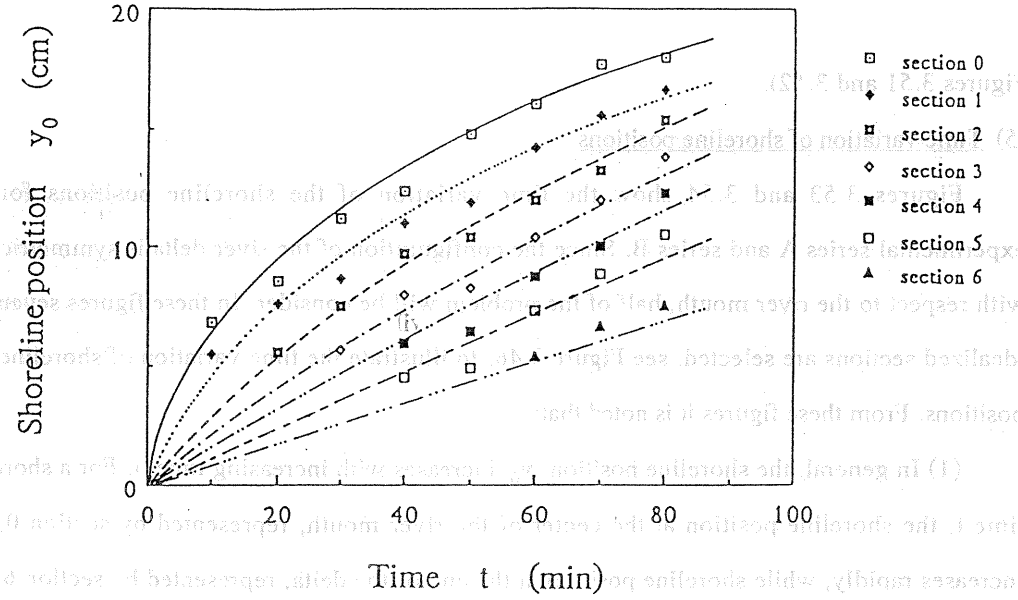

Figure 3.53 Time variation of shoreline positions, (series A).

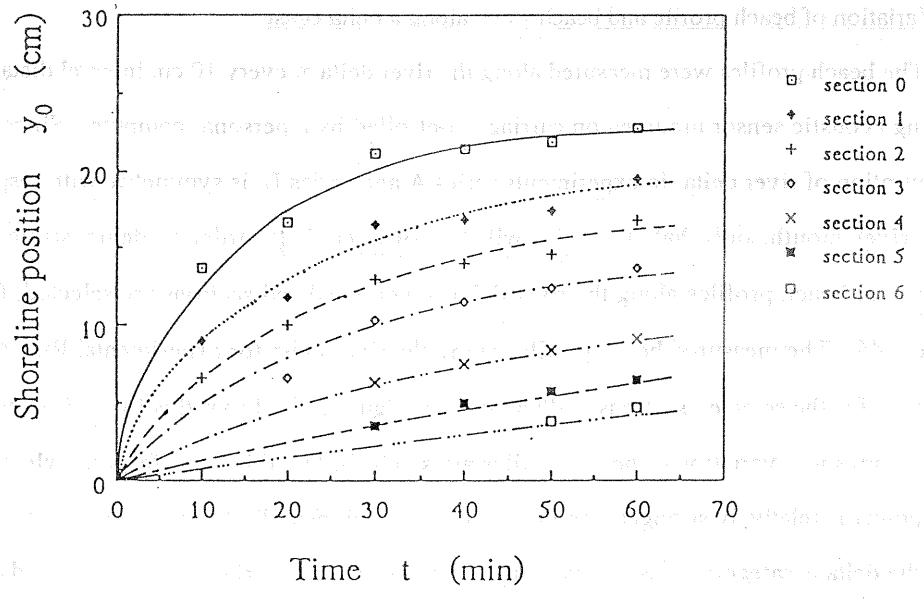

Figure 3.54 Time variation of shoreline positions, (series B).

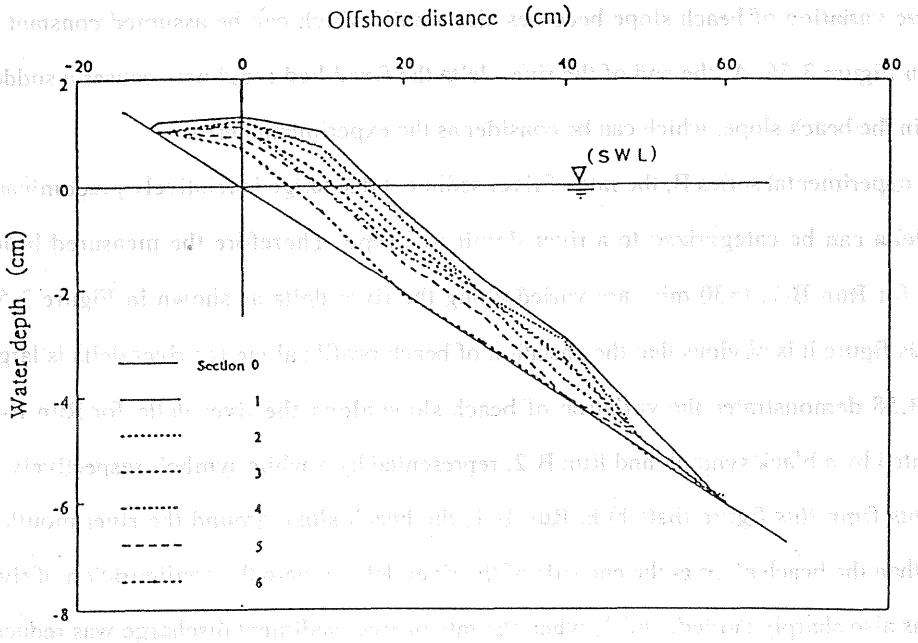

Figure 3.55 Variation of beach profiles along shoreline of river delta, (Run A-2).

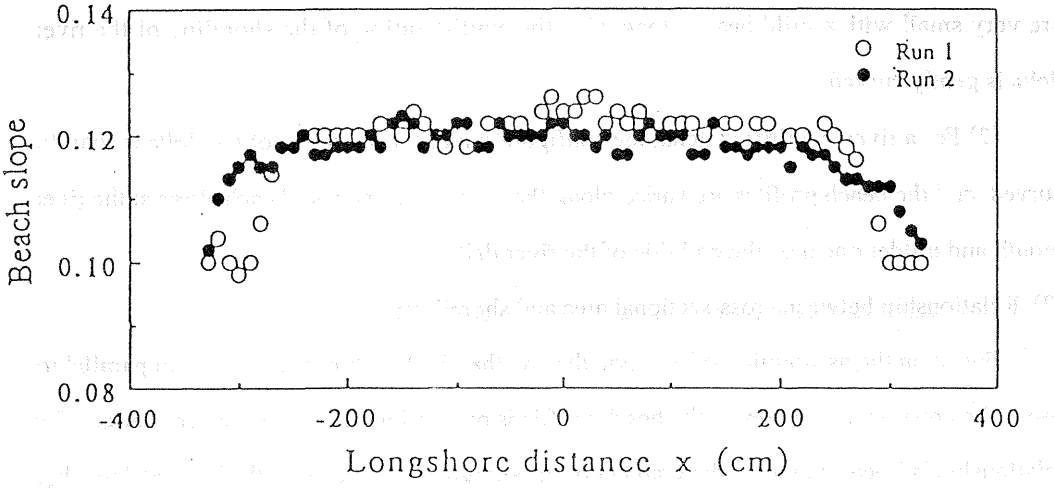

Figure 3.56 Changes of beach slope along shoreline of river delta, (series A).

longshore variation of beach slope becomes also small, which can be assumed constant as shown in Figure 3.56. At the end of the river delta the fixed bed roughness causes a sudden change in the beach slope, which can be consider as the experimental error.

In experimental series B, the rate of river sediment discharge is relatively predominant, or the delta can be categorized to a river-dominated type. Therefore the measured beach profiles for Run B-1, t=30 min, are varied along the river delta as shown in Figure 3.57. From this figure it is obvious that the variation of beach profile along the river delta is large. Figure 3.58 demonstrates the variation of beach slope along the river delta for Run B-2 represented by a black symbol, and Run B-1 represented by a white symbol, respectively. It is obvious from this figure that; 1) in Run B-1, the beach slope around the river mouth is steeper than the beach slope at the end side of the river delta, where the configuration of river delta was also sharply curved, and 2) when the rate of river sediment discharge was reduced by half in Run B-2, the configuration of the shoreline of the river delta is changed, it becomes more gently curved, and therefore the variation of beach slope along the river delta became (more or less) small.

From Figure 3.55 to Figure 3.58 it can be inferred that:

(1) For a wave-dominated delta, the variations of the beach profile along the river delta are very small with a mild beach slope, also the configuration of the shoreline of the river delta is gently curved.

(2) For a river-dominated delta, the configuration of the shoreline of the delta is sharply curved, and the beach profiles are varied along the delta with a steeper beach slope at the river mouth and milder one near the end side of the river delta.

(7) Relationship between cross-sectional area and shoreline position

Based on the assumption of one-line theory, that the beach profile moves in parallel to itself, the cross-sectional area of the beach profile is proportional to the shoreline change. The relationship is linear, in which the gradient of the straight line is equal to the limited depth h_k, mathematically it is written as:

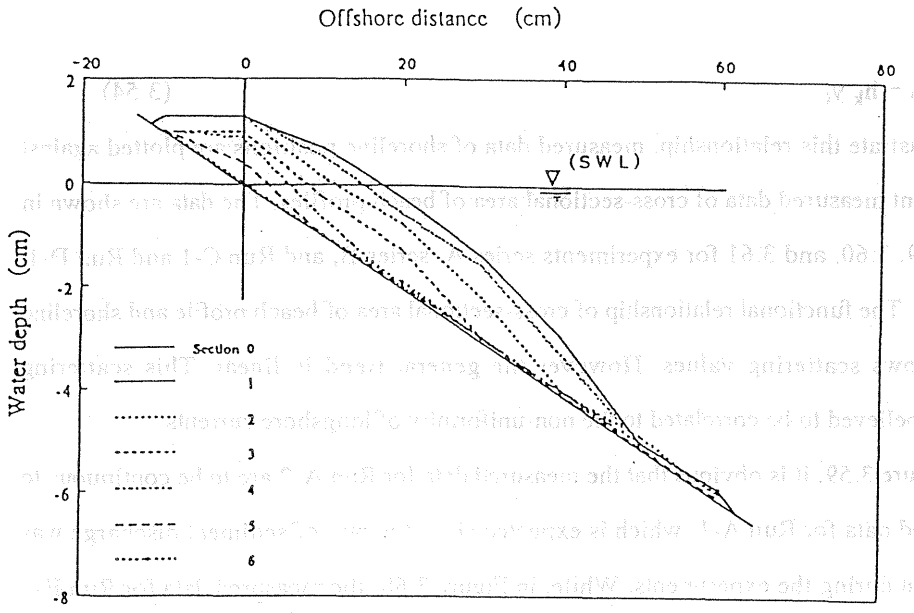

Figure 3.57 Variation of beach profiles along shoreline of river delta, (RunB-1).

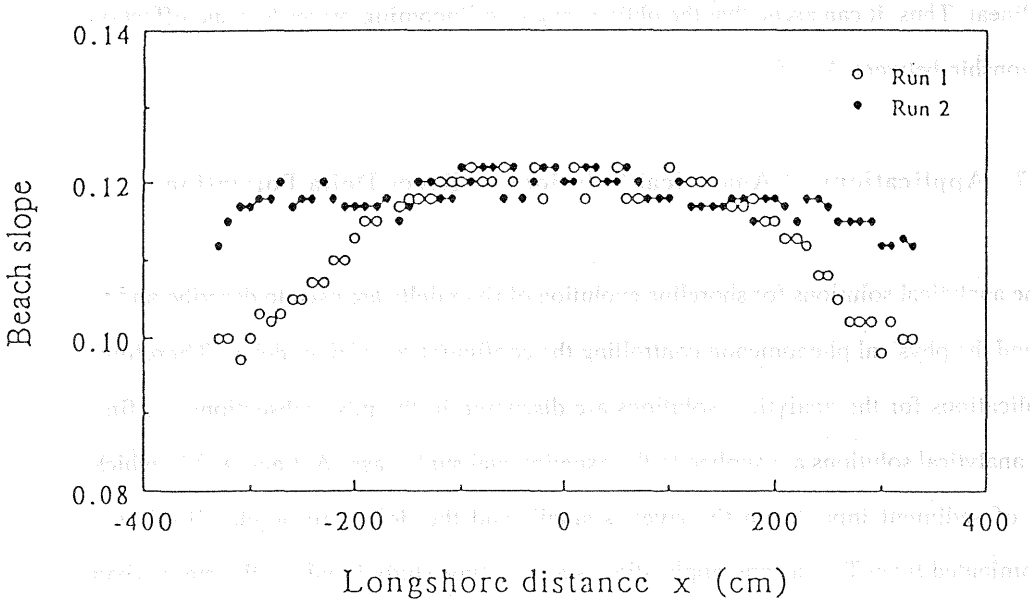

Figure 3.58 Changes of beach slope along shoreline of river delta, (series B).

$$A = h_k y_0 \qquad (3.54)$$

To illustrate this relationship, measured data of shoreline positions are plotted against the equivalent measured data of cross-sectional area of beach profiles. The data are shown in Figures 3.59, 3.60, and 3.61 for experiments series A, series B, and Run C-1 and Run D-1, respectively. The functional relationship of cross-sectional area of beach profile and shoreline position shows scattering values. However the general trend is linear. This scattering behavior is believed to be correlated to the non-uniformity of longshore currents.

In Figure 3.59, it is obvious that the measured data for Run A-2 are to be continuous to the measured data for Run A-1, which is expected since the rate of sediment discharge was kept constant during the experiments. While, in Figure 3.60, the measured data for Run B-2 are plotted above the measured data for Run B-1, moreover, the measured data fluctuate around the mean values while they are increasing linearly. This behavior in the measured data of this figure is probably due to the non-uniformity of sediment transport. Figure 3.61 illustrates the relationship between A and y_0 for Run C-1 and Run D-1 where the oblique angles are 7.5° and 15°, respectively. Although the measured data are scattered, the general trend is linear. Thus, it can argue that the oblique angles of incoming waves have no effect on the relationship between A and y_0.

3.7 Applications of Analytical Solutions of River Delta Formation

The analytical solutions for shoreline evolution of river delta are used to describe and to understand the physical phenomenon controlling the configuration of river deltas. Therefore, two applications for the analytical solutions are discussed in the next subsections. In first one, the analytical solutions are applied to the experimental study cases A-1 and A-2 in which the rate of sediment input from the river is small, and the delta can be classified as a wave-dominated type. The second application is a prototype study in which the major river deltas in Lake Biwa are investigated. The river deltas in Lake Biwa are classified as

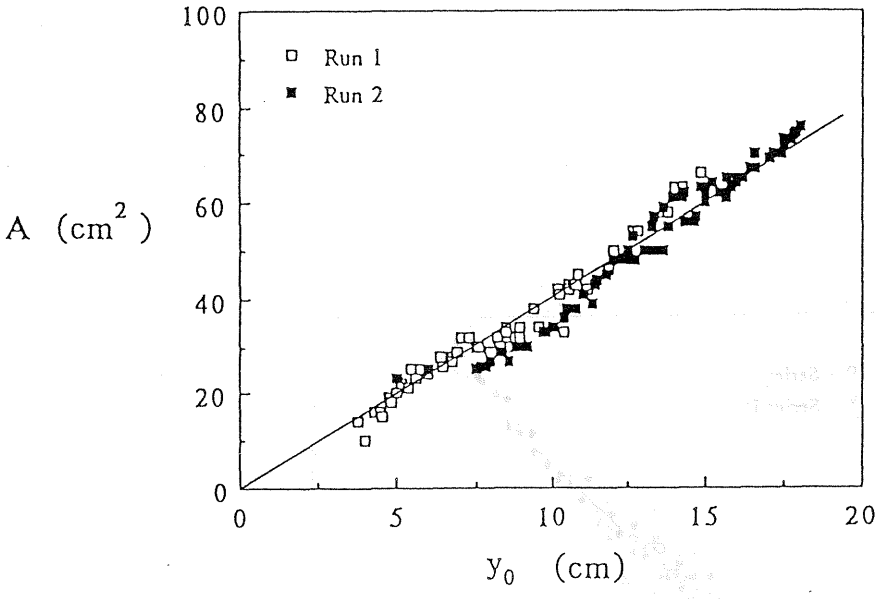

Figure 3.59 Cross-sectional area of beach profile as a function of shoreline position, for symmetrical configuration river delta (series A).

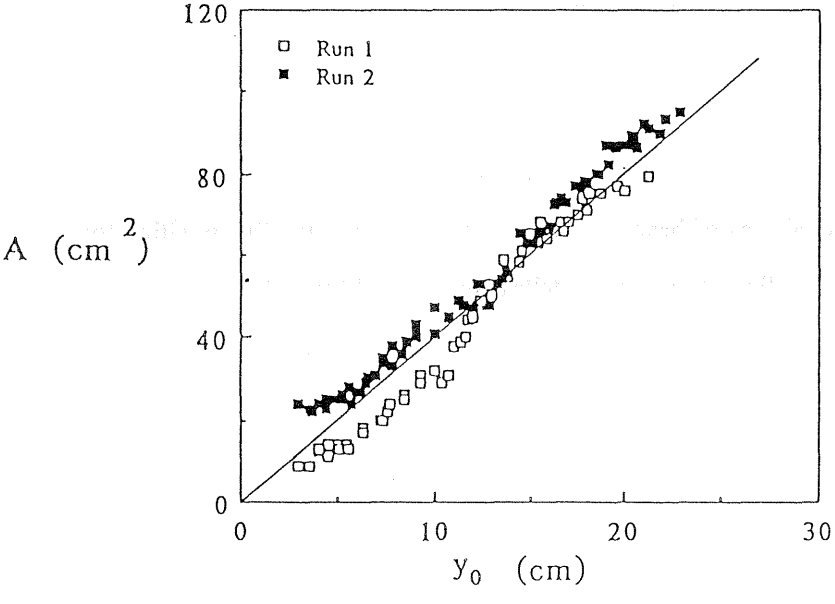

Figure 3.60 Cross-sectional area of beach profile as a function of shoreline position for symmetrical configuration of river delta (series B).

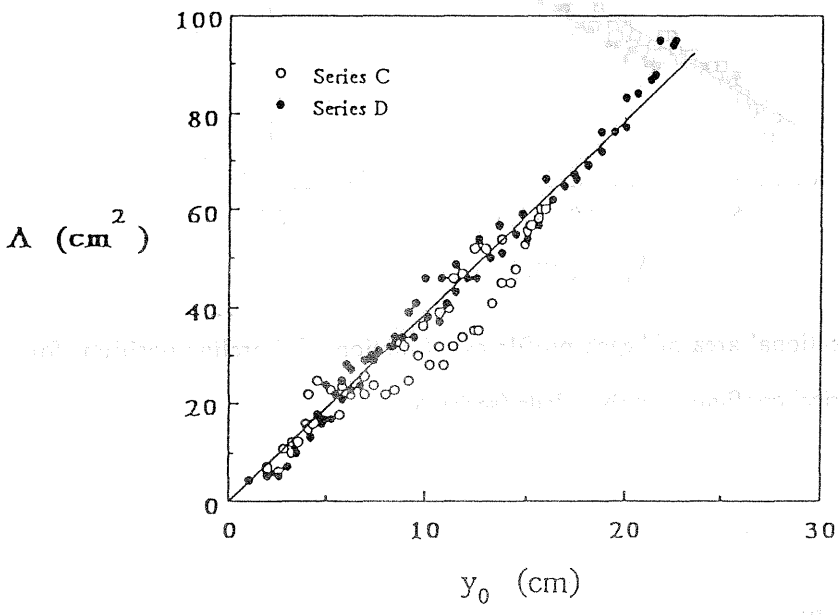

Figure 3.61 Cross-sectional area of beach profile as a function of shoreline position for a symmetrical configuration of river delta (Run C-1 and Run D-1).

river-dominated type, since the river discharge is predominant and wave power is minimal. The results are straightforward.

3.7.1 Application of analytical solutions to experimental study

The measurements of shoreline evolution of a river delta for experimental runs A-1 and A-2 are compared with the analytical solution given by Eq. (3.19), the results are shown in Figure 3.62. It is seen, that the evolution of the shoreline near the river mouth is well predicted. However, near the end side of the river less agreement between the measured and computed shoreline position is observed. This is due to the effect of the bed roughness which causes the measured shoreline to rapidly decrease.

Figure 3.63 shows the time variation of measured shoreline positions at the measuring sections compared with the analytical solution. As previously mentioned a good prediction between the measured and the computed shoreline is observed for the measuring sections near the river mouth. At the end side of the river, represented by section 6, the evolution of shoreline by analytical solution is overestimated.

3.7.2 Applications of analytical solutions to river deltas in Lake Biwa

The river deltas in Lake Biwa are classified as river-dominated types, since the river discharge is predominant and wave power is minimal. Therefore, the effect of beach slope variation plays an essential role in the process of formation. Using the wave data and bottom topography information described in the section 3.3, the wave conditions for each river are calculated. The significant wave height and period are 0.75 m and 3.0 sec, respectively. Table 3.9 presents the field conditions of the major river deltas in Lake Biwa. Since the river deltas in Lake Biwa were formed a long time ago, say some million years ago, it is very difficult to estimate the original basin of the river delta. In addition, the lake basin has been formed due to geological activities as well as the hydrological effects. All these factors make the determination of the initial shoreline for river delta formation impossible.

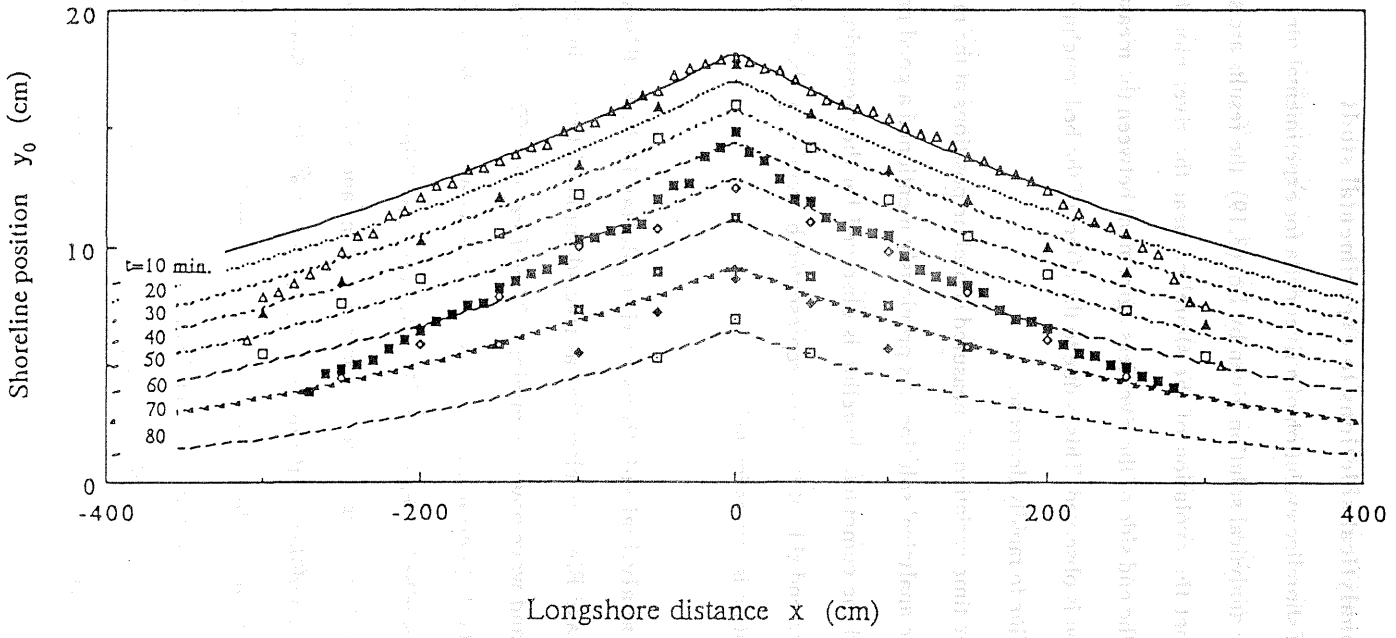

Figure 3.62 Comparison between measured and computed shoreline positions of river delta, (series A).

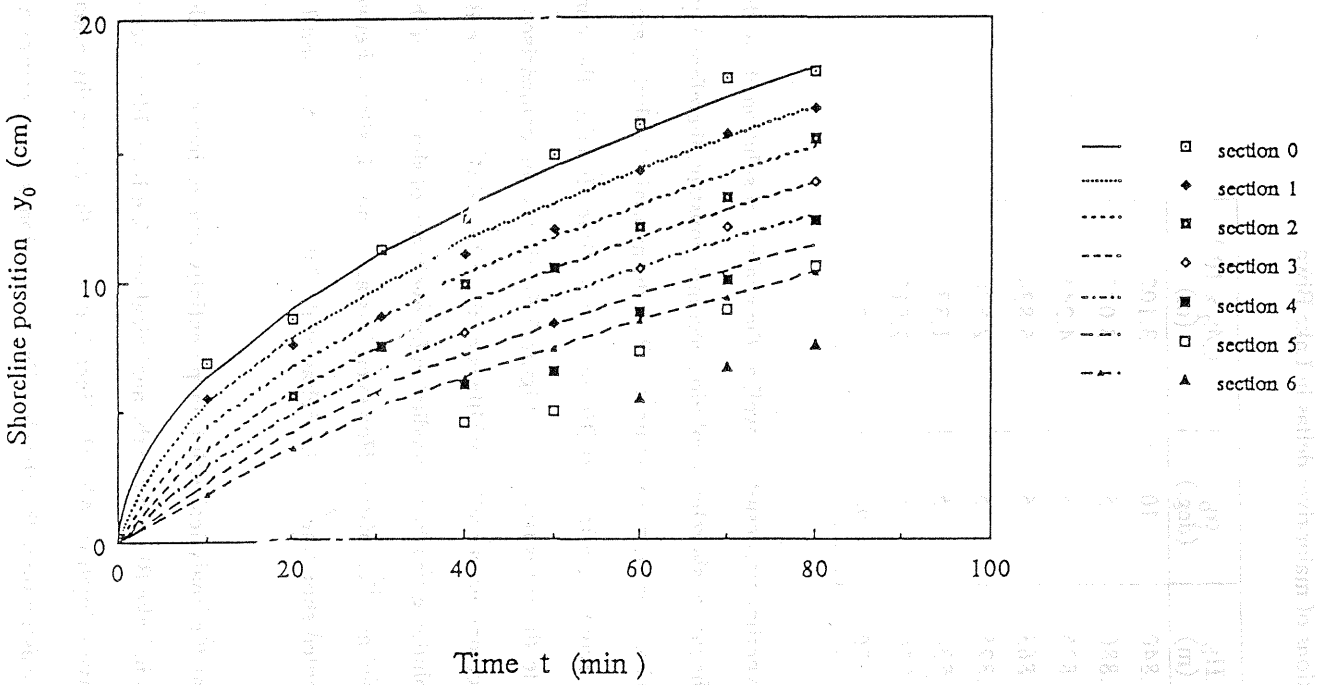

Figure 3.63 Time variation of measured and computed shoreline position of river delta, (series A).

Table 3.9 Field conditions of major river deltas in Lake Biwa.

River Name	H_b (m)	α_b (deg.)	$\varepsilon_1/\varepsilon_2 \times 10^{-3}$ (m)
Ishida	0.840	10	3.102
Ado	0.880	5	3.027
Kamo	0.825	5	4.244
Otani	0.863	5	5.834
Wane	0.825	5	2.876
Ane	0.830	5	1.334
Inugami	0.770	5	2.912
Echi	0.770	20	3.200

Fortunately, the experimental results as well as the analytical solution show that after sufficiently long time, the rate of shoreline evolution becomes constant, therefore any datum line can be selected as a base for the measurements. Then the analytical solution are used to estimate the shoreline evolution after a sufficiently long time. Finally, the computed shorelines are adapted to the measured ones. Figure 3.64 shows the comparison results between measured and computed shoreline positions of the selected river in Lake Biwa. In general, the analytical solution give a better prediction for evolution of shorelines of the deltas of the Kamo, Otani, Wani and Echi rivers. However, less agreement is shown between the measured and the computed shorelines of the deltas of the Ishida, Ado, Ane and Inugami rivers.

It is indicated that the analytical solution potentially overestimates the shoreline evolution of river deltas in Lake Biwa, since the analytical solution is unable to account for bottom changes and wave refraction. Also the linearization of the continuity equation of sediment transport by the assumption that the shoreline orientation is small, causes a greater error in the overestimation of shoreline evolution. Therefore the one-line theory is limited to estimate the shoreline evolution of a river-dominated delta type. Instead, numerical solution must be used. However, with the aid of the one-line theory, the physical phenomenon

controlling the shoreline evolution of river delta could be interpreted. Moreover, the one-line theory produces only small errors for the shoreline evolution of a wave-dominated delta.

3.8 Conclusions

The formation process of river deltas was investigated analytically and experimentally. The general configuration of the river deltas depends on the relative importance of the deposited river sediment and the transported one by the action of waves and tidal currents. The river deltas are mainly categorized as: 1) river-dominated type in which the river discharge is predominant and wave energy is minimal, 2) wave-dominated type which represents higher wave energy situations, and tidal-dominated type where the tidal currents are impinging on coastal waters near river deltas cause river discharged sediments to be transported and dispersed along the coast at considerable distances from the river mouth. A modified version of a ternary diagram proposed by Galloway (1975) and Wright (1985) was adapted.

The physical description of the river delta formation was studied by investigating two field cases: the Nile Delta coast in Egypt and the major river deltas in Lake Biwa, Japan. The geographical and topographical investigation of these sets has been made. The main conclusions drawn from this investigation are:

(1) Most of the river sediment discharge are carried during the flood seasons as suspended load. These sediments are responsible for building up the river deltas.

(2) Since the river deltas have been formed long time ago, the beach profiles have reached an equilibrium shape. Therefore Dean's expression for equilibrium beach profile can be applied with reasonable accuracy.

(3) In general, the average beach slope varies along the river delta beach, with a steeper slope at the river mouth and milder one near the end sides of the river delta.

(4) The sediment size typically varies along the coast of river delta, in which the coarser

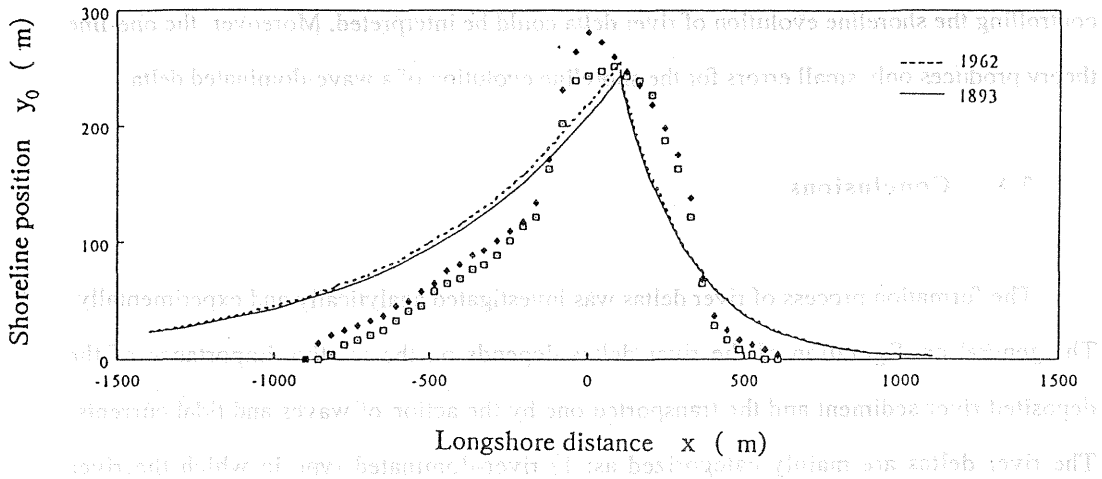

a) Ishida River

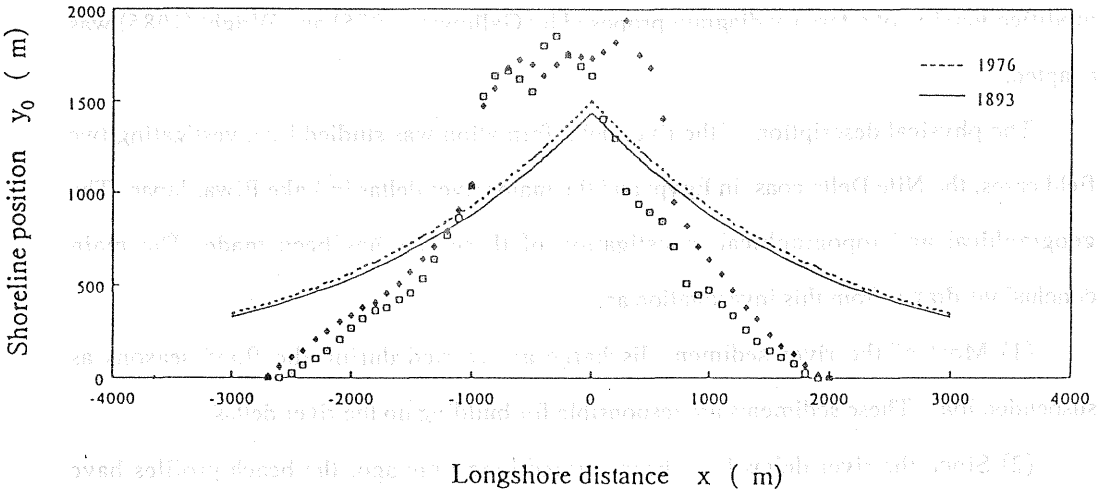

b) Ado River

Figure 3.64 Comparison between measured and computed shoreline positions of selected river deltas in Lake Biwa, a) Ishida river , b) Ado river.

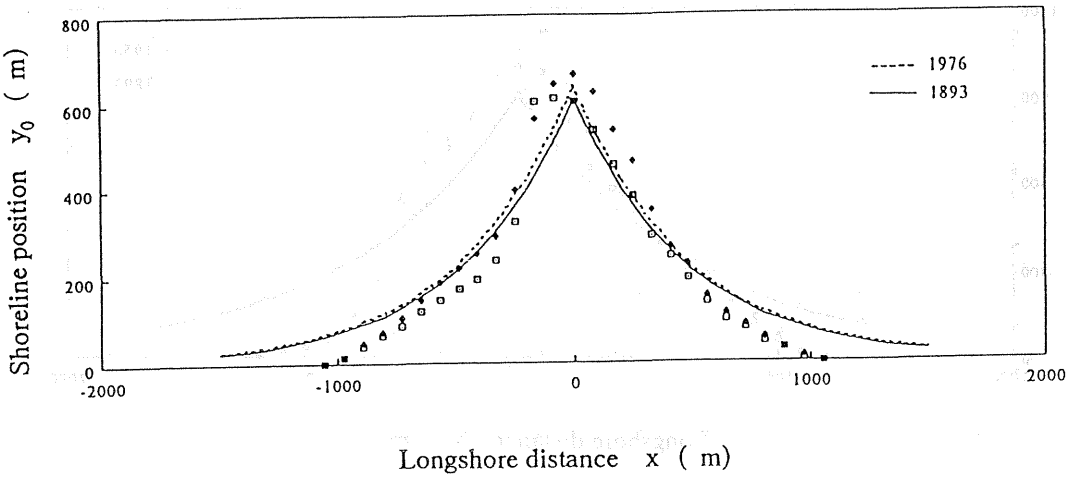

c) Kamo River

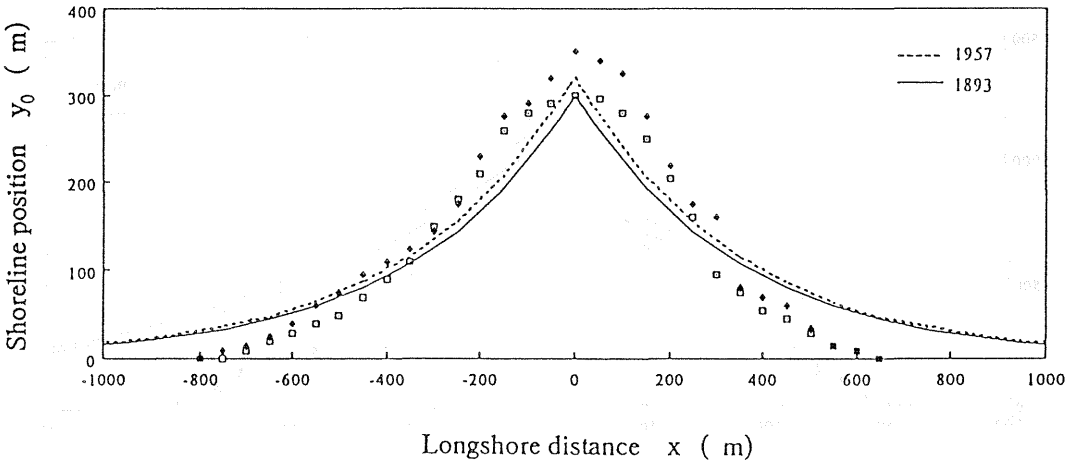

d) Otani River

Figure 3.64 Comparison between measured and computed shoreline positions of selected river deltas in Lake Biwa, c) Kamo river , d) Otani river.

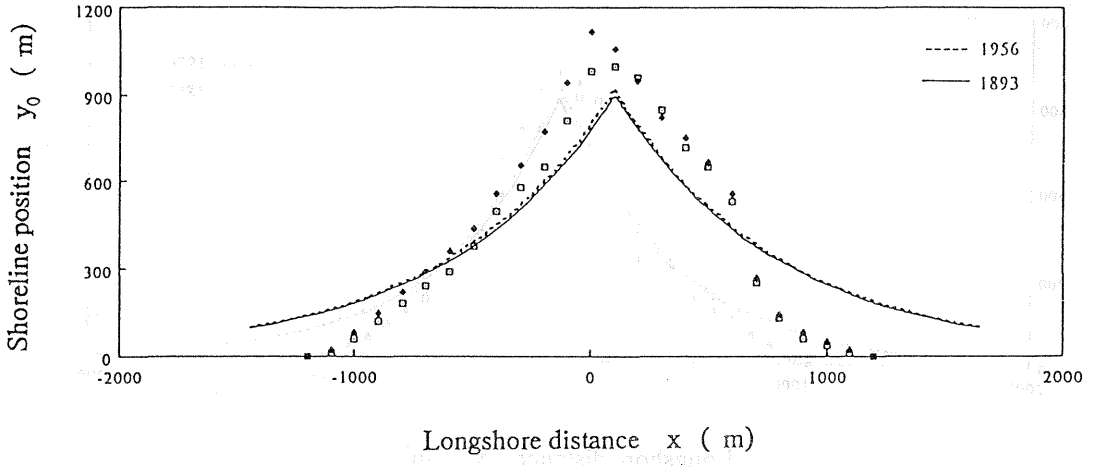

e) Wani River

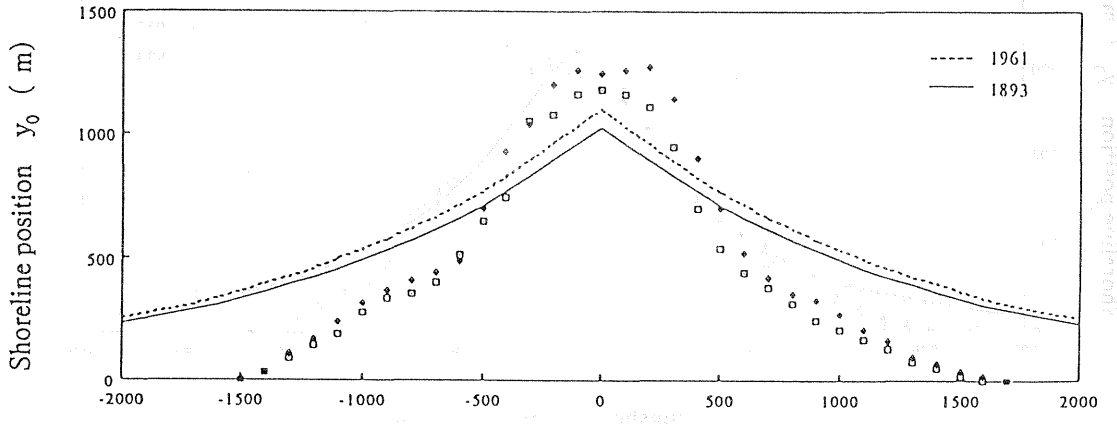

f) Ane River

Figure 3.64 Comparison between measured and computed shoreline positions of selected river deltas in Lake Biwa, e) Wani river , f) Ane river.

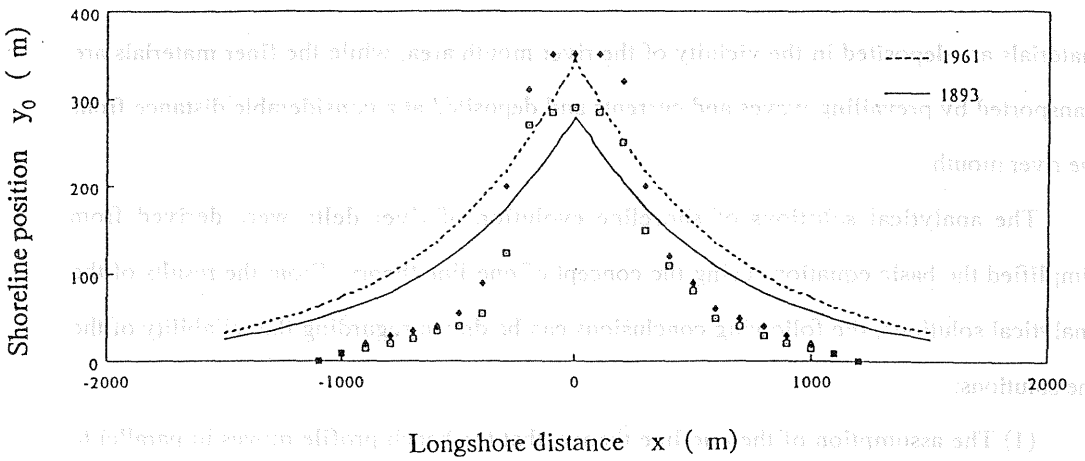

g) Imugami River

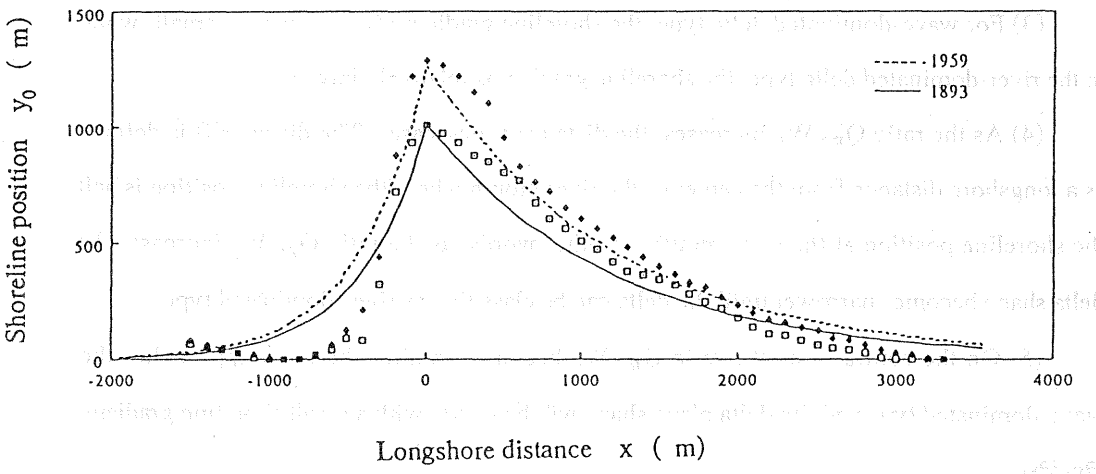

h) Echi River

Figure 3.64 Comparison between measured and computed shoreline positions of selected river deltas in Lake Biwa, g) Inugami river , h) Echi river.

materials are deposited in the vicinity of the river mouth area, while the finer materials are transported by prevailing waves and currents and deposited at a considerable distance from the river mouth.

The analytical solutions of shoreline evolution of river delta were derived from simplified the basic equations using the concept of one-line theory. From the results of the analytical solutions, the following conclusions can be drawn regarding the reliability of the the solutions:

(1) The assumption of the one-line theory, that the beach profile moves in parallel to itself is limited when it is applied to the formation of the river delta of a river-dominated type, where the beach slope change along the river delta as, at the river mouth the beach slope is steeper than the beach slope near the end sides of the delta.

(2) The obliquely incident waves produce an asymmetrical configuration of the river delta. The degree of asymmetric increases as the angle of the incoming wave increases.

(3) For wave-dominated delta type, the shoreline gradient,$|\partial y_0/\partial x|$, is very small, while in the river-dominated delta type, the shoreline gradient is relatively larger.

(4) As the ratio Q_{R0}/W_E increases, the distance B decreases. The distance B is defined as a longshore distance from the center of the river mouth where the shoreline position is half the shoreline position at the river mouth. In other words, as the ratio Q_{R0}/W_E increases the delta shape becomes narrower until the delta can be classified as river-dominated type.

(5) On the contrary, as the ratio Q_{R0}/W_E becomes smaller the delta approaches the wave-dominated type and the delta plane shape will be gentle with a small shoreline gradient, $|\partial y_0/\partial x|$.

(6) For a specific ratio Q_{R0}/W_E, the distance B decreases with increasing the time t, which implies that the rate of deposited sediment around the river mouth increases by time.

An experimental study on the formation process of river deltas was carried out and the important factors affected the formation process were discussed. The methods of modeling a river sediment discharge were examined, showing the advantage and disadvantage of every

method. Since the river mouth width is very small compared with the finite length of the shoreline, we decided to use the point source method for modeling the river sediment discharge. Additionally, the point source technique is easier to apply than the other methods and it gives a reasonable accuracy for the measurements. The following conclusions can be drawn from the experimental study:

(1) During the formation process the river delta consists of a series of layers, each layer represents a complete evolution of shoreline cycle.

(2) For wave-dominated delta type, the shoreline of river delta propagates with nearly same rate as the propagation of the front line of the delta. Therefore, one-line theory can be used to describe long term variations in shoreline configuration of river deltas. Oppositely, for river-dominated delta type, the shoreline of the delta propagates with a faster rate than the front line of the delta.

(3) For wave-dominated delta type, the longshore variation of beach slope is very small with a gently mild beach profile. The shoreline gradient is gently change resulting gently curved of river delta shape. In the contrary, for river-dominated delta type, beach slope is remarkable varied along the delta coast with steeper beach slope at the river mouth and milder one at the end sides of the delta. The shoreline gradient, $|\partial y_0/\partial x|$, is steeply varied resulting in sharply curved shape of delta.

(4) The interaction between the configuration of river delta and the longshore currents is belong to the so-call feedback mechanism, in which the configuration of river delta affects and affected by the longshore currents.

(5) The longshore currents affect on the symmetrical shape of river delta. Under normal wave incident, the configuration of delta is symmetric with respect to the center of the river. The configuration of delta will be changed to asymmetric shape when incoming waves are obliquely incident.

(6) With asymmetrical configuration of river delta, the longshore currents at the downcoast side are stronger than the longshore currents at the upcoast side. As a result much

sediment are moving and depositing at the downcoast side than at the upcoast side.

(7) The cross-sectional area of beach profile of river delta is proportional to the shoreline position. The relationship is nearly linear with a gradient equal to the limited depth of littoral drift, h_k.

In comparing of the analytical solutions for shoreline evolution of river deltas with the experimental measurements of delta formation and the major river deltas in Lake Biwa, favorable agreement is found. For wave-dominated delta type, the analytical solutions can predict the shoreline evolution with a high level of accuracy. While, less accuracy is considerable for evolution of shoreline changes of river-dominated delta type.

REFERENCES

Abramowitz, M. and Stegun, I.A., 1972, Handbook of Mathematical Functions, 9th ed., Dover Pub. Inc., New York.

Bakker, W.T., 1968," The Dynamics of a Coast with a Groin System," Proc. 11th Coastal Eng. Conf., ASCE, pp. 492-517.

Bakker, W.T. and Edelman, T., 1964," The Coastline of River Deltas," Proc. 9th Coastal Eng. Conf., ASCE, pp. 199-218.

Carslaw, H. and Jaeger, J., 1959, Conduction of Heat in Solids, 2nd ed., Clarendon Press, Oxford.

Coleman J. M. and Roberts H. H. , 1987 " Deltaic Coastal Wetlands " Proc. of the symp. on Coastal Lowlands Organized by the Royal Geological and Mining Society of the Netherlands (KNGMG).

CRI, 1980," Report on grain size analysis of bottom sediment samples," Part 2, Semi-annual data, Ministry of Irrigation, Water Research Center, Coastal Research Institute.

Dean, R.G., 1973," Heuristic models of Sand Transport in the Surf Zone," Proc. of the Australian Conf. on Coastal Eng., pp. 208-214.

Dean, R.G., 1977," Equilibrium Beach Profiles," US Atlantic and Gulf Coastal, Ocean Engineering, Report No. 12, University of Delaware Press.

Dean, R.G., 1984. CRC Handbook of Coastal Processes and Erosion, Komar, P.D., editor, CRC Press Inc., Boca Raton, Fla.

Elwany, M. H. S., Inman, D. L. and Khafagy, A. A., 1984," Wave Climate and Sand Transport Along the Nile Delta," Research and Experimental Station, Ministry of Irrigation.

Fishawi, N., Fahmy, M., Sestinine G. and Shawki A., 1976," Grain Size of the Nile Delta Beach Sand," Proc. Seminar on Nile Delta Sedimentology, Alexandria, pp. 79-94.

Galloway, W. E. 1975 " Process Framework for Describing the Morphologic and Stratigraphic Evaluation of Deltaic Depositional Systems ", in M. L. Broussared (ed.): Deltas, models for exploration, Houston Geol. Soc. , Houston, Texas, pp. 87-98.

Grijm, W., 1961," Theoretical Forms of Shoreline," Proc. 7th Coast. Eng. Conf., ASCE, pp. 197-202.

Grijm, W., 1964," Theoretical Forms of Shorelines," Proc. 9th Coastal Eng. Conf., ASCE, pp. 219-235.

Hanson, H. and Larson, M., 1987," Comparison of Analytic and Numerical Solutions of the One-Line Model of Shoreline Change," Proc. of Coastal Sediment'87, ASCE, pp. 500-514.

Holeman, J.N., 1980," The Sediment Yield of Major Rivers of the World," Water Resources Res., Vol. 4, No. 4, pp. 737-741.

Hurst, H.E., 1952, The Nile, Constable Pub. London.

Inman, D.L., Audrey D.G. and Pawka S.S., 1975," Application of Nearshore Processes to the Nile Delta," Proc. of Seminar on Nile Delta sedimentology, Alexandria, pp. 205-255.

Inman, D.L. and Jenkins, S.A., 1984, " The Nile littoral Cell and Man's Impact on the

Coastal Zone of the Southeastern Mediterranean," Proc. 19th Coastal Eng. conf., ASCE, Texas, pp. 1600-1617.

Iwagaki, Y., 1966," A Treatise on Beach Erosion," Summer Seminar on Hydraulics Eng., JSCE, pp. B-17.1-17.17 (in Japanese).

Kadib, A.A., 1969," Sand Movement Along a Portion of the Northern Coast of U.A.R.," 22nd Int. Navigation Congress, Section 2, pp. 273-287.

Khafagy, A.A.et al., 1981," Autumn Hydrographic Profiles Along the Egyptian Coast from Abu Quir to Port Said; 1974-1979," Coastal Research Institute, Alexandria, Cooperative Marine Technology Program for the middle East, CMSP/81/81/, 23 pp.

Komar, P.D., 1973," Computer models of Delta Growth due to Sediment Input from Waves and Longshore Transport," Geological Society of America Bulletin, Vol. 84, pp. 2217-2226.

Kraus, N.C., Hanson, H. and Harikai, S., 1985," Shoreline Change at Oarai Beach - Past, Present and Future," Proc. 19th Coastal Eng. Conf., ASCE, pp. 2107-2123.

Kreyszig, E., 1983, Advanced Engineering Mathematics, 5th ed., John Wiley & Sons, Inc., Canada.

Le Méhauté, B. and Brebner, A., 1961," An Introduction to Coastal morphology and Littoral Processes," Report No. 14, Civil Eng. Dept., Queens University at Kingston, Ontario, Canada.

Le Méhauté, B. and Soldate, M., 1979," Mathematical Modeling of Shoreline Evolution," Proc. 16th Coast. Eng. Conf., ASCE, pp. 1163-1179.

Mobarek, I.E., 1972," The Nile Delta Coastal Protection Project," Proc. 13th Coastal Eng. conf., ASCE, pp. 1409-1426.

Moore, B., 1982,' Beach Profile Evolution in Response to Changes in Water Level and Wave Height", M.S. Thesis, University of Delaware Press.

Pelnard-Considére, R., 1956," Essai de l'Evolution des Forms de Rivage en Plage de Sable et de Galets," 4th Journee de l'Hydralique, des Energies de la Mar, Question III ,

Rapport No. 1, pp. 289-298.

Price, W.A., Tomlinson, D.W., and Willis, D.H., 1972," Predicting Changes in the Plan Shape of Beaches," Proc. 13th Coastal Eng. Conf., ASCE, pp. 1321-1329.

Ross, D.A. and Uchupi, E., 1977," Structure and Sediment history of Southeastern Mediterranean Sea - Nile Cone Area," Amer. Assoc. Petrol. Geol. Bull., Vol. 61, pp. 872-902.

Said, R., 1981, The Geological Evolution of the River Nile, Springer-Verlag, New York and Berlin, 151 pp. and sheets.

Sasaki, T.O. and Sakuramoto, H., 1978," Field Verification of a Shoreline Simulation Model," International Conference on Water Resources Engineering, IAHR, pp. 501-518.

Sestini, G., 1975," Geomorphology of the Nile Delta," Proc. Seminar on Nile Delta Sedimentology, Alexandria, pp. 12-24.

Shahin, M., 1985, Hydrology of the Nile Basin, Elsevier Science Publishers, The Netherlands.

Shibano, T., Yamashita, T., Inoue, M.and Tsuchiya, Y., 1985," Sediment Properties along the West beach of Lake Biwa," Annuals, D.P.R.I., Kyoto University, No. 28 B-2, pp. 1-19 (in Japanese).

Tsuchiya, Y.,1973," Coastal Sediment Balance and Beach Change," Summer Seminar on Hydraulics Engineering , JSCE , pp. B-3.1-3.19 (in Japanese).

Tsuchiya, Y., 1978," Beach Erosion and its Prediction," Annuals, D.P.R.I., Kyoto University, No. 21A, pp. 1-18 (in Japanese).

UNDP, 1973," Coastal Erosion Studies," Arab Republic of Egypt UNESCO project, EGY 70 581, Technical Rept. No. 1, Alexandria.

UNDP, 1978," Coastal Erosion Studies, Final Technical Report; UNDP EGY 73 063, Paris.

Walton, T. and Chiu, T., 1979," A Review of Analytical Techniques to Solve the Sand Transport Equation and Some Simplified Solutions," Proc. Coastal Structures'79,

ASCE, pp. 809-837.

Wright, L. D. 1985 " River Deltas " In: R. A. Davis (ed.) : " Coastal Sedimentary Environments", second edition, Springer-Verlag pub. New York : pp. 76.

Wright, L. D , Coleman J. M. and Ericson M. W. , 1974 " Analysis of Major River Systems and their Deltas ", coastal studies Institute, Louisiana State University, Techn. Rept. 156, 114 pp.

Chapter 4 BEACH EROSION DUE TO RIVER DELTA REDUCTION AND ITS CONTROL

4.1 Introduction

Man's intervention with coastal processes takes many forms. However, the most serious, large scale and long term coastal erosion results from the construction of dams which block the river sediment supplied to the coast. This loss of sediment may have a catastrophic effects along the coastal line of a river delta. Many investigations have been performed on the erosion of the river delta mainly around the river mouth where navigation can be hindered by problems such as erosion of the river mouth , deposition of the sediment in the estuarine, and closing of the navigation channels. Most of these investigations have been focused on protection methods of river mouths from wave and current actions by the construction artificial structures such as jetties or seawalls. However these structures interrupt the littoral drift and produce a dramatic change in the shoreline; accretion occurs on the upcoast side of the structure, and erosion occurs on the downcoast side.

Because of the previous methods of beach erosion control failed to prevent or even reduce the beach erosion, many coastal engineers are being advised to let nature takes its courses. Silvester (1979) states the methodology for beach erosion control as " How to copy nature ". Nature always adapts the beach profiles which are in an equilibrium shape, in which the incident wave energy is dissipated without causing a significant net beach profile change. Also, nature forms beautiful stable sandy beaches between reefs or headlands. These beaches will be in static equilibrium when no further beach recession occurs, no littoral current exists, no sediment deposition beyond the downcoast headland occurs, or when waves are breaking

simultaneously along the shoreline.

The aim of this chapter is to investigate the reduction process of river deltas and to study the methodology of beach erosion control, through the investigation of the stable beach configuration. Firstly, an experimental study was carried out. The main purpose of this experiment is to study the reduction process of river deltas due a decrease or lack of sediment input from the river. Secondly, a theory of formation of stable sandy beaches is derived. The derivation of this theory is based on the formulation of non-uniform longshore sediment transport presented in Chapter 2 together with the aid of one-line theory. Next, an application of the theory is made to the stable sandy beaches at Amanohashidate beach, which is located in Miyazu Bay, northern part of Kyoto Prefecture, Japan. In the last portion of this chapter, the methodology of beach erosion control is investigated with a brief description of the previous and new methods for beach erosion control. A new proposal is made for beach erosion control around the river deltas. This proposal is based on Tsuchiya's ideal methodology for beach erosion control and the concept of configuration of stable beaches. Two ideal examples are presented for controlling beach erosion around symmetrical and asymmetrical river delta configurations.

4.2 Experimental Study on Reduction Process of River Delta

The protection of beach against erosion is one of the important problems which coastal engineers must face, especially near the river mouth and adjacent coasts. In order to prevent erosion of the river delta coast, it is important to study the process of river delta reduction (erosion), which is very difficult to investigate it in the field coast. Therefore laboratory experiments must be relied upon. By hydraulic experiments it is possible to simulate a hundred year prototype phenomenon in only few hours in laboratory by controlling the experimental conditions and measurements. Beach erosion mainly occurs due to the

predominant longshore currents which carry the sediment alongshore. When the longshore current dose not exist, in other words, when waves approach the beach in a normal direction for a sufficiently long time, the beach profiles will be in equilibrium condition.

The basic idea is that the beach profile in its equilibrium condition dissipates incident energy without significant net change in shape. Dean (1977) derived an analytical expression for the equilibrium beach profile shape based on the concept of constant wave energy dissipation per unit water volume. The main objectives of this experimental study are to investigated the reduction process of river deltas, to examine the time variation of the shoreline positions and the rate of beach erosion, and finally to verify the relationship between shoreline position and cross-sectional area of the reduced beach profile.

4.2.1 Experimental procedure

The experiments were performed in the fan-shaped wave basin of Ujigawa Hydraulics Laboratory, Disaster Prevention Research Institute, Kyoto University. The initial shorelines and beach profiles in these experiments were the final shorelines and beach profiles of the experiments on the formation process of river delta presented in Chapter 3, (series A and B). The experiments were halted once the longshore current died away and only the on-offshore movement exist. To verify this condition color tracers were used and the trajectories were observed.

Measurements of shoreline changes were made at every 5 min interval during the first 30 min of the experiment, this interval was then increased as equilibrium conditions were approached, which is determined by tracing the movements of color paper tracers which should be only in the on-offshore direction. The measurements of shoreline changes were made along the delta coast at 13 idealized sections at 50 cm intervals, see Figure 3.46. At the end each experiment, beach profiles as well as shoreline changes were measured at 10 cm intervals along the delta. The beach profiles measurements were made by an acoustic sensor

mounted on a movable carriage, controlled by a personal computer.

The reduction process of river delta was observed by taking photographs at 5 min intervals during the first 30 min of the experiment, this interval was then increased as equilibrium conditions were approached. Measurements of wave height in the constant depth part of the basin were made using capacitance type wave gauges. While on the sloping part, the measurements were made using a wave gauge mounted on a movable carriage controlled by a personal computer.

4.2.2 Experimental results

Two experiments were performed, A-3 and B-3, for a still water depth in the constant depth part of 30 cm, a wave height of 2.0 cm and a wave period of 0.8 sec. The incoming waves were normally incident during the experiments. The experimental results are given as follows:

(1) General description of river delta reduction process

The reduction process of the river delta is significantly different from the formation process of the river delta. During the experiment it was observed that:

(1) In general the shoreline of the river delta significantly erode while the front line of the delta retreats shoreward at a very slow rate. This phenomenon occurs because the breaking wave energy more strongly affects the shoreline of delta than on the front line of the delta which is located out side the surf zone.

(2) The sediments move alongshore from the river mouth area and deposit at the end sides of the river delta, as a result, a nearly straight shoreline is formed nearly at the middle of deltaic area.

(3) The rate of longshore sediment transport decreases as the shoreline becomes nearly straight. The on-offshore sediment movement becomes predominant, and therefore an equilibrium beach profile is formed.

(2) Characteristic of reduction of river delta

Figures 4.1 and 4.2 show the behaviors of river delta reduction for experiments A-3 and B-3. The shoreline of the delta rapidly changes to a nearly straight one, with erosion at the center of river delta and deposition at the end sides of the river delta. It is noted that the new shoreline position in Figure 4.1 is shoreward the shoreline position in Figure 4.2, that is because the total sediment volume for experiment A-3 was smaller than the total sediment volume for experiment B-3, while the wave conditions were same in both experiments.

(3) Time variation of shoreline positions

The time variation of the shoreline positions for experiments A-3 and B-3, is shown in Figures 4.3 and 4.4, respectively. From these figures it is noted that; 1) the shoreline position at the center of the river delta decreases significantly with increasing time t, while the shoreline position at the end of river delta increases with increasing time t, and 2) the physical process of erosion at center of the river delta and accretion at the end sides of the river delta occurs for a short time of about 30 min, following by a nearly constant shoreline position.

(4) Equilibrium beach profiles

The beach profiles were measured every 10 cm interval along the shoreline. The measurements reveal that the beach profiles along the river delta are nearly similar in shape. Figures 4.5 and 4.6 illustrate the different between the shape of the beach profiles in the formation and reduction processes. Since the configuration of river delta is symmetry with respect to the center of the river delta, only seven idealized sections in one side are presented in these figures, in which section 0 denotes the measured profile at the center of the river delta and section 6 denotes the measured profile at the end side of the river delta. From these figures it is noted that the curvature of the profile shape changes from a divergent mode shape to convergent one. This convergent mode shape absorbs and dissipates the incoming wave energy without significant net change in the beach profile shape. Therefore, the beach is

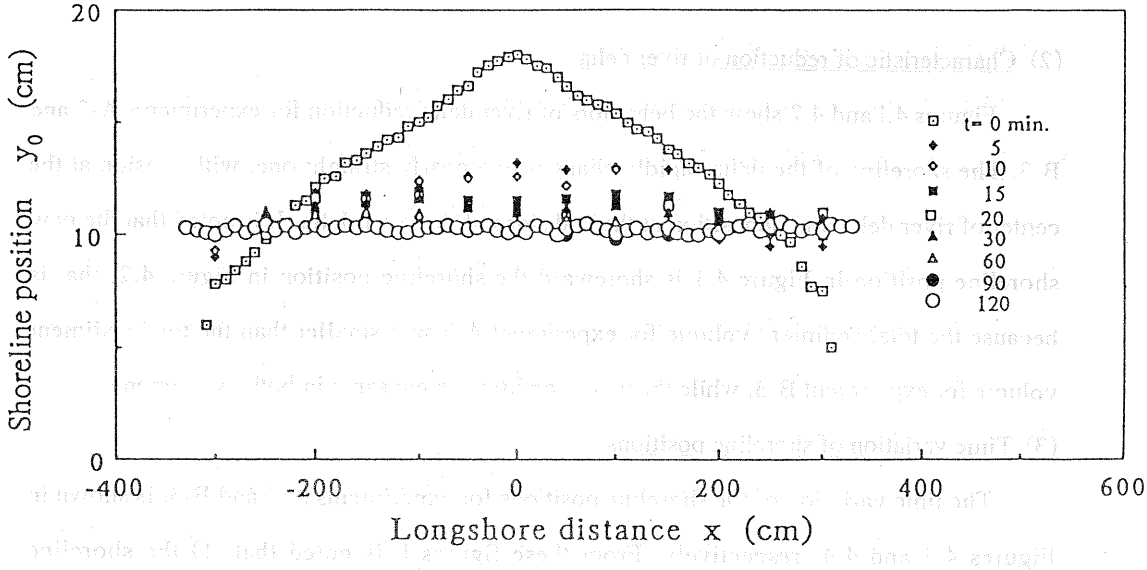

Figure 4.1 Reduction process of shoreline of river delta, (Run A-3).

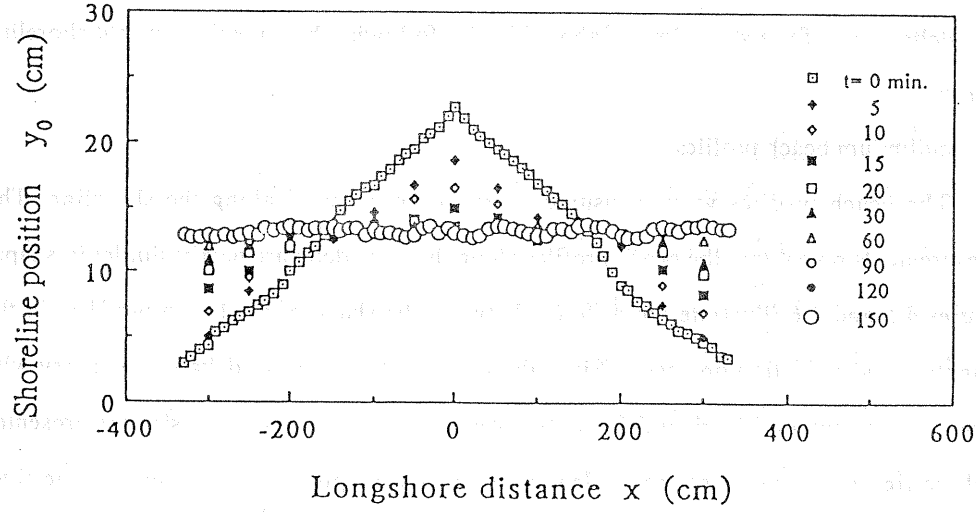

Figure 4.2 Reduction process of shoreline of river delta, (Run B-3).

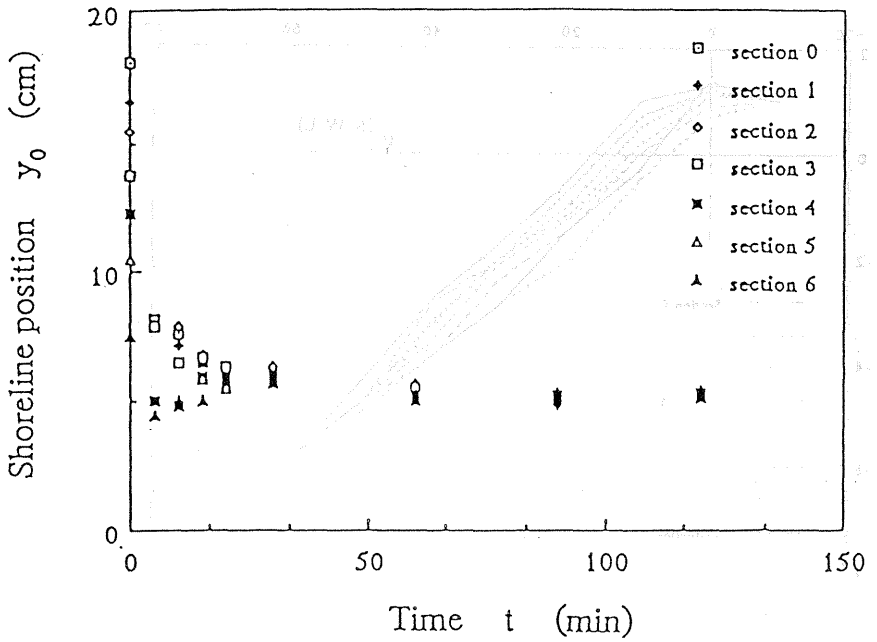

Figure 4.3 Time variation of shoreline positions, (Run A-3).

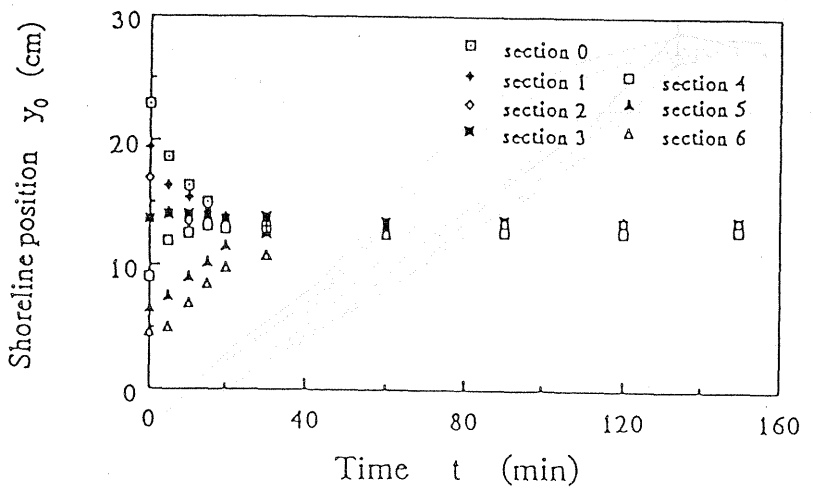

Figure 4.4 Time variation of shoreline positions, (Run B-3).

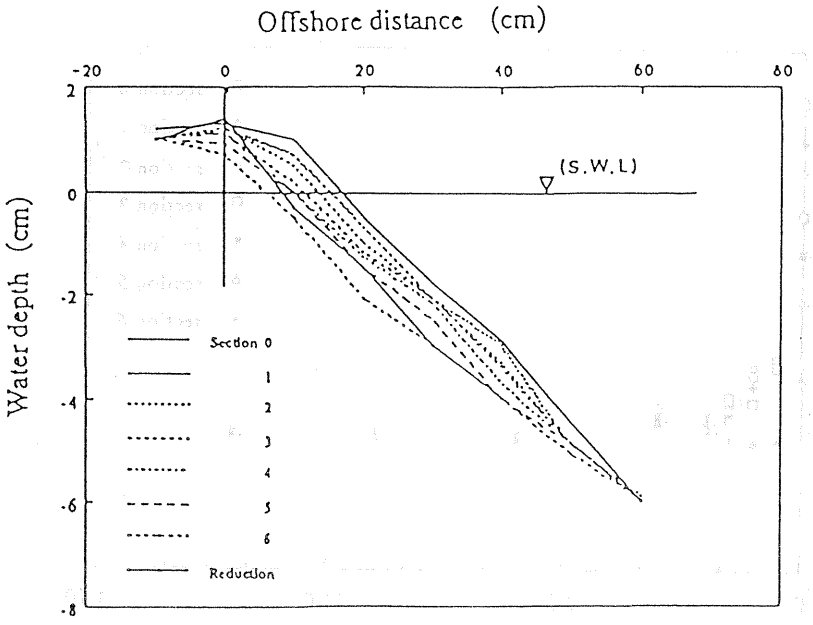

Figure 4.5 Different between mode shape of beach profile of river delta and mode shape of equilibrium beach profile, (Run A-3).

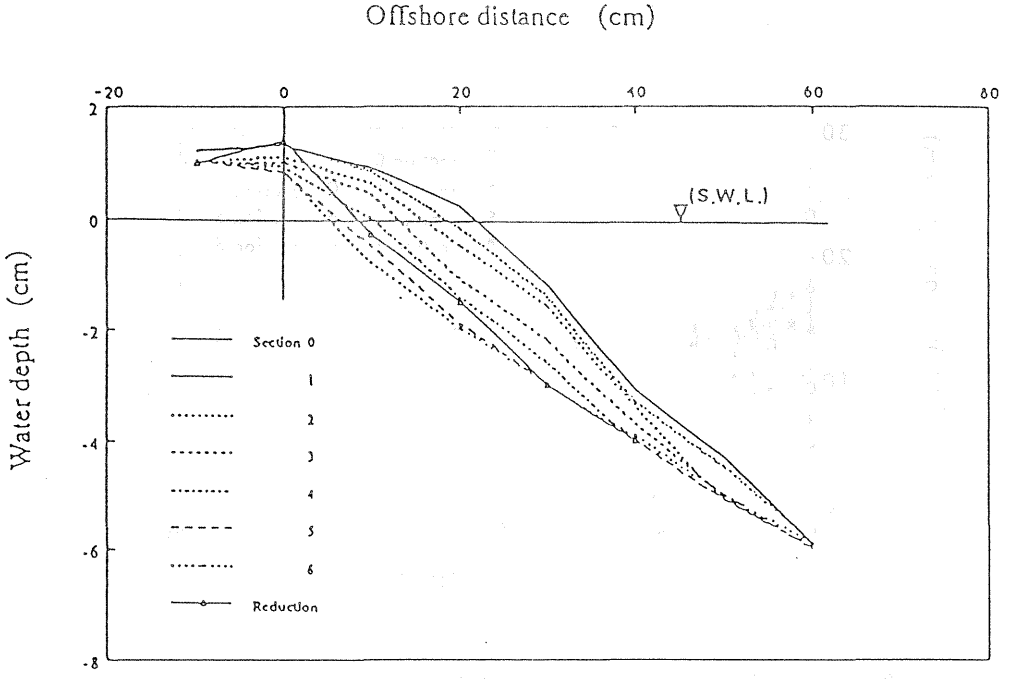

Figure 4.6 Different between mode shape of beach profile of river delta and mode shape of equilibrium beach profile, (Run B-3).

believed to be in equilibrium condition.

(5) Relationship between shoreline position and cross-sectional area

The cross-sectional area of the beach profile was measured at every 10 cm interval along the shoreline, and plotted versus the measured shoreline position. The results are shown in Figures 4.7 and 4.8 for experiment A-3 and B-3 respectively, combined with the experimental results of the formation process of river delta presented in Chapter 3. From these figures it is noted that the relationship between the cross-sectional area and the shoreline position is nearly linear, like the formation process of river delta, but the gradient of the relation in the reduction process is larger than the gradient of the relation in the formation process.

4.3 A Theory of Formation of Stable Beaches

Many methods have been used previously to reduce or prevent beach erosion, but few have worked satisfactory. It is commonly observed that the construction of breakwaters for harbors and groins extended out of the surf zone has a harmful effect by intercepting the littoral drift. Although, the use of groins and seawalls has been shown to promote erosion, relatively little progress has been made in recent years resulting in the construction of large and more impressive groins and seawalls. However, in explaining the reasons for these new installations no explanation is often given for either the failure of the previous construction or for the new feature working any better. However, the reason appears to be very simple, in fact all these methods are working against nature. The most effective method of controlling beach erosion is to let nature takes its courses, and to learn how to duplicate nature.

It is commonly accepted that the formation of a shoreline between two headlands under obliquely incident waves is the most stable beach generated by nature (Silvester, 1974). The configuration of the stable beach has received various names in the literature, such as

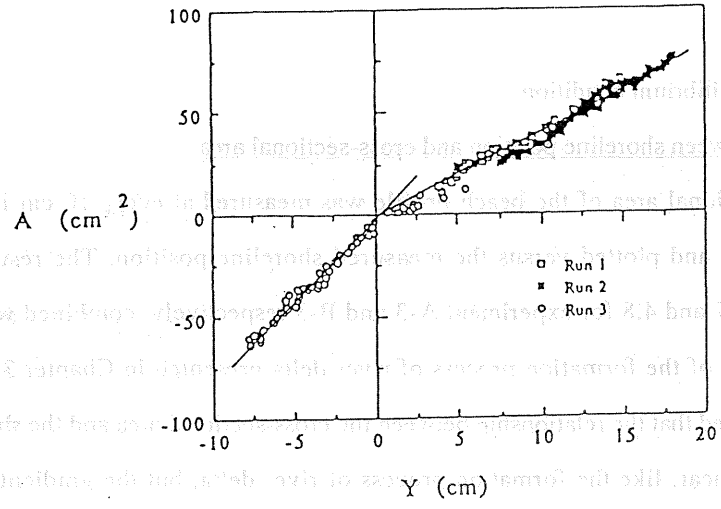

Figure 4.7 Cross-sectional area of beach profile as a function of shoreline position, (Run A-3).

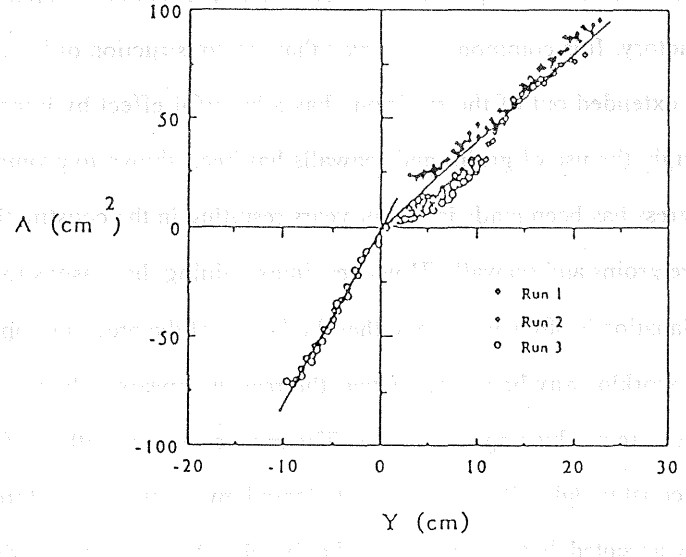

Figure 4.8 Cross-sectional area of beach profile as a function of shoreline position, (Run B-3).

half-heart bay (Silvester, 1960), crenelate shaped bays (Ho, 1971, Silvester and Ho, 1972), spiral beaches (LeBlond, 1972), curved-or hooked beaches (Rea and Komar, 1975), headland bay beaches (LeBlond, 1979), or zeta bays and pocket beaches (Silvester, Tsuchiya and Shibano, 1980). Some authors have equated the offshore breakwater concept to that of headland control, (e.g. Dally and Pope, 1986, Loveless, 1986, and Pope and Dean, 1986). This is unfortunately not true because the principles of each concept are quite different. With the former, where long offshore breakwaters are placed parallel to the shore with a small spacing in between, there is little length of beach available to the waves. It has been said that a system of offshore breakwaters is used to prevent cross-shore and longshore sediment movements rather than to form a beach behind the breakwater. Nevertheless, erosion occurs on the beach at the maximum recession of the shoreline in between. In the case of headland control, the stability of the beach is left to nature, where restored land remains in position with added benefit of beautiful beaches for recreation.

4.3.1 Literature review

Since Lewis (1938) pointed out a relation between the configuration of shoreline and predominant wave direction, the study of the configuration of beaches formed behind offshore structures has been the subject of considerable coastal engineering work. Sauvage, Marc and Vincent (1954) analyzed the equilibrium shapes of these coastal formations, they showed that the shape of the beach was markedly elliptical. Yasso (1965) measured and analyzed the shape of many natural bays and concluded that they, or portions of them at least, followed a logarithmic spirals. Johnson (1965) also investigated and examined the Yasso results and found that there are significant distribution of sediment alongshore the stable beach.

Silvester (1970) extensively investigated the configuration of stable sandy beaches for a number of beaches in the world and concluded that the configuration of the beach between

headlands consists of three distinct zones; an arc behind the upcoast headland; a stretch which is logarithmic spiral in shape, and a straight stretch which extends downcoast towards the next headland. Applying these conclusions, Silvester and Ho (1972) used the logarithmic spiral approach for the stabilization of artificial reclaimed land in Singapore through the concept of headland control. Silvester has attempted to proselytize the coastal engineering community to this concept for many years (Silvester, 1976, 1978) without much success, probably due to the difficulty of utilizing the logarithmic spiral pattern.

Rea and Komar (1975) developed a numerical model for evolution of spiral beaches behind a rocky headland. Dean (1978) presented a method for calculating the equilibrium shape of stable beaches. In his method the bathymetry is considered stable when the wave front is tangent everywhere to the local bottom contours. The calculation was carried out for relatively narrow openings with normal and oblique wave, the shape of the beach was markedly semi-circular.

In Japan, beach erosion is one of the serious problems, since the Japanese Islands are faced on the open sea and are always attacked by severe waves. Mashima (1961) studied bays within limited bodies of water, such as Tokyo Bay, in which he derived vectors of wave energy, accounting for wind velocities, duration and fetch. These formed half ellipse whose major axes were related to the shape of the bay. Mashima (1973) investigated theoretically the stable configuration of sandy beaches taking into consideration the wave energy distributions. Toyoshima (1976) investigated a field case, Kaike coast on Japan Sea, for configuration of sandy beaches behind the offshore breakwaters. He proposed a design system for the offshore breakwaters.

Tsuchiya (1978) proposed the methods of prediction and prevention of beach erosion from the view point of mechanics of sediment transport by fluid motion. He described some comments on beach erosion control for new applicable methods such as headland control which based on the intensive functions of natural sandy beaches in wave dissipation.

Tsuchiya, Silvester and Shibano (1979) proposed two kinds of equilibrium beaches, static equilibrium, in which no longshore sediment transport exists along the beach and dynamic equilibrium, where the longshore sediment transport exists along the beach. Recently, Tsuchiya (1982) proposed an ideal methodology for beach erosion control from view point of controlling the total rate of longshore sediment transport. For this purpose a new formulation of the total rate of longshore sediment transport is made. He established the practical methods to control the total rate of longshore sediment transport and explained two typical, but ideal examples for beach erosion control by this methodology. The first example is for beach erosion due to decrease of sediment input from the river. By Figure 4.9, he explained the ideal methodology for beach erosion control, in which Figure 4.9(a) shows the situation when the sediment input from the river is reduced from Q_R to Q'_R. Thus, beach erosion is advanced on the downcoast of the river delta, the lift-side coast of the river as shown in Figure 4.9(a). From the view point of controlling the total rate of longshore sediment transport, the rate of longshore sediment transport must be reduced along the downcoast of the river delta according to the decreased sediment input from the river. A possible solution of this problem is depicted a shown in Figure 4.9(b), in which a series of headlands is inserted at suitable angles and distances to make the total sediment transport rate decreases according to the decreased sediment input from the river. The second example is for beach erosion due to the lack of sediment sources. The solution for such beach erosion is proposed by this methodology as shown in Figure 4.10, in which a series of headlands (Silvester, 1976) or offshore breakwaters (Toyoshima, 1976) is employed to make the total rate of longshore sediment transport vanish.

More recently, Hsu, Silvester and Xia (1987) showed that the configuration of stable beach using the logarithmic spiral does not follow the complete boundary of the beach. They found that the logarithmic spiral is not an effective method for defining curvature of the stable beach and hence they proposed a new computerized method named "Parabolic Form", in

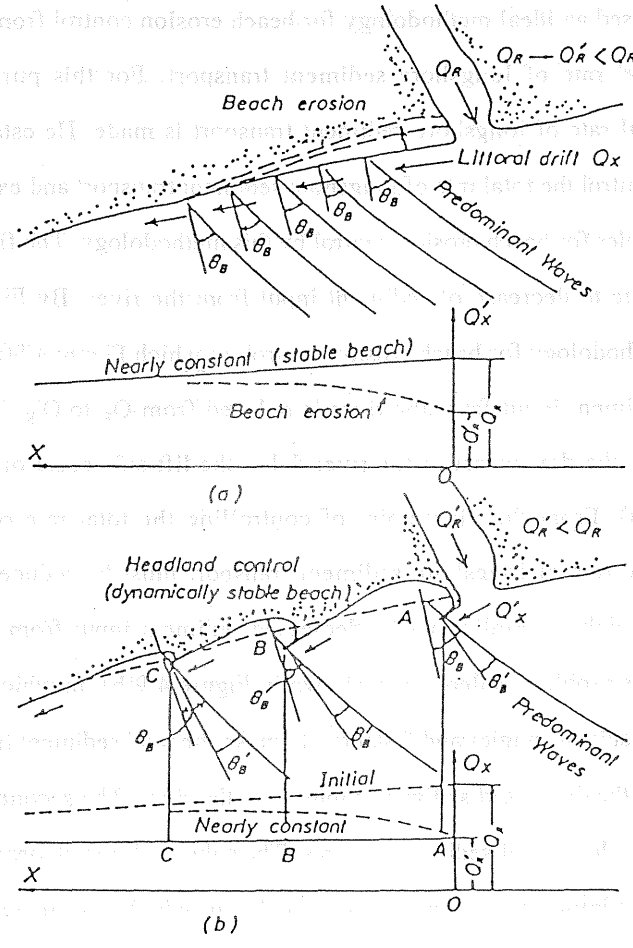

Figure 4.9 Beach erosion contorl for the decrease in sediment input from a river, (after Tsuchiya, 1982).

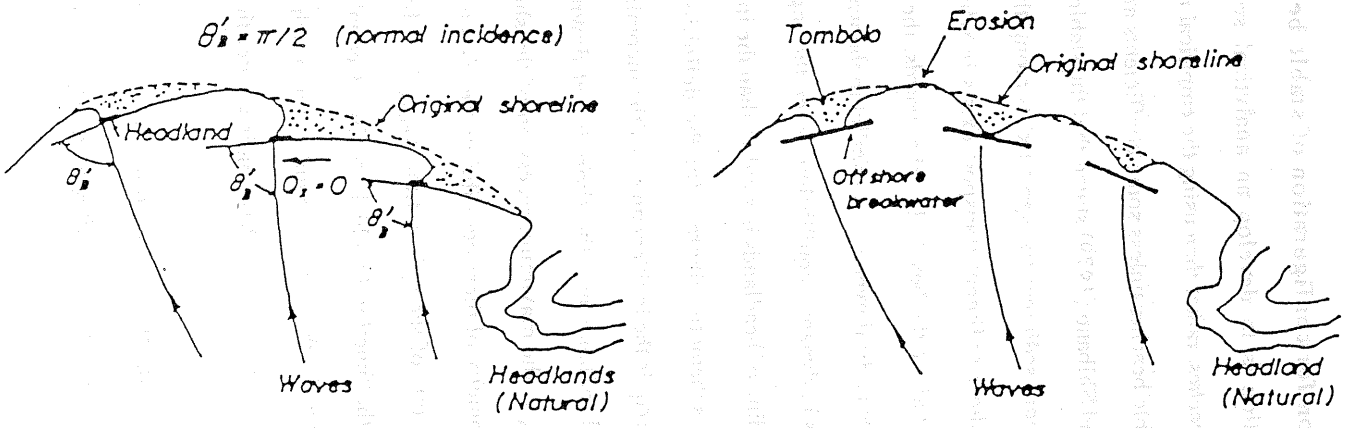

(a) Headlands

(b) Offshore breakwaters

Figure 4.10 Beach erosion control for the lack of sediment sources, (after Tsuchiya, 1982).

which a polynomial equation derived empirically from best fitting of model studies and observation data of prototype bays in Australia known to be in static equilibrium conditions.

4.3.2 Analytical solution for configuration of stable beaches

The aim of this portion is to develop an analytical solution for the shoreline configuration of the stable beaches, rather than using the empirical methods which fail to give a good prediction for the stable beaches unless some coefficients are adapted for each model study. Tsuchiya, Silvester and Shibano (1979) stated that the stable beach is either in a static equilibrium, when no longshore sediment transport exists along the beach, or in a dynamic equilibrium, when the longshore sediment transport exists in which the rate of longshore sediment transport is constant along the beach. In other words, the stable beach is in a static equilibrium when the shoreline at the downcoast is parallel to the wave crests approaching the coast from offshore. And it is in dynamic equilibrium when the angle between the shoreline at downcoast and the control line of headlands is smaller than the incident angle of incoming waves. Figure 4.11 shows a schematic diagram for the definition of static and dynamic equilibrium beaches, in which α_b is the incident angle of the incoming waves, β_b is the angle between the control line of headlands and the shoreline at downcoast, L is the distance between headlands, and y_{0max} is the maximum recession of the shoreline from the control line of the headlands. The geometry of these equilibrium beaches are shown in Figure 4.12. This figure describes that the rate of the indentation y_{0max}/L for the static equilibrium beach is practically given by the function in which α_b/β_b is equal to one as shown by the solid curve (Silvester, 1976), but for the dynamic equilibrium beach the indentation y_{0max}/L may be practically given by a function in which α_b/β_b is greater than one as also shown in Figure 4.11.

In order to predict, theoretically, the configuration of stable beaches, two basic equations are used; the continuity equation of sediment transport and a specific equation for

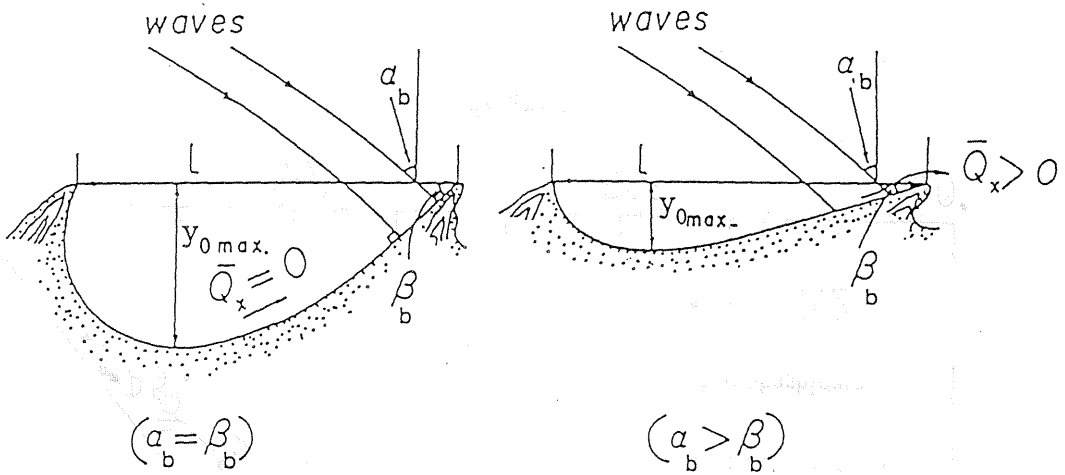

Figure 4.11 Schematic diagram of static and dynamic equilibrium beaches.

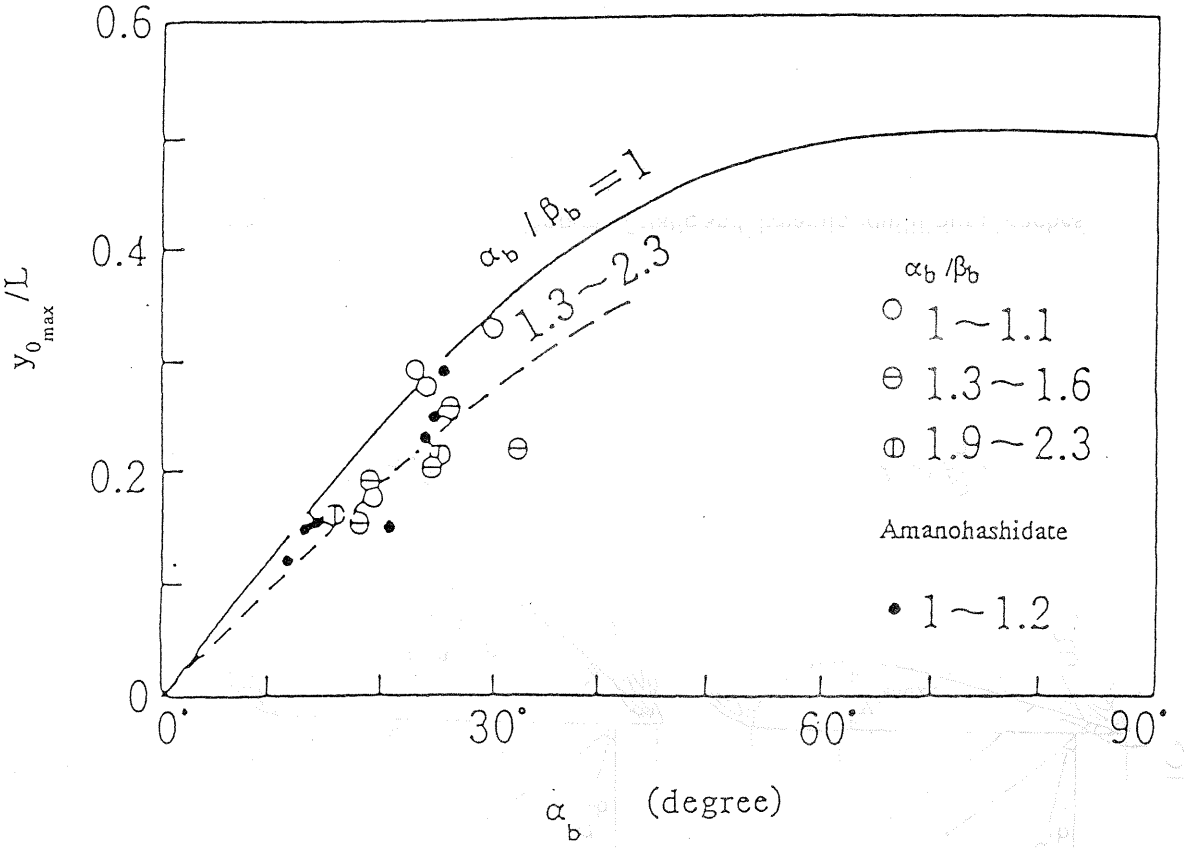

Figure 4.12 Geometry of stable beaches.

predicting total rate of longshore sediment transport. In Chapter 2, a new formulation of total rate of non-uniform longshore sediment transport was derived. This formula is used in this portion to develop an analytical solution for the shoreline configuration of the stable sandy beaches.

(1) Continuity equation of sediment transport

Iwagaki (1966) used a prismatic element to derive an equation of the continuity of sediment transport for long-term beach changes, which was modified by Tsuchiya (1973,1978) for the one-line theory expressed as:

$$\frac{\partial y_0}{\partial t} + \frac{1}{(1-\lambda)h_k}\frac{\partial Q_x}{\partial x} = 0 \qquad (4.1)$$

in which y_0 is the shoreline position, λ is the correction factor for the pore space of beach sediment (approximately 0.4 for most beach deposits), h_k is the limited depth for sediment transport, and Q_x is the total rate of longshore sediment transport. Equation (4.1) states explicitly that the non-uniformity of the rate of longshore sediment transport, $\partial Q_x / \partial x$, is inversely proportional to the evolution of shoreline change, and that for a positive $\partial Q_x / \partial x$ value shoreline erosion will occur, contrarily, for a negative $\partial Q_x / \partial x$ value the shoreline will accrete. In order to solve Eq. (4.1) we have to specify an equation for predicting a total rate of longshore sediment transport.

(2) Total rate of longshore sediment transport

In Chapter 2 the details of the theory of non-uniform longshore current have been presented together with an evaluation of the expression for the total rate of non-uniform longshore sediment transport. The expression of the total rate of non-uniform longshore sediment transport, Eq. (2.68) is expressed as:

$$Q_x = \frac{c_0}{m}\left(\frac{\rho}{\sigma}\right) I(R,F_r)\, h_b^2\, U_0 \qquad (4.2)$$

in which the function $I(R,F_r)$ includes the effect of wave properties and some effects of

sediment size. In the field, this function becomes nearly constant, while in the laboratory the function is strongly affected by the sediment size as well as the wave properties. The non-uniform longshore current velocity U_0 is given by, Eq. (2.41), as:

$$\alpha_1 \frac{\partial}{\partial t}(U_0 h_b^2) + \alpha_2 \frac{\partial}{\partial x}(U_0^2 h_b^2) + \alpha_3 \frac{\gamma C_f c_b}{\pi} U_0 h_b = f(x) \qquad (4.3)$$

where

$$f(x) = \frac{\gamma^2}{16} g h_b^2 \{ \sin 2\alpha_b - 2 \cos^2 \alpha_b \frac{\partial y_b}{\partial x} - (5\beta_1 - 6\beta_2 + 6\beta_3 \sin^2 \alpha_b) \frac{\partial h_b}{\partial x} - 2\beta_3 h_b \sin 2\alpha_b \frac{\partial \alpha_b}{\partial x} \} \qquad (4.4)$$

Now, we have a set of simultaneous equations Eqs. (4.1), (4.2) and (4.3) which are the basic equations for the evolution of any shoreline. The initial and boundary conditions should be specified for every case of shoreline evolution. In the case of stable beach, the shoreline charge will be steady, i.e. the derivative with respect to time will be equal to zero, mathematically expressed as, $\partial/\partial t = 0$. Substitution into Eq. (4.1) leads to, Q_X being constant, which implies that if Q_X is equal to zero the beach will be in a static equilibrium, and if Q_X is greater than zero the beach will be in dynamic equilibrium. The solution now is pending evaluation of the total rate of longshore sediment transport. A small change in the orientation of the shoreline causes a small change in the incident wave angle, mathematically expressed as:

$$\Delta \alpha_b = \frac{d y_0}{d x} \quad \text{or} \quad \frac{d \alpha_b}{d x} = \frac{d^2 y_0}{d x^2} \qquad (4.5)$$

Introducing the concept of the one-line theory, which assumes that the beach profile moves in parallel to itself, with substituting Eqs. (4.1) and (4.5) into Eq. (4.3) through Eq. (4.2), one can obtain an ordinary linear differential equation as:

$$\frac{d^2 y_0}{d x^2} + d_1 \frac{d y_0}{d x} = d_2 \qquad (4.6)$$

where

$$d_1 = \frac{2 m}{\tan \alpha_b} \frac{1}{h_b} \qquad (4.7)$$

$$d_2 = \frac{2 m}{h_b} [1 - \bar{Q}_x] \qquad (4.8)$$

in which m is the beach slope, and $\bar{Q}_x$ is the ratio between the longshore sediment transport rate along the stable beach and the uniform longshore sediment transport rate along a straight infinite beach. Equation (4.6) is the general equation for evolution the plane shape of the stable beach, with setting boundary conditions $y_0 = 0$ at $x = 0$ and at $x = L$ the solution is given as:

$$\frac{y_0}{L} = \frac{d_2}{d_1} \left(\frac{x}{L}\right) + \frac{d_2}{d_1} \exp (d_1 L) \left[\frac{1 - \exp (- (x / L) d_1 L)}{1 - \exp (d_1 L)} \right] \qquad (4.9)$$

where $$d_1 L = \frac{2 m}{\tan \alpha_b} \frac{L}{h_b} \qquad (4.10)$$

and $$\frac{d_2}{d_1} = [1 - \bar{Q}_x] \tan \alpha_b \qquad (4.11)$$

In Equation (4.9), two parametric quantities control the configuration of the stable beach, they are; $d_1 L$ which represents a ratio of distance between headlands, L, to breaker depth h_b, and d_1 / d_2 which represents a rate of longshore sediment transport along the stable beach. The parametric investigation for the effect of the quantities L / h_b and $\bar{Q}_x$ on the configuration of stable beach is illustrated in Figures 4.13 and 4.14 respectively. In order to investigate the effect of one parameter on the configuration of stable beach, the other parameters must be fixed. Form this purpose the value $\bar{Q}_x$ is selected to be equal zero in Figure 4.13, which represents a case of statically stable beaches. In Figure 4.14 the value of

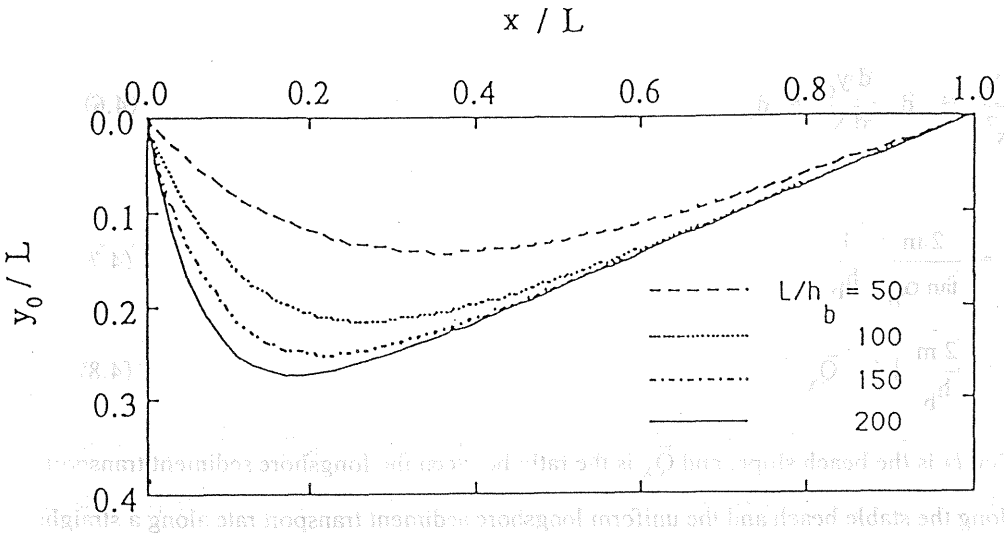

Figure 4.13 Effect of L / h_b on configuration of stable beach where $\bar{Q}_x = 0$.

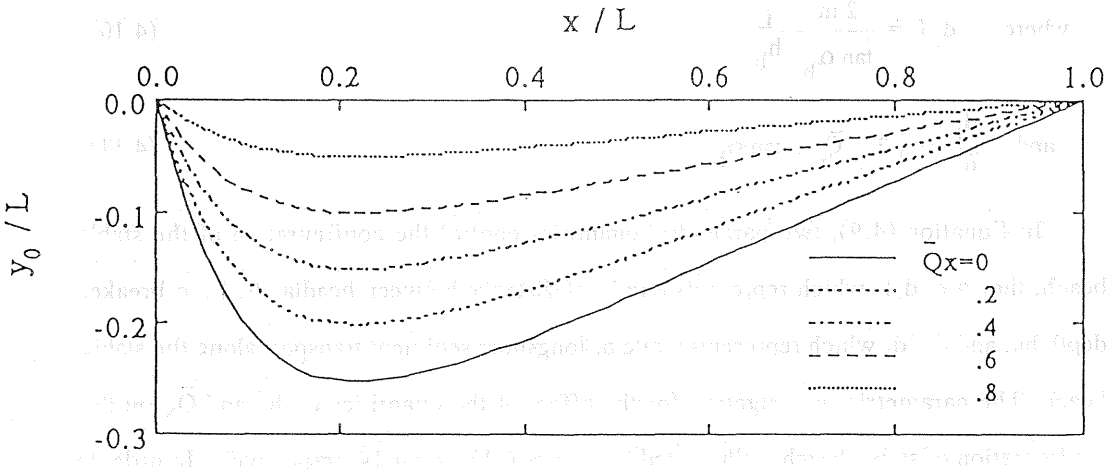

Figure 4.14 Effect of $\bar{Q}_x$ on configuration of stable beach where $L / h_b = 150$.

L/h_b is selected to be equal 150 from a practical view point. Selected other values for L/h_b will lead to the same configuration but with some different values. From these figures it is noted that:

(1) The general configuration of the stable beach follows that of a logarithmic spiral behind the upcoast headland connected with a straight stretch which extends downcoast towards the next headland.

(2) The recession of stable beach increases with increasing L/h_b and decreasing $\bar{Q}_x$.

(3) The position of maximum shoreline recession moves upcoast toward the headland as the L/h_b increases.

(4) The decreasing of $\bar{Q}_x$ does not affect the distance from the upcoast headland to the position of maximum shoreline recession, that can be verified mathematically from differentiation of Eq. (4.9) with respect to x and equating it to zero. The result given as:

$$\left(\frac{x}{L}\right)_{y_{0\max}} = \frac{1}{d_1 L} \ln\left[\frac{d_1 L}{1-\exp(-d_1 L)}\right] \tag{4.12}$$

From Eq. (4.12) it is clear that the distance from upcoast headland the location of maximum shoreline recession is proportional to L/h_b. This relationship is illustrated in Figure 4.15. It is observed that the position of the maximum shoreline recession moves in the upcoast headland of a rate which decreases with increasing values of L/h_b. In Figure 4.16 the incident wave angle is plotted versus the ratio y_{0max}/L for different valves of L/h_b where $\bar{Q}_x$ is equal zero, which represents the case of statically stable beach. From this figure it is obvious that ; 1) y_{0max}/L increases with increasing α_b, 2) y_{0max}/L increases with increasing L/h_b, and 3) the curves become flatter as the incident wave angle α_b increases and L/h_b decreases. This indicates that the ratio y_{0max}/L tends to be a constant value with a small ratio of L/h_b ,and to be independent of the incident waves. In other words, as the distance between the headlands becomes smaller, the headland control concept changes to the offshore breakwater control concept , thus the configuration of the shoreline behind them will

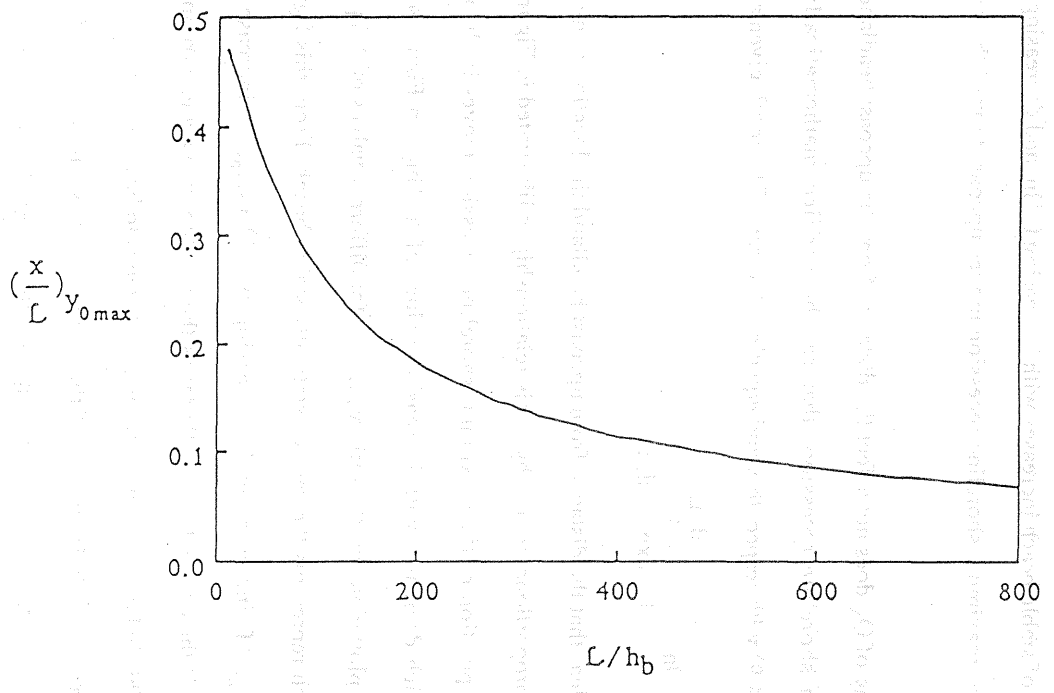

Figure 4.15 Distance from upcoast headland to position of maximum recession of shoreline as a function of L / h_b.

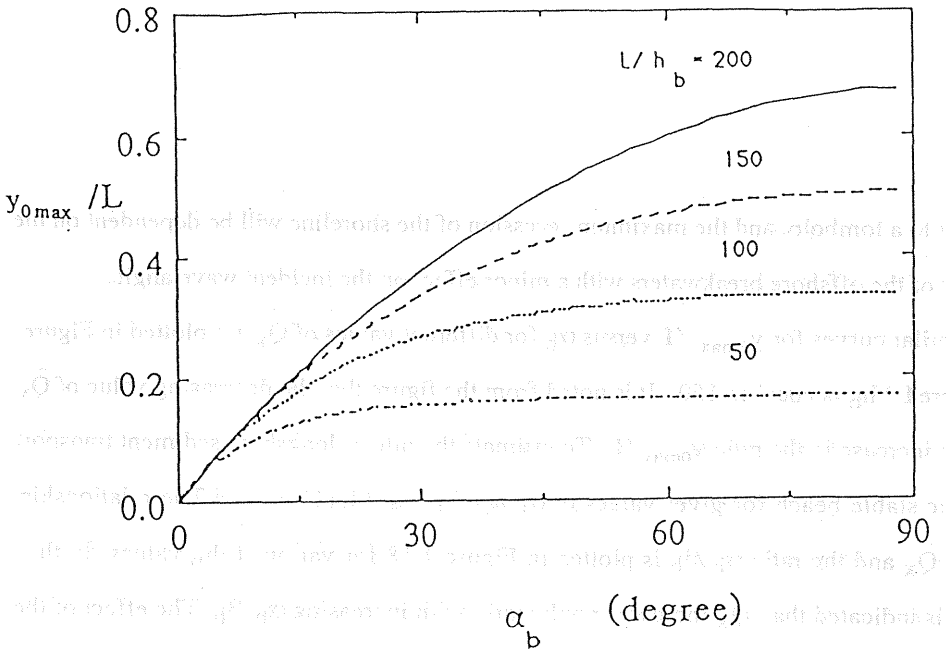

Figure 4.16 Effect of incident wave angle on maximum recession of shoreline for various L / h_b values where $\bar{Q}_x = 0$.

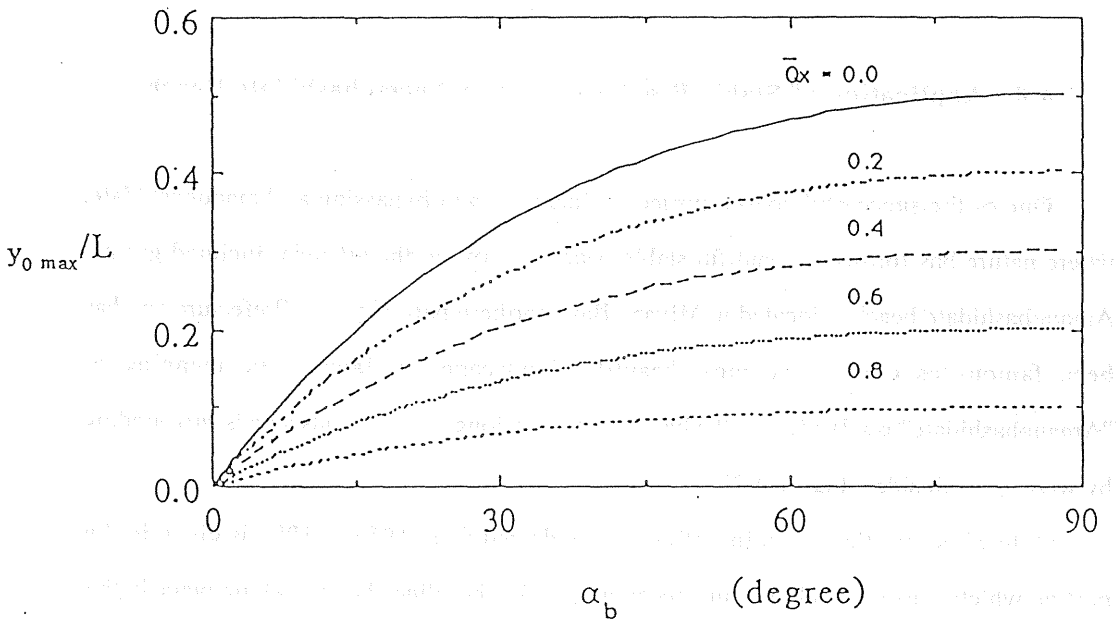

Figure 4.17 Effect of incident wave angle on maximum recession of shoreline for various $\bar{Q}_x$ values where $L / h_b = 150$.

be similar to a tombolo, and the maximum recession of the shoreline will be dependent on the geometry of the offshore breakwaters with a minor effect on the incident wave angle.

Similar curves for y_{0max}/L versus α_b for different values of $\bar{Q}_x$ are plotted in Figure 4.17 where L/h_b is equal to 150. It is noted from the figure that the decreasing value of $\bar{Q}_x$ causes an increase in the ratio y_{0max}/L. To estimate the rate of longshore sediment transport within the stable beach for giver values of α_b and β_b Eq. (4.11) is used.The relationship between $\bar{Q}_x$ and the ratio α_b/β_b is plotted in Figure 4.18 for various L/h_b values. In this figure it is indicated that $\bar{Q}_x$ increases nonlinearly with increasing α_b/β_b. The effect of the ratio L/h_b on the relationship between $\bar{Q}_x$ and α_b/β_b becomes unaffected as the value of L/h_b increases. The applicability of the analytical solution is examined with the laboratory and field data. The result is shown in Figure 4.19, in which the solid curves represent the analytical solution for static equilibrium beach and the dotted curve indicates the Silvester's empirical curve for static equilibrium beach.

4.4 Application of Stable Beach Concept to Amanohashidate Beach

One of the successful coastal project in Japan is sand bypassing at Amanohashidate, where nature has formed a beautiful stable beaches between the artificial inclined groins. Amanohashidate beach is located in Miyazu Bay, northern part of Kyoto Prefecture and has been famous as one of the most beautiful landscapes in Japan. The meaning of "Amanohashidate" is a Bridge to the heaven, where a long narrow landscape is surrounding by water in both sides, Figure 4.20.

A brief description of an investigation conducted from 1956 to 1989 is given in this portion which aims to develop an understanding of the shoreline changes taking place in this area. In addition, the analytical solutions are used to simulate development of stable beaches between the groins. The field data was previously presented in Yajima, Yezono, Yauchi and

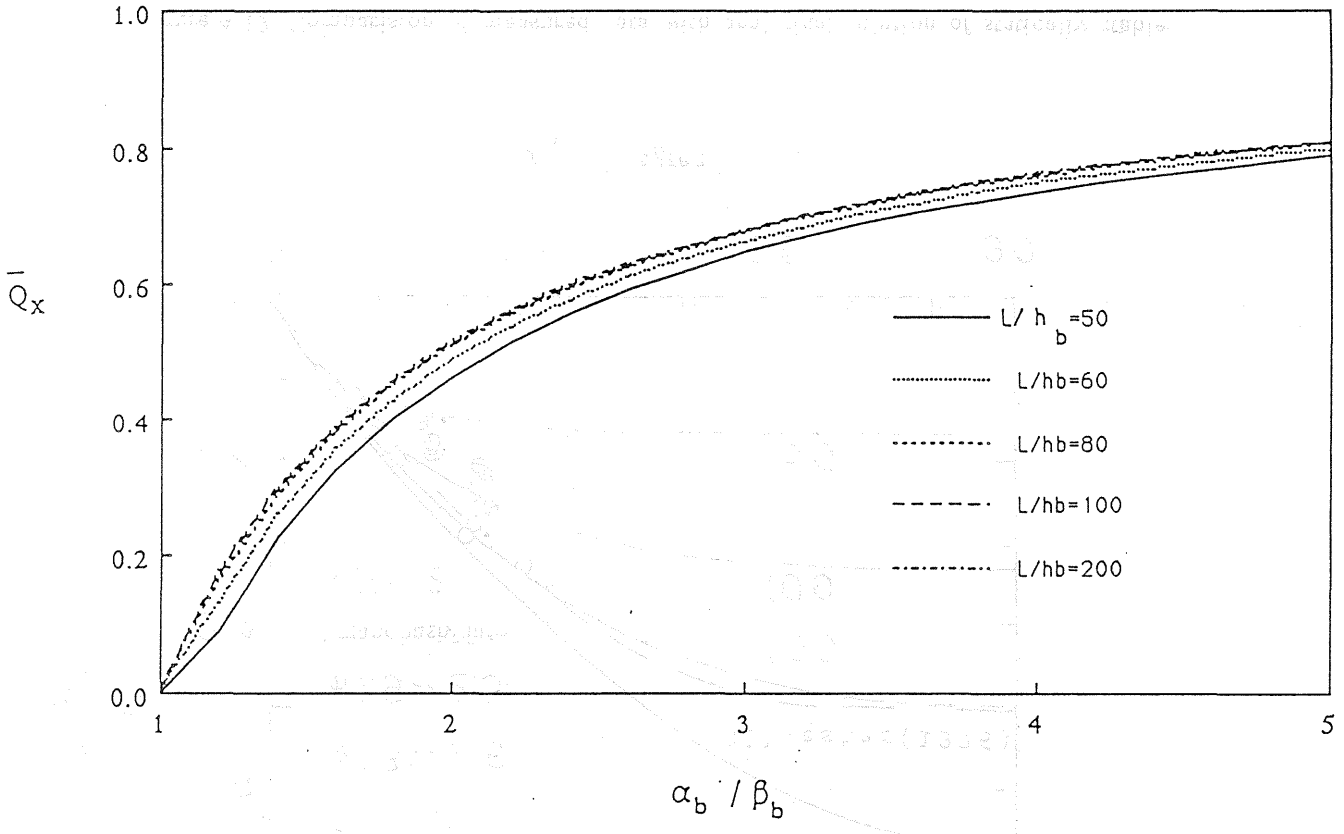

Figure 4.18 Relationship between $\overline{Q}_x$ and α_b / β_b.

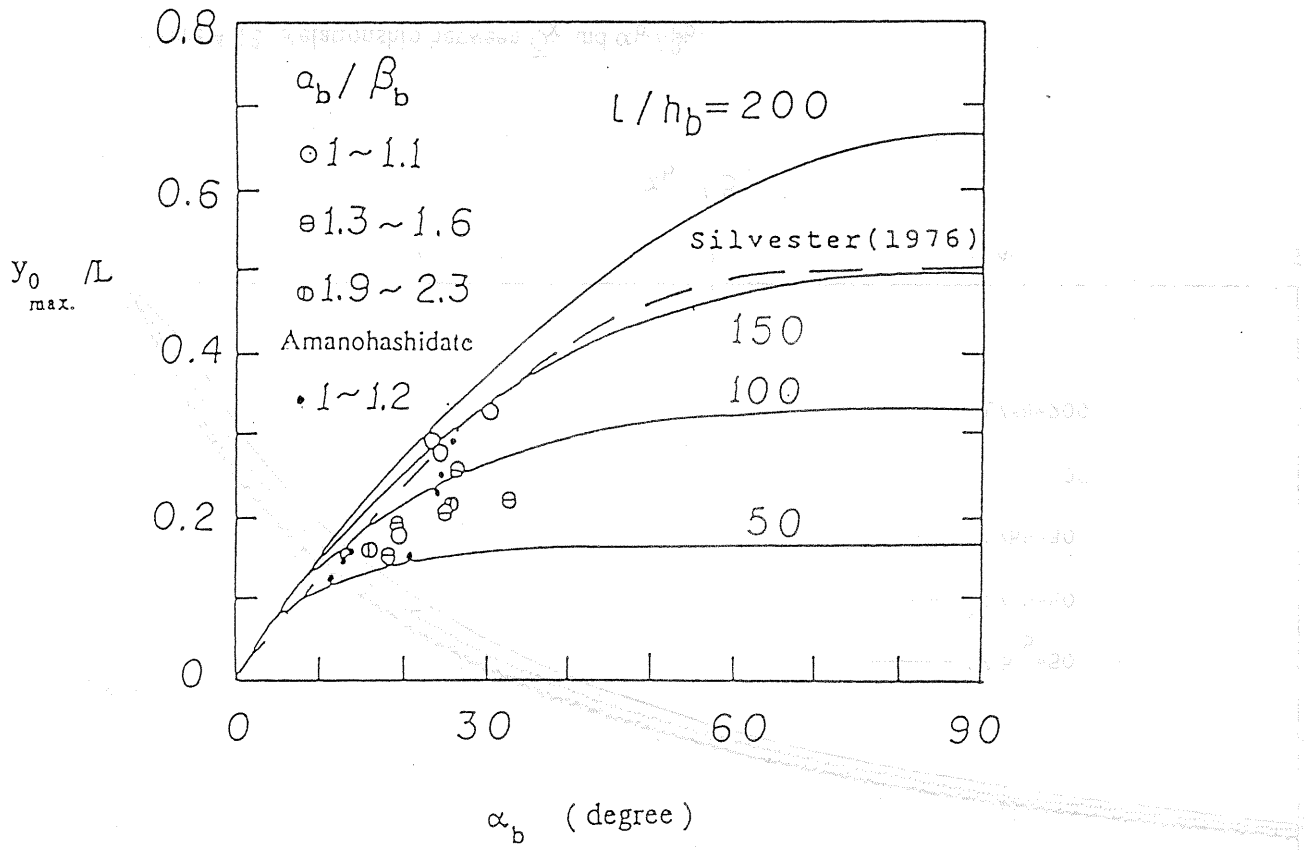

Figure 4.19 Comparision of measured data with analytical solution of statically stable beaches.

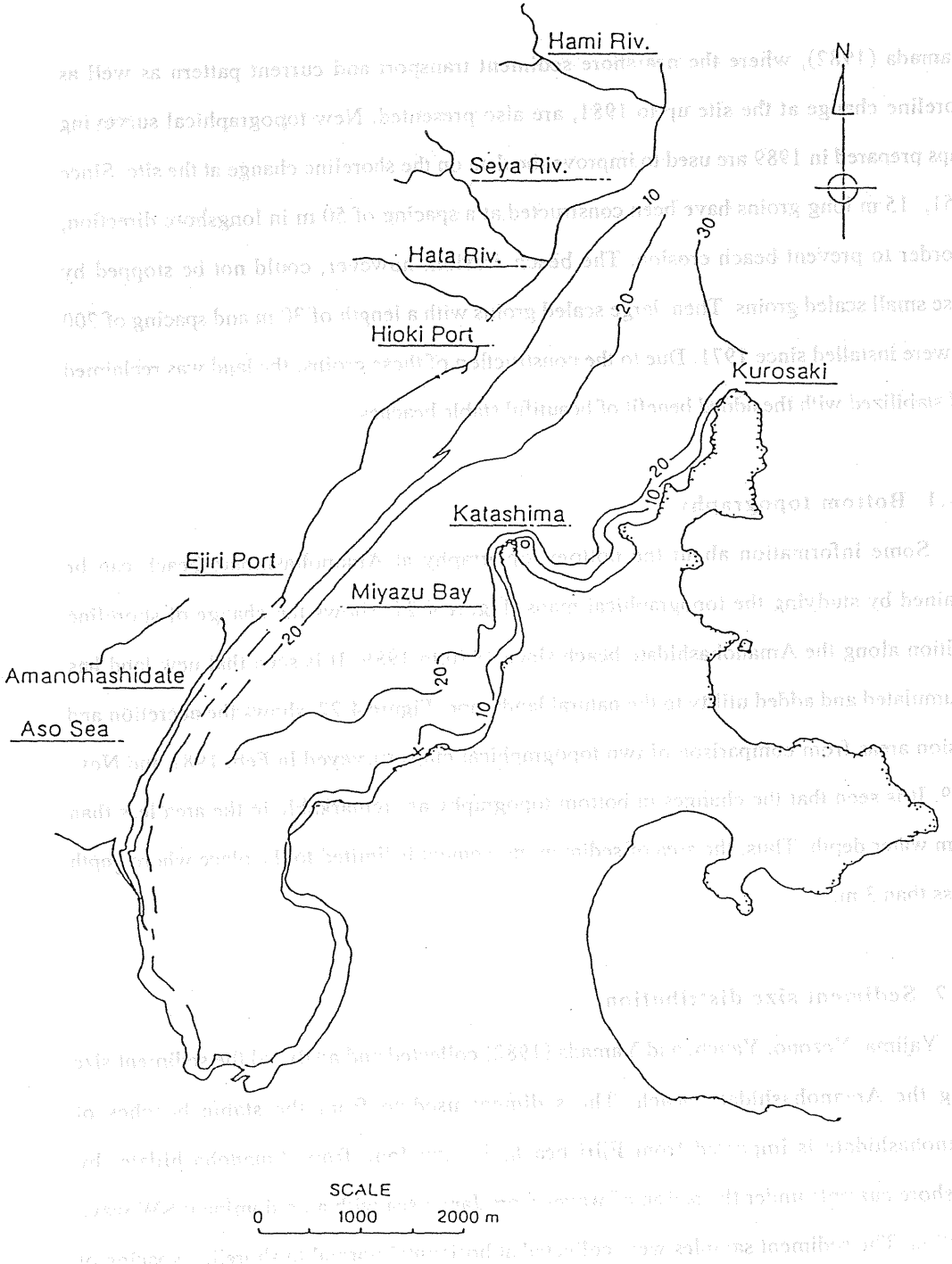

Figure 4.20 Topographical map of Amanohashidate beach.

Yamada (1982), where the nearshore sediment transport and current pattern as well as shoreline change at the site up to 1981, are also presented. New topographical surveying maps prepared in 1989 are used to improve the data on the shoreline change at the site. Since 1951, 15 m long groins have been constructed at a spacing of 50 m in longshore direction, in order to prevent beach erosion. The beach erosion, however, could not be stopped by these small scaled groins. Then, large scaled groins with a length of 30 m and spacing of 200 m, were installed since 1971. Due to the construction of these groins, the land was reclaimed and stabilized with the added benefit of beautiful stable beaches.

4.4.1 Bottom topography

Some information about the bottom topography at Amanohashidate beach can be obtained by studying the topographical maps. Figure 4.21 shows the change of shoreline position along the Amanohashidate beach since 1970 to 1989. It is seen that new land has accumulated and added utility to the natural landscape. Figure 4.22 shows the accretion and erosion areas from comparison of two topographical maps surveyed in Feb. 1981 and Nov. 1989. It is seen that the changes in bottom topography are remarkable in the area less than 3.0 m water depth. Thus, the area of sediment movement is limited to the place where depth is less than 3 m.

4.4.2 Sediment size distribution

Yajima, Yezono, Yauchi and Yamada (1982) collected and analyzed the sediment size along the Amanohashidate beach. The sediment used to from the stable beaches of Amanohashidate is imported from Ejiri beach, 3.6 km long from Amanohashidate, by longshore currents under the action of waves from Japan sea with a predominant SW wave direction. The sediment samples were collected at horizontal normal to shoreline spacing of one meter, up to a depth of 10 m. The sediment size distributions results and specific gravity

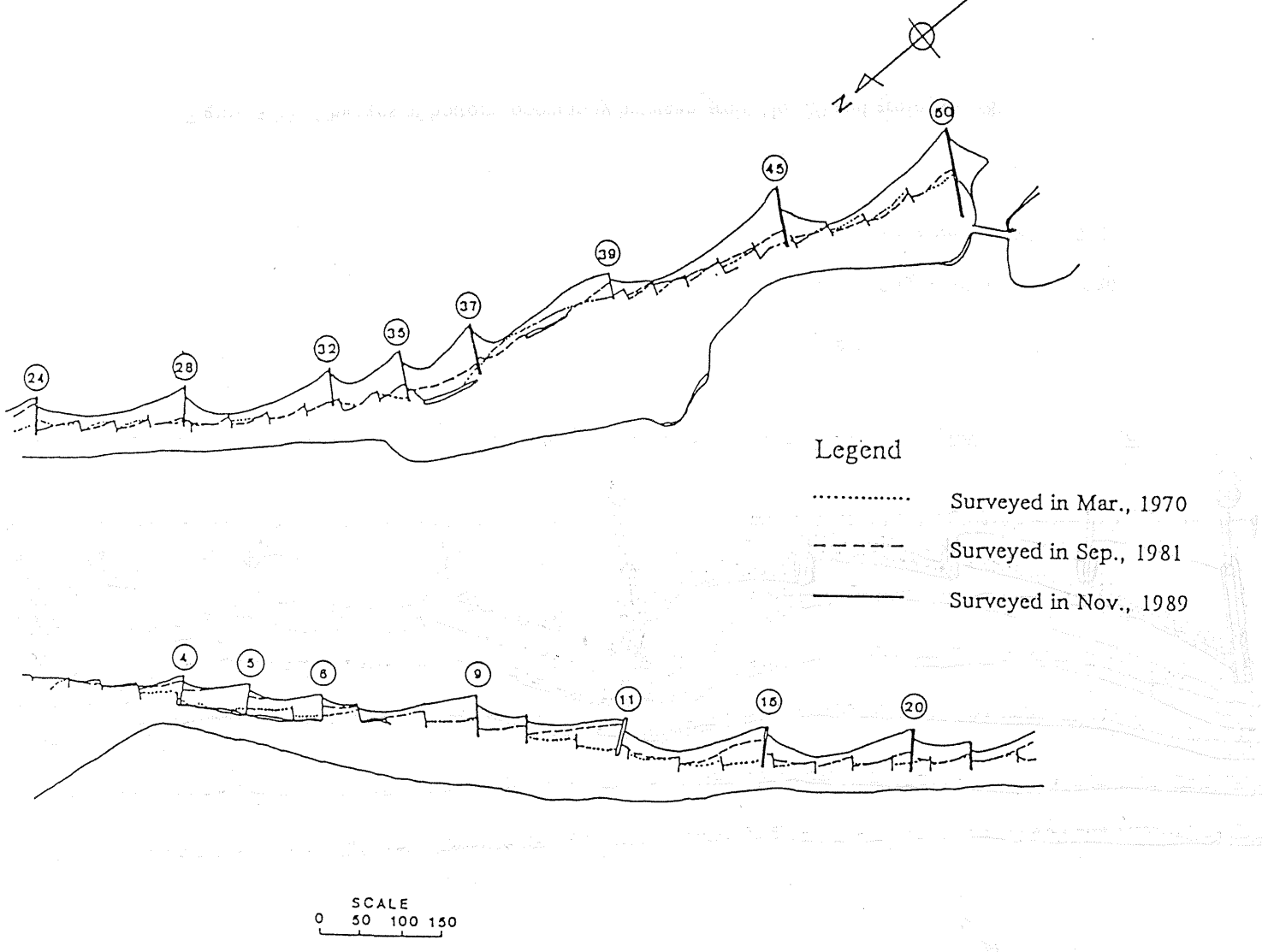

Figure 4.21 Changes of shoreline at Amanohashidate beach.

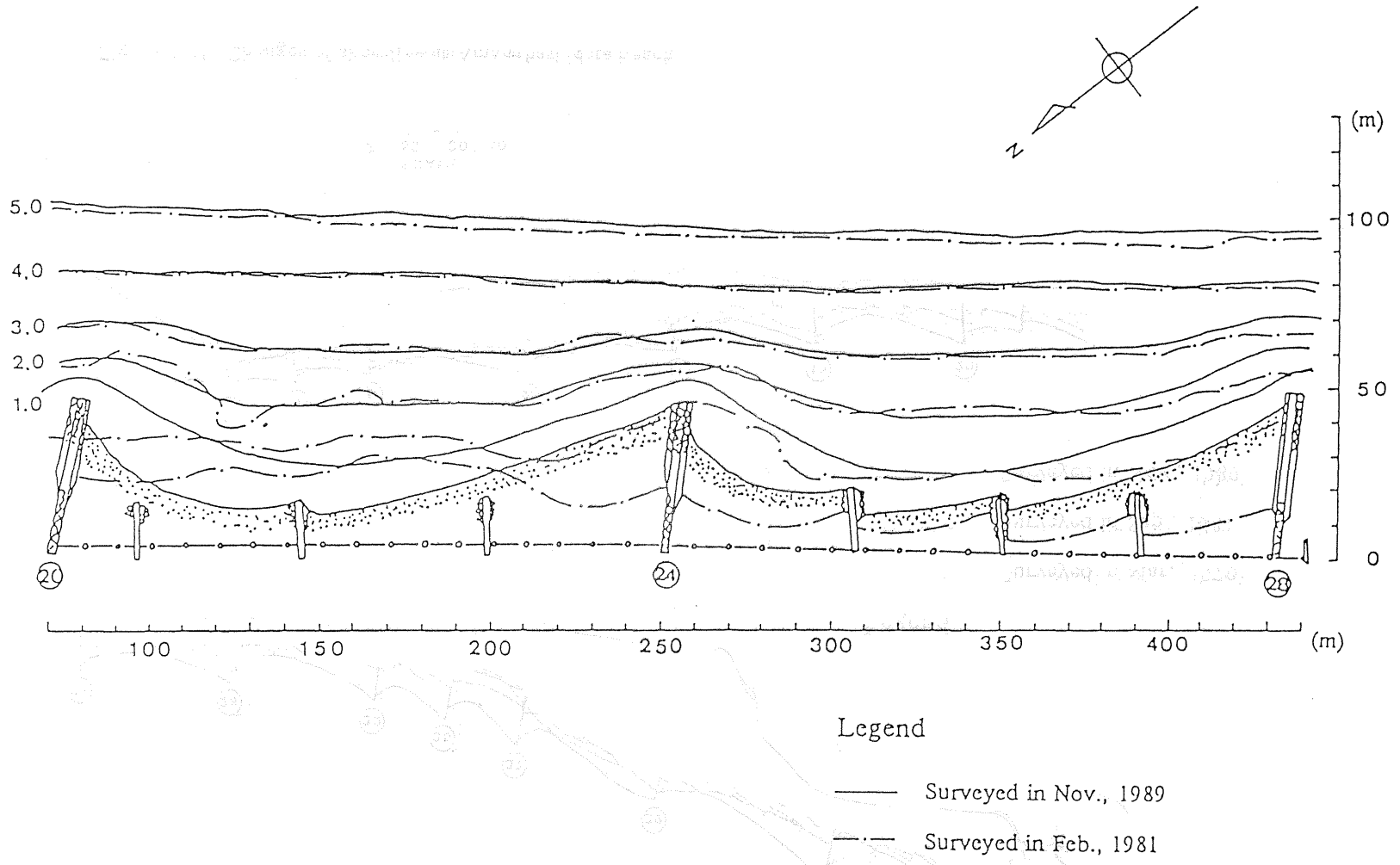

Figure 4.22 Changes of bottom topography between groin No. 20 and groin No. 28.

of there samples are shown in Table 4.1. The sediment medium diameter d_{50} ranges between 0.1 mm and 0.2 mm, and it becomes smaller with increasing water depth.

Table 4.1 Characteristics of bed material at Amanohashidate beach.

Water depth (m)	1.0	2.0	3.0	4.0	5.0	6.0	7.0	8.0	9.0	10.0	11.0
d_{50} mm	0.36	0.11	0.17	0.15	0.21	0.10	0.18	0.11	0.12	0.089	0.095
Spcific gravity	2.67	2.686				2.662					

4.4.3 Wave climate

Waves have been observed in Hioki port, north part of Miyazu bay, Figure 4.20, by using an ultrasonic type wave gauge at the water depth of 8 m, and in Amanohashidate by using a pressure type wave gauge at the water depth of 9 m. The significant wave height and period at Hioki port are 0.8 m - 1.5 m and 7 sec, respectively. The predominant wave direction is in southwest. The refraction diagrams have been used to estimate the refraction coefficients and incident wave angles along the Amanohashidate beach.

4.4.4 Beach profiles

The general bottom configuration of the stable beach presents a characteristic that makes it different from the typical pattern of open beach. Four stable beaches along the Amanohashidate were selected. The beach profiles were measured along each stable beach at 20 m intervals, the beach profiles were measured perpendicularly to the shoreline. Figure 4.23 presents the location of the selected stable beaches by referring to the groin numbers shown in the general layout of Figure 4.21. The numbers shown in Figure 4.23 indicate the

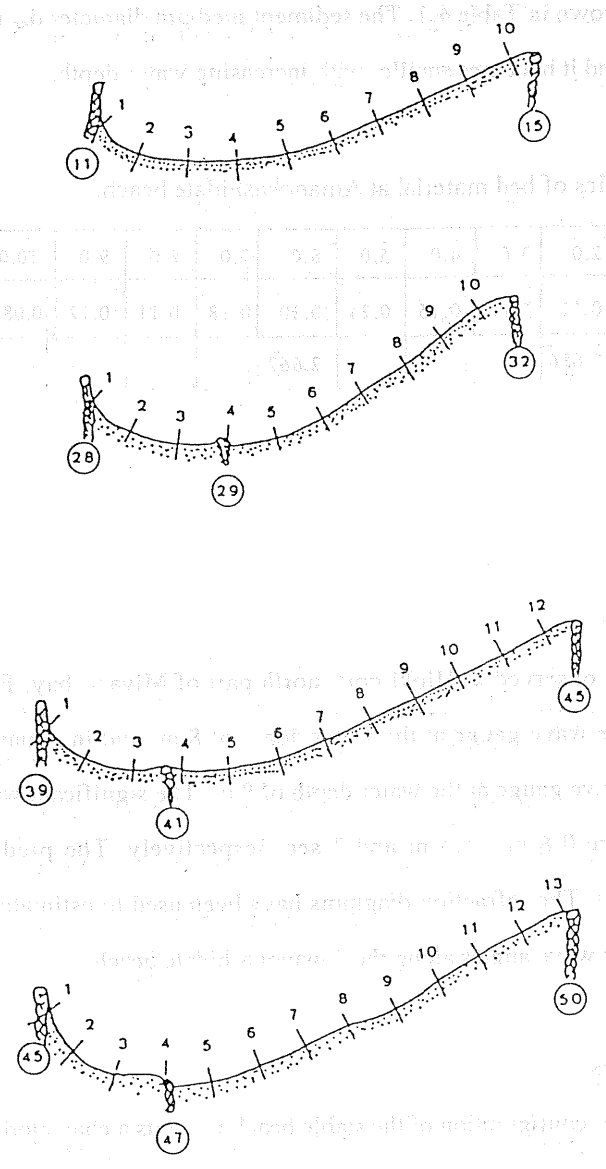

Figure 4.23 Points of measurement of beach profile along four selected stable beaches.

measured beach profile sections. The results of the beach profile measurement are shown in Figures 4.24 to 4.27. These figures show similar results in that the beach slopes on the upcoast side of the groin are gentle, and they become steeper towards the downcoast side of the groin. Up to a water depth of 1.5 m, the contour lines are nearly parallel to the shoreline with an average slope of 1/10. For water depth deeper than 2 m up to 6 m the beach slope is varied between 1/20 on the upcoast side of the groin to 1/5 on the downcoast side.

4.4.5 Prediction of shoreline changes

The shoreline changes along the Amanohashidate beach are measured from a topographical map prepared in 1989. By knowing the wave properties along the beach, and the tangential angle β_b on downcoast side the analytical solution, presented in Eq. (4.9), for a stable beach can be applied. The results of the comparison between the theoretical curves and the measured data of shoreline change are presented in Figures 4.28, 4.29 and 4.30. These figures have been categorized based on the ratio of α_b/β_b. From these figures it is obvious that the theoretical curves fits the measured data well on the downcoast side of the groin. However, less agreement between the theoretical curves and the measured data is seen on the upcoast groin side where the wave diffraction effects are strong. An improved prediction can be made if the numerical solution is introduced with a feedback mechanism. In these figures the ratio of α_b/β_b is always greater than 1.0 which indicates that the beaches still in dynamic equilibrium stage. Figure 4.31 illustrates the comparison between the analytical solution and the measured data of maximum recession of shoreline, y_{0max}, normalized by L, plotted versus the incident wave angle α_b. In this figure the ratio L/h_b is calculated, for each group of α_b/β_b, based on the estimated rate of sand bypass along Amanohashidate coast to be 4,000 m^3/y.

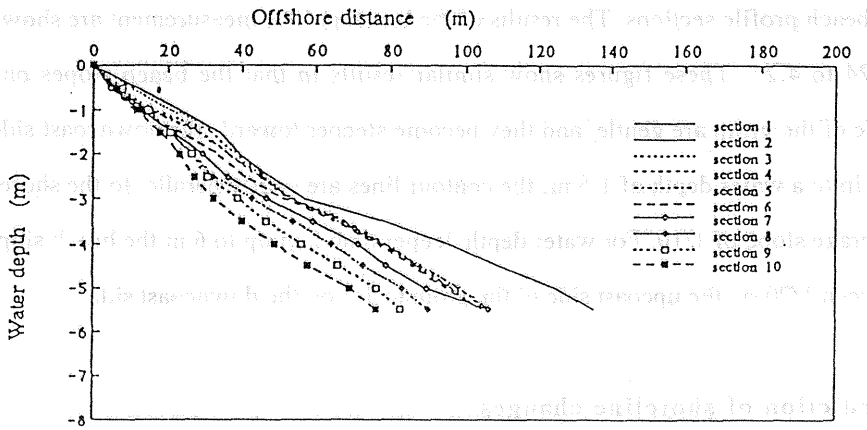

Figure 4.24 Variation of beach profiles along a stable beach between grain No. 11 and groin No. 15.

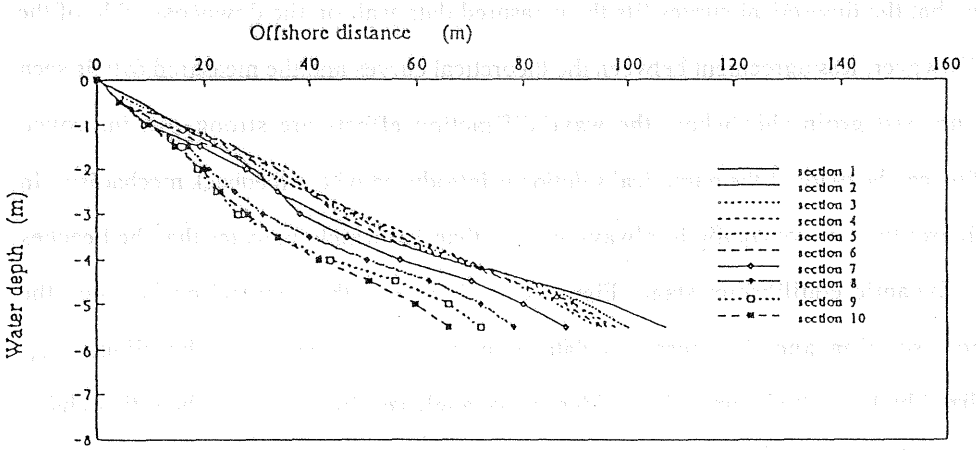

Figure 4.25 Variation of beach profiles along a stable beach between groin No. 28 and groin No. 32.

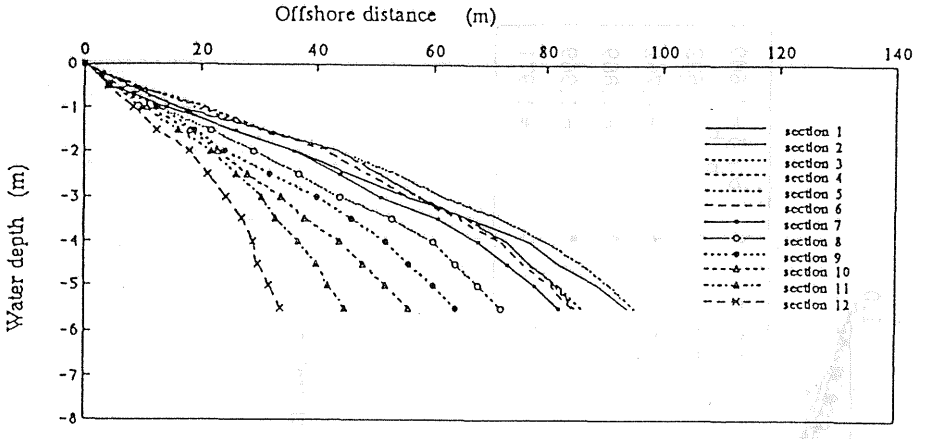

Figure 4.26 Variation of beach profiles along a stable beach between groin No. 39 and groin No. 45.

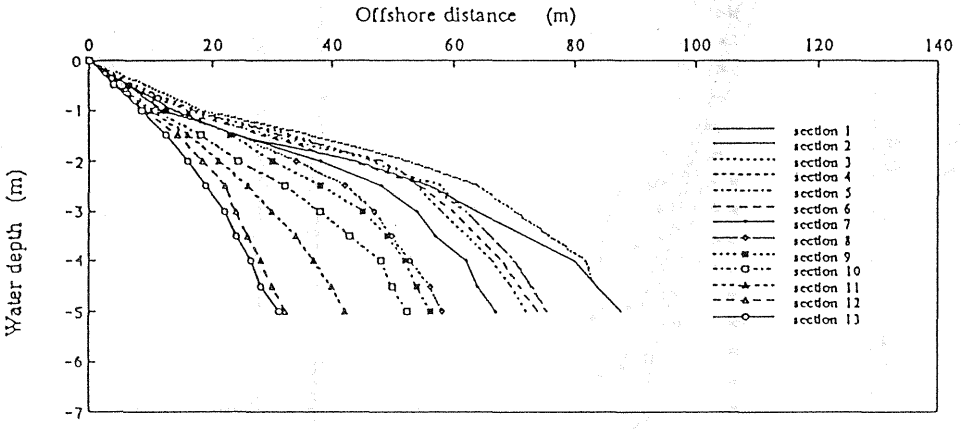

Figure 4.27 Variation of beach profiles along a stable beach between groin No. 45 and groin No. 50.

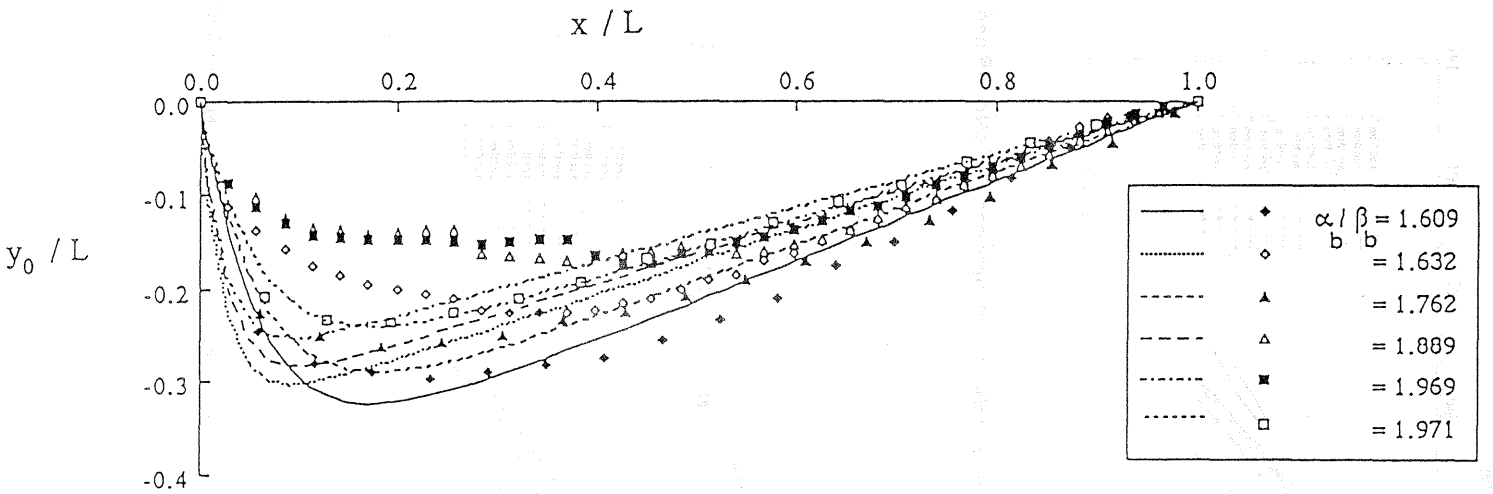

Figure 4.28 Comparison between measured and computed shoreline positions of stable beaches at Amanohashidate, ($\alpha_b / \beta_b < 2.0$).

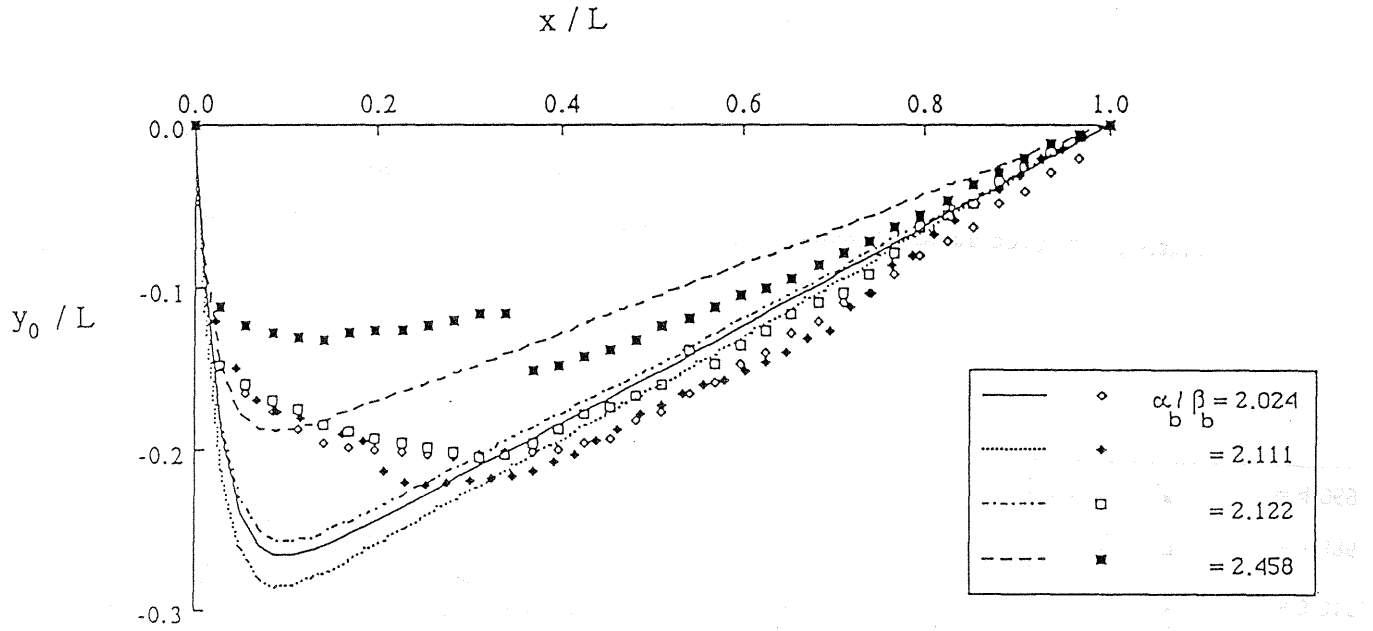

Figure 4.29 Comparison between measured and computed shoreline positions of stable beaches at Amanohashidate, ($2.0 < \alpha_b / \beta_b < 2.5$).

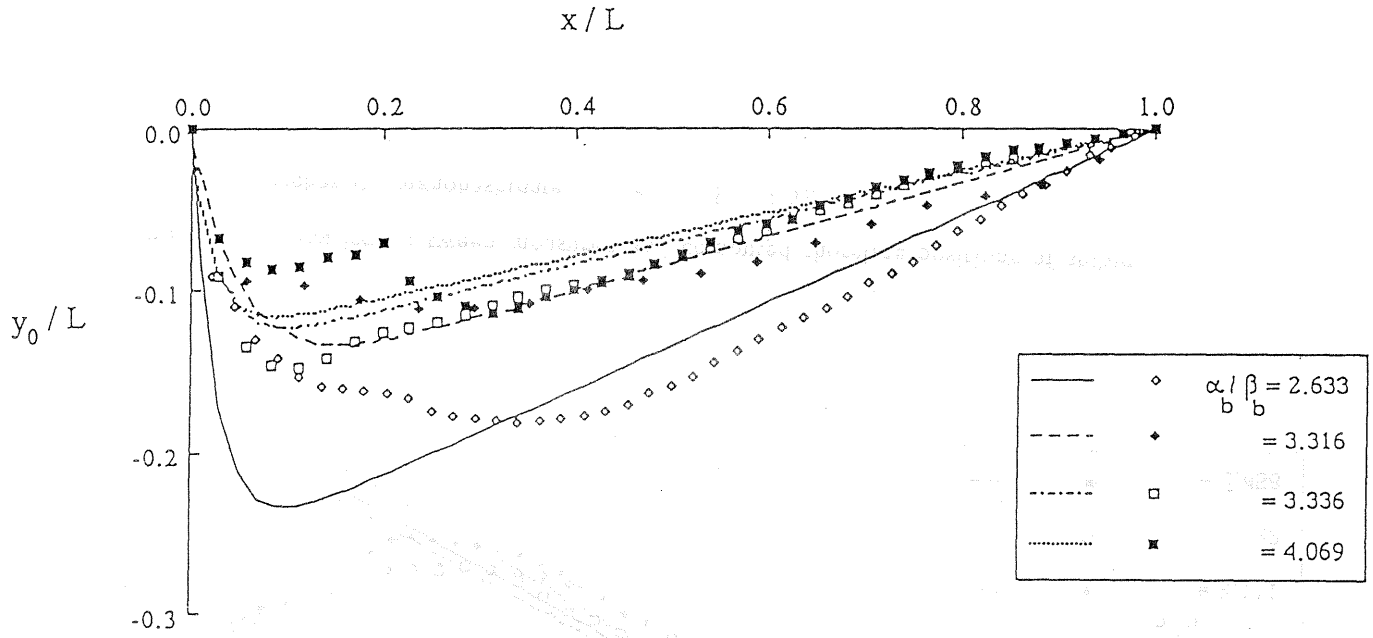

Figure 4.30 Comparison between measured and computed shoreline positions of stable beaches at Amanohashidate, ($\alpha_b / \beta_b > 2.5$).

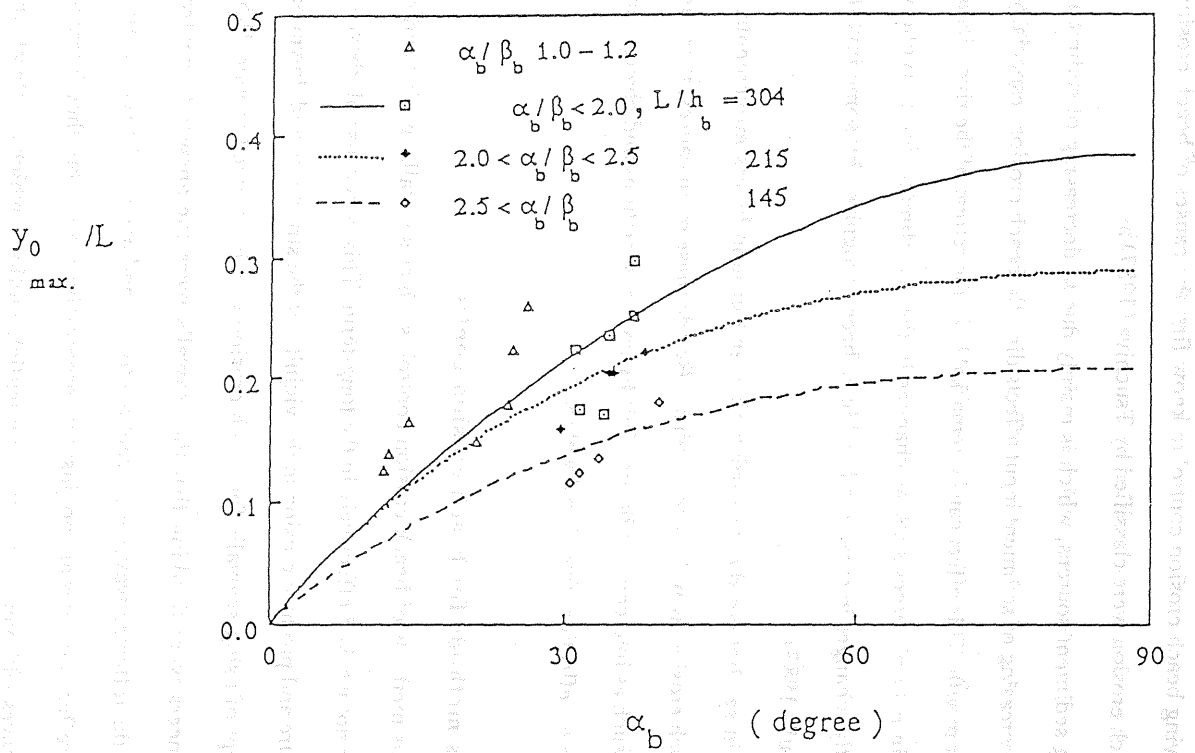

Figure 4.31 Comparison between measured and computed data of maximum recession of shoreline of stable beaches at Amanohashidate beach.

4.5 Methodology for Beach Erosion Control

Recently, beach erosion has been remarkable in many counties in the world. It is very important for studying beach erosion control to know first the causes of beach erosion. The main causes of beach erosion were classified by Tsuchiya (1987) as:

(1) Reducing sediment sources, which is mainly due to decreasing of sediment input from rivers. The decreasing of sediment input affects directly beach erosion, especially in the vicinity of the river mouth. This effect can be remarkable in the retreat of the river delta.

(2) Change in natural forces such as changes in the sea climate due to typhoons and monsoons. Recently, changes in mean sea level have been recognized by some investigators (e.g. Pugh and Faull, 1983).

(3) Change in sea bottom due to earthquakes and ground layers movements. It may directly affect beach erosion as well as sea climate. Beside these main causes, there are other additional causes such as intercept the littoral drift by coastal structures and changes in waves characteristics due to reflection from breakwaters.

4.5.1 Previous methods for beach erosion control

The previous methods of beach erosion control, such as seawalls, groins and offshore breakwaters have not worked effectively in the long-term. This is because all these structure work against nature and produce erosion in the vicinity of the structures and downcoast from them. The concept of using seawalls for beach erosion was introduced around 1950, when the coastal engineers were thinking that the seawalls were the answer to control beach erosion, because the reflected waves were sent out to sea, and never to be seen again. In fact, the incident and reflected waves are not just two progressive waves, but they interact to form a short crested waves with very complex water particle motions, which accelerate the rate of sediment transport and cause the beach slopes in front of the seawalls to become steeper.

Furthermore, this may cause the failure of the structure.

Groins are generally built at right angles to the shore, and usually extended beyond the surf zone. They were constructed to intercept the littoral drift and hence form a beach to the tip of the groin. During storm wave, a strong littoral current is generated toward the upcoast groin. This is deflected seaward as a rip current and carries sediment to a deeper depths. When swell wave returns, this sediment will be carried to the next groin. Thus, using groins can not stop the littoral drift and therefore they promote beach erosion.

The offshore breakwaters are placed parallel to the shore with small spacing between. This little opening available for waves to form tombolo behind the structure, but erosion will occur at the far end beach between the structures. Brunn (1972) stated in his lecture at the 13th Coastal Engineering Conference that, "Water shall not be compelled by any fortse (force) or it will return that fortse onto you". This means that the more powerful man acts on nature the more nature reacts upon man's ambitions. So that man should not act against nature, but check the reaction of nature (Tsuchiya, 1987).

4.5.2 New methods for beach erosion control

Recently, many coastal engineers are being advised to let nature takes its courses. Nature always adapts the beach between reefs or natural headlands, to minimize the littoral drift and to form a beautiful stable shape for sandy beach. Silvester (1979) states the methodology of beach erosion control in his paper as "How to copy nature". Tsuchiya (1987) proposed new methods for beach erosion control and beach preservation which are generally being applied in the field. He summarized these methods as:

(1) To avoid offshore sediment drift by making beach slopes as mild as possible for reducing reflected waves by the beaches. The number of structures for beach preservation even for preventing nourished sediment from offshore drift should also be reduced. It should be expected to form sandy beaches naturally.

(2) To conserve the continuity of sediment drift. When the sediment sources change or disappear beach erosion will take place. In this case, essentially, sand bypassing should be carried out at once to conserve the continuity of sediment drift.

When sediment input from river decreases, the rate of longshore sediment transport should be reduced for the same order. To reduce the total rate of sediment transport, practically, two ways which would be suitable from the expression proposed in Chapter 2 for the total rate of sediment transport. The first is to reduce the breaker depth by either changing bottom topography or constructing submerged breakwaters or offshore breakwaters. The second is to reduce the breaking wave angle by changing either the bottom topography or the inclination of the shoreline to be parallel to the predominant wave crests.

4.5.3 Beach erosion control of river delta

One of the major problems of coastlines is the decrease of sediment input from the river. Severe erosion generally takes place at the river mouth. To control the reduction of the river delta two methods are considered. First, to increase the sediment input from the river. A direct sand bypassing may be considered from the river basin to the coast. This method would be most effective for beach erosion control, but it be difficult. Secondly, to reduce or prevent longshore sediment transport by forming a series of stable beaches.

Based on Tsuchiya's ideal methodology for beach erosion control of river delta shown in Figure 4.9, in which the sediment input from the river is reduced, the second solution is recommended. Two ideal examples can be presented for controlling beach erosion of river deltas. The first is for beach erosion control of symmetrical river delta configuration, where the predominant waves are normally incident. The second example is for beach erosion control of asymmetrical river delta configuration, where predominant waves are obliquely incident. Suppose that a river flows into the sea in which the predominant waves are normally incident as shown in Figure 4.32, the configuration of the delta is symmetric. The

sediment input from the river was Q_R and has recently been reduced to Q'_R, therefore severe beach erosion occurs on both sides of the river delta, especially at the vicinity of the river mouth. Based on Tsuchiya's ideal methodology for beach erosion control and the theory of formation of stable sandy beaches, the solution is depicted as shown in Figure 4.32(b), in which a series of headlands is constructed on both sides of the river delta at suitable angles and distances. As a result, a series of dynamically stable beaches is naturally formed.

Figure 4.33(b) demonstrates the situation for asymmetrical river delta configuration when the sediment input from the river reduces from Q_R to Q'_R, therefore severe beach erosion occurs on the downcoast side of the river delta. The solution as stated before is to construct a series of headlands in order to form a series of dynamically stable beaches as shown in Figure 4.33(b). The upcoast side of the river delta may be suffered from a local, small scale beach erosion since the main sediment transport is moving with the direction of littoral drift towards the downcoast side as shown in Figure 4.33(a).

4.6 Conclusions

In this chapter the reduction process of river delta due to decrease or lack of sediment input from the river was experimentally investigated. A theory of formation of stable sandy beaches was derived based on the formulation of non-uniform longshore sediment transport associated with the aid of one-line theory. Through the investigation of the methodology of beach erosion control, a new proposal is made for beach erosion control of river delta. This proposal is based on Tsuchiya's ideal methodology for beach erosion control and the theory of formation of stable sandy beaches. From the experimental study on the reduction process of river delta, the following conclusions are given as:

(1) The reduction of formation processes are significantly different. For the reduction process, the shoreline of the delta is rapidly eroded while the front line of delta retreats at a

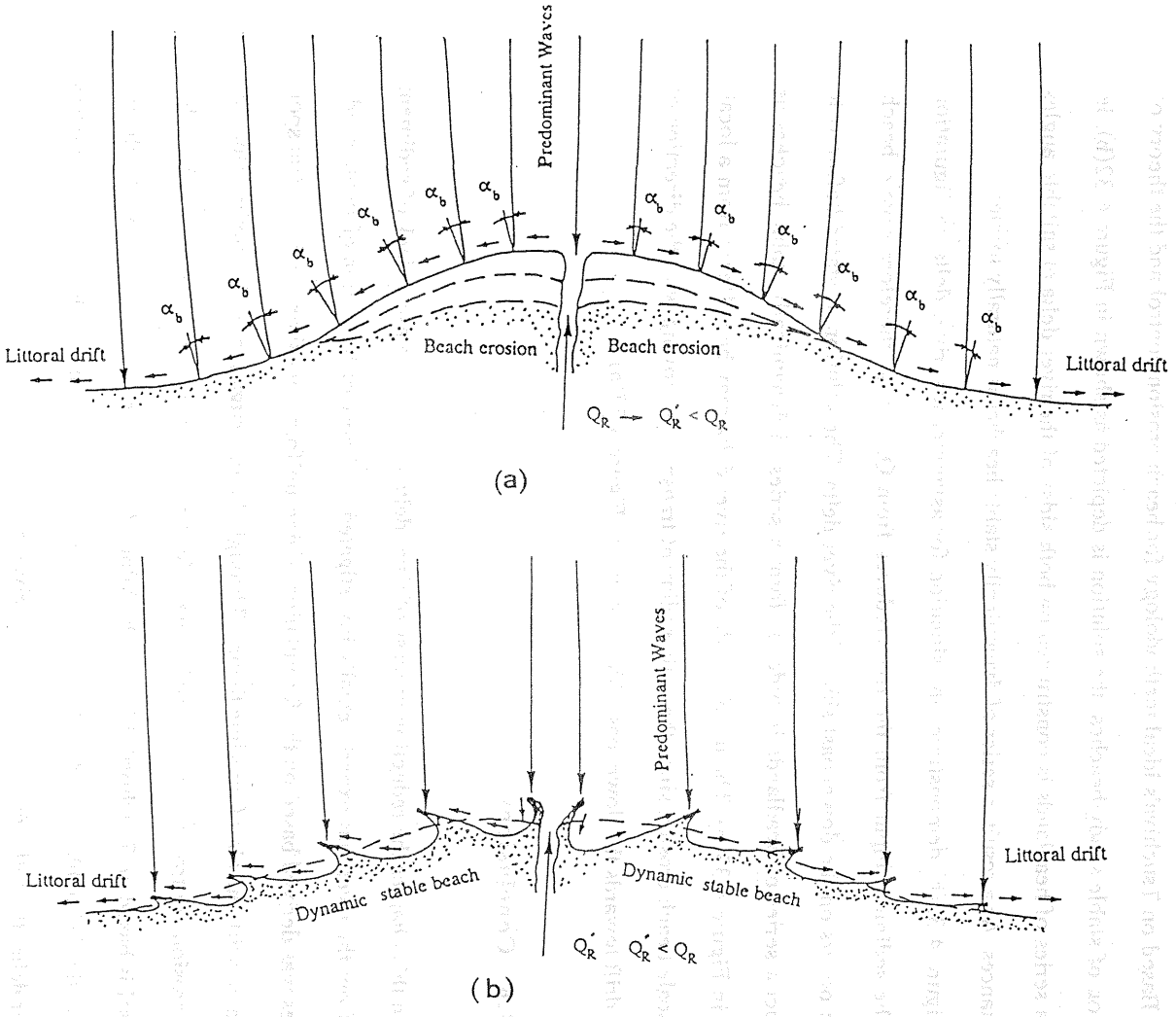

Figure 4.32 Beach erosion control of symmetrical river delta configuration due to the decrease of sediment input from the river.

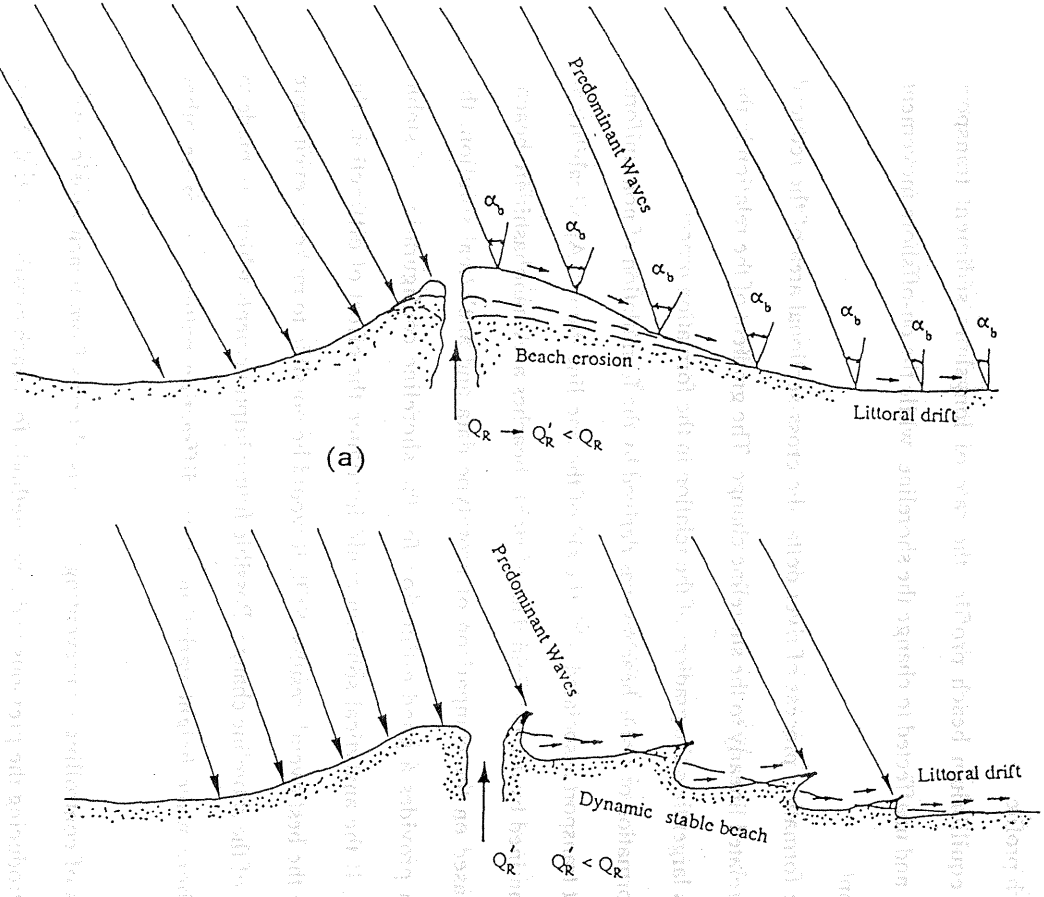

Figure 4.33 Beach erosion contol of asymmetrical river delta configuration due to the decrease of sediment input form the river.

very slow rate. For the formation process, both of the shoreline and the front line of the delta propagate at the same rate, they are almost parallel.

(2) After a sufficient long time the beach profile reaches an stable shape which called the equilibrium beach profile.

(3) With the equilibrium beach profile, the rate of longshore sediment transport becomes very small and unaffected to change the shoreline, while the on-offshore movement becomes predominant.

(4) Likely the formation process of river delta, the cross-sectional area of the reduced beach profile is correlated linearly to the shoreline change. The gradient of the relation in the reduction process is larger than the gradient of the relation in the formation process.

A theory of formation of stable beaches was derived by the formulation of non-uniform longshore sediment transport associated with the aid of the one-line theory. Applicability of this theory was examined by use the field data of stable beaches at Amanohashidate beach. As a conclusion based on the comparison of prototype data and analytical solution, the analytical solution provides a good estimation for the shoreline configuration of stable beaches. However, if the analytical solution could introduce the effect of diffraction, the result may provide the best overall results. Still, it would be possible to make an even more accurate prediction of the shoreline change. Possible future improvements which can made to include the longshore wave height variation, wave diffraction pattern and more other parameters.

The methods of controlling or preventing the coastal areas from beach erosion were investigated by introducing the previous and new methods for beach erosion control. Since the previous methods of beach erosion control failed to prevent or even reduce the beach erosion, we should allow nature takes its courses. Nature always forms the beach between reefs or natural headlands to minimize littoral drift and to form a beautiful stable shape for sandy beaches. A new proposal was made for controlling the beach erosion around the river

delta which is based of Tsuchiya's ideal methodology and the theory of formation of stable sandy beaches. Two ideal examples were presented for controlling beach erosion around symmetrical and asymmetrical river delta configurations. By constructing a series of headlands at the areas where severe beach erosion occurs, a series of stable beaches is formed and a new land reclaimed from the sea will add benefit of beautiful stable beaches for recreation.

REFERENCES

Brunn, P., 1972," The History and Philosophy of Coastal Protection," Proc. 13th Coast. Eng. Conf., ASCE, pp. 33-74.

Dally, W. R. and Pope, J., 1986," Detached Breakwaters for Shoreline Protection," US Army Engrs., Waterways Expt. Station, Coastal Eng. Res. Center, Tech. Report CERC - 86 - 1.

Dean, R.G., 1977," Equilibrium Beach Profiles," US Atlantic and Gulf Coastal, Ocean Engineering, Report No. 12, University of Delaware Press.

Dean, R.G., 1978," Diffraction Calculation of Shoreline Planforms", Proc. 15th Conf. Coastal Eng., ASCE, pp. 1903 - 1917.

Ho, S.K., 1971," Crenelate Shaped Bays," M. Eng. thesis No. 346, Asian Institute of Technology, Bangkok.

Hsu, J.R.C., Silvester, R. and Xia, Y.M., 1987," New Characteristics of Equilibrium Shaped Bays," Proc. 8th Austral. Conf. Coastal & Ocean Eng., pp. 140 - 144.

Iwagaki, Y., 1966," A Treatise on Beach Erosion," Summer Seminar on Hydraulics Engineering, JSCE, pp. B-17.1-17.17 (in Japanese).

LeBlond, P. H., 1972," On the Formation of Spiral Beaches," Proc. 13th Internl. Conf. Coastal Eng., ASCE, pp. 1331 - 1345.

LeBlond, P. H., 1979," An Explanation of the Logarithmic Spiral Shape of Headland Bay Beaches," J. Sed. Petrol., Vol. 49, No. 4, pp. 1093 - 1100.

Loveless , J. H., 1986," Offshore Breakwaters : Some New Design Consideration ," J. Inst. Water Engrs.& Scientists, Vol. 40, pp. 511 - 522.

Mashima, Y., 1961," Stable Configuration of Coastline," Coastal Eng. in Japan, Vol. 4, pp. 47 - 59.

Pope, J. and Dean, J. I., 1986," Development of Design Criteria for Segmented Breakwaters," Proc. 20th Conf. Coastal Eng., ASCE, pp. 2144 - 2158.

Pugh, D.T. and Faull, H.E., 1983," Tides, Surges and Mean Sea Level Trends," Shoreline Protection, Thomas Telford, pp. 59-69.

Rea, C.C. and Komar, P.D., 1975," Computer Simulation Models of a Hooked Beach Shoreline Configuration," J. Sed. Petrol., Vol. 45, pp. 866 - 872.

Sauvage de. St., Marc, M. G., and Vincent, M. G., 1954," Tranport Littoral, Formation de Fleches et de Tombolo," Proc. of 5th conf. on Coastal Eng., ASCE.

Silvester, R., 1960," Stabilization of Sedimentary Coastlines," Nature, Vol. 188, No. 4749, pp. 467 - 469.

Silvester, R., 1970," Growth of Crenulate-Shaped Bays to Equilibrium," J. of the Waterway and Harbours Division, May 1970, WW 2, pp. 275 - 287.

Silvester, R., 1974, "Coastal Engineering," V. 11, Elsevier publ.Co., Amsterdam.

Silvester, R., 1976," Headland Defense of Coasts," Proc. 15th Conf. Coastal Eng., ASCE, pp. 1394 - 1406.

Silvester, R., 1978," Some Facts and Fancies on beach erosion," Proc. 16th Conf. Coastal Eng., ASCE, pp. 1888 - 1902.

Silvester, R., 1979," A New Look at Beach Erosion Control," Annuals, D.P.R.I., Kyoto Univ., No. 22A, pp. 33-74.

Silvester, R. and Ho, S. K., 1972, " Use of Crenelate Shaped Bays to Stabilize Coasts,"

Proc. 13th Conf. Coastal. Eng., ASCE, pp. 1347 - 1365.

Silvester, R., Tsuchiya, Y. and Shibano, T., 1980," Zeta Bays, Pocket Beaches and Headland Control," Proc. 17th Conf. Coastal Eng., ASCE, pp. 1306 - 1319.

Toyoshima, O., 1976," Changes of Sea Bed Due to Detached Breakwaters," Proc. 15th Conf. Coastal Eng., ASCE, pp. 1572-1589.

Tsuchiya, Y., 1973," Coastal Sediment Balance and Beach change," Summer Seminar on Hydraulics Engineering, JSCE, pp. B 3.1- 3.19, (in Japanese).

Tsuchiya, Y., 1978 ," Beach Erosion and its Prediction," Annuals, D.P.R.I., Kyoto Univ., No.21A, pp. 1-18, (in Japanese).

Tsuchiya, Y., 1982," The Rate of Longshore Sediment Transport and Beach Erosion Control," Proc. 18th Coast. Eng. Conf., ASCE, pp. 1326-1334.

Tsuchiya, Y., 1987," Beach Erosion Control," Jour. Hydr. and Senitary Eng., JSCE, No. 3871/II-8, pp. 11-23, (in Japanese).

Tsuchiya, Y., Silvester, R. and Shibano, T., 1979," Beach Erosion Control by Method of Equilibrium Beaches," 26th Japanese Conf. on Coast. Eng., JSCE, pp. 191-194, (in Japanese).

Yajima, M., Yezono, A., Yauchi, T.and Yamada, F.,1982," Application of Sand Bypassing to Amanohashidate Beach," 29 th Japanese conf. on coastal Eng., JSCE, (in Japanese).

Yasso, W. E., 1965," Plan Geometry of Headland Bay Beaches," Jour. Geology, Vol. 73, pp. 702 - 714.

Chapter 5 CONCLUSIONS

The formation and reduction processes of river deltas, and their control have been investigated in this study. A new formulation of non-uniform longshore currents and the associated longshore sediment transport has been derived based on introducing of the concept of boundary layer theory. This formula of non-uniform longshore sediment transport rate has been employed with the aid of the one-line theory to develop analytical solutions for evolution of the shorelines of the river delta and to derive a theory of formation of stable sandy beaches. Three experimental studies were carried out, 1) on the similarity of velocity profiles of non-uniform longshore currents, 2) on the formation process of river deltas and 3) on the reduction process of river deltas. The methodology for beach erosion control due to the reduction process of river deltas has been studied. A new proposal is made for beach erosion control of river deltas based on Tsuchiya's ideal methodology for beach erosion control and the concept of formation of stable sandy beaches. Two ideal examples were presented for controlling beach erosion of symmetrical and asymmetrical river delta configurations from the view point of mechanism of longshore sediment transport. The following conclusions can be drawn from this study as follows:

In Chapter 2, the concept of boundary layer theory is introduced to the nearshore region based on the similarity process between the flow motion within the boundary layer and the nearshore currents within the surf zone. The boundary layer theory is authorized by two essential assumptions; they are the velocity profiles of longshore currents are similar and wave set-up is independent of longshore direction. Employing these assumptions the nearshore currents equations could be simplified to arrive a new equation of non-uniform longshore currents. This equation is similar to the boundary layer integral equation and contains integration coefficients which depend only on the velocity profiles of longshore currents. Therefore, an experimental study on the similarity of velocity profiles in

non-uniform longshore currents was carried out. The experimental results reveal that the coefficients which appeared in the new equation of non-uniform longshore currents are not functions of longshore direction nor time. The comparison of the new equation of non-uniform longshore currents with detailed laboratory measurements indicates that the similarity of the velocity profiles is very satisfactory.

Tsuchiya and Yasuda's formula for estimating of the total rate of longshore sediment transport is extended to include the non-uniform terms. The general equation of the total rate of longshore sediment transport is then formulated. This new formulation of non-uniform longshore current includes the effects of sediment size, beach slope and bed roughness, and has been verified with the field and laboratory data plotted in the well known Komar's figure. With this formula, the CERC empirical formula could be modified.

In Chapter 3, the physical description of river delta formation has been investigated through studying two field cases; the Nile Delta coast, Egypt, and the major river deltas in Lake Biwa, Japan. The formulation of non-uniform longshore sediment transport has been employed with the aid of the one-line theory to derive a general formal solution of river delta formation. This formal solution takes into account the effect of longshore variation of beach slope. For various initial and boundary conditions, several analytical solutions for evolution of the shorelines of river deltas have been derived. The formation process of river delta has been also studied experimentally. The main conclusions drawn from the experimental study on the formation process of river deltas are: 1) For wave-dominated delta type, the longshore variation of beach slope is very small with a gently mild beach profile. The shoreline gradient in the longshore direction is gradually change resulting in gently curved of river delta shape. In the contrary, for river-dominated delta type, beach slope is remarkably varied along the river delta with steeper beach slope at the river mouth and milder one at the end sides of the river delta, resulting in sharply curved shape of river delta. 2) When predominant waves are obliquely incident, the configuration of delta will be asymmetric. With asymmetrical configuration of river delta, the longshore currents on the downcoast side are stronger than the longshore currents on the upcoast side. As a result much sediment are moving and

depositing on the downcoast side than on the upcoast side.

In comparing of the analytical solutions for shoreline evolution of river deltas with the experimental measurements of delta formation and the major river deltas in Lake Biwa, favorable agreement was found. For wave-dominated delta type, the analytical solutions can predict the shoreline evolution with a high level of accuracy. While, less accuracy was considerable for evolution of shoreline changes of river-dominated delta type.

In Chapter 4, the reduction process of river delta due to decrease or lack of sediment input from the river was experimentally investigated. The experiment reveals that the reduction process is significantly different from the formation process. In the reduction process, the shoreline of river delta significantly is eroded in a very short time, while the front line of the delta retreated shoreward at a very slow rate. After a sufficient long time the beach profile reaches an stable shape which called equilibrium beach profile, where the longshore sediment transport is not exist anywhere.

A theory of formation of stable sandy beaches was established by employing the new formulation of non-uniform longshore sediment transport rate with the aid of one-line theory. The applicability of the theory of formation of stable sandy beaches was examined using data of stable beaches at Amanohashidate beach, Japan. From the comparison of measured and calculated date of stable beaches, it is concluded that this theory provides a good estimation for the configuration of the shoreline of stable beaches.

One of the principle goal of this study is to control beach erosion of the river delta, which occurs due to decrease or lack of sediment input from the river. The methodology for beach erosion control was investigated by introducing the previous and new methods for beach erosion control. The previous methods of beach erosion control, such as seawalls, groins and offshore breakwaters, failed to control the beach erosion, oppositely these structures promote beach erosion. Tsuchiya established his ideal methodology for beach erosion control from the view point of controlling the total rate of longshore sediment transport. By introducing his methodology and the theory of formation of stable sandy beaches, a new proposal is made for controlling beach erosion of the river deltas. Two ideal

examples were presented for controlling beach erosion of symmetrical and asymmetrical river delta configurations. In order to control beach erosion of symmetrical river delta configuration from the view point of mechanism of longshore sediment transport where the sediments input from the river move and deposit on both sides of river delta, a series of headlands is constructed on both sides of river delta at suitable angles and spacings. The theory of formation of stable sandy beaches is used to determine the suitable angles and distances of the headlands. For asymmetrical river delta configuration, beach erosion often occurs on the downcoast side of the river delta, in which most of sediments input from the river move and deposit on this side. Therefore, a series of headlands is constructed on the downcoast side of the river delta. Consequently, a series of stable beaches is naturally formed with reclaiming a new land from the sea and adding benefit of beautiful sandy beaches.

Finally, in future the extension of the present study should be directed towards the practical applications of the new concept of formation of stable beaches to control beach erosion of river deltas. Since the bases of this concept were already established, it is still possible to make even more better understanding and more better controlling of beach erosion, which can be made in the near future.